THE DETERMINATION OF MOISTURE VARIATION PATTERNS IN CLAY SOILS UNDER A LIGHT STRUCTURE HOUSE

By

Dirk Maartens Bester

A thesis submitted in fulfilment of the requirements for the degree

Master of Engineering in Civil Engineering

in the

Department of Civil Engineering

of the

Faculty of Engineering and Information Technology

of the

Central University of Technology, Free State, South Africa

Supervisor: Prof. E Theron

Co- Supervisor: Dr. PR Stott

December 2017

DECLARATION

I, the undersigned, declare that the thesis hereby submitted by me for the degree *Master of Engineering in Civil Engineering* at the Central University of Technology, Free State, is my own independent work and has not been submitted by me to another University and/or Faculty in order to obtain a degree. I further cede copyright of this thesis in favour of the Central University of Technology, Free State.

Dirk Maartens Bester

Signature: …….

Date: December 2017

Bloemfontein, South Africa

ABSTRACT

The South African Government's attempts to provide affordable, subsidized housing for the very poor have suffered from a large number of structural failures, many due to heaving foundations. These houses are particularly susceptible to damage by heaving clay because they are relatively light and clay heave can lift them very easily. Rational design requires knowledge of the pattern of heave which will occur under the foundation. The pattern of heave depends on the pattern of moisture movement. Currently available methods of rational design rely on assumptions about the shape of the mound which will develop due to moisture movement under the foundation. The shape assumed is largely guided by measurements made on mock foundations.

Instrumentation has been installed under a Government Subsidy house in the Free State and moisture movement is being monitored. The actual pattern of moisture movement observed is substantially different to what is normally assumed and could point to more reliable estimates of the heave which needs to be designed for.

ACKNOWLEDGEMENTS

A number of special acknowledgements deserve specific mention:

I. I would like to take this opportunity to acknowledge the Central University of Technology (CUT), and the Department of Civil Engineering of CUT, for their support to me during this research work.

II. My hearty gratitude and special thanks to Prof. E Theron, Senior lecture at the Department of Civil Engineering for her wonderful support and continuous encouragement.

III. I would like to express my sincere gratitude to my co-supervisor, Dr. PR Stott for his encouragement, contribution, guidance and patience throughout this research project.

IV. My sincere appreciation to the University of the Free State for their co-operation with the assistance of data collection as well as the students who assisted me in the soils laboratory at CUT.

V. The various agencies for funding and in particular the Central University of Technology, Free State and National Research Foundation.

VI. My special thanks and hearty gratitude to my family for their constant encouragement, support and understanding.

Table of Contents:

LIST OF FIGURES:

LIST OF TABLES:

APPENDIX LIST:

LIST OF ABBREVIATIONS:

%	Percent
°C	Celsius
3D	Three dimensional
Bd	Bulk density
CLSM	Continuous logging soil moisture
COLTO	Committee of land transport officials
e	Edge moisture variation distance
ESP	Exchangeable Sodium Percentage
IDW	Inverse distance weighted
k_s	Modulus of the subgrade reaction
kPa	Kilopascal
L	Length
LL	Liquid limit
SL	Shrinkage limit
m	Meter
M	Mound exponent
mm	Millimetre
NWM	Neutron water meters
PI	Plasticity index
PL	Plastic limit
RBF	Radial Basis Functions
SAR	Sodium absorption ratio
Ym	Differential heave
z	Expansive layers
Zw	Influence depth of penetrated precipitation
δ/l	Allowable deformation
θd	Gravimetric moisture content
θvd	Volumetric moisture Content

CHAPTER 1: INTRODUCTION AND RESEARCH DESIGN

1.1 Introduction

The South African Government has been attempting to provide subsidized housing for the very poor communities throughout the country. Since 1994, the South African government has built more than 2,68 million subsidized houses throughout the country (Anonymous 2015). These subsidized houses have been plagued by failures due to expansive soils which heave and damage the structures. In many cases these houses failed to meet the expected design life time. The South African Government and human settlement stakeholders have committed to deliver 1.5 million housing opportunities throughout the country by 2019.

The construction of raft foundations for Government Subsidy housing has become common in areas affected by expansive soils such as most of the Free State and Northern Cape. The objective of raft foundations constructed on active soils is to limit the differential movements of the underlying soils to a level which can be tolerated by the superstructure (Day, 1991). The large number of failures suggests that the raft foundations are not properly designed for these soils. Observations reinforce this view since many houses built on "stock design" rafts cannot cope with magnitude and distribution of heave. There is an apparent lack of understanding how the soil and foundation interact to cause the extensive structural damage. This assertion is further supported by the practice of builders who find it more economical to demolish the entire structure rather than attempt repairs (Bester, Stott & Theron 2016).

Current raft design relies on assumptions about the shape of the mound or dome which will develop due to moisture movement in the soil underneath the foundation. The assumed deformation pattern is often based on heave measurements on model foundations e.g. (Pidgeon, 1987), (Pidgeon & Pellisier 1987) or foundations simulated by sheet covers e.g. (Fityus, Smith & Allman 2004), (Miller, Durkee, Chao & Nelson 1995), (de Bruijn 1973). Such model foundations do not take two significant factors concerning the influence of a building constructed on the foundation into account: the influence of the building on the temperature regime under the slab and the influence of the building on solar energy reaching the soil surrounding the slab. Both of these

factors can have a profound effect on moisture movement under the foundation. Fityus *et al* (2004) found that over a period of measurement lasting seven years, temperature appeared to have a greater effect than rainfall on moisture movement and consequent heave of clayey soils at their test site.

This study used a foundation of an actual light structure house (Government Subsidy housing) that was built on expansive soils and is occupied by residents. The location of the study area is in Botshabelo section K, which forms part of the Mangaung metropolitan area and is situated 45 km east of Bloemfontein (Figure 1-1). Each year many Government Subsidy houses are built throughout Botshabelo. A significant number of them experience structural distress well short of their design lifetime.

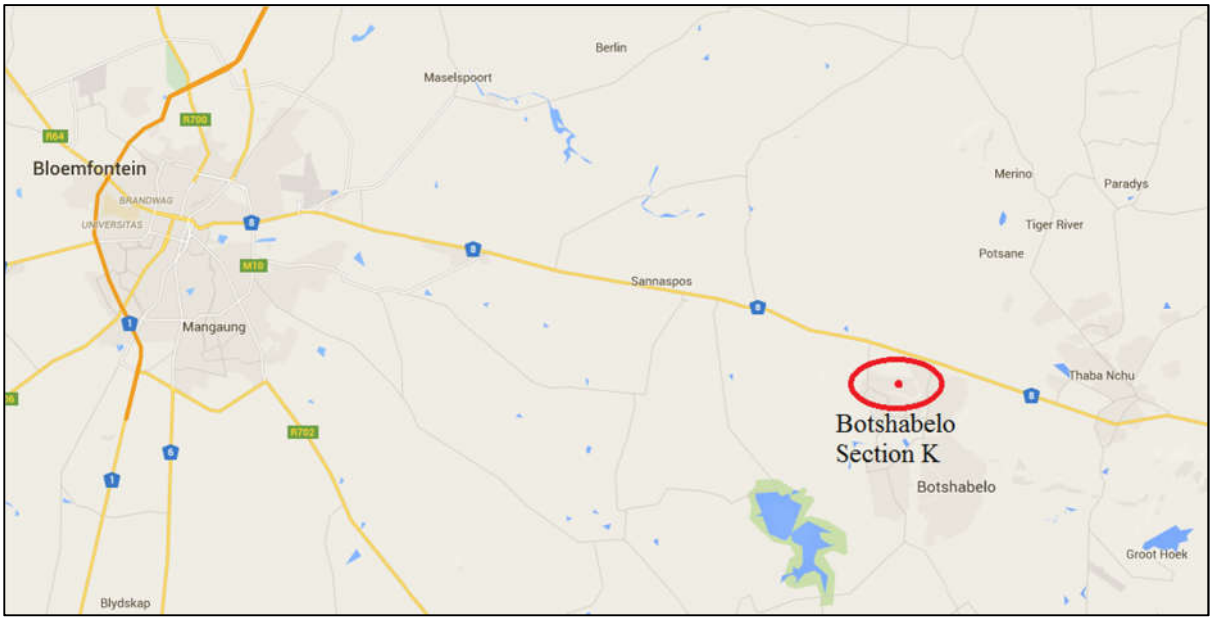

Figure 1-1: Study area in Botshabelo section K

The underlying geology where Botshabelo is situated consists of shale, mudstone and sandstone of the Beaufort group, with frequent intrusions of dolerite. All of these rocks frequently produce to expansive clays when weathered in the semi-arid conditions of the central Free State. The area is therefore considered very suitable for the study being undertaken. The Government Subsidy house was selected based on the soil conditions and the fact that it has a raft foundation of a very common “stock” design. Continuous logging soil moisture probes (CLSM probes) were installed into the foundation (Figure 1-2) to measure water content at various depths under the house. Measurements were taken automatically at hourly intervals. The installation layout

follows two linear alignments transecting the house: one east west, the other north south. The CLSM probes allow measurement of temperature and water content at depths of 150mm, 300mm, 450mm, 600mm, 800mm and 1000mm respectively. The soil profile underneath the house has a thin layer of dark brown clayey sand with a thickness of 150mm. This is underlain by a layer of black clay and a layer of olive-coloured residual clay. Both clays are assessed by Van der Merwe's method as having medium expansiveness. Rock is found at a depth of approximately 1100 mm. The first clay layer is from 150-900mm, the second clay layer is from 900 – 1100mm.

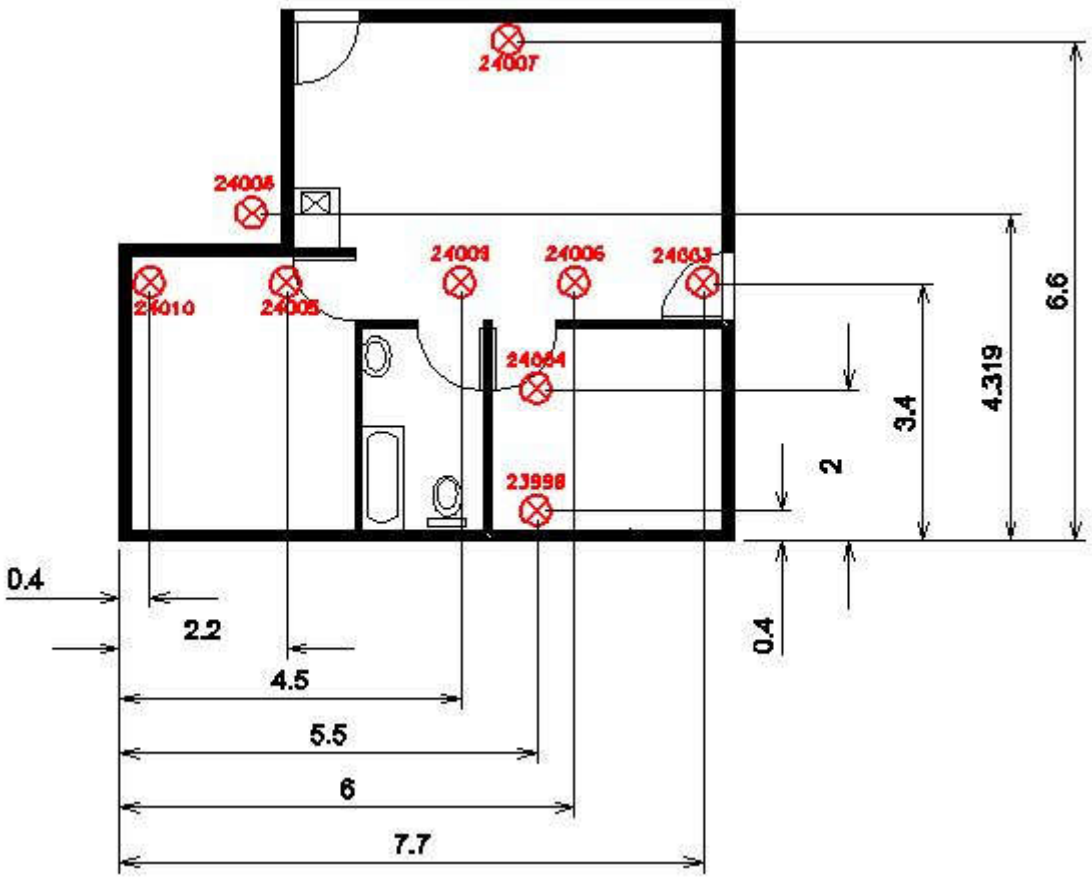

Figure 1-2: CLSM probe layout in raft foundation: dimensions meters

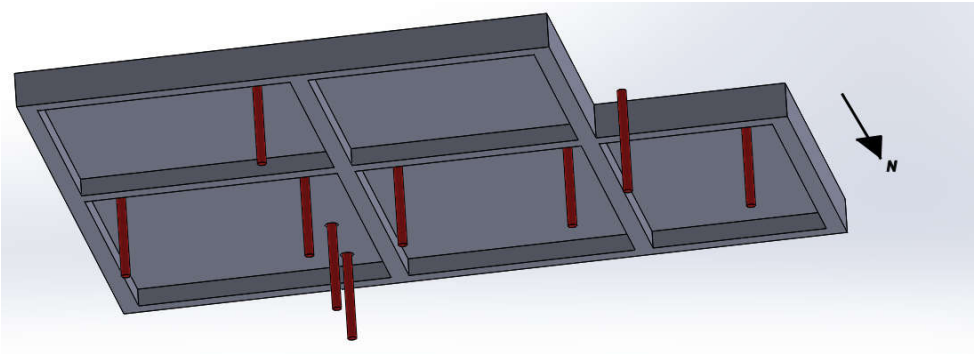

Figure 1-3: 3D layout of CLSM probes

1.2 Problem statement

In South Africa, expansive clays soils are the most widespread of problematic soils. Expansive clays pose a significant risk to light weight buildings such as Government Subsidy houses. The leading cause of heave or settlement in expansive soils is change in soil moisture in active clays. There are two notable heave patterns which can occur depending on the building and weather conditions:

I. Edge heave (Figure 1-4): This occurs when the expansive clay is wetter along the outer edges of the structure and drier near the centre. This might be observed relatively soon after the completion of construction where vegetation has been removed and the lack of surface grading both lead to increased soil moisture. The moisture increase is immediately seen along the periphery of the structure.

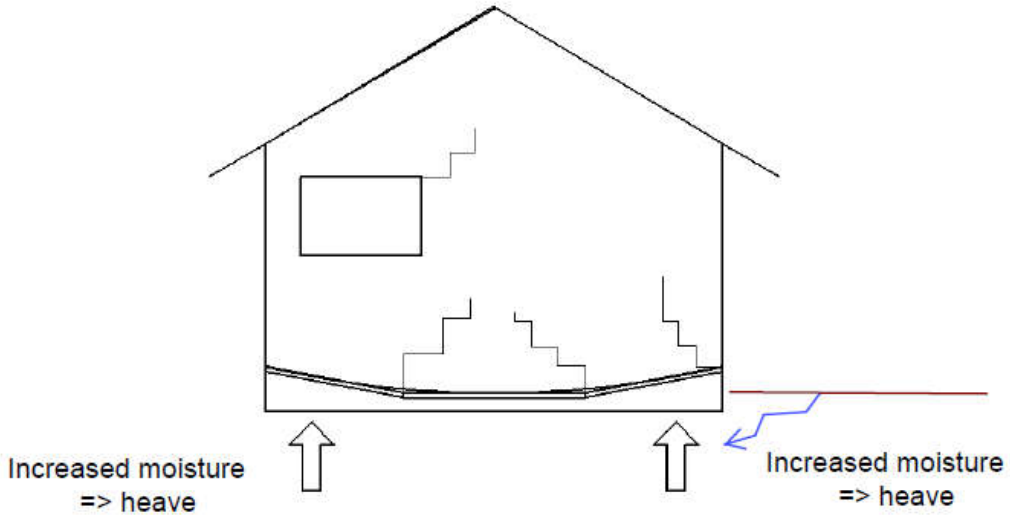

Figure 1-4: Edge heave

II. Centre doming (Figure 1-5): of foundations can occur with an upward, long-term, dome-shaped movement that develops over a period of a few years. This dome shape pattern heaves toward the centre of the structure and follows a decrease of the natural soil moisture content around the perimeter or increase of moisture content under the centre of the building. Figure 1-5 illustrates some commonly observed exterior cracks in brick walls from centre doming. This pattern of heave generally causes the external walls in the superstructure to lean outward. The result is horizontal, vertical, and diagonal fractures with larger cracks near the top of a structure.

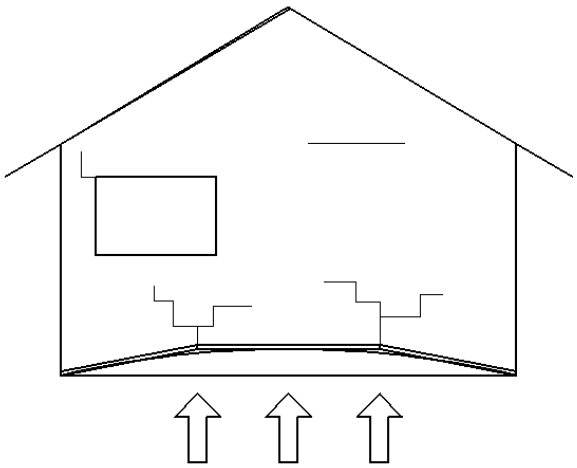

Figure 1-5: Centre Doming

The design of foundations on expansive clay materials is a challenging problem. This requires a good understanding of unsaturated soil behaviour, moisture movement through soil, shrink-swell behaviour of the soil, foundation response, and soil-foundation-structure interaction. Raft design involves assumptions such as the distance for water penetration from the edge to the interior of the foundation. Additionally, the magnitude of heave is dictated by soil characteristics and moisture patterns. The shape and sized of the dome is guided by experience from road construction, however there is no evidence that this is an accurate assumption for building foundations. This study will give insight into this problem and will give an indication of what can be expected in a real scenario beneath a light weight structure house.

The study used the foundation of an actual Government Subsidy house that was built and completed in 2014. The house was constructed using a raft foundation built on expansive soils and is presently occupied by residents going about their daily lives; a rather unique set of circumstances. This study site is in the Mangaung Municipality district which forms part area where surface evaporation of moisture exceeds rainfall for significant portions of the year. The instrumentation used are continuous logging soil moisture probes (CLSM probes). These probes measure the moisture content and soil temperature at various depths. The data will then analysed to establish moisture distribution patterns underneath the foundation. This information will facilitate the development of more refined foundation models on problematic heaving clays.

1.3 Purpose of the study

1.3.1 Research aims of the study

The main aim of this study was to advance our understanding of moisture movement underneath a raft foundation of a lightweight house. This was done by identifying external factors such as orientation of the sun and quantify their influence on moisture movement in the soil.

The secondary aim was to measure moisture distributions during different times of the year when temperature and rainfall vary in seasonal patterns. These fluctuations could result in significant moisture content redistribution and significant changes in heave patterns.

1.3.2 Objectives of the study

For the purposes mentioned (section 1.3.1), a set of objectives was framed. The objectives of this investigation were:

I. To measure soil moisture movement underneath a foundation and track its variation with the seasons. Two and three dimensional interpretations will be made based on measurements at six depths between 150 and 1000 mm.

II. To assess the validity of the edge penetration concept as it applies to raft foundations for small, lightweight buildings. Additionally to study the influence of soil characteristics, permeability, layering, soil density, and building orientation to the sun.

III. To determine the effect of depth on the degree of seasonal moisture variations.

IV. To estimate the potential heave that may occur within the different soil layers at the various moisture contents measured throughout the study.

1.4 Hypothesis

A reasonable hypothesis based on the investigative work which was tested on the present investigation, may be expressed as:

I. The moisture movement underneath a light structure depends on the orientation of the structure to the sun.
II. In the Southern hemisphere, the north side of the structure has a greater difference in moisture over time than the south side.
III. Moisture stays more constant at areas where sunlight is limited.

1.5 Scope of the study

The scope of the investigation was to develop models and a set of design tools to improve our understanding of soil moisture movement and the factors that influence it. This includes design and construction guidelines to reduce moisture movement and potential foundation heave. As a consequence, raft foundations for lightweight structures will become more reliable and require less maintenance and repair. The investigator hopes that if the recommendations of the present investigation are implemented it will help in the overall design process of raft foundations.

1.6 Research design

The research design of the study is represented in Figure 1-6. The figure outlines the methodology which was followed to conduct this investigation in moisture variation underneath a foundation.

1.6.1 Methodology of the study

This investigation in the variation of moisture followed the orderly and step-wise methodology presented in Figure 1-6. The various steps followed in the investigation were the identification of problems and the formulation of objectives which was followed by the collection of data, analysis and modelling.

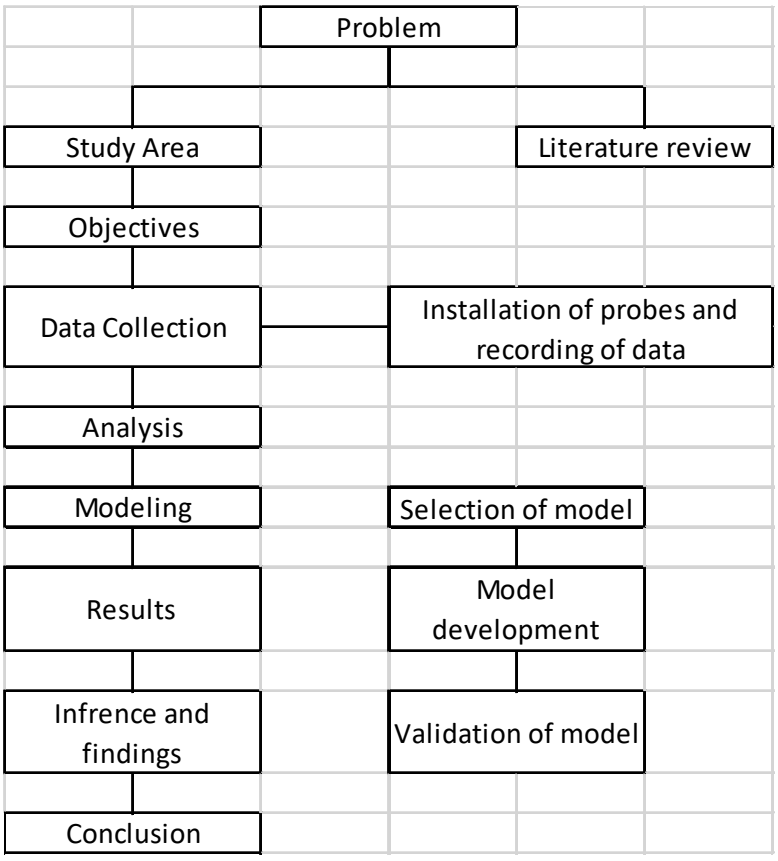

Figure 1-6: Research design

1.6.2 Data collection

Primary data was collected by means of visiting the study location each month and downloading the data using a data logger. This data was uploaded onto Microsoft Excel after which it was sorted according to date and time.

1.6.3 Analysis of data

After compilation, the data was checked for completeness and correctness, and errors in the readings were eliminated by crosschecking, and subsequently, carefully transferred into Excel sheets and then to a computer for analysis. Errors where determined by going through all the data manually and looking for readings which does not match the current trend, for example if the readings are constant and one reading changes extremely and the next readings are constant again then that was deemed as a error reading and eliminated.

The analysis was done by inspection and evaluation of graphical output showing moisture readings over time as profile lines or areal contours. The graphs show the seasonal changes of each measured point for a period of two years. Other graphs and tables illustrate moisture variation distance on the vertical depth for each measured point underneath the raft foundation. All of this information is used to generate graphical models by means of 3D field software.

1.6.4 Modelling

3D Field was selected for processing and displaying the moisture variation patterns. The software develops easy to understand graphical model to illustrate the moisture patterns via a colour scale. The model generated shows the influence of different factors such as the orientation of the building to the sun. Information from these models can be used for the development of design tools and guidelines for the construction of raft foundations for lightweight structures.

1.6.5 Results

The results and modelling of the data has been discussed in detail to arrive at reasonable findings in chapter 4 and 5. For detailed results including all modelling done over the two year period see the appendices A to E.

1.6.6 Inference and findings

Reasonable inferences were drawn for development of moisture variation models and derivation of partial engineering recommendations.

1.6.7 Conclusion to the study

Soil moisture movement under a very common type of Government subsidy house built on clayey soil is very difficult to determine. It is hoped that this study will help to understand how the moisture variation patterns will develop over time and how the orientation of the sun to the building can have an influence. This study should allow reliable forecasts of the moisture conditions which need to be considered when designing common raft foundations. This should allow reliable and economic design of a wide range of raft foundations with the prospect of fewer failures. By applying the findings of this study it should be possible to, at least, achieve a better estimation of moisture pattern development and to determine more realistic and accurate heave patterns which can develop.

1.7 Limitations

I. One of the limitations of the study is that some aspects such as soil conditions and specific raft foundation design cannot be generalized. Other aspects, such as the influence of solar radiation should be universally applicable.

II. Time limit – for this study to be of greater value the measurements should be taken for a period of many years. This would give the study greater value, but the probes gradually stop working.

III. In addition, one of the major limitations of this investigation was the availability of funds to install more CLSM probes in not just one house but multiple houses throughout different climatic areas.

IV. CLSM probe 24006 broke a few weeks after installation and could not be repaired.

1.8 Chapter scheme

Chapter 1: This chapter consists of an introduction, the problem statement, and objectives, the hypothesis, Scope of the study, research design, inferences, strategies and recommendations and limitations of the research.

Chapter 2: This chapter consists of the literature review. This chapter presents the literature review on problematic soils, heaving and expansive clays, raft foundation design, factors affecting water change underneath foundations, testing procedures and the orientation of the sun to the earth.

Chapter 3: This chapter focuses on the profile of study area, laboratory test methods and results, 3D field and data analysis. This chapter also covers the process which was conducted to calibrate the CLSM probes and how the data was collected in this study.

Chapter 4: This chapter covers the data obtained in the study and discussions thereof. Presentations of results obtained is represented in graphs and discussed in detail.

Chapter 5: This chapter contains the findings, the discussion, recommendations and the conclusion.

CHAPTER 2: LITERATURE REVIEW

2.1 Introduction

To a Civil Engineer, soil is any uncemented or weakly cemented accumulation of mineral particles formed by the weathering of rocks during the rock cycle. The weathering process may be physical or chemical, or both (Knapnet & Craig, 2012). Soil is used as a structural support of building foundations and a construction material in many construction projects. It is therefore important to study the properties and features of soil. Soil mechanics is the science where soils are studied for their physical properties and the behaviour under different types of actions. *Soil engineering* is the principles of soil mechanics used in real life practical problems. Geotechnical engineering is, therefore, the discipline where the application of soil mechanics is used in the design of foundations, retaining structures, and earth structures (Das, 2015).

2.2 Geology in the Free State and Botshabelo

Botshabelo is underlain by sandstone, shale and mudstone belonging to the Adelaide Subgroup of the Beaufort Group in the Karoo Sequence. These rocks were extensively intruded during the Karoo period by numerous dolerite sills and dykes.

2.3 Problematic soils

Problematic soils behave in ways that lead to poor performance of engineering structures. According to Diop, Stapelberg, Tegegn, Ngubelangaand and Heath (2011) the five common problematic soils which could be encountered in South Africa are as follows.

2.3.1 Collapsible soils

Collapsible soils are usually poorly graded (with respect to particle size) by nature. Collapsible soils can experience minor compression if imposed stresses are applied at low in-situ moisture content. When wetted or excessively loaded a collapsible soil

display a sudden and substantial decrease in volume or large settlements under stresses. The occurrence of these types of soils is restricted to very specific geological conditions which usually lead to the formation of silts and sands with a low fraction of clay sized particles. It is common to find collapsible soils in wind deposited sands or highly weathered and leached granite soils. Failure of these soils often do not occur below the entire structure but usually only in areas where collapse conditions are favourable and therefore leading to restricted damage to structures. In the event of construction on a collapsing soil preventative measures are straight forward with the proper compaction or densification sufficient (Diop, et al, 2011). Figure 2-1 shows the distribution of potential collapsible soils in South Africa.

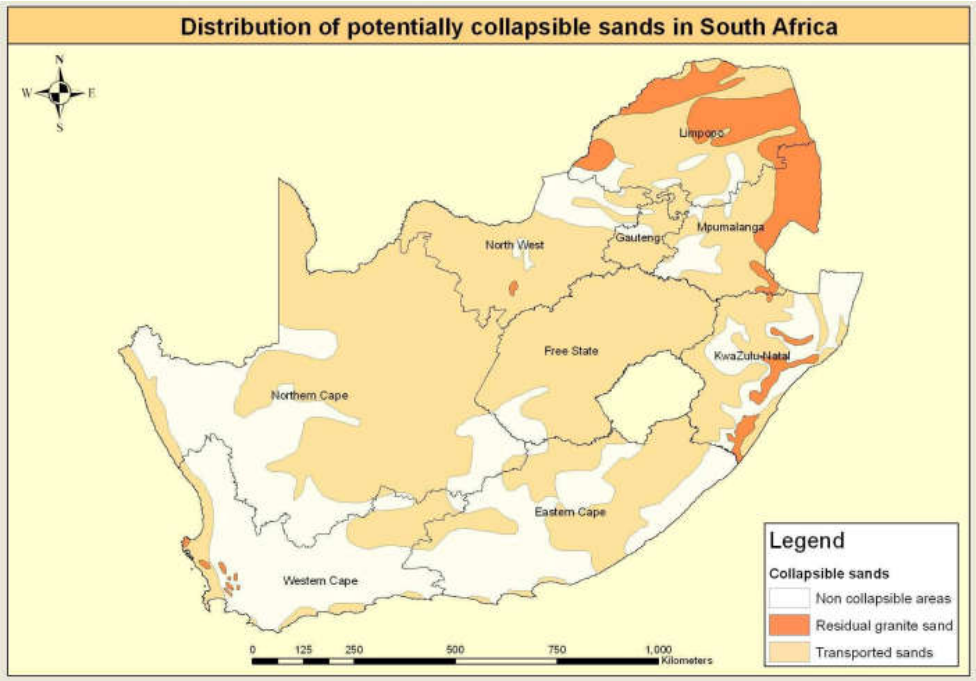

Figure 2-1: Regional distribution map of potentially collapsing sand in South Africa (Diop, et al, 2011)

2.3.2 Shallow dolomitic bedrock

Dolomite is a single mineral consisting of calcium and magnesium carbonate. It is commonly found in Gauteng Province, some parts of the North West Province and the gold-mining regions in the West Rand. Dolomites are problematic because when rain water takes up carbon dioxide from the atmosphere or soil, it will then form a weak carbonic acid. This weak acidic water infiltrates fissures in the dolomite, leaching

carbonate minerals and generating larger and larger pathways through the rock. As the carbonates are removed by the groundwater, large sinkholes can develop. In South Africa, at certain locations where underlining dolomite rocks are located, it is possible for the soil to suddenly collapse. This may lead to injuries or structural damage to buildings due to sinkholes developing (Oosthuizen and Richardson, 2011).

2.3.3 Dispersive clays

Dispersive clays can, according to Diop (2011), occur in any soils with a high percentage of exchangeable sodium cations. They generally exhibit a pale colour in the field. Dispersive soils are mostly restricted to arid and semi-arid climates, but erosion problems associated with the presence of dispersive soils have been found in areas with humid climates in recent years Diop (2011). Dispersive clays mostly result from argillaceous sedimentary rocks of Karoo Supergroup, Cape Supergroup, Uitenhage group and residual soils of all granites. It is typical of these soils to occur in areas of water scarcity.

Dispersive clays can develop under the following circumstances:

I. In low-lying areas where the rainfall is such that seepage water has a high SAR (Sodium absorption ratio) value. Soils which developed from granite are particularly prone to the development of high Exchangeable Sodium Percentage (ESP) values in low-lying areas.
II. In locations where the original sediments contained large quantities of illite-smectitic clays (such as montmorillonite) with high ESP values. This is predominantly the situation with the mudstone and siltstone of the Beaufort Group.
III. In the arid areas where the development of dispersive soil is commonly inhibited by the presence of free salts despite high SAR values. Highly dispersive soil can develop if the free salts with high SAR values are leached out.

2.3.4 Soft clays

Soft clays have low shear strength and high compressibility. These types of clays are typically related to settlement problems. Soft clays commonly have undrained shear strengths of less than 40 kPa (Diop, 2011). They also are susceptible to a very high magnitude of settlement due to consolidation when loaded. The consolidation may require decades to arrest completely. Generally, soft clays have high moisture contents which will be close to the saturation point. Common problems associated with soft clays are: they lead to collapsing, slope instability and failure of underlying road embankments. In South Africa, it is generally to the eastern and southern coastal areas of the country. They usually occur in the locations of existing or old river channels, but could also occur in poorly drained areas. Soft clays occur primarily as transported soils and are mostly found in a number of areas along the coasts including Durban, Richards Bay, Knysna and Langebaan (Diop, 2011).

2.3.5 Heaving or expansive clays

The term "clay" is applied both to materials having a particle size of less than 2 microns and to the family of minerals (i.e. phyllosilcates) that have similar chemical compositions and common crystal structural characteristics (Velde, 1995). The most common clays consist of kaolinite, montmorillonite-smectite, illite, chlorite or a combination of these minerals. When clay minerals are present in the soil, their influence on behaviour is disproportionately large. One of the main reasons for this is that all clay minerals have a great attraction to water. Some swell easily when wet and shrink when dry (Salgado, 2008). The process of swelling of some types of clays when they adsorb water is reversible. Hydration and dehydration can vary the thickness of a single clay particle by almost 100% (Velde, 1995).Moisture variation also causes changes in the matrix suction stress state variable (Nelson and Miller, 1992). Expansive soils are normally found in an unsaturated condition. Clay soil’s suction varies from zero kPa when it is wet (in a saturated condition) to 10,000kPa when it is dry. (Vanapalli and Fredlund, 2000). The volume change behaviour, and the flow and shear strength behaviour of expansive soils, are greatly affected over the entire suction range.

Expansive clay are widely distributed throughout South Africa. It's distribution mainly is dictated by geology, soil type and by local climatic conditions. These expansive soils are considered to be problematic to geotechnical engineers designing foundations. Expansive soils, particularly pose a significant hazard to foundations for light structured buildings (Rogers, Olshansky & Rogers, 1985). On wetting expansive clays soils get wet the clay minerals absorb water molecules and expand. During dry periods they shrink, and therefore leave large air voids or cracks in the soil. Variations in the moisture content of expansive soils will result in volumetric change occurring in the soil structure. The continuous change in moisture content is problematic for structures' foundations and especially lightly loaded structures since it gives rise to volumetric changes underneath in the soil. This results in stresses in the foundation and super-structure resulting in strain and cracking. Generally crack repairs are unsuccessful due to the repetitive nature of the stress variations. The main problem of expansive clays rests in the fact that the magnitude of the soil movement is often not predictable. Structural damage can, in fact, occur when as little as 2% to 3% of soil volume expansion and contraction is experienced (Diop et al, 2011).

Clay minerals are complex aluminium silicates which are usually less than 2 microns in size and are composed of two basic units: Silica tetrahedron and aluminium octahedron (Das, 2008). Clays form part of minerals which are called silicates. The silicon tetrahedrons link together with each another to form thin tetrahedral sheets. The aluminium octahedrons also link together to form octahedral sheets. The actual clay crystals are compounds of aluminium and silicon sheets which are held together by intra-molecular forces as seen in figure 2-2 (Mitchell 1993).

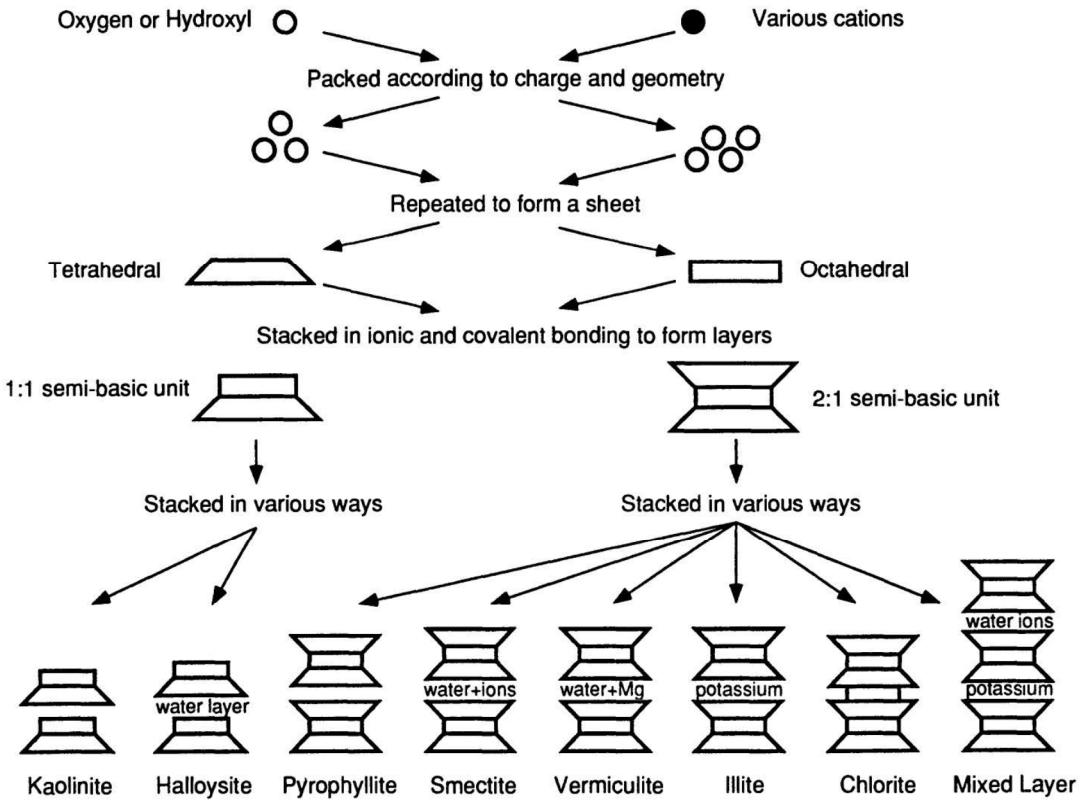

Figure 2-2: Schematic diagram of Swelling clay and Non-swelling clay

Highly expansive clay minerals named Smectites consist of of one octahedral sheet between two tetrahedral sheets to produce the mineral structure (Figure 2-2). Since the charge distribution within each structure is nearly neutral, in clay crystals will attract and hold onto cations surrounded by water molecules in between their crystalline sheets. The electrical structure of water molecules allow them to interact with other charged particles to form stable hydrated cations structures. The process where water molecules will become attached to the microscopic clay crystals is commonly called adsorption. Clay configuration and electrical charge in the thin sheets have an electro-chemical attraction for water molecules. Montmorillonite is the most notorious and active of the Smectites. Montmorillonitecan absorb large quantities of water molecules among its crystalline sheets and has a large shrink and swell potential (Das, 2008). The swelling of clays such as montmorillonite causes the bulk volume of the soil to increase (or swell) and in many cases also cause a decrease in the capacity or strength of the soil. In dry periods, when the moisture in the clay soil is removed by evaporation, the water molecules among the clay sheets are released. This will cause the volume of the clay soil to decrease. As the moisture is being removed the shrinking

clay soil can develop voids or cracks These shrinkage cracks can be seen on the surface of clay soils and thus give a sign of expansive clay soils.

According to the NHBRC (National Home Builders registration Council of South Africa) as indicated in figure 2-3 expansive soils are widely distributed across South Africa and occur in most parts of the country with the exception of the Little Karoo, the extreme Northern Cape, the northern portion of the Limpopo Province and the extreme eastern regions of the Mpumalanga Province. The areas most affected by expansive soils include the Free State gold fields, the North West Province and the Pretoria Witwatersrand Vereeniging complex, which are some of the most densely populated areas in South Africa (NHBRC, 1999).

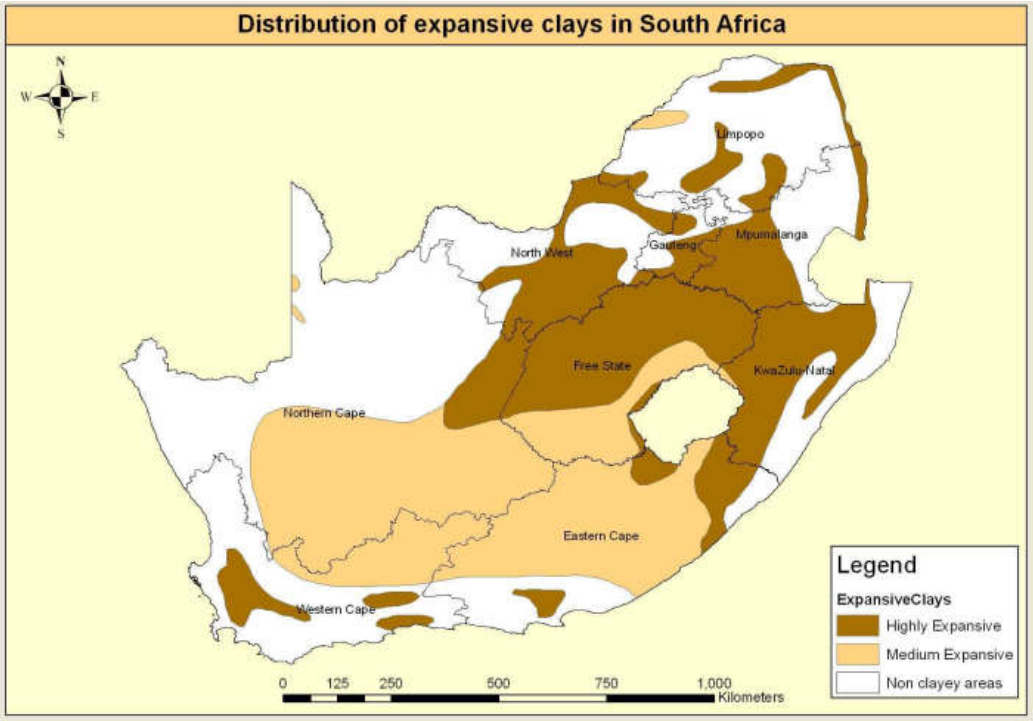

Figure 2-3: Regional distribution map of swell clay occurrence in South Africa (Diop, 2011).

2.4 Shallow foundations

Foundation engineering has been practiced as an art in absence of soil science since ancient times up until the early 1920's when it had achieved a considerable amount of

academic attraction. A foundation is the part of a structure which transmits loads directly to the underlying soil. This process is known as soil–structure interaction (Whitlow, 1995). To perform in an acceptable way, the foundation must be designed to meet two principal performance requirements which are known as (1) ultimate limit state and (2) service limit state. These are specified in such a way that the foundation's capacity or resistance is sufficient to support the loads applied to the foundation and to avoid excessive deformation under these applied loads which might damage the supported structure (ultimate limit state) or lead to a loss of function (service limit state) (Knapnet *et al.,* 2012).

When it is found that a soil layer near the surface is capable of adequately supporting the structural loads it is advised to use either pad, strip footings or raft foundations. These types of foundations are generally referred to as shallow foundations. Pad or strip footings are relatively small slabs of concrete reinforced with steel giving independent support to part of the structure. The resistance of these shallow foundation types is quantified by its bearing resistance or bearing capacity (Knapnet, *et al*., 2012). Pad and strip footings, however, are not recommended or advised for expansive heaving clays which can be found in the Free State.

A raft foundation (also commonly called a mat foundation) is a combined footing that covers the entire area beneath a structure and supports the entire structures. A raft foundation normally rests directly on the soil and raft foundation is generally suggested the following situations (Gupta, 1997):

I. When structural loads are so heavy or acceptable pressures on the soil so small that a individual footing would cover more than the structure's floor area.
II. When soil behaviour is unpredictable and it is difficult to define and assess the extent of settlement or movement.
III. If structures and equipment to be supported are very sensitive to movement such as settlement or heave.
IV. Where structures naturally lend themselves to the use of raft foundation such as silos and water towers.

V. Compensated foundation cases wherein soil has a very poor bearing capacity and the weight of the super-structures is supposed to be balanced by the weight of the soil removed.

VI. Buildings where basements are to be provided or pits located below ground water table.

VII. Buildings where individual foundation will be subjected to large bending moments which may result in differential rotation and differential movements causing distress in the building.

The construction of raft foundations for Government Subsidy housing has become common in areas affected by expansive soils as is the case in much of the Free State and Northern Cape (Bester *et al.*, 2016). As discussed in points III & VII the objective of a typical raft foundations is to limit the differential movements of the underlying soils to a level which can be tolerated by the superstructure (Day 1991).It is therefore recommended by the NHBRC that the following guidelines be followed (NHBRC, 1999) - If the estimated total heave to be expected is 15mm or greater, then the foundation should be recommended to be a stiffened or cellular raft foundation.

2.5 Design of Raft foundations

2.5.1 Raft design Peck, Hanson and Thornburn

A raft foundation is typically designed as a continuous slab with continuous beams supported on soil or, in some cases, bedding material. The soil pressure acting against the slab is usually assumed to be uniformly distributed. This pressure acting on the raft foundation is equal to the total of all loads multiplied by load factors and divided by the area of the raft foundation (Gupta, 1997). The moment and shear in the raft foundation is determined by the use of appropriate coefficients listed in the specifications for the design of flat slab floors. This method by Peck, Hanson and Thornburn has been widely used often with success, but it has also led to structural failure not only of the slab but also of the super structure (Gupta, 1997).

According to Peck *et al*. (1954) raft foundations are designed as if they rests on a bed of elastic springs of equal stiffness. The contact pressure underneath the small areas

which are close and equal are then proportional to the deflection of the spring in that area. The constant of proportionality is called the modulus of sub-grade reaction. Although the theory has been well developed, in the case of real soils, it is not constant and depends not only on the stress deformation characteristics of the soil but also in a complex manner on the shape and size of the loaded area and the magnitude and position of nearby loaded areas. Evaluation of modulus of sub-grade reaction for design is difficult on active soils (Lytton, 1972).

2.5.2 Lytton raft design

Lytton's raft design methodology involves many simplified assumptions and has its drawbacks, it is a method well suited to routine design (Day, 1991). This method involves the dividing non-rectangular raft foundations into a series of overlapping rectangles and analysing each of these rectangle blocks separately. The important input parameters are: the differential heave (Ym) below the building; depth to the bottom of the expansive layers (z); allowable deformation (δ/l) of the supported structure; and the modulus of the subgrade reaction (k) (Lytton 1972). With this procedure the modulus of subgrade is calculated as a suppression of heave. It is also generally accepted with the method that the heave which will occur will be a centrally located dome on the middle of the structure where moisture concentration will take place.

The determination of mound exponent "m" is usually an empirical estimate linked to field observations. Lytton (1972) assessed a number of field studies and he found a rough approximation to mound exponent value. (Lytton, 1972) suggested that the mound exponent (m) is: $m = L/Z$. Where L is the length of the shortest side of the foundation and Z is the depth of the active clay layer.

2.5.3 Lytton and Woodburn

Lytton and Woodburn (1973) stated that the design of stiffened raft foundations on expansive clays is primarily affected by the variation of the soil moisture content supporting the raft foundation underneath. They established that the predicted soil

movement in laboratory tests for expansive soils match the observed field soil water content movement. Their methodology is built on the fact that soil to raft foundation contact is not uniform due to soil moisture variations. The raft foundation interacts with the soil surface within the contact areas. This results in pressing down the high spots and bridging the low spots underneath. This soil-structure interface can be expressed as a partial differential equation for the deflections of an isotropic plate resting on a coupled spring mound (Lytton & Woodburn, 1973).

2.5.4 Swinburne method

The Swinburne method was suggested by Fraser and Wardle (1975). This was largely to improve the interaction models of the soil to the raft foundation which have been suggested by Lytton. This was also an attempt to find an economical design methodology for housing raft foundations on active soils. The researchers conducted their studies on the performance of several housing raft foundations which were built on different types of expansive soils in Australia. The raft foundations were monitored for their movement over time in order to measure the actual field mound which will develop. The researchers modelled the raft foundations and its stiffening beams using the finite element method as a plate with beams resting on semi-infinite elastic soil layers. The two main parameters determined by the researchers were:

I. Maximum differential heave (Ym) and;
II. The edge moisture variation distance (e).

2.5.5 Pidgeon

Pidgeon observed that design methods for raft foundation for houses on heaving clays had drawbacks. Raft designs relied on the foundations to be constructed on an already formed mound or dome and required an estimation of the initial mound shape (Pidgeon, 1980). Pidgeon assumed that the raft foundation is cast initially on a flat levelled ground surface. When the raft foundation is built, instant undrained surface settlement will occur followed by changes in stresses, strain and suctions throughout the soil layers. Considering these limitations Pidgeon developed a rational design

procedure which depends on a detailed laboratory and field data to identify the original soil state and changes in boundary conditions.

To analyse the soil underneath the stiffened raft foundation Pidgeon split the foundation soil into a series of vertical soil columns. The number of soil columns should be adequate to offer suitable accuracy. Each soil column consists of several layers with different moisture contents. The heave of each column is then calculated. An iterative process was required to reach agreement between the deflected slab shape and the soil contact pressure. Pidgeon (1987) recommended that the worst conditions should be considered for the design of raft foundations. This will be when the soil under the centre of the raft approached the maximum moisture content or swell conditions (Pidgeon, 1987).

Pidgeon proposed the following figure 2-4 a-d for representing the initial condition, edge heave and moisture content migration. This also illustrates the possible transitional phase and finally centre doming as shown in figure 2-4 a-d.

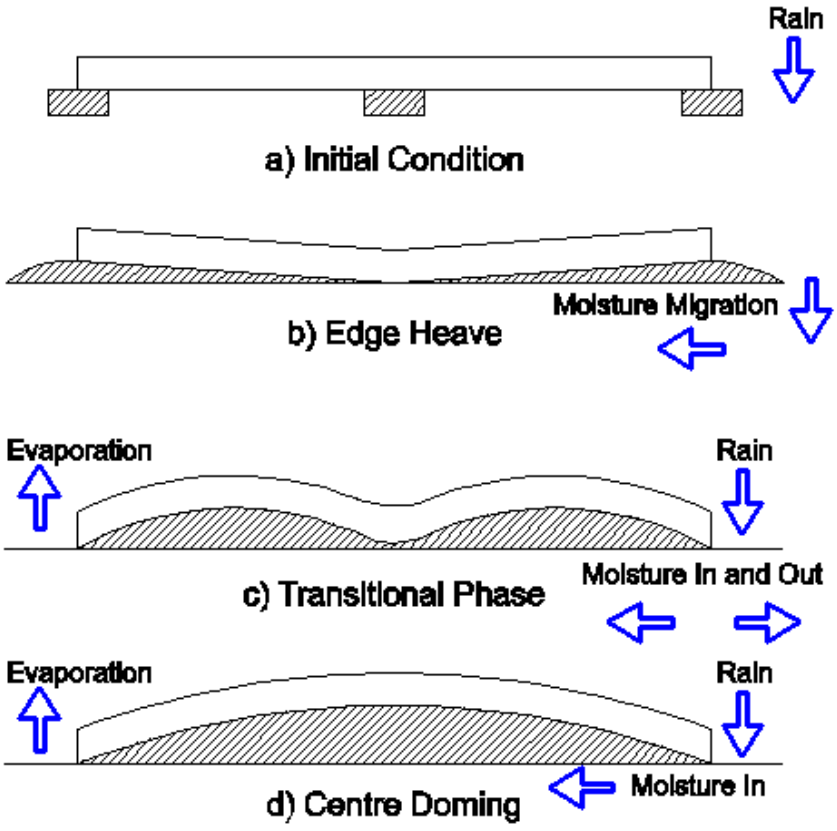

Figure 2-4: Centre doming under an impermeable cover (Pidgeon, 1987)

2.5.6 Post-tensioning institute design of slabs-on-ground

Post Tensioning Institute method (PTI) is first developed from the program SLAB2 which was developed by Huang (1974) and then later improved on by Wray (1978). PTI design method is one of the several design approaches for the slab on ground or raft foundations used in USA in Texas.

The main objective of the PTI design method is to arrive at an adequate and simple design method. This was hoped to improve the rationality of the previous design methods used. This method is developed to provide sufficient, rigid and stiffened foundations that are reinforced by either conventional steel bars or post-tensioned cables, which is mostly preferred by the PTI method. These rigid foundations are designed in such a way that they will move as a single unit in the event of differential soil movement.

2.5.7 Expansive soil test site near Newcastle in Australia

Researchers conducted a field study of surface movements on a flexible cover in Maryland, Australia near Newcastle. This study was conducted to investigate the long term expansive soil behaviour underneath a flexible impervious cover and a stiffened raft slab. The site was established in 1993 and was monitored for a period of seven years.

The physical processes that drive reactive soil behaviour were investigated to develop more reliable models of expansive soil behaviour. The site was instrumented to allow measurements of soil water content, moisture suction and the ground water movements underneath a simulated lightly loaded building foundation. The effects of trees on soil water content changes and ground movement were also taken into account. (Fityus *et al*., 2004). The outcome of the study highlighted aspects of foundation behaviour that is important in expansive soil foundation practice. However, the great disadvantage of this study was the fact that they used two ground covers to simulate moisture boundary conditions due to the presence of typical structures. This

does not model reality since moisture movement is dependent on temperature conditions.

2.6 Factors affecting water changes underneath foundations

There are several reasons why water content changes can occur underneath a foundation.The first reason is environmental factors such as wet and dry conditions and temperatures. Swelling clay expands or contracts in response to changes in the moisture content. The evaporation of moisture from within the clay soil due to hot weather or drought will cause a decrease in the moisture content. In wet seasons the influx of water due to high rainfalls combined with inadequate drainage around the house will contributed to much higher moisture content in the clay soil (Chester & Duncan, 1992).

The second reason is on-site construction and landscaping as this plays a major role in moisture content changes. An example is the excavation during the construction process of foundations. Large areas of underground soil get exposed, which leads to the loss of moisture content due to evaporation, especially in hot summer days. Another consequence of construction is the removal of plants and trees which can result in a major change of moisture content in the soil over time (Chester et al, 1992). Another reason why changes in moisture content can occur is unforeseen circumstances such as leaking pipes underneath a building. This can result in an increase in moisture content in the surrounding area (Chester et al, 1992).

Water content change is the main reason for expansive soil problems. If problem soil underneath a foundation swells or shrinks it’s likely to cause problems. When a foundation heaves or settles, differential movement causes cracks and other damage to the structure. Most differential movement is caused by differences in soil moisture. After construction, soil underneath the foundation becomes wetter or drier than the rest of the soil. Soil at the foundation edges regains moisture first because it is directly exposed to rain water. Soil at the slab edges swells and causes the edges to curl up. This is what is known as edge heave of the structure and usually occurs soon after construction (Department of the Army USA, 1983).

Water does not move rapidly through dense expansive clay soils so the return to normal moisture content is slower beneath the foundation slab centre. The clay soil retains the water longer underneath the slab and can thus create higher moisture content in the middle of the structure. This can create centre doming and causes the middle of the slab to move upwards (Department of the Army USA, 1983).

2.7 Movement of water in saturated and unsaturated soils

2.7.1 Saturated soils

All soils have voids which are connected and forms continuous pathways for water movement. One of the main problems encountered in foundation engineering is the prediction of water flow in soils due to hydrostatic pressures. In soil mechanics, engineers are often concerned with the flow of water through soil. This information is used to determine seepage loss of water from dams or to determine the required pumping rate to keep construction locations dry such as ground pits, trenches and dewatering schemes. It is also used in the design of tailing dams and the determination of groundwater pollution under tailing dams. This resistance to the flow of water through soil affects the seepage. This resistance is quantified as hydraulic conductivity (k) or coefficient of permeability (Withlow, 1995).

2.7.2 Unsaturated soils (expansive soils)

The construction of sites in arid climates commonly results in the increase in water content underneath the soil profile due to two factors. The first is irrigation at the surface that introduces water into the soil. The second is the building of waterproof surfaces such as foundations and roadways which stop the evaporation of water. Factors which can lead to extra sources of water underneath structures include broken pipes, leaky sewers, etc. The soil may become saturated or remain unsaturated during the wetting process, depending on the rate of infiltration, site conditions, and soil properties (Nelson, Chao, Overton, & Nelson, 2015).

When water migrates into the soil it may become fully wetted. Fully wetted refers to the degree of saturation of soil which is required to cause the soil to expand. With expansive soil, where it has a low hydraulic conductivity and high soil suction, the degree of saturation of the soil will increase to higher than 90%. For non-expansive soils with higher values of hydraulic conductivity the degree of saturation will be much less (Nelson et al, 2015). Figure 2-5 shows a wetting profile moving downward with time due to infiltration. The analysis is complicated because across the wetting front the water content and the soil suction is varying. The wetting front changes over distance from higher water content to that of the soil below. There is no distinct point that expresses the actual depth of wetting. In clays soils with low permeability the changeover zone may extend over a much greater distance compared to sandy soils with high permeability.

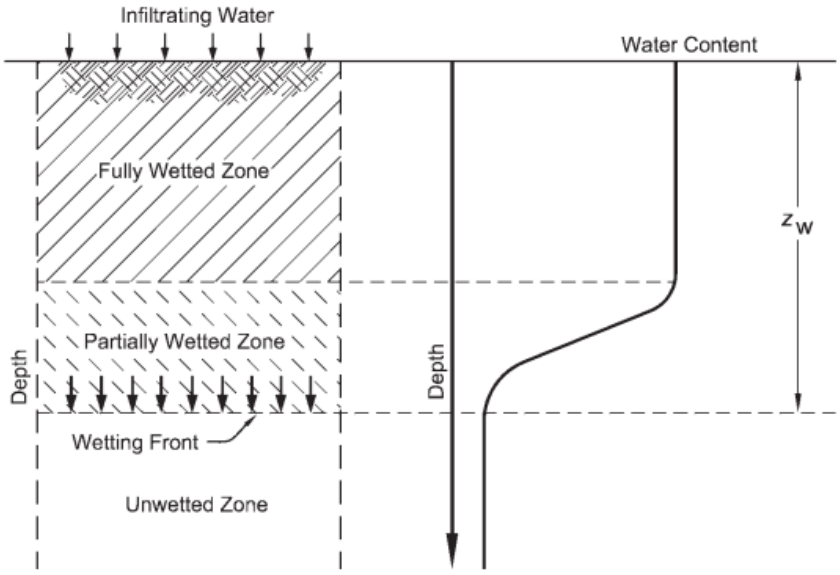

Figure 2-5: Progression of wetting in unsaturated soil where the depth of wetting is shown as the depth to the bottom of the transition zone (Nelson el, 2015).

2.7.3 Active zone

Problems associated with expansive soils arise mostly with an increase of water content in the upper layers of the soil. The moisture content in these upper layers of soil are affected by climatic environmental factors. This area is termed the active zone

(Nelson, 1992). Figure 2-6 shows a diagram of the active zone. The depth of the active zone can differ with time and the concept mainly applies only if external influences such as surface drainage, or irrigation are not present.

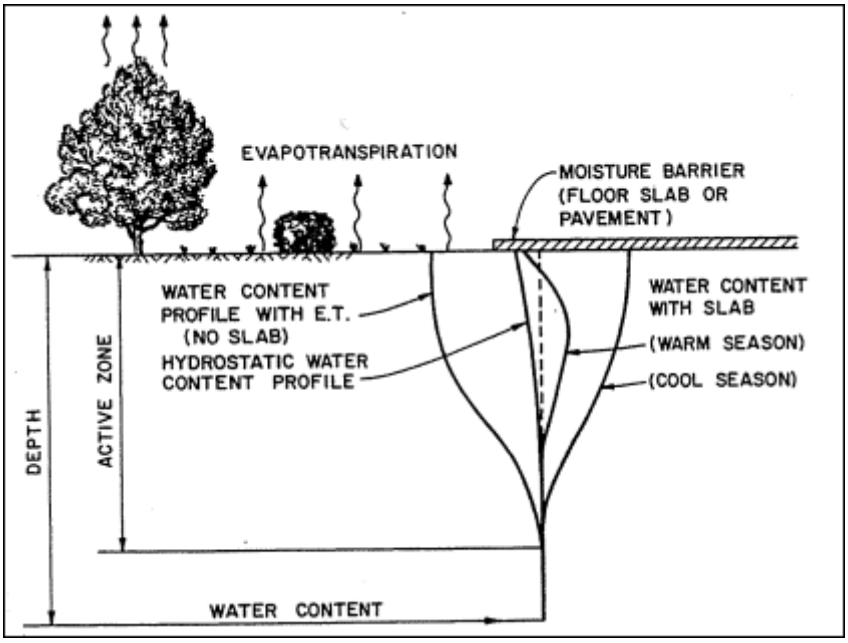

Figure 2-6: Water content profiles in the active zone (Nelson, 1992)

2.8 Soil suction

If one were able to attach a stress gauge onto one end of a horizontal water column and soil onto the other end, the soil suction would be the tensile stress that is measured in the water. Soil suction is defined as the potential energy of water in soil relative to some reference state (Nelson et al, 2015).

Total suction is the sum of the matric suction and the osmotic suction of a soil. Matric and osmotic suction will vary with the water content of soils.

Matric suction comes from the pore size distribution, texture, and surface adsorptive forces of the soil. Matric suction is the force which soil applies on adjacent soil particles to equalise the moisture content. The matric suction represents the value of the tension in the water and represents a physical process. It can be expressed as the height to which water can be sucked up into an unsaturated soil. This process is

commonly referred to as capillary rise. This is normally established by allowing water to rise in a capillary tube of initially dry soil (Nelson et al, 2015). A diagram showing the relationship between soil water and matric suction at three different stages of water content is shown in Figure 2-7.

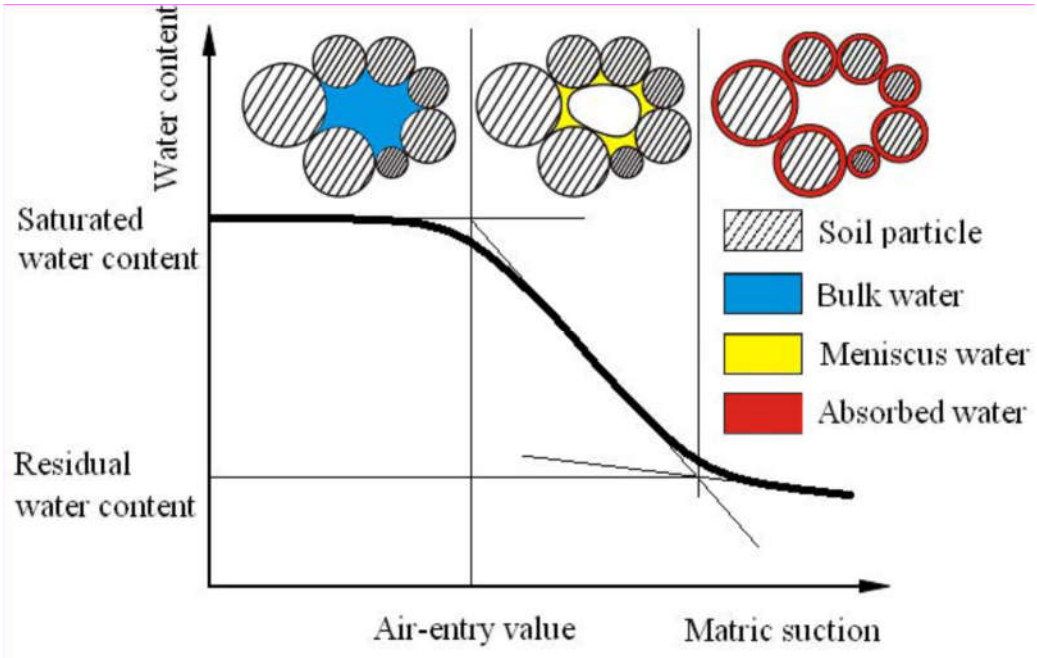

Figure 2- 7: Soil water and matric suction at three different stages of water content

Osmotic suction is caused by the difference in salt concentration in positions in the soil water. The way in which the osmotic suction works in soil is illustrated below in Figure 2-7 two ideal clay particles are placed close to each other. The electrical charges on the clay particles hold salt cations in the clay micelle. The concentration of salt in the water in the space around particles is higher than that outside of the micelle. The electrical field around the clay particle can be thought of as creating a “pseudo-semipermeable” membrane, as shown below. The fairly high concentration of salt between the particles causes pressure to be exerted on the water molecules. This pressure is the osmotic suction of the soil (Nelson et al, 2015).

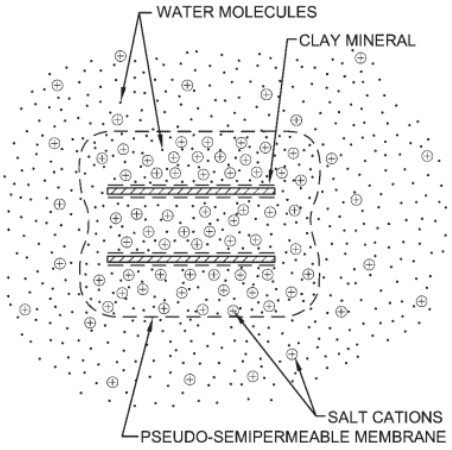

Figure 2-8: Pseudo-semipermeable membrane effect causing osmotic suction in clay (Nelson et al, 2015)

Frequently used methods for measuring soil suction are: Tensiometer methods, axis translation techniques, filter papers, thermal conductivity sensors, electrical resistance sensors, the pore fluid extraction techniques, and psychrometers (Fredlund, 2002).

2.9 Soil Sampling and testing

2.9.1 Guidelines for soil and rock logging in South Africa, 2nd impression 2002 by editors ABA Brink and RMH Bruin

A soil profile is a record of the vertical succession of the different layers of soil as they occur at any particular location on site. Each soil layer should be described in terms of its moisture condition, colour, consistency, structure, soil texture and origin. The inspection of a soil profile should be done before the soil has dried to any extent. All inspections done in trial holes should be done in accordance with the 1991 Code of Practice for Safety (Brink and Bruin, 2002).

The recommended procedure for the field observations of the moisture condition, colour, consistency, structure, soil texture and origin of each layer are as follows as recommended by Brink *et al*. (2002):

I. The description used for moisture condition of the soil should be described as a precursor to assess the consistency which is largely dependent on the moisture content at the time of inspection. This is documented as one of the following: dry, slightly moist, moist, very moist, wet.

II. Soil colours descriptions should simply be limited to two, for example: reddish-brown or green-blue. Secondary colour patterns are described according to their size limits.

III. Consistency is the hardness or stiffness of the soil. This is an observation based on the effort required to dig into the soil. The assessment of consistency is a rough measure of its shear strength of soil.

IV. The soil structure indicates the presence of discontinuities in the soil and its nature. Non-cohesive soils have a granular structure while cohesive soils have several types of structural characteristics such as "slickensided", shattered, etc.

V. Soil texture is described on a base of its grain sizes. Most soils are a mixture of one or more textures. Such examples are silty clay which is a clay with some silt or sandy clay is a clay with some sand in it.

VI. The origin of soils is an attempt to determine the origin or source of each layer in the soil profile. The origin of soils can be described either as transported or residual soils. Local knowledge of the geology and references of geological maps is essential and will be a useful tool to determine the origin of soils.

2.9.1 Laboratory testing methods

I. Grain size analysis:

This is performed by mechanical sieving to determine the percentages of soil fractions passing a set of standard sieve sizes to a minimum opening of 0,075mm. A hydrometer analysis which is used to determine the particle size distribution to 0,002mm. The classification of soil types according to particle size is shown below in Table 2-1. The clay content is defined as the percentage of material smaller than 0,002mm (TMH1, 1986).

Boulders	Cobbles	Gravel			Sand			Silt			Clay
		Coarse	Medium	Fine	Coarse	Medium	Fine	Coarse	Medium	Fine	
200	60	20	6	2	0.6	0.2	0.06	0.02	0.006	0.002	
PARTICLE SIZE (mm)											

Table 2- 1: Soil particle sizes

II. Atterberg Limits:

The fraction passing the 0,425mm sieve size is used to determine the Atterberg limits which are: the liquid limit (LL) and plastic limit (PL), followed by computing the determine the plasticity index (PI) and determination of the shrinkage limit (SL) as specified in the (TMH1, 1986). They are defined as follows:

I. The liquid limit of a soil as defined in this method is determined by using the device specified to plot a curve of the number of taps necessary to obtain a specific consistency of the soil fines against the moisture contents (TMH1, 1986).

II. The plastic limit of a soil as defined by measuring the lowest moisture content at which the soil can be rolled into threads 3 mm in diameter without the threads crumbling (TMH1, 1986).

III. The determination of the linear shrinkage of soils is the linear shrinkage of soil when it is dried from a moisture content equivalent to the liquid limit to the oven-dry state (TMH1, 1986).

2.10 Semi-empirical measurements for heave

Numerous methods exist to determine or predict the expected heave of clayey soils in South Africa. The choice of which methodology to used depends on the design engineer or laboratory. The engineer or technician should be familiar with the limitations of the method(s) he or she decides to use. It is good practice to determine the expected heave by using more than one method.

2.10.1 Van der Merwe's method (1964)

This method is the most commonly used method in South Africa to predict expected heave. This method is based on the results obtained from indicator tests. The method was originally developed for clays soils on the Highveld (Van der Merwe 1964). Required inputs are:

I. The Plasticity Index (PI)
II. The percentage material passing the 0,425 mm sieve
III. The clay content.

On the Van der Merwe's swell prediction chart Figure 2-10 the PI of the whole sample is plotted against the clay content to determine the heave potential of the clay. This heave potential can be either low, medium, high or very highly expansive. The in situ moisture content should also be considered, because the heave potential of the soil is the potential total heave for a moisture change from a dry to a saturated condition.

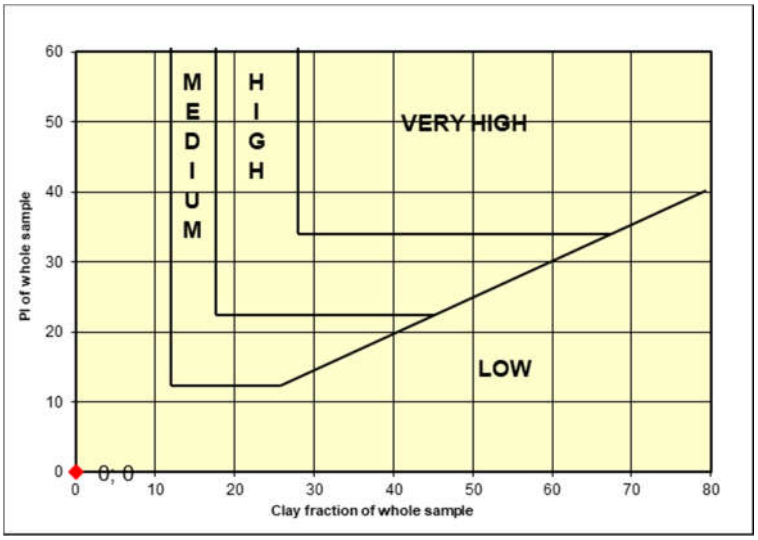

Figure 2- 9: Van der Merwe's chart for heave prediction (Van der Merwe 1964)

2.10.2 Savage method (2007)

This heave prediction method is based on a study of different clays that showed a ratio between the Liquid limit and Plastic limit to identify the different types of clay present in a soil. The plasticity ratio (R) is related exponentially to Skempton's activity index.

The Savage method, using the van der Merwe's zones of swell potential, is mathematically calculated or read from a chart giving the swell potential of a soil from the value of R and material passing the 0.425mm sieve. The use of the R value (LL/PL) for a soil and the PI gross will allow assessment of active soils quickly by using the chart below in Figure 2-10 (Savage, 2007). Savage has established a mathematical derivation of lines representing swell potential by a factor K, certain values of which define the swell zones approximating those of van der Merwe (1964)

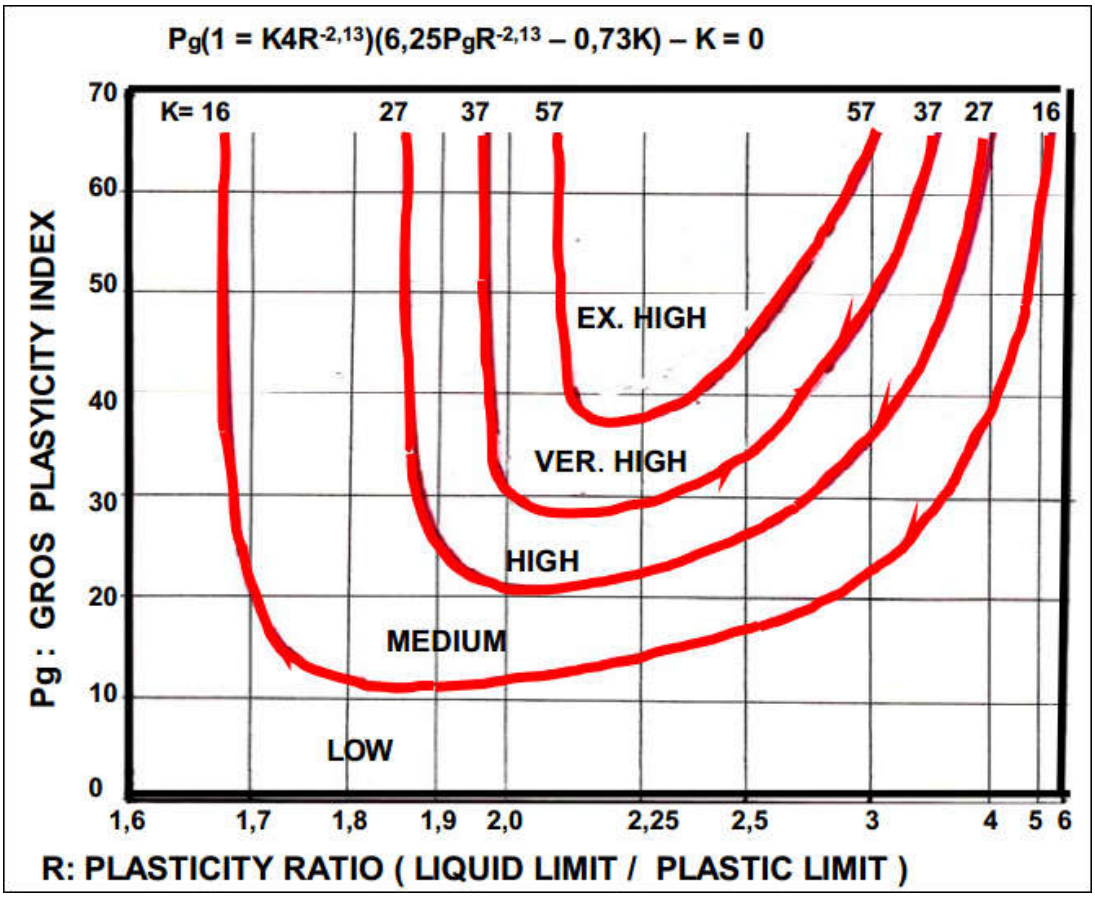

Figure 2-10: Swelling potential of soil by use of the Atterberg Limits of Plasticity Index and Plasticity Ratio (Savange, 2007)

2.11 Field moisture measurement methods

Measuring moisture content by moisture probes is a common procedure in agricultural work and soil science. There are a great number of commercial products available, however, for this study CLSM probes were selected. Users are suggested to first have

the basic understanding of the uses, advantages and limitations before they can effectively use the probes.

The CLSM probes can measure moisture content and temperature at different depths in a soil profile. These readings can be taken hourly, but the operator has the option to customize reading intervals. If the intervals were left to the default setting the probe can store readings for approximately 5 months. The measurements of soil water evaporation with CLSM probes and neutron water meters (NWM) were compared by Zerizghy, van Rensburg & Anderson, 2013. It was found that the measurements of the CLSM probes and NWM closely agreed with the gravimetric soil water content. The researchers established through the results that CLSM probes provided more accurate measurements than the NWM. The researchers did note that proper installation is vital to insure full contact with the soil.

2.12 Sun path

During daytime the sun follows a spherical arc which is symmetrical along the vertical plane. The sun rises in the south-east and sets south-west, and is at its highest at solar noon. Declination will vary according to the cycles of the seasons as seen in Figure 2-11 (CSIR, 2004). When radiation from the sun strikes, for example, a building surface at a normal angle less energy is reflected and more is absorbed so the energy density per unit area is higher than at a slanting angle. The magnitude of solar radiation striking a surface can be calculated based on the cosine of the angle of incidence of the radiation and a line normal to the plane of the object. The orientation of a building has a direct influence on the availability and magnitude of solar radiation reaching the structure and the surrounding soils (CSIR, 2004).

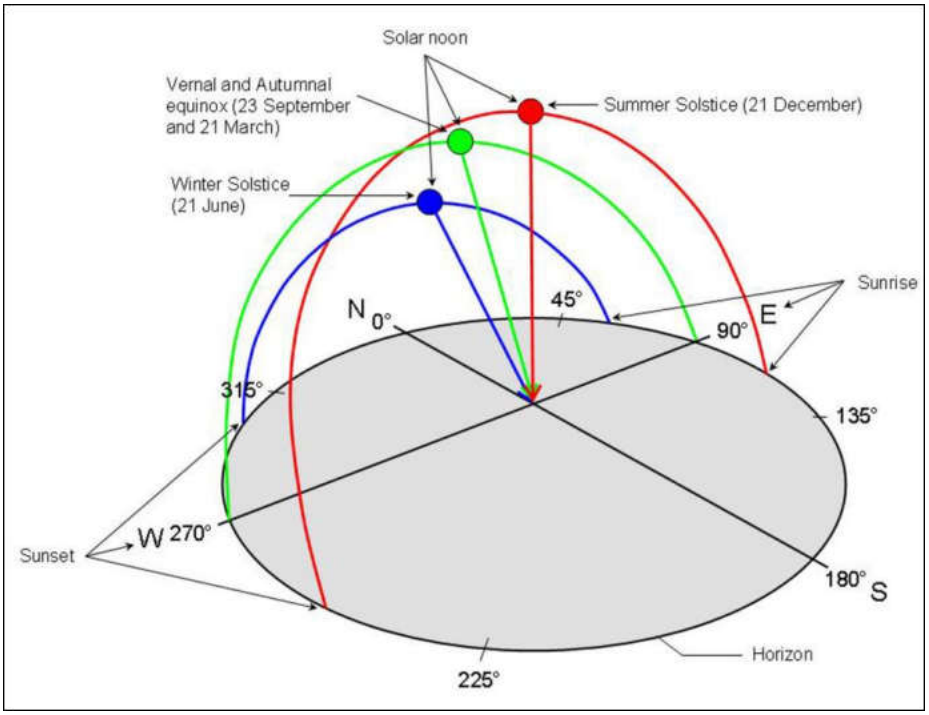

Figure 2-11: Sun's apparent path in the sky during different seasons (CSIR. 2004)

2.13 Data analytics method

Contouring is a technique to accurately describe the terrain or areas of a map by means of shading, colour contorting, hachure and layer tinting in the best way that fits the data. There are a great number of commercial interpolation software packages, however, for this study 3D Field was selected. 3D Field has multiple interpolation methods that can be used. Users are suggested to first have the basic understanding of every interpolation method before they can successfully select the best one. The interpolation methods are.

2.13.1. Interpolation

I. The inverse distance method is a weighted average interpolator. This method uses data that is weighted during interpolation where influence of one point relative to another declines with distance from the grid node. Usually the inverse distance behaves as a precise interpolator.

II. The Kriging Method is a geostatistical gridding method. This method produces visually attractive maps from irregularly spaced data. Kriging attempts to

express trends suggested in the data. For example high points might be connected along a ridge rather than isolated contours.

III. The minimum curvature method is widely used in the earth sciences. The interpolated surface generated by this method is a linearly elastic line passing through each of the data values with a minimum bending. Minimum curvature generates the smoothest possible surface while attempting to honour the data as closly as possible. This however is not an exact interpolator.

IV. The natural neighbour method is taking into consideration a set of Thiessen polygons (the dual of a Delaunay triangulation). If a new point is added to the data the polygons will be modified and some of the polygons would shrink in size although none would increase in size. This method algorithm uses a weighted average of the neighbouring point, however this method does not extrapolate contours beyond the convex hull of the data points.

V. Triangulation creates triangles by drawing lines between data points. The original points are connected in such a way that no triangle edges are intersected by other triangles. The result is triangular faces over a grid. This method is an exact interpolator. Triangulation works best when the data is evenly spread over the grid area.

VI. Radial Basis Functions (RBF) is a varied group of data interpolation methods. These methods are exact interpolators an exact interpolator and it attempts to honour the data. Smoothing factors are introduced to attempt producing a smoother surface. The functions outline the optimal set of weights to apply to your data when interpolating.

2.14 Summary

The literature reviewed above forms the basis for this investigation on moisture movement underneath a light weight house built a raft foundation on active clays. Research has shown the use of ground covers to simulate moisture boundary conditions due to the presence of typical structures. This does not model reality since moisture movement is also dependent on temperature conditions. Furthermore, external factors such as the orientation of the building can also play a role in the moisture underneath a structure, which was not taken into consideration. Moisture

movements in active clay soils is a complex problem, especially with respect to foundation design assumptions. It was concluded that assessment of factors not normally taken into account was needed to gain a better understanding further research is needed to understand the problems associated with construction on active clay soils and practical solutions which are needed.

CHAPTER 3: PROFILE OF STUDY AREA AND METHODS

3.1 Introduction

An investigation was undertaken to determine a suitable area with history of problematic soils and where the Government has constructed multiple subsidized houses. In this chapter an attempt is made, firstly, to examine and understand the numerous influences of the soil conditions in Botshabelo, Section K that affect Government subsidized housing. Secondly, to discuss the instrumentation and data analysis that took place which provided the primary data used in this study.

3.2 Government subsidy house selection for case study

The study location was selected to be in Botshabelo due to the fact this area is known to have very problematic soil conditions for light structures. The selection of the Government Subsidy house was done by searching in Botshabelo, section K for a local who would like to volunteer. Permission was obtained from the owners of the property and CLSM probes were installed underneath their house's foundation. The Government Subsidy house which was selected was a newly constructed building. The owners of the property had not moved into the building due to the fact that doors and plumbing had not yet been installed.

Before the installation was done the CLSM probes were calibrated first in identical soil conditions next to the light structure house in order to calibrate the probes according to the site conditions. This means the probes were installed temporary next to the house. The calibration took a few weeks since it depended on the weather conditions and moisture content of the soil. In order to calibrate the probes it was necessary to determine the volumetric moisture content, gravimetric moisture content and bulk densities as discussed in section 3.8. CLSM Probe calibration. These values were used to determine a correction factor for moisture content reading of the CLSM probes.

When the calibration was completed the CLSM probes from the control area next to the house were removed. The installation was done by drilling holes into the

foundations slab and soil underneath the house. The CLSM probes were placed inside these holes and covered with concrete to seal them. Therefore these probes could not be removed again after the study was completed.

3.3 Site description

The study site is situated 50km East-South-East of Bloemfontein, just to the South of N8 highway, 15km West of Thaba Nchu in the Free State. Botshabelo, Section K covers an area of approximately 200 hectares. The position is shown in the locality plan below in Figure 3-1. The Free State Department of Human Settlement in the study actively engaged in the construction of numerous Government subsidy houses.

Figure 3-1: Study area in Botshabelo Section K

Figure 3- 2: Rock found on the Southern side of Section K

Overall drainage generally flowed towards a watercourse starting in section F and flowing eastwards between sections K and J before turning South through the eastern end of section J (refer to Figure 3-3). This watercourse flows into the Klein Modderrivier about one kilometre from the end of section J. Storm-water drains away adequately over much of the general area. There are, however, some level areas where drainage is poor.

Figure 3-3: Locality plan of Section K

The site is mainly covered by residential development which has been gradually expanding for about 20 years. The housing in the area is Government subsidized housing together with poorly constructed mud houses and structures built from scrap metal. It was also observed that much of the Government subsidized housing is poorly constructed or much of Section K, Botshabelo.

3.4 Site geology and Ground water conditions

According to the 1:250 000 series geological map (2926 Bloemfontein) (Department of Mines and Geological Survey, 1966) the site is underlain by shale, sandstone and mudstone of the Adelaide Subgroup of the Beaufort group of the Karroo Super Group. Dolerite intrusions into these rocks are prevalent.

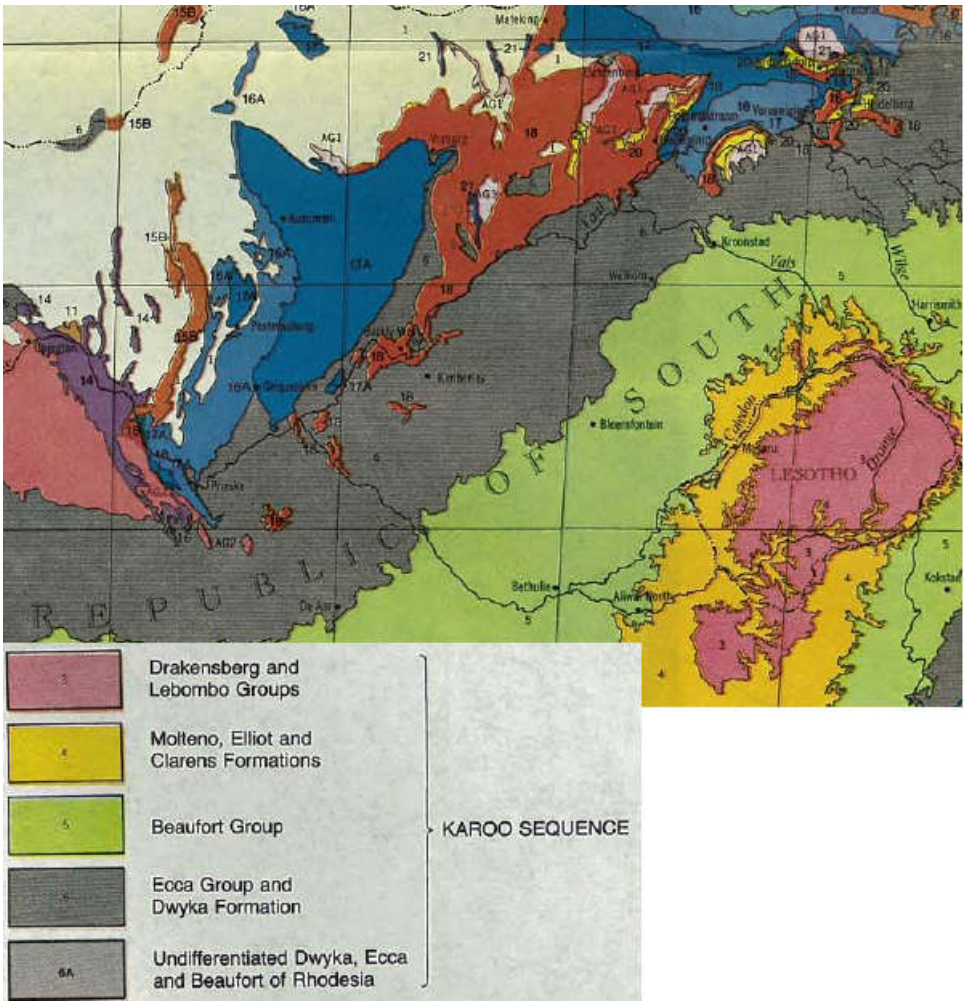

Figure 3-4: Geological map ABA Brink, 1979

3.4.1 Climate

The climate is warm sub-humid with about 500mm to 550mm of annual rainfall per year, most of which falls during the summer months. The lowest rainfall is during July and the height rainfall can be expected during February and March. The monthly distribution of average daily maximum temperatures ranges from 15°C in the winter to 29°C in the summer. The region is coldest during June and July when temperatures can drop below 0°C regularly during the night and early mornings. Rainfall, evaporation and climate maps are shown in figure 3-5.

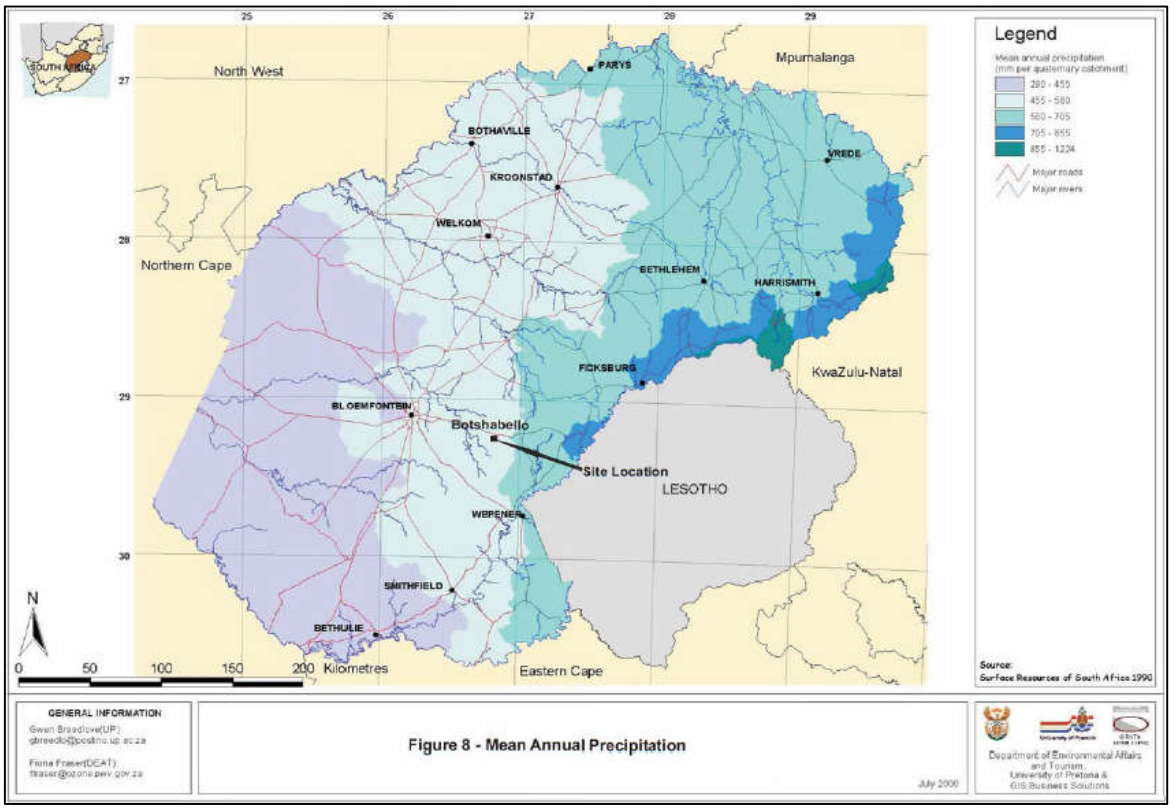

Figure 3-5: Rainfall, evaporation and climate map (Botshabelo climate, SA explorer)

3.4.2. Dolomite

Dolomite is not expected in this area and no evidence of its existence was found. Sink-hole formation is considered very unlikely anywhere in this area.

3.4.3 Seismicity

Earthquake activity is not expected to be a serious limiting factor. A map of probable seismic event severity is shown in Figure 3-6.

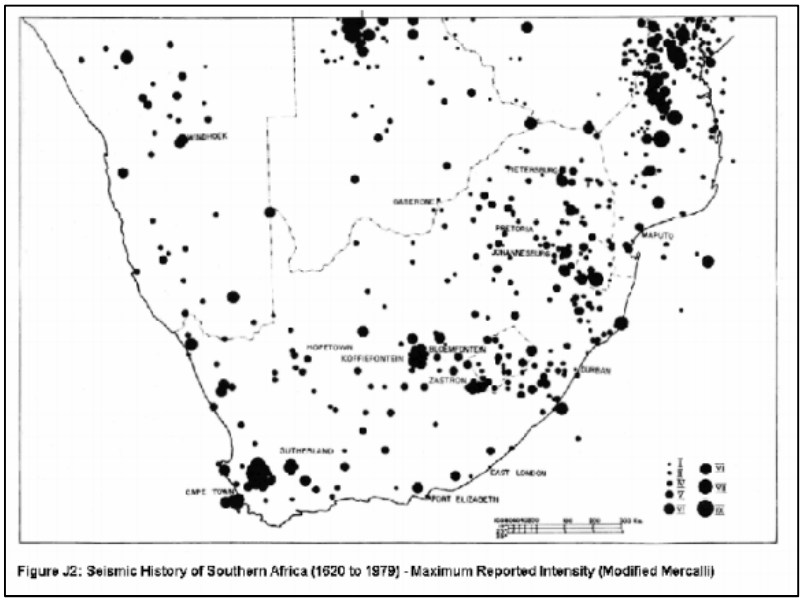

Figure 3-6: Seismic history of southern Africa

3.4.4 Soil Profile and conditions

A photograph of the soil profile exposed in the test pit next to the Government subsidized house is shown in figure 3-7. The soil profile underneath the house has a thin layer of dark brown clayey sand with a thickness of 150mm. This is underlain by a layer of black transported clay and a layer of olive residual clay. Samples of each different type of soil were taken for soil testing at the Central University of Technology Geotechnical Laboratory and subjected to the full range of indicator and grading tests. Laboratory results are presented in section 3.5.1.

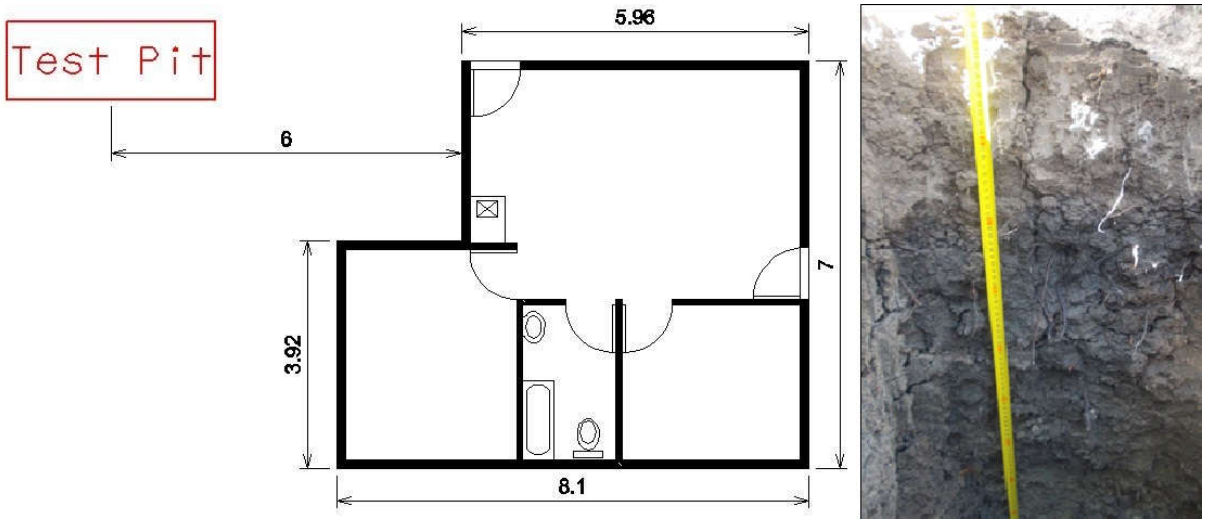

Figure 3-7: Soil profile location and exposed soil in the test pit

3.4.4 Water table

The hole which was made struck relatively impermeable rock fairly near to the surface (approximately 1.1 meter below the surface). This points to the possibility of short term, shallow, perched water tables following heavy rainfall. No water table was encountered in proximity to the Government subsidized house.

3.5 Geotechnical evaluation at the location of the instrumented government subsidy house

3.5.1 Engineering and material characteristics

Potentially active clays were found at the location of the instrumented Government Subsidy House. Expansive conditions should be expected throughout the area of section K. The dolerite rocks underlying the site have the potential to decompose into active clays.

3.5.2 Slope stability and erosion

The area is gently undulating with slopes mainly less than 2% to 3%. An area of rock outcrop is found on the Southern side of Section K. Erosion tends to be a problem where dispersive soils are found. Erosion tends to be less problematic where expansive clays predominate. Expansive soils are evident throughout the area of

investigation. No dispersive soils were noted. No evidence of serious erosion was observed. All the houses in Section K were constructed on levels close to that of the existing ground. It is therefore determined unlikely that slope instability will be a problem. No evidence of slope instability was observed in Botshabelo section K.No major cut or fill is visible at the study site of the Government subsidy house. The Government subsidized house instrumented in the study was constructed at a level close to that of the existing ground. It is therefore unlikely that slope instability is a problem since no indication of slope instability was observed. There was no observation of erosion found around the surrounding area of the study location where the house was constructed.

3.6 Soil testing

The sampling of material on site and profiling was done in accordance to: Guidelines for soil and rock logging in South Africa, 2nd Edition 2002 by Editors ABA Brink & RMH Bruin. All laboratory tests were conducted in accordance to the TMH1: 1986. The results obtained in this report relates only to the materials collected on site and materials which were tested. The tests and results which were obtained are as follows:

I. The wet preparation and sieve analysis of gravel, sand and soil samples, TMH1: 1986, Method A1 (a).

II. The determination of the liquid limit of soils by means of the flow curve method, THM1: 1986, Method A2.

III. The determination of the plastic limit and plasticity index of soils, TMH1: 1986, Method A3.

IV. The determination of the linear shrinkage of soils, THM1: 1986, Method A4.

V. The determination of the grain size distribution in soils by means of a hydrometer, TMH1, 1986, Method A6.

VI. The determination of the moisture content of a field sample, TMH1: 1986, Method A17.

VII. The determination of the potential expansiveness of soil according to Van der Merwe's and Savage's methods.

3.6.1 Sieve analysis and hydrometer results

BOTSHABELO SECTION K				
HOLE NO.		Test Pit 1	Test Pit 1	Test Pit 1
MATERIAL DEPTH (mm)		0 - 150 mm	150 - 900	900 - 1100 mm
SAMPLE NO.		A	B	C
MATERIAL DESCRIPTION		Moist dark brown stiff clayey sand	Moist dusky blue firm clay	Moist dark yellow firm clayey sand
SIEVE ANALYSIS, PERCENTAGE OF MATERIAL PASSING 0.007mm SIEVE (TMH 1: 1986, METHOD A1 (a), A5) - % PASSING SIEVES				
SIEVE ANALYSIS	63.0 mm	100	100	100
	53.0 mm	100	100	100
	37.5 mm	100	100	100
	26.5 mm	100	100	100
	19.0 mm	100	100	100
	13.2 mm	100	100	100
	4.75 mm	99	100	99
	2.00 mm	90	99	98
	0.425 mm	84	97	95
	0.075 mm	39	66	61
	0.002 mm	18	25	26
	% CLAY	18	25	26
	% SILT	21	41	35
	% SAND	51	33	37
	% GRAVEL	10	1	2

Table 3-1: Sieve analysis and hydrometer test

3.6.2 Atterberg limits results

BOTSHABELO SECTION K				
HOLE NO.		Test Pit 1	Test Pit 1	Test Pit 1
MATERIAL DEPTH (mm)		0 - 150 mm	150 – 900mm	900 - 1100 mm
SAMPLE NO.		A	B	C
MATERIAL DESCRIPTION		Moist dark brown stiff clayey sand	Moist dusky blue firm clay	Moist dark yellow firm clayey sand
ATTERBERG LIMITS ANALYSIS (TMH 1 : 1986, METHOD A2, A3, & A4)				
	ATTERBERG LIMITS PASSING SIEVE 0.425mm			
L.L	LIQUID LIMIT	31.1	58.6	59.6
P.L	PLASTIC LIMIT	13.3	19.0	19.0
P.I	PLASTICITY INDEX	17.8	39.6	40.6
L.S	SHRINKAGE LIMIT	8.2	10.5	16.4

Table 3-2: Atterberg limits

3.7 Heave potential

BOTSHABELO SECTION K				
HOLE NO.		Test Pit 1	Test Pit 1	Test Pit 1
MATERIAL DEPTH (mm)		0 - 150 mm	150 – 900mm	900 - 1100 mm
SAMPLE NO.		A	B	C
MATERIAL DESCRIPTION		Moist dark brown stiff clayey sand	Moist dusky blue firm clay	Moist dark yellow firm clayey sand
POTENTIAL EXPANSIVENESS (mm)				
VAN DER MERWE		Medium (3mm)	High (26mm)	High (6mm)
SAVAGE		Medium (3mm)	High (29mm)	High (6mm)

Table 3-3: Heave potential

The results indicate material which is expansive at the study location of the Government Subsidy House and therefore it can be expected that heave and swell may cause damage to the structure. As seen in the results the heave potential for sample B is much greater than sample C. This is due to two reasons. Firstly, the layer for sample B is much thicker than layer C and secondly layer B is on top of layer C which will result in the moisture reaching layer C to much longer.

3.8 CLSM probe calibration

Calibration was performed over a period of three weeks. Soils were sampled at depths corresponding to probe depths to determine gravimetric water content and bulk density. The process was repeated four times over the duration of calibration. Volumetric water contents could then be deduced from the data and compared to the probe readings.

3.8.1 Gravimetric moisture content

The soil moisture content is expressed by weight as the ratio of the weight of water present to the dry weight of the soil sample. It can also be expressed by volume as ratio of volume of water to the total volume of the soil sample. To determine gravimetric moisture content for a specific soil sample the water mass must be determined by drying the soil to its dry weight and measuring the mass before and after drying. The water mass is the difference between the weights of the wet soil weighed and oven dry soil weighed. The drying of the soil sample is done at temperatures between 100 – 110 °C. The water content in Gravimetric moisture content is expressed in equation 1. All results are shown in figure 3-8, 3-9 and 3-10. The calibrations final results are shown in Chapter 4 and Appendix A.

$$\theta_d = \frac{(Weight\ of\ wet\ soil+tare)-(Weight\ of\ dry\ soil+tare)}{(Weight\ of\ dry\ soil+tare)-(tare)} \quad \text{.....[1]}$$

3.8.2 Bulk density

Bulk density, equation 2, is the weight of dry soil per unit of volume. Soil which is more compacted with less pore space will have a higher bulk density whereas soil which is less compacted will have a lower bulk density. Bulk density has an effect on the infiltration, available water capacity, and soil absorbency, which all have an influence on moisture content in soil. Bulk density normally increases with soil depth since subsurface layers are usually more compacted and have less organic matter and less compared to surface layers and therefore contain less pore space.

$$Bd = \frac{Mass\ of\ soil}{Soil\ Volume} \quad \text{.....[2]}$$

The Bulk densities were determined and plotted against gravimetric moisture content for each horizon in the test pit, after which a linear regression was done to determine a formula which was used in the determination of the bulk density at a specific moisture content.

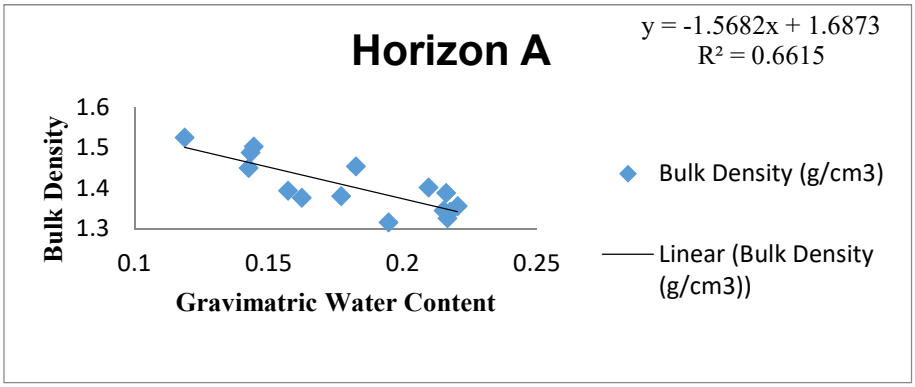

Figure 3-8: Horizon A

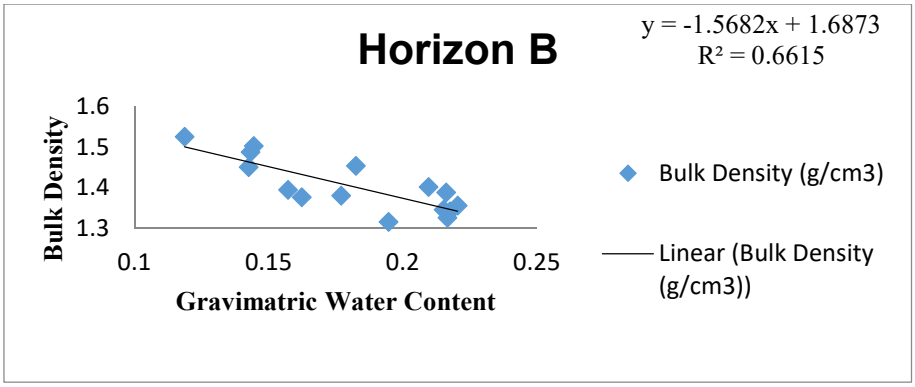

Figure 3-9: Horizon B

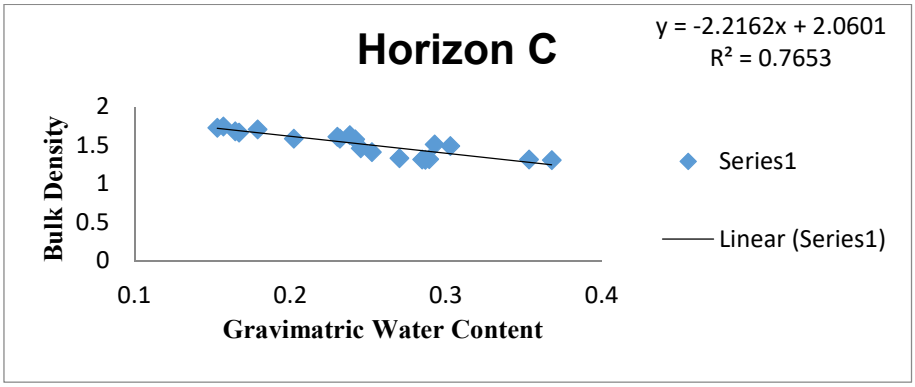

Figure 3-10: Horizon C

3.8.3 Volumetric moisture content

Water content in volumetric basis is expressed as:

$$\theta_{vd} \frac{Volume\ of\ water}{Volume\ of\ soil} \quad \text{.....[3]}$$

But:

$$Volume\ of\ water = \frac{Weight\ of\ water}{Water\ density} \quad \text{.....[4]}$$

And:

$$Volume\ of\ soil = \frac{Weight\ of\ dry\ soil}{Bulk\ density} \quad \text{.....[5]}$$

Thus:

$$\theta_{vd} = \frac{Weight\ of\ water}{Weight\ of\ dry\ soil}\ x\ \frac{Bulk\ density}{Water\ density} \quad \text{.....[6]}$$

Thus:

$$\theta_{vd} = \theta_d\ x\ \frac{d_b}{d_w} \quad \text{.....[7]}$$

3.8.4 Final Moisture calibration equations

The following graphs were determined by plotting the volumetric moisture content against the readings from the CLSM probes. Then a linear regression was conducted to determine a correcting equation to calibrate the volumetric moisture content of each probe.

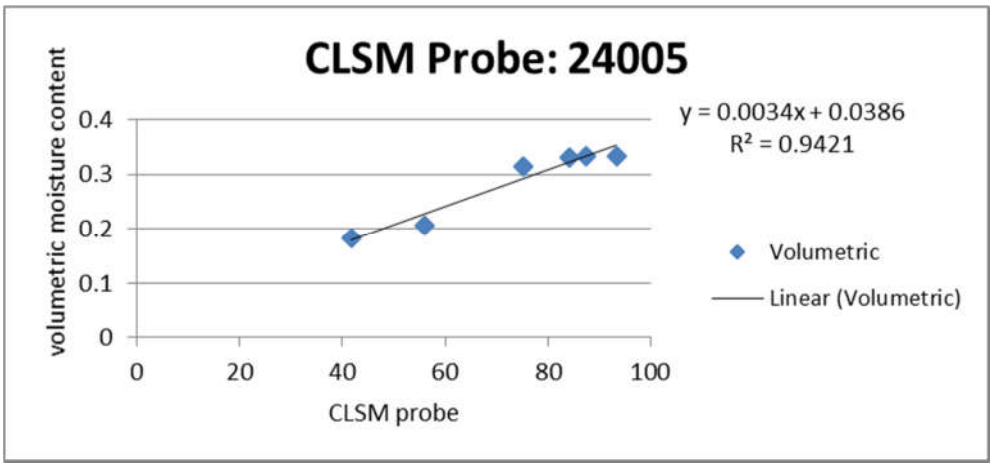

Figure 3-11: CLSM probes 24005

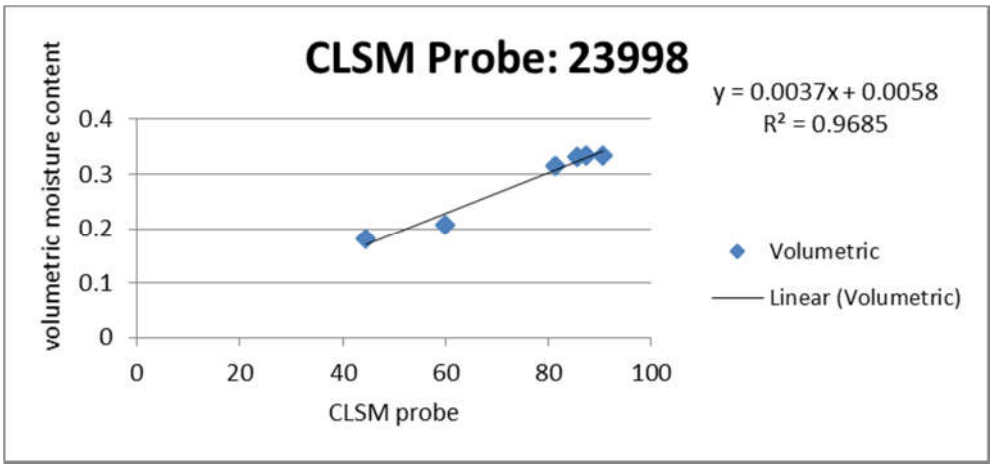

Figure 3-12: CLSM probes 23998

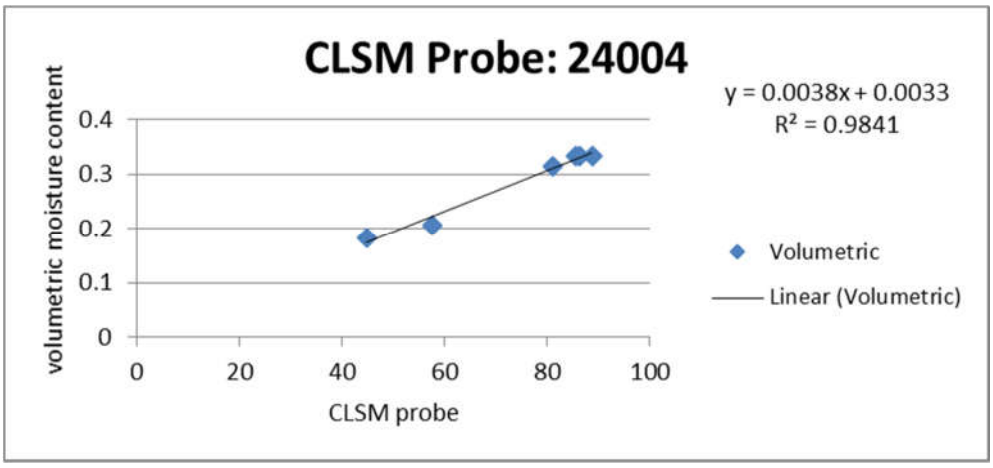

Figure 3-13: CLSM probes 24004

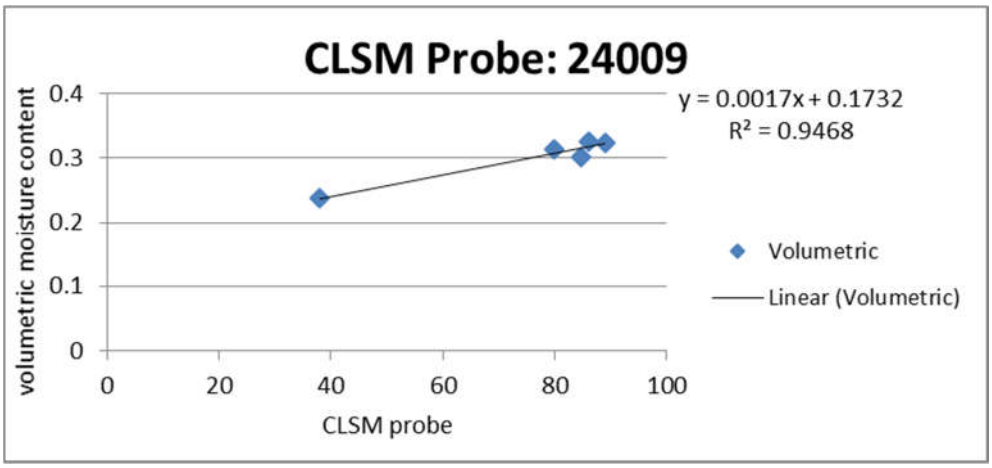

Figure 3-14: CLSM probes 24009

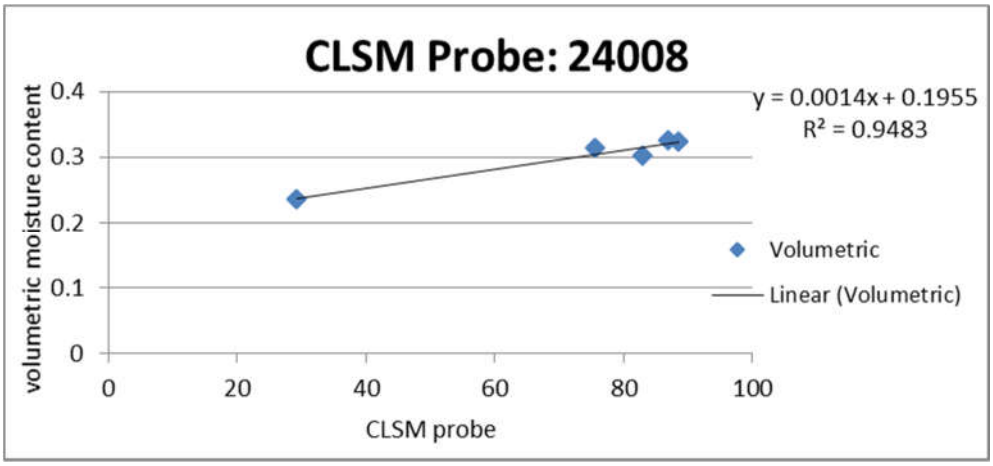

Figure 3-15: CLSM probes 24008

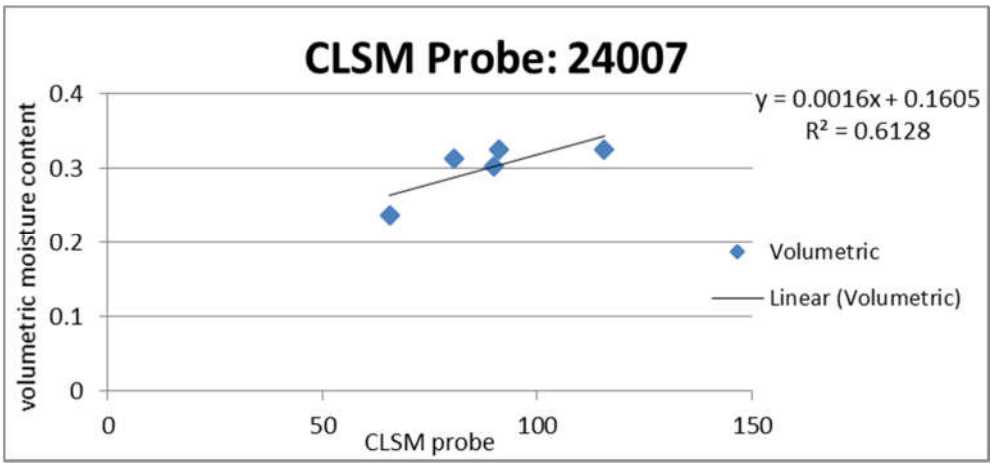

Figure 3-16: CLSM probes 24007

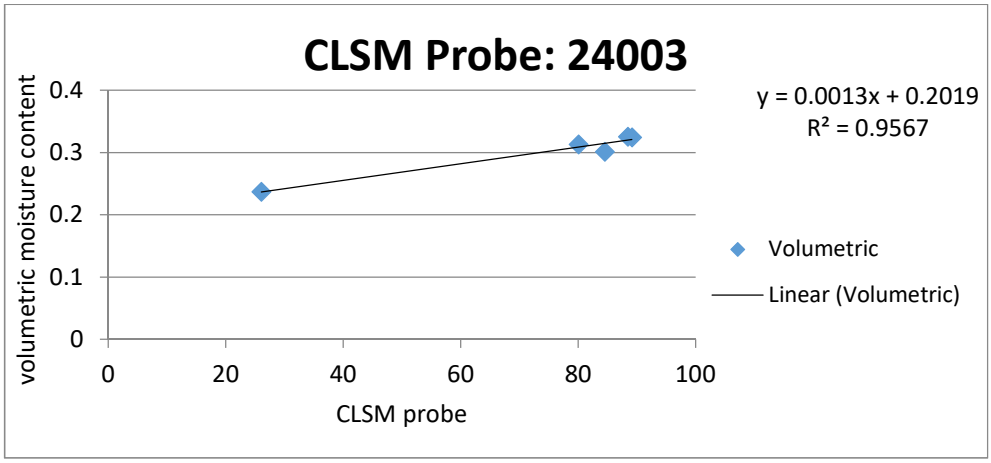

Figure 3-17: CLSM probes 24003

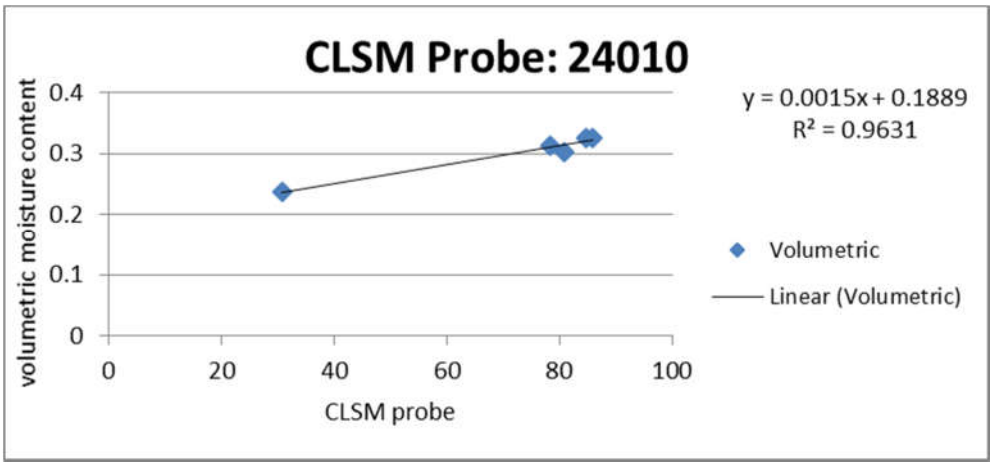

Figure 3-188: CLSM probes 24010

3.9 Data collection

Data was collected each month by using a CLSM data logger. While the collection of data was carried out, the moisture probes were monitored and inspected to ensure they are still in working condition. Unfortunately, one CLSM probe stopped working for a period of 5 weeks where no information could be collected. The errors in the logged data were filtered out to ensure quality control. After the collection was completed the correction factors mentioned above were applied. The data was used to plot the monthly moisture content averages.

3.10 Processing of data

All data was processed using excel spread-sheet analysis. The moisture variation patterns were determined by modelling it on 3D Field. A comparison will be made between seasonal changes and how the shape of the structure can have an influence on moisture condition underneath the structure.

3.11 Modelling using 3D Field

As discussed in the literature 3D Field is a software application which is used to convert data into colour contour maps and surface plots. The software creates 3D maps from data which one collects and fixes the points one has on a site. The data which was collected was used to make a model to identify the moisture distribution underneath the foundation. The areas with higher moisture concentrations are dark blue where lower moisture areas are a lighter blue. These coloured contours were used as a tool to identify areas where the greatest moisture concentration is located and how it changes as the seasons progressed. These areas where these changes are most likely to occur are areas of concern for any raft foundation. Finally the model was evaluated against the accepted norms and to identify where the changes are and the reasons thereof.

CHAPTER 4: RESULTS AND DISCUSSION

4.1 Introduction

This chapter details the investigation of moisture variations which occurred during this study period and to determine the extent and impact the change of moisture can have on a raft foundation of a typical Government Subsidy House. The data which was collected was examined by the candidate and cross checked for correctness. Thereafter, the data was transferred to Microsoft Excel sheets and 3D Field where appropriate analyses were done. The various analyses done include:

I. Time plots of moisture change using line graphs
II. Depth plots of moisture content using line and bar graphs.
III. Modelling on 3D Field of moisture using the inverse distance weighted (IDW) interpolation.

All data is summarised in the appendixes as follows:

I. Appendix A: Moisture content summary tables per month.
II. Appendix B: Graph of moisture content over time.
III. Appendix C: Moisture content change at specific depths for all CLSM probes.
IV. Appendix D: Moisture Content seasonal change models using 3D Field.
V. Appendix E: Orientation of the sun in Botshabelo.

4.2 Moisture content at each CLSM probe and discussion

The study was conducted over a time period of two years from the beginning of 2014 to the end of 2015. Eight CLSM probes took readings at six different depth levels on the soil profile of 150mm, 300mm, 450mm, 600mm, 800mm and 1000mm. The position of the CLSM probes is from North to South and East to west. The reason for this was to get the best possible picture of what is happening underneath the foundation with the limited CLSM probes that were available. All measurements were taken hourly. The results used in this chapter are the average moisture contents per month over this period. This was primarily done to observe the seasonal changes

which will occur in this study period. All these results are discussed below in detail at each specific point of measurement.

4.2.1 Continuous logging soil moisture probe: 24010

CLSM probe 24010 is located at the furthest east corner of the building underneath the raft foundation. The moisture variation throughout the whole soil profile at this specific location has a very similar pattern that follows the seasonal changes as seen in figure 4-1. In wet seasons the moisture content is higher due to higher rainfall since this is typically the rainy season in Botshabelo, Free State. During the dry seasons the moisture content decreases due to the lack of rainfall during this time. The moisture content pattern shows only small variations during the two year monitoring period. When studying the Appendix E it is observed that the solar energy reaching this specific location of the building is only during the early mornings.

Figure 4-2 illustrates how much the moisture content will change with depth. At a depth of 150mm, the moisture content changes by 8% during this study period. The deeper recorded readings, such as at a depth of 800 mm, observed that the greatest change in moisture content change is 9.4%. This is most likely due to the edge beam of the raft foundation protecting the soil from rapid moisture changes up to a depth of 300mm. Readings taken at depths of 600mm, 800mm and 1000mm were more prone to moisture content changes during the study period. Figure 4-3 illustrates the distribution between minimum (Blue line) and maximum (Red line) moisture content. As seen in figure 4-3 the moisture content increases as the depth increase into the soil profile.

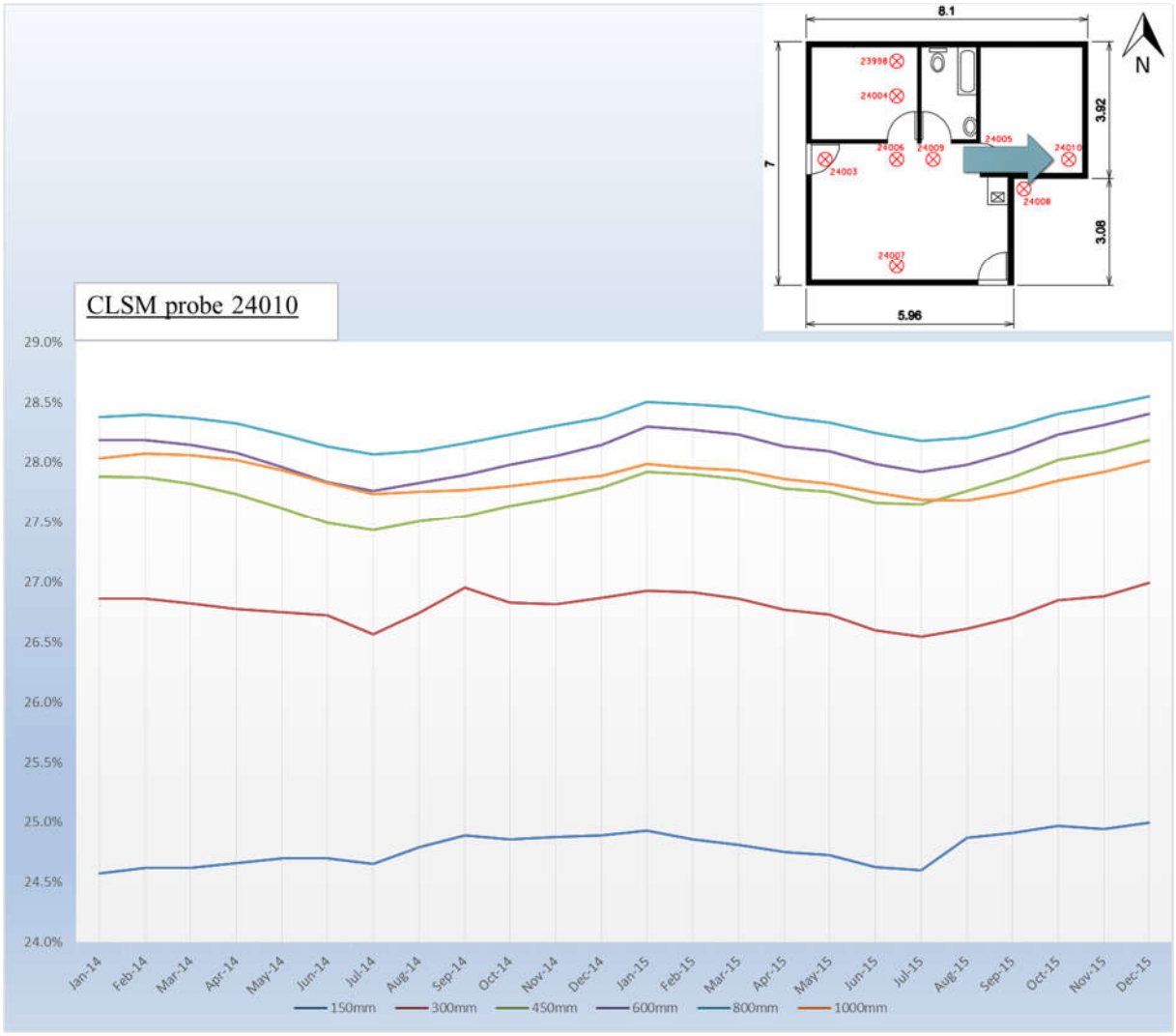

Figure 4-1: CLSM probe 24010 monthly average moisture variation for 2014 and 2015

Figure 4-2: CLSM probe 24010 maximum and minimum moisture difference to depth

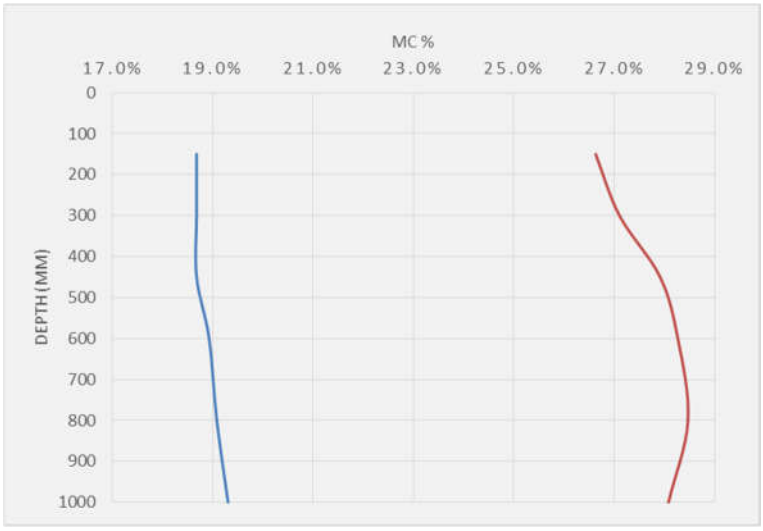

Figure 4-3: CLSM probe 24010 maximum and minimum moisture distribution to depth

4.2.2 Continuous logging soil moisture probe: 24008

CLSM probe 24008, figure 4-4, is located just outside the building at the re-entry corner of the building. This is the only probe not located underneath the foundation of the building. The reason for the placement of this CLSM probe was that in closer inspection of the building when doing the site investigation it was observed that this corner was constantly wet. It was therefore decided by the candidate to measure this location as it was particularly interesting.

The moisture readings at this specific point tracks a clear pattern following the seasonal changes, but with the exception of the upper most layer reading at 150mm. The reason for this exception is due to external factors such as rainfall and the owner of the property watering that specific location. For the other recorded depths, the average moisture content is about 2-3% higher during wet seasons and decreases during the dry seasons.

The location where probe 24008 was placed experienced minimum solar energy. This also contributed to the moisture content being much higher in this zone. This phenomena is also observed at CLSM probe 2005 discussed in section 4.2.3. Both of these locations have similar characteristics and features except CLSM probe 24005 is located underneath the raft foundation and protected by an edge beam.

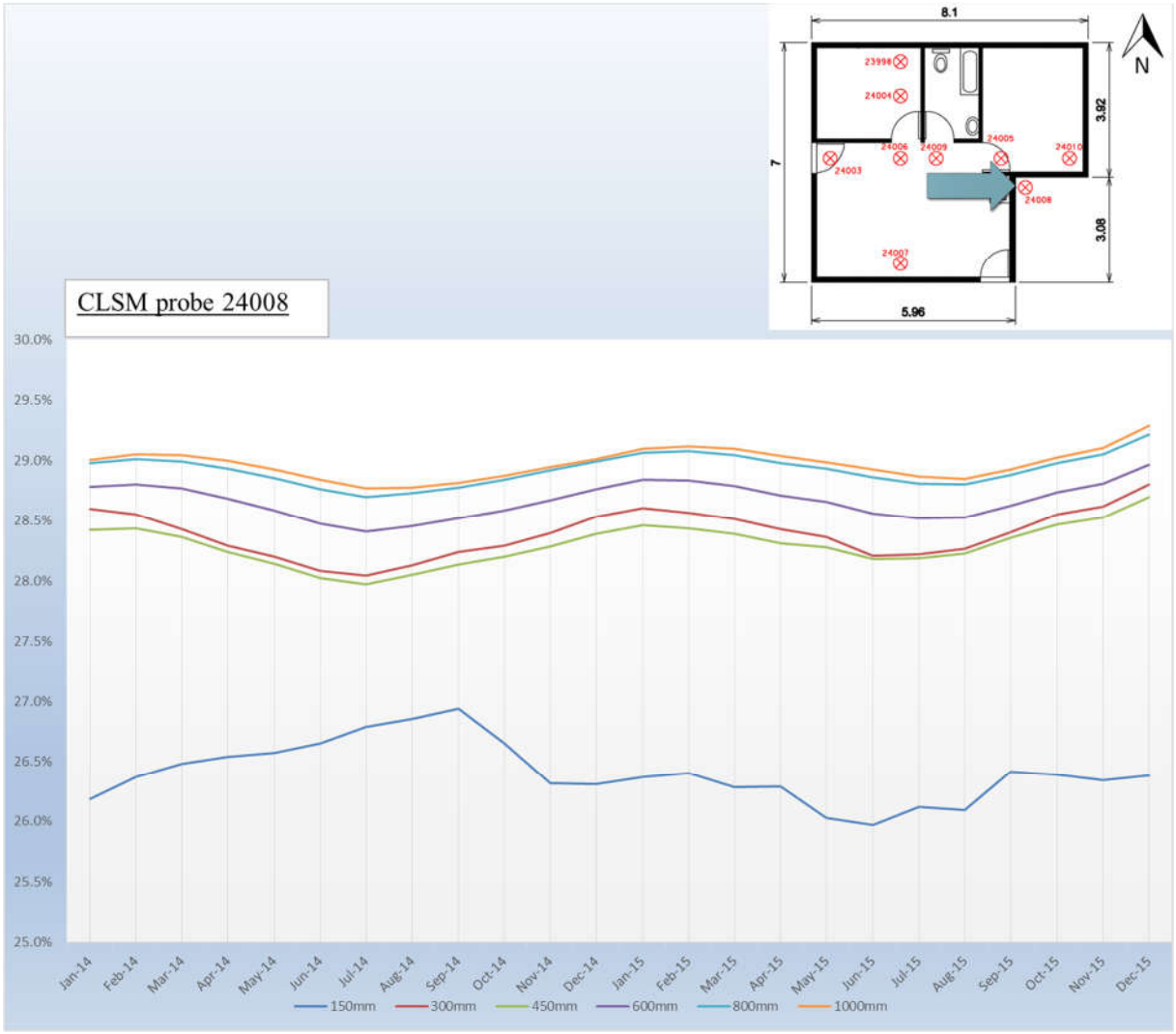

Figure 4-4: CLSM probe 24008 monthly average moisture variation for 2014 and 2015

In figure 4-5 the moisture distribution is observed at various depths. Figure 4-6 illustrates the distribution between minimum (Blue line) and maximum (Red line) moisture content. The first 150mm of the distribution graph of moisture change is where the most erratic change occurs. In the rest of the soil profile the change in moisture content is much more constant and predictable.

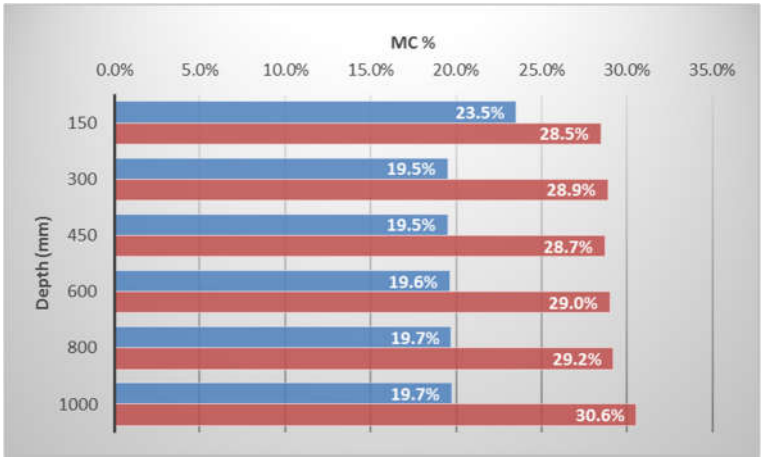

Figure 4-5: CLSM probe 24008 maximum and minimum moisture difference to depth

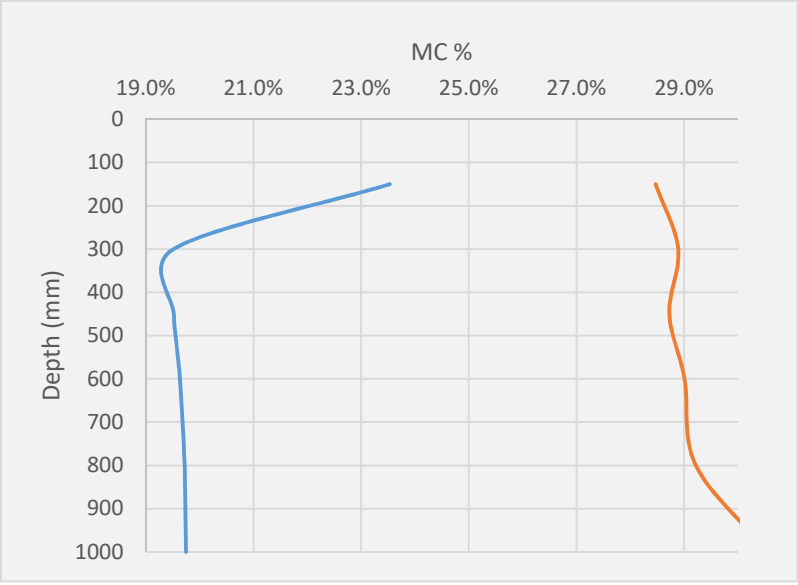

Figure 4-6: CLSM probe 24008 maximum and minimum moisture distribution to depth

4.2.3 Continuous logging soil moisture probe: 24005

Similar to CLSM probes24008 and 240010, CLSM probe 24005 is located on the east side of the building. It is situated just inside the re-entry corner of the building and was installed underneath the raft foundation. The architecture of the building guarantees that this re-entry corner is almost always in the shadow of the building and will not be exposed to the solar energy of the sun. In this study, it was found that this CLSM probe had the highest moisture content among all the CLSM probes. This zone has a

tendency to be very wet and water tends to collect at the re-entry corner. The change in moisture content is approximately 3% throughout the soil profile. It can also be clearly observed that the moisture content also follows the seasonal changes. This was the result of having higher rainfall during wet seasons compared to dry seasons.

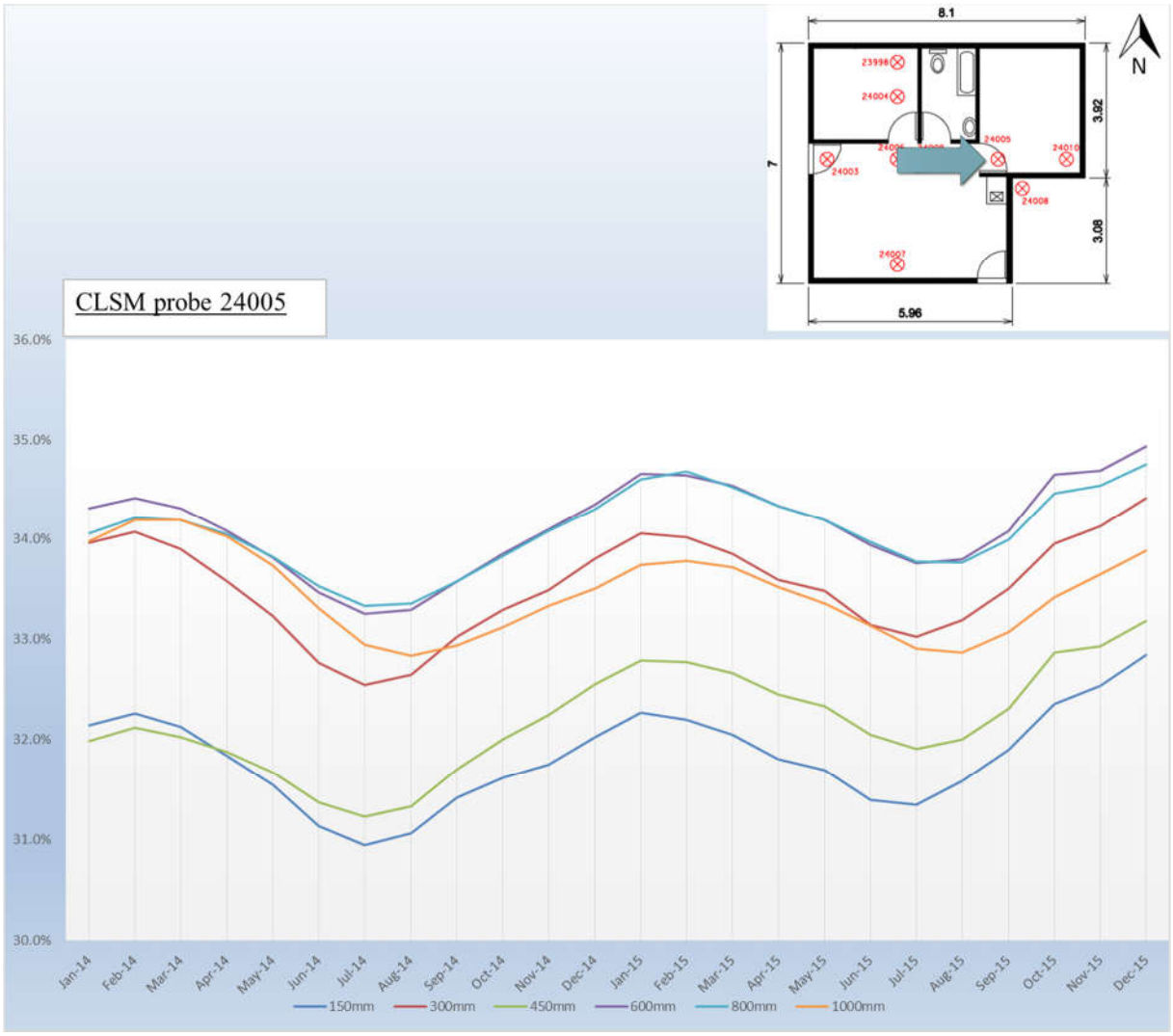

Figure 4-7: CLSM probe 24005 monthly average moisture variation for 2014 and 2015

Figure 4-8 and 4-9 it is observed that the moisture difference stays constant. The change in moisture content is approximately 3-4% throughout the soil profile. It can also be clearly observed that the moisture content also follows the seasonal changes. It would have been expected that the first 150mm to 450mm readings would have had lower moisture content, but this was not the case in reality. This was certainly due to

this location being well isolated from factors such as solar energy that the only change in moisture content can be attributed to factors such as rainfall during the wet seasons. Another observation which can be seen is that the moisture content from 300mm to 450mm decreases and from 450mm to 600mm increases again. This is most probably due to that the soil at a depth of 450mm has less soil suction than compared to the soil at a depth of 600mm.

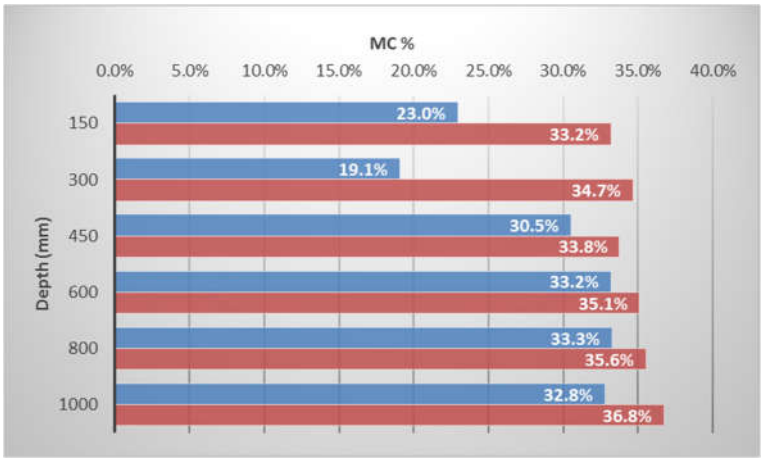

Figure 4-8: CLSM probe 24005 maximum and minimum moisture difference to depth

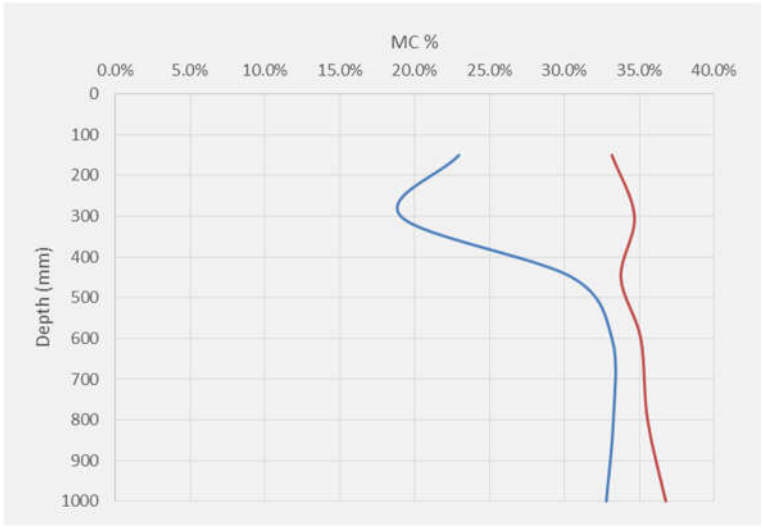

Figure 4-9: CLSM probe 24005 maximum and minimum moisture distribution to depth

4.2.4 Continuous logging soil moisture probe: 24007

CLSM probe24007 is the only sensor located at the south side of the building. The south-facing sides of buildings in the southern hemisphere are not exposed to direct sunlight thus very little solar energy will reach this location. During the dry seasons the south facing sides of the building tends to be cold and in the shadow. As seen in figure 6, the moisture content follows a similar pattern, tracking seasonal changes at all depths. It's also notable that the upper layer of 150mm has the lowest moisture content compared to the rest of the soil profiles. This sensor may be in the compacted fill layer beneath the raft as is thought to be the case for probe 23998. The moisture variation does not exceed 1%. The moisture content tends to stay stable in this area.

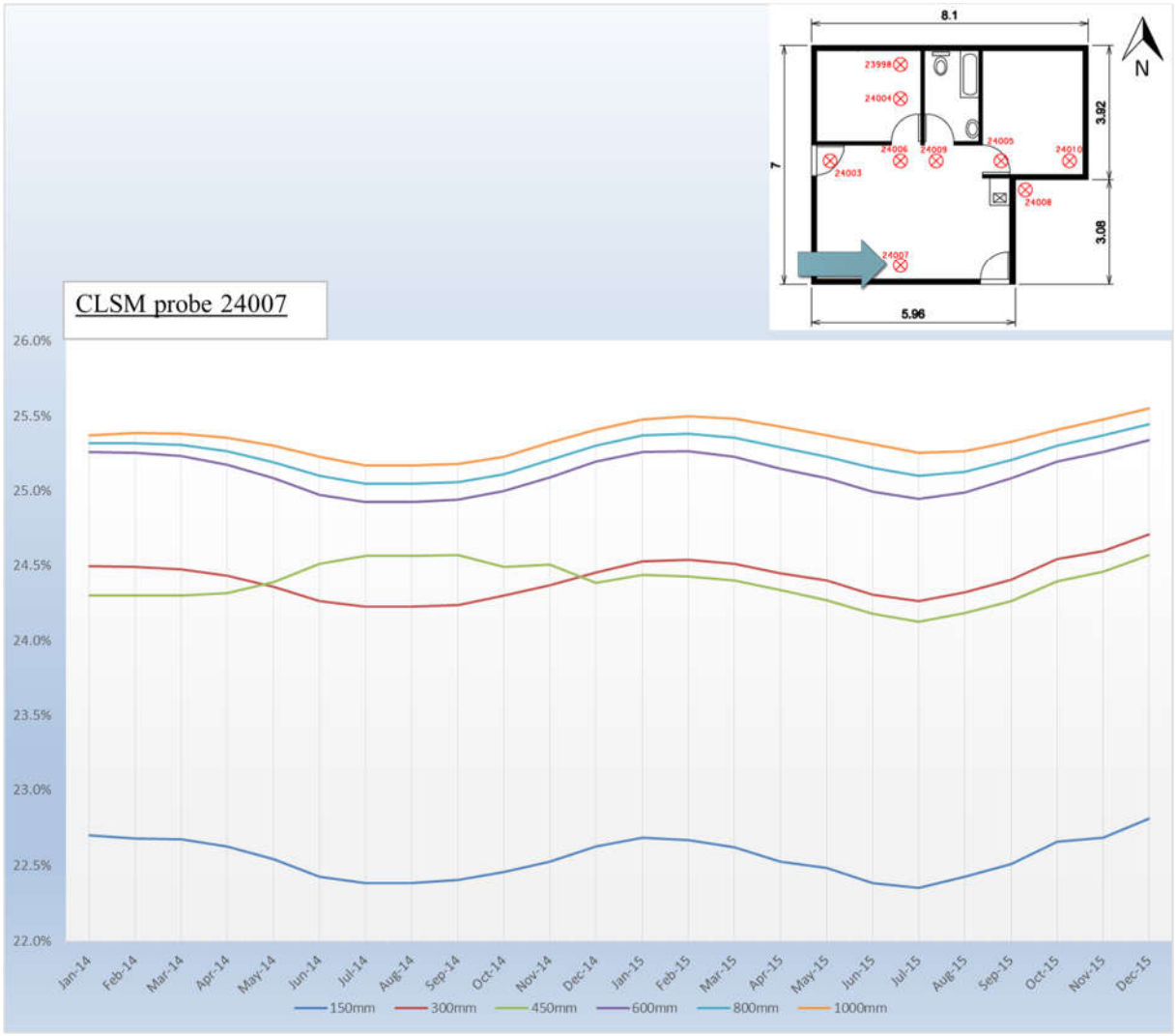

Figure 4-10: CLSM probe 24007 monthly average moisture variation for 2014 and 2015

In figures 4-11 and 4-12 the moisture variation does not exceed 0.7%, except at a depth of 800mm on the southern side, underneath the foundation.

Figure 4-11: CLSM probe 24007 maximum and minimum moisture difference to depth

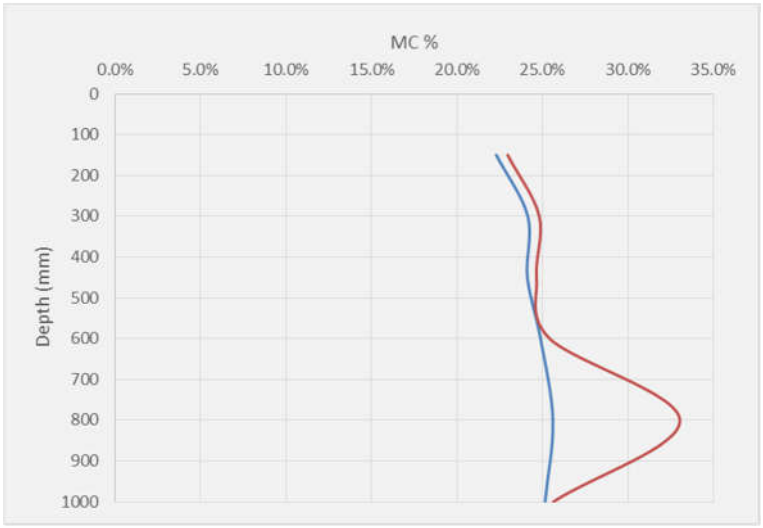

Figure 4-12: CLSM probe 24007 maximum and minimum moisture distribution to depth

4.2.5 Continuous logging soil moisture probe: 23998

The northern sides of buildings are mainly exposed to direct sun light in the southern hemisphere. The heat energy's effect at this location is the Greater than anywhere else in the building the building. CLSM probe 23998 is located just underneath the

raft foundation as seen in figure 4-13. It can be seen that the north side consistently shows the lowest moisture content compared to the rest of the recorded readings anywhere under the building. This is likely due to the fact that solar energy reaching the ground on the northern side is more intense than that reaching the other sides of the building. The clay experiences more shrinkage and cracking than at the other sides. This will also have an effect when rainfall occurs and will cause the north side to have rapid moisture changes. At the north side water contents range from less than 5% to 23%.

The candidate also observed that the readings of 150 mm and 300mm are much lower compared to the deeper depths. It is believed that these sensors may be in the gravel fill layer typically used to level the ground before casting of the slab. This is usually a G6 graded material which is natural gravel or rocks that have been crushed. The properties of this material could not be determined since this material is located underneath the building. It does, however, fit into the typical requirements of G6 material where it's stated as follows: The PI shall not exceed 12 or a value equal to 3 times the grading modulus plus 10 (COLTO specifications, 1998). In this case the moisture content varies between 4% and 8%.

What can also be noticed is that in the first year of recording moisture content at CLSM probe 23998 the readings are very unpredictable before it starts to flatten out in 2015. This is especially true at a depth of 150mm where a 6-8% increase can be seen. The reason for this was that this Government Subsidy House was newly constructed to the end of 2013 and builders where still present on site. When the installation of the CLSM probes were done, the house did not have finishes attached like doors or plumbing. In February 2014, the builders installed water to the house but it was done poorly. This poor workmanship resulted in water leaking at the location close to where the CLSM probe was installed. After a period of a few months the problem was resolved. This resulted in the soil in the surrounding drying out and the average moisture content decreasing over time.

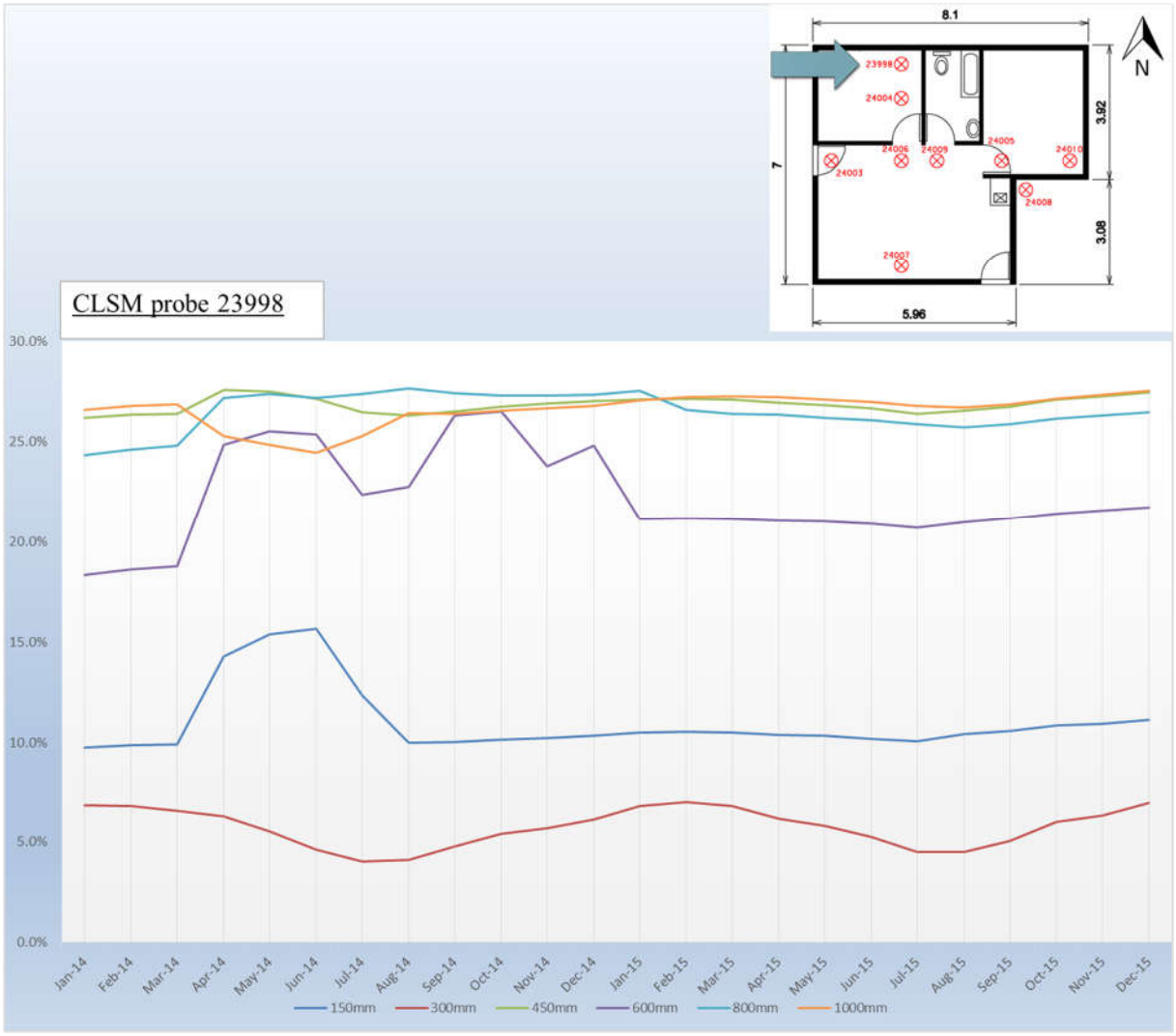

Figure 4-13: CLSM probe 23998 monthly average moisture variation for 2014 and 2015

As seen in figures 4-14 and 4-15 the moisture variation exceeds 6% in some cases at the north-facing side underneath the foundation. The highest recorded moisture contents occur at a depth of 450mm to 1000mm where the two main clay soil layers are found with the highest soil suction.

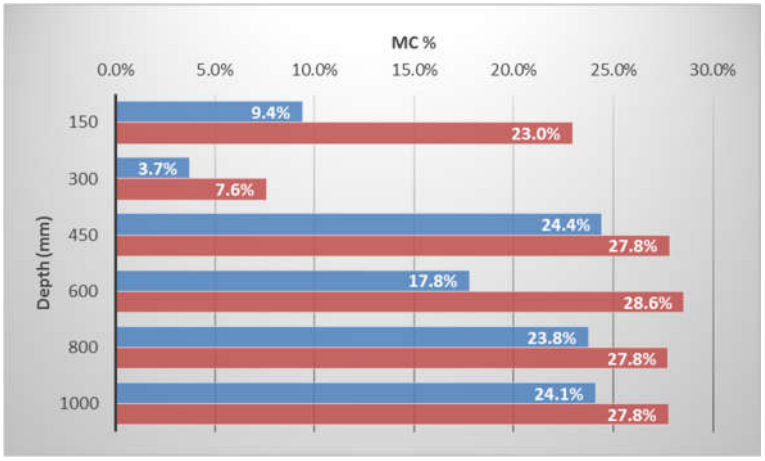

Figure 4-14: CLSM probe 23998 maximum and minimum moisture difference to depth

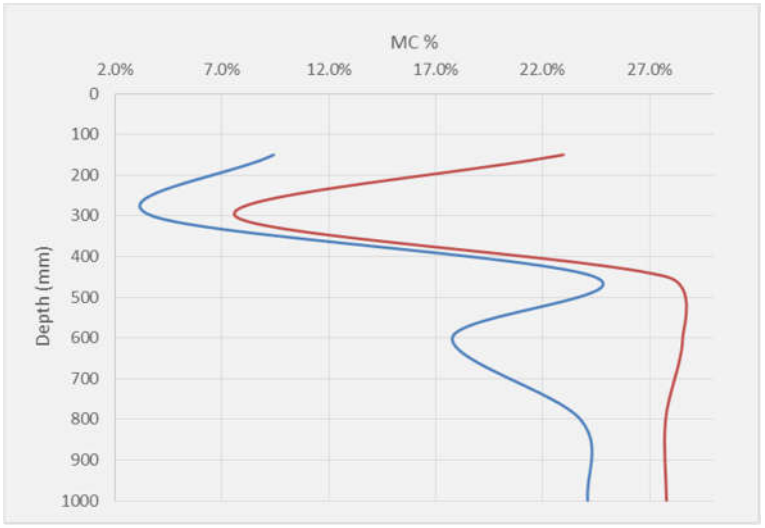

Figure 4-15: CLSM probe 23998 maximum and minimum moisture distribution to depth

4.2.6 Continuous logging soil moisture probe: 24004

CLSM probe 24004 is situated in the north-central location of the Government Subsidy House. It appears that this location underneath the raft foundation can also be affected by solar energy of the sun. But not to the extent of the far north facing side of the building. The recorded data below in figure 4-16 and 4-17 observes that the moisture over the study period stays very constant with very little change occurring. Something that can be noticed is that a the upper most soil layers readings (150mm, 300mm and

450mm) are less than the readings on the centrally located CSLM probe 24009 as seen in figure 4-23.

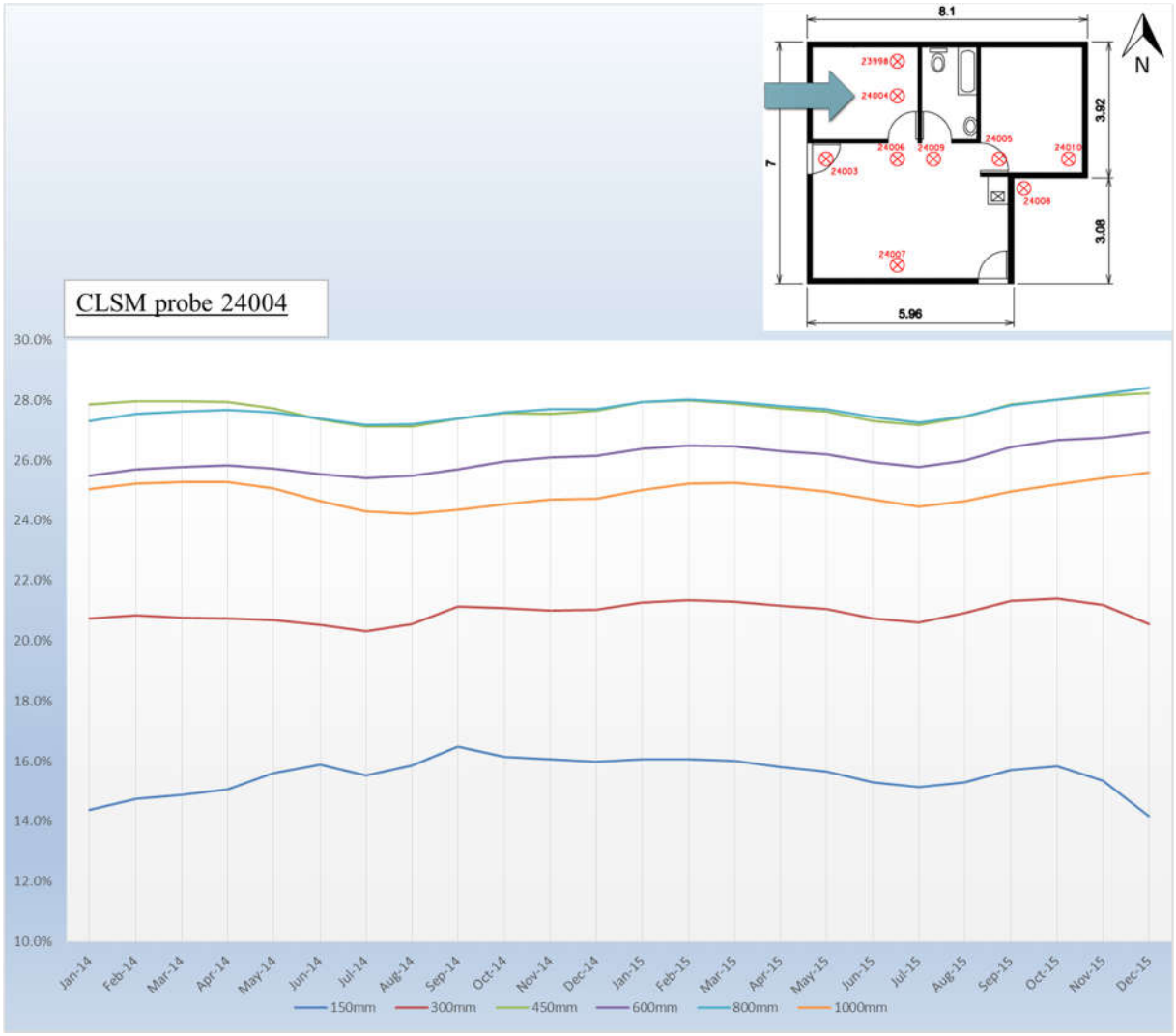

Figure 4-16: CLSM probe 24004 monthly average moisture variation for 2014 and 2015

Moisture distribution data is illustrated in figure 4-17 and 4-18 for CLSM probe 24004. There is a slight change in the moisture content over the recorded two year period. What can be observed is that the moisture content from 450mm to 600mm decreases and from 600mm to 800mm increases again which is due to the soil at the depth of 600mm having less soil suction than compared to the soil at the depth of 800mm. This effect, however, is not as great as in the previous case with CSLM probe 24005 due to the distance the moisture has to infiltrate to the centre of the foundation.

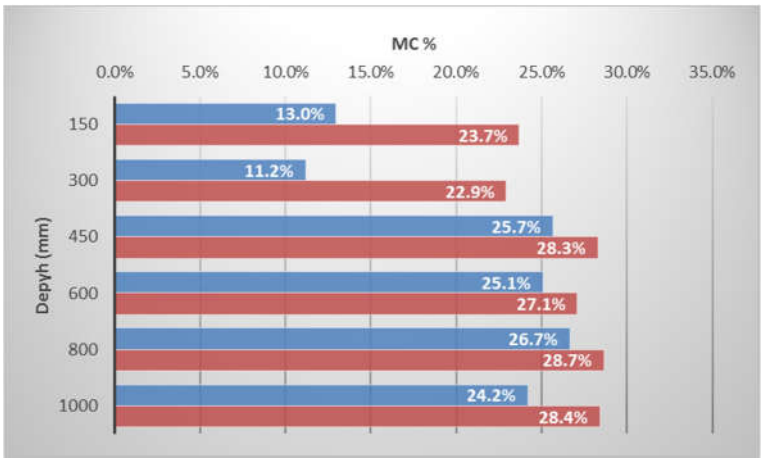

Figure 4-17: CLSM probe 24004 maximum and minimum moisture variation for 2014 and 2015

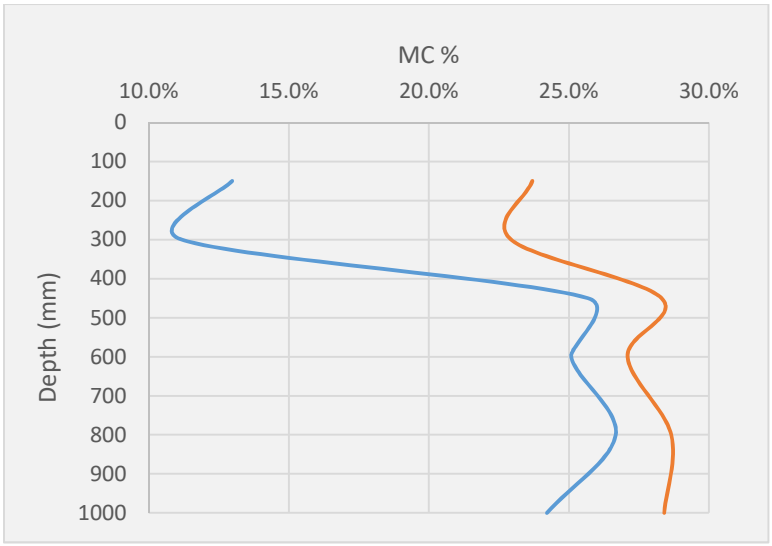

Figure 4-18: CLSM probe 24004 maximum and minimum moisture distribution to depth

4.2.7 Continuous logging soil moisture probe: 24003

As seen in Figure 4-19, Probe 24003 is situated at the west side of the building, close to the edge beam. This area of the building is mainly exposed to the afternoon sun and tends to be warmer than the previous locations. This specific area of the building had experienced a dramatic influence on its moisture content where CLSM probe 24003 is located. The reason being the owner of the house installed paving in front of the main door entrance. The owner installed this paving in August of 2014. This had a

major influence, causing a significant drop in the moisture content. The paving as seen in figure 19 was done at the beginning of spring while temperatures were rising. There was no rainfall and moisture content fell due to evaporation. The observed decrease in moisture content varied between 1% and 4%, depending on the depth of the CSLM probe readings. This highlights the fact that post construction practices and extensions to a house are beyond the control of the designing engineer. Such changes in the surroundings can cause distress to a structure that was constructed on active clay soils. Paving around the house or even planting vegetation or shrubs next to the foundation can cause a decrease in the moisture content.

All these external influences could either prevent moisture from penetrating the foundation or withdrawing moisture and causing soil shrinkage in the region. To minimize movements in soil, landscaping should be done on all sides adjacent to the foundation and drainage should be provided and maintained. The data shows that the change in moisture content levels out towards the end of March 2015. The greatest change as seen in figure 4-21 and 4-22 in moisture content is at a depth of 800-1000 mm where the variation is 9%. It should be noted that the placement of the paving skews the data since there was a drop in moisture content over a period of a few months. If the data is compared as follows: January 2014 to June 2014, and May 2015 to December 2015 it can be seen that there is in reality, very little variation in the equilibrium moisture content underneath the raft foundation. It can therefore be assumed that unless drastic landscaping takes place, such as in this scenario, very little might have happened in this location in terms of moisture change.

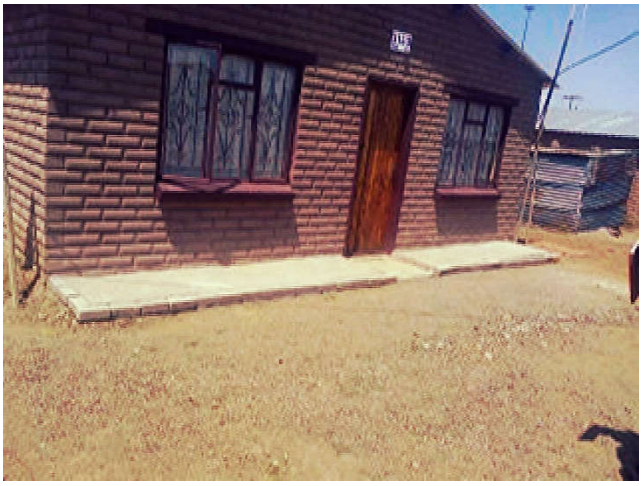

Figure 4-19: Paving in front of the house

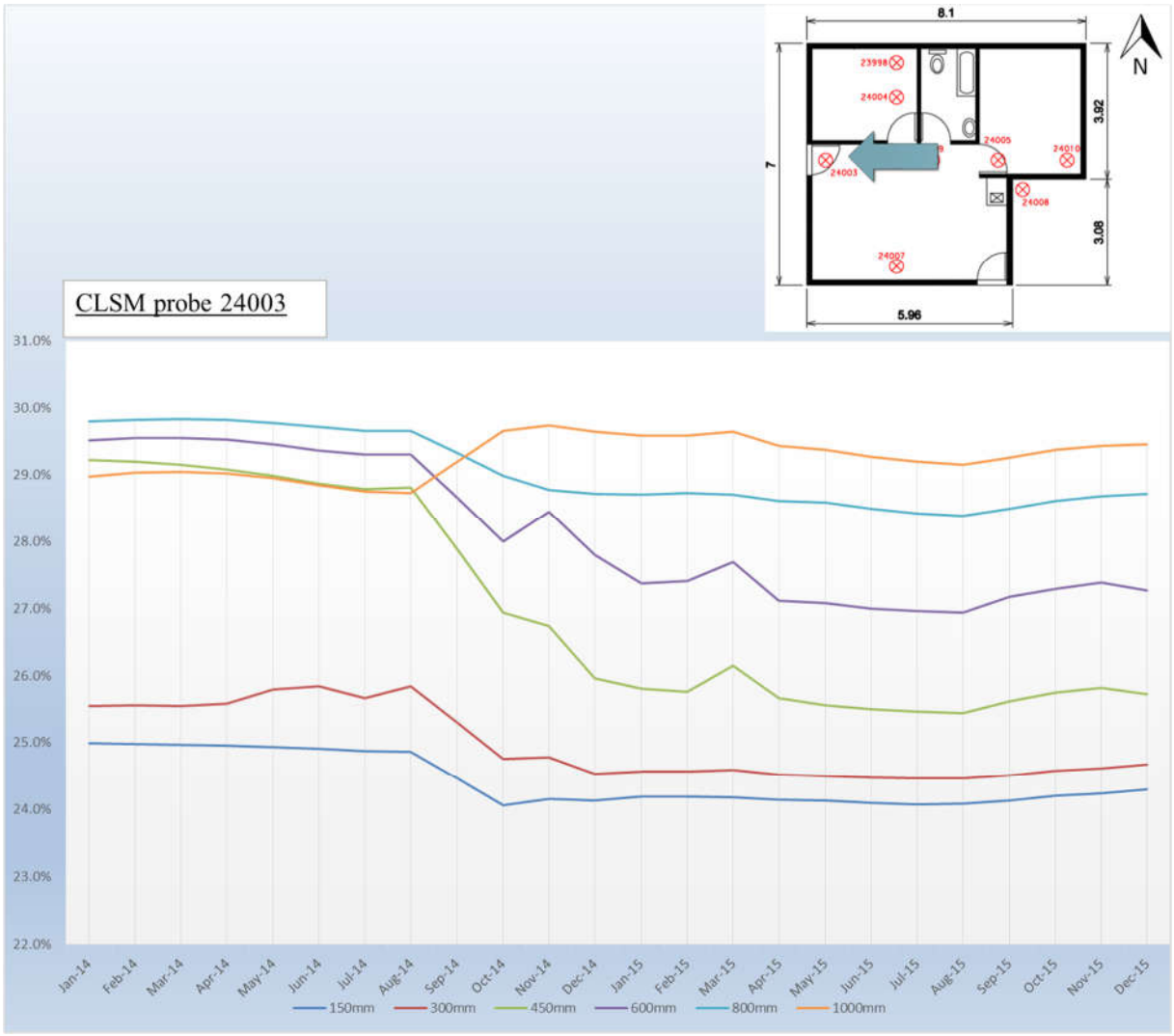

Figure 4-20: CLSM probe 24003 monthly average moisture variation for 2014 and 2015

Figure 4-21: CLSM probe 24003 maximum and minimum moisture difference to depth

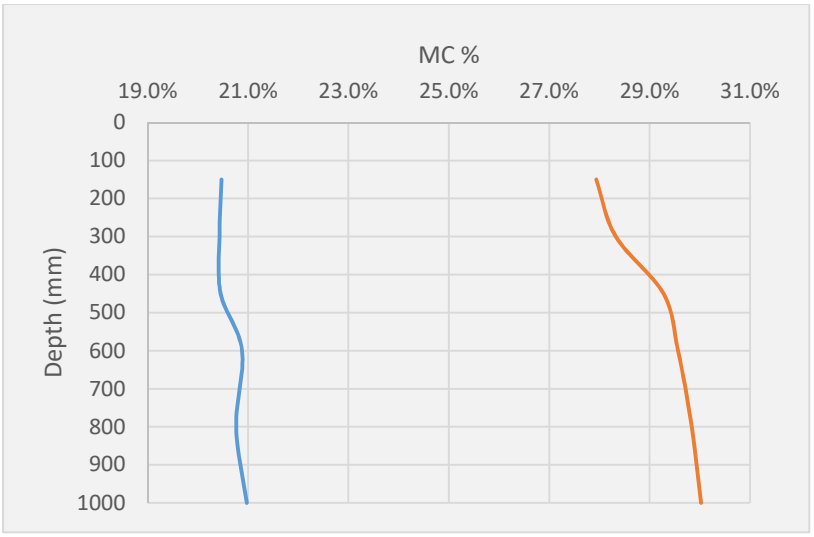

Figure 4-22: CLSM probe 24003 maximum and minimum moisture distribution to depth

4.2.8 Continuous logging soil moisture probe: 24009

CLSM probe 24009 is located centrally underneath the raft. This location is where the literature suggest the highest moisture concentration should be located. By studying the data in figure 4-23, and comparing it to the data of CLSM probe 24005, it is observed that the moisture content throughout the soil profile is constantly lower. The possible reason for this is that the soil conditions at this specific site is of such a nature that it is very difficult for moisture to infiltrate to the centre of the raft foundation. The moisture throughout the soil profile underneath the raft foundation will simply not reach

the middle in active clays; and therefore the moisture content stays constant. Between September 2014 and December 2014 a very slight change did occur. The only factor that could have contributed to this is the landscaping, which was done by the owner of the house when she installed paving at the west side of the building. This did cause a short-term change, but shortly afterwards the moisture readjusted itself. This can support the theory that the moisture content located in the centre of a raft foundation will never exceed certain moisture content and that in reality the east-southern corners of a building are more susceptible to having a moisture concentration. As seen in figures 4-24 and 4-25 which illustrates the difference in moisture variations at CLSM probe 24009. The variation in moisture content stays constant throughout this study period. This is due to the central location underneath the raft foundation.

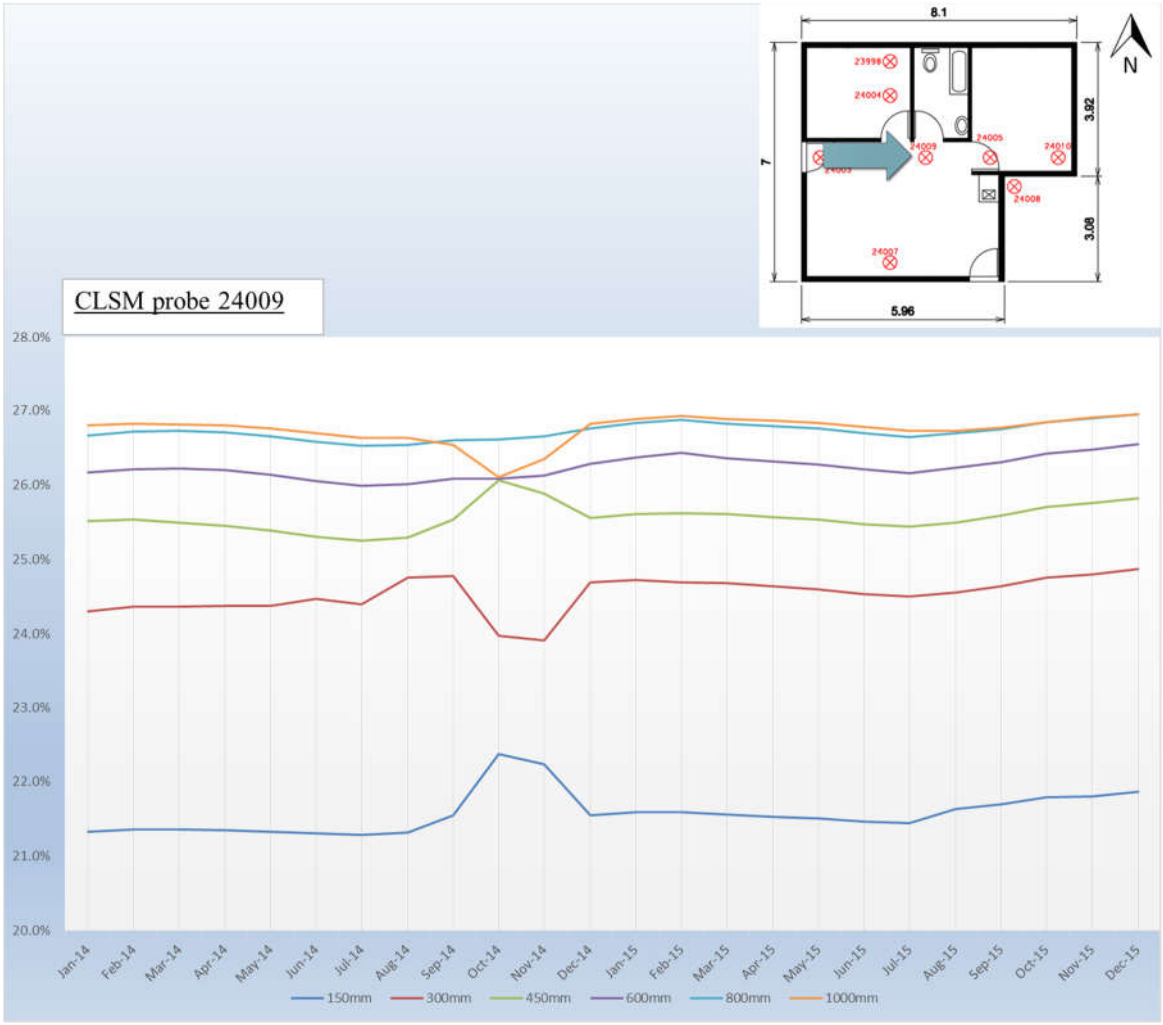

Figure 4-23: CLSM probe 24009 monthly average moisture variation for 2014 and 2015

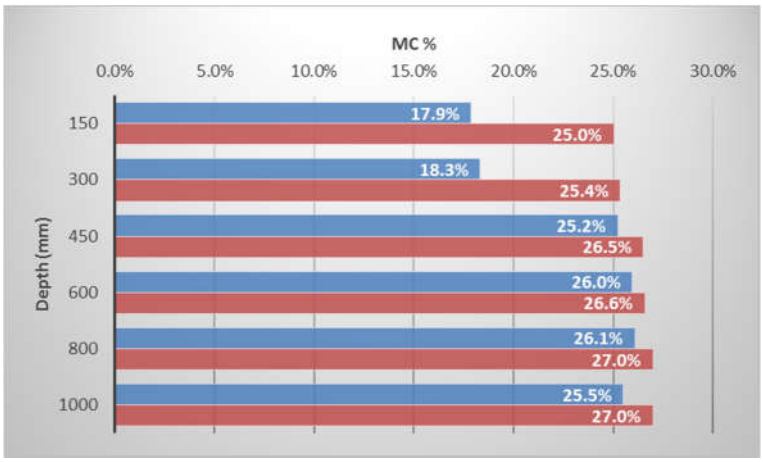

Figure 4-24: CLSM probe 24009 maximum and minimum moisture difference to depth

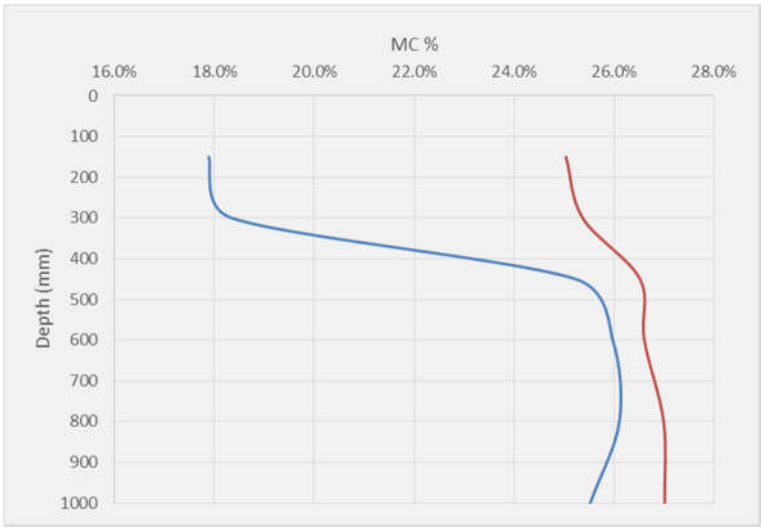

Figure 4-25: CLSM probe 24009 maximum and minimum moisture distribution to depth

4.3 Moisture variation underneath the raft foundation

All of the results obtained in this study were modelled using 3D Field to see the effect of moisture distribution that will appear underneath the raft foundation as in appendix D. For the purpose of this study it was conducted over a period of two years and modelled at six different depths, namely: 150mm, 300mm, 450mm, 600mm, 800mm and 1000mm. A model was then generated for each month and each depth as discussed above to see how the moisture variation will appear over this period.

The methodology used in 3D Field for the modelling of moisture content was the inverse distance method (IDW) interpolation. This method makes the assumption readings closer to each other are more alike or similar than those that are far away. To predict a value of any unmeasured location this method uses the surrounding location to make its prediction. The values close to the measured locations have much more influence on the predicted value than those far away. The weights are reduced as the distance between points increase. The main reason for the selection of the IDW interpolation is more realistic representation of geographic phenomena. The analysis was done on a plan view at each specific depth.

In Appendix D it can be observed that there are a wide range of different moisture variations over the periods of January 2014 to December 2015. Typically the north side below the structure has the lowest moisture content throughout the foundation. Whereas the re-entry corner constantly shows the highest moisture content throughout the six layers measured. This can be accredited to the orientation of the building to the sun. The orientation of the sun in Botshabelo in summarised in Appendix E. Constantly the re-entry corner of the building has minimum exposure to any solar energy during the day in the wet seasons. In dry seasons, there is no solar energy reaching the re-entry corner. Thus the end result is a very high moisture concentration located underneath the structure at the east side of the re-entry corner.

In contrast, the north is very exposed to the solar energy during the dry seasons and wet seasons. This was due to the solar energy reaching the ground on the northern side more intensely than that reaching the other sides of the building. This resulted in the soil being much dryer and the north side's soil being more prone to rapid moisture change, especially after rainfall, which could cause distress to the building. This is probably due to the fact that the dry, cracked soil allows immediate access for rainwater. The dry north facing location underneath the raft foundation will rapidly heave when rainfall occurs and rapidly shrink afterwards.

At closer inspection the moisture concentration is not located in the middle of the raft foundation. It tends to be located at the location which is least exposed to solar energy.

The observed moisture variations in this study, executed in Botshabelo in the Free State, suggests that an approximately symmetrical dome-shaped heave shape which is located roughly on the centre of the foundation, as found by Pidgeon (1987), Pidgeon and Pellissier (1987), Fityus et al. (2004) etc. in simulated foundation tests is not likely to occur or develop. In effect by studying all the models in Appendix D it tends to suggest that the dome that develops will rather depend on the shape of the building and its orientation to the sun.

4.4 Edge moisture variation distance, em

Edge penetration distance is the distance measured from the edge of the outside beam inwards to the area where moisture content of the soil is nearly constant. The magnitude of the edge penetration distance is dependent on the temperature, rainfall and soil conditions in the area. This study suggests that those accepted norms are not the only influence on the edge moisture distance. Previously shape and shadow of the building was ignored, because all previous studies were done on simulated foundations, there was no shadows cast since there was no super structure. The whole foundation in previous studies was equally exposed to sunlight. The following figures illustrate the absolute minimum and maximum readings obtained in this study to determine the edge penetration distance.

Figure 4-26 shows the length of the building going from North to South in meters as the y-axis and the moisture contents as the x-axis. Where Figure 4-27 shows the length of the building from west to east in the x-axes and the moisture content in the y-axis. The whole measured soil profile moisture content was taken into consideration because the whole soil profile can have an influence on the edge penetration distance. It should be noted that it is not possible to use a factoring value or correction factor in determining the influence each layer will have on the edge penetration distance. To provide satisfactory stiffness to a raft foundation is important in the rational design methods to determine the edge penetration distance. This has been done for many years now using information obtained from mock foundations as in the case with Fityus et al (2004) and Pidgion (1987). This assumes that the edge distance is the same throughout the raft foundation. Figure 9 suggests that the edge penetration distance

is very similar from East to West. The edge distance in the east side approximately 2 meters, and in the West approximately 2.5 meters. Figure 8 however shows no clear pattern defining an edge penetration distance. At the North there is a very wide range of moisture variation to the south. This means that the edge penetration distance on the North side may be far greater than previously believed. The findings tend to suggest that the failure of many raft foundations constructed on active clay materials may be due to due to a lack of stiffness in the North-South beams.

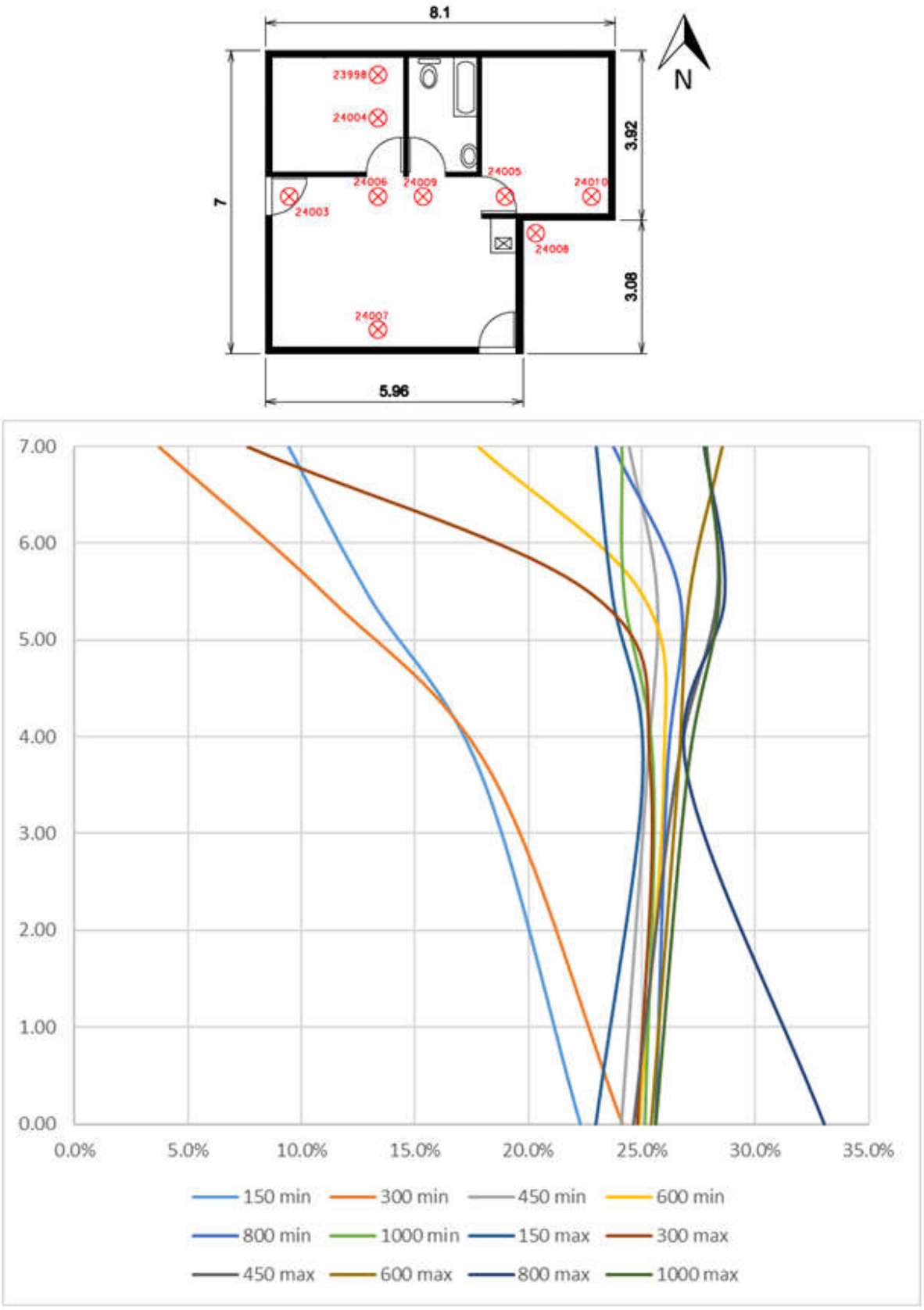

Figure 4-26: Edge penetration North to South

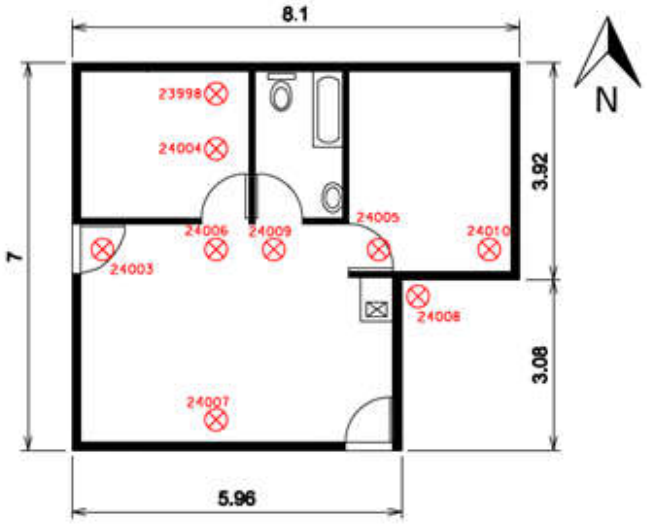

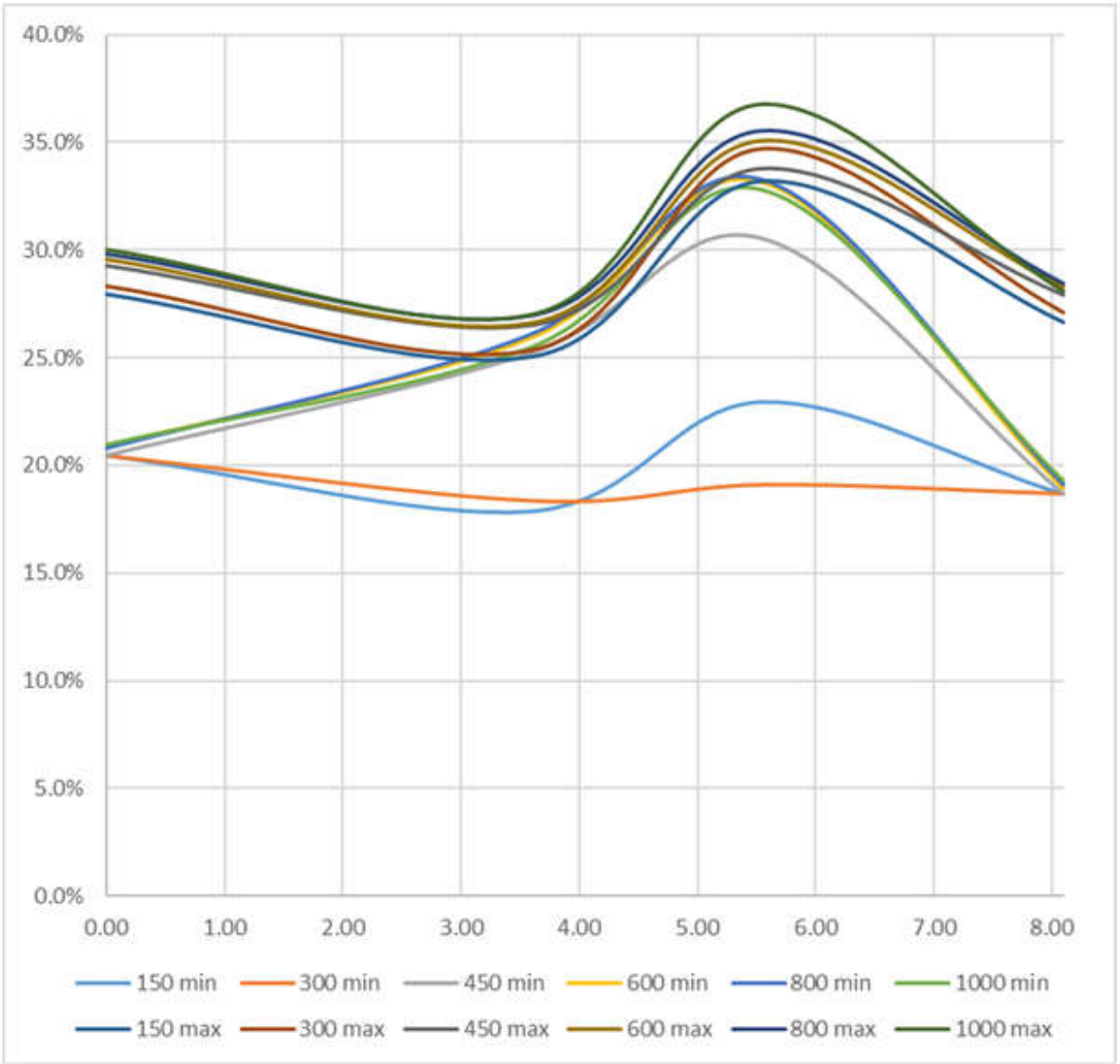

Figure 4-27: Edge penetration West to East

CHAPTER 5: CONCLUSION

5.1 Conclusion

The department of Human Settlement is committed to delivering over 1.5 million housing opportunities by 2019. These Government Subsidy Houses are particularly susceptible to damage in the Free State by heaving clay because they are exceptionally light and clay can lift them very easily. In this final chapter, the main conclusions of this thesis are summarized and some recommendations are given.

5.2 Acceptance of Hypothesis

I. The moisture movement underneath a light structure depends on the orientation of the structure to the sun. Seasonal changes will result in different angles to which the sun will shine relative to the building. As seen in Chapter 4 the north side of the building consistently shows a lower moisture content compared to the rest of the building. This is certainly due to the fact that in the southern hemisphere the North facing side of the building is most exposed to solar energy. Seasonal changes will result in different angles to which the sun will shine relative to the building.

II. The north side of the structure will have a greater differences in moisture over time than the south side. As seen in figure 4-26 there is a very wide spread at the North side of the foundation. The north side of the structure will have a greater difference in moisture variation due to the fact it will dry out much quicker and thus when it rains the water absorption will be far greater. This will result in higher evaporation during warmer months compared to colder months and cause much greater heaving at the north facing side of the structure.

III. Moisture will stay more constant at areas where sunlight is limited. At the re-entry corner of the building it constantly shows the highest moisture content compared to the rest of the structure. This side tends to not be exposed to direct sunlight and will have higher moisture content due to temperature being lower than the north facing areas of the structure. Thus causing the dome forming not being centre but rather to the south east side of the structure.

5.3 Applications

Applying the findings of this study, it should be possible to at least achieve better estimates of moisture pattern development and to consider more realistic heave patterns than are currently being employed. The edge penetration also needs rethinking since this study shows that there is no clear indication of the value of this parameter which should be used in estimating mound shape and required stiffness. The use of a flat-top dome is not recommended since there is no clear evidence to support it. The soil underneath this foundation predominately stays Close to the fully expanded state except on the northern side, where water content in the upper layers may fall to the shrinkage limit.

5.4 Recommendations

The following recommendations can be adopted to improve the raft design of Government Subsidy Houses:

I. If the foundation conditions are likely to be troublesome (active clays) stiffened raft foundations will probably be the most satisfactory alternative for the new Government Subsidy House. The provision of raft foundations will also take care of the secondary possible geotechnical problem, that of shallow, temporary, short-term perched water tables after heavy rainfall.

II. Stiffened raft foundations and chemical improvement are likely to present the most satisfactory and economic solution. The raft foundation design should aim to limit long-term differential deflections and distortions of the rafts to ensure that the deflection ratios across the centre and along the edges of the rafts do not exceed 1: 1000. This deflection ratio is adequate if the buildings have both internal and external articulation joints and the brickwork meets the standards. If there are no articulation joints then the rafts will need to provide approximately twice this stiffness

III. The installation of an apron of paving which is sloping away from the building can increase the distance, which the moisture must migrate to underneath the

foundation. This can vastly improve the success of the building if it is constructed on active clays.

IV. In locations with very active clays it is particularly important that both the water and sewerage connections be made with flexible connections. No water must be allowed to pond close to any of the buildings and no trees or shrubs should be planted closer to the houses than one and a half times their mature height.

5.5 Summary

It has been noted by (Bester et al, 2016) that the measurements of moisture content under a very common type of Government subsidy house built on clayey soil suggest that currently accepted patterns of heave are unlikely to provide good guidance for foundation design. The instrumentation used in the study has proved itself convenient and reliable. It is hoped that it will be possible to instrument several other light structures in order to work towards a general modelling procedure. This should enable reliable predictions of the moisture conditions which need to be designed for in the general case. This in turn should allow reliable and economic design of a wide range of raft foundations with the prospect of fewer failures. In the meanwhile, by applying the findings of this investigation it should be possible to at least obtain better estimates of moisture pattern development and to estimate more realistic heave patterns than are currently being employed.

CHAPTER 6: REFERENCES

Anonymous, 2015. *Government Communication and Information System. 2015. Housing delivery in.* [Online]
Available at: http://www.sanews.gov.za/south-africa/housing-delivery-sa-how-havewe-fared
[Accessed 20 January 2016].

Bester, DM, Stott, PR ,Theron, E, 2016. The movement of soil moisture under a Government subsidy house. In: S. Jacobsz, ed. *Proceedings of the first Southern African Geotechnical* Conference. Netherlands: CRC Press/Balkema, pp. 41-47.

Brink, ABA & Bruin, RMH, 1990. Guidelines for soil and rock logging in South Africa. In: *Proceedings of the Geoterminology Workshop.* South Africa: SAICE, pp. 8-14.

Brink, ABA, 1979. *Engineering Geology of Southern Africa.* 1 ed. South Africa: Building Publications.

Bruijn, C. D., 1974. Moisture redistribution in Southern African soils. In: *Proceedings of the 8th International Conference on Soil Mechanics and Foundation Engineering.* Moscow: NBRI Reprint No R/Bou 442, pp. 37-44.

Chester, I & Duncan, JR, 1992. Soils and Foundations for architects and Engineers. In: *Reasons why water content changes.* New York: Pringer Science Business media, pp. 296-297.

Das, B., 2006. Principles of Geotechnical Engineering. In: K. R. Burrell, ed. *Principles of Geotechnical Engineering.* Canada: Chris Carson, pp. 1-2.

Das, B., 2008. Soil aggregate, Plasticity and classification. In: *Advanced Soil Mechanics.* New York: Taylor & Francis, pp. 4-8.

Day, P., 1991. Design of Raft foundations for houses on expansive clay using Lytton's method. *SAICE Structural Division,* Volume Course on design of foundation to suit various soil conditions, pp. 1-15.

Diop, S, Stapelberg, F, Tegegn K, Ngubelangaand, S & Heath L, 2011. General background and overview of problem soils in South Africa. In: *A review on Problem Soils in South Africa.* Cape Town: Council for Geoscience, pp. 5-18.

Explorer, S., n.d. *Botshabelo Climate.* [Online]
Available at: http://www.saexplorer.co.za/south-africa/climate/botshabelo_climate.asp
[Accessed 20 November 2013].

Field, 3., n.d. *Contour Maps - Create 2D and 3D Countour plots.* [Online]
Available at: 3dfmaps.com/
[Accessed 02 December 2015].

Fityus, SG, Smith, DW & Allman, MA, 2004. Expansive soil test site near Newcastle. In: *Journal of Geotechnical and Geoenvironmental Engineering.* s.l.:ASCE, pp. 686-695.

Frazer, RA & Wardle, LJ, 1975. The Analysis of Stiffened Raft Foundations on Expansive Soils. In: *Recent Developments in the Analysis of Soil Behaviour and their Application to Geotechnical Structures.* Australia: s.n., pp. 301-307.

Gupta, S., 1997. Types of raft foundations. In: *Raft foundations design and analysis with a practical approach .* India: ew age international (P) limited publishers, pp. 6-10.

Knappett JA, Craig RS, 2012. Basic characteristics of soils. In: *Craig's Soil Mechanics.* Eight edition ed. New York: Spon Press, pp. 3-5 .

Knappett JA, Craig RS, 2012. Shallow foundations. In: *Craig's Soil Mechanics.* New York: Spon Press, pp. 269-272.

Lytton, RL & Woodburn JA, 1973. Design and Performance of Mat Foundations on Expansive Clay. In: *Proceeding of the 3rd Int. Conf. on Expansive Soils.* s.l.:Haifa, pp. 301-307.

Materials, T. S. M. o. T. R. C., 1986. *asphalt.csir.co.za/tmh/.* [Online] Available at: asphalt.csir.co.za/tmh/ [Accessed 2 January 2013].

Miller, DJ, Durkee, DB, Chao, KC & Nelson, JD, 1995. Simplified heave prediction for expansive soils. In: *Unsaturated soils/sols Non Satures.* Roterdam: Balkema: lonso &Delage (eds).

Mitchell JK, (1993)(reproduced from *Fundamentals of Soil Behavior.* John Wiley & Sons, Inc.

Nelson, JD & Miller DJ, 1992. Identification and Classification of Expansive Soils. In: *Expansive Soils: Problems and practice in foundation and pavement engineering.* New york: John Wiley & Sons, Inc., pp. 40-44.

Nelson JD, 2015. Soil Suction. In: *Foundation Engineering.* USA: John Wiley & Sons, Inc., pp. 74-86.

NHBRC, 1999. Design and construction requirements. In: *Home building manual.* s.l.:NHBRC, pp. 7-20.

Oosthuizen, AC & Richardson, S, 2011. Mechanism of sinkhole formation. In: *Sinkholes and subsidence in South Africa.* Cape Town: Council for Geoscience, pp. 1-8.

Pidgeon, JT & Pellissier, JP, 1987. The behaviour of an L-shaped raft subjected to non-uniform support conditions. In: *International Conference on Soil Structure Interactions.* Paris: ENPC Press.

Pidgeon, J., 1980. The rational design of raft foundations for houses on heaving soil. In: *Seventh Regional Conference for African Soil Mechanics and Foundation Engineering .* South Africa: ACCRA, pp. 291-299.

Pidgeon, J., 1987. he results of a large scale field experiment aimed at studying the interaction of raft foundations and expansive soils. In: *nternational Conference on soil structure Interactions.* Paris: ENPC Press.

PTI, 2008. Design and Construction of PostTensioned. In: *Standard Requirements for Design of Shallow Post Tensioned.* s.l.:s.n.

RL, L., 1972. Design methods for concrete mats on unstable soils. In: *Proc 3rd Inter- American Confrence on Materials Technology.* Brazil: s.n., pp. 171-177.

Rogers, JD Olshansky, R & Rogers, RB, 1985. Damage to foundations for expansive soils. In: *Submitted to Ground Failure, National Research Council.* Washington D.C. : s.n.

Savange, P., 2007. Evaluation of Possible Swelling Potential of Soil. In: *Proceedings of the 26th Southern African Transport Conference.* Pretoria: Produced by: Document Transformation Technologies cc , pp. 277-283.

Smith ,GN & Smith, Ian GN , 1995. In: *Elements of soil mechanics.* England: Blackwell science.

Space, C. R., 2010. *Maximising the sun.* [Online]
Available at:
researchspace.csir.co.za/dspace/bitstream/10204/7519/1/Conradie_2010.pdf
[Accessed 4 December 2015].

USA, D. o. t. A., 1983. Technical Manual TM 5-818-7. In: *Foundations in Expansive Soils.* Washington. DC.: s.n.

Van der Merwe, D., 1964. The prediction of heave from the Plasticity Index and the percentage clay fraction. In: *he Civil Engineer in South Africa Vol.6.No.6.* South Africa: s.n.

Vanapalli, S & Fredlund, D, 2000. Comparison of Different Procedures to Predict Unsaturated Soil Shear Strength. In: C. D. Shackelford, S. L. Houston & a. N. Chang, eds. *Advances in Unsaturated Geotechnics.* s.l.:ASCE, pp. 195-209.

Velde, B., 1995. Composition and mineralogy of clay minerals. In: *Origin and mineralogy of clays.* New York: Springer-Verlag, pp. 8-20.

Whitlow, R., 1995. Bearing capacity of foundations. In: *Basic soil mechanics.* England: Longman group limited, pp. 449-450.

Zerizghy, MG, van Rensburg, LD & Anderson, JJ, 2013. Comparison of neutron probes and DFM capacitance instruments in measuring soil water evaporation. In: *Water SA vol.39.* Pretoria: s.n.

APPENDIX: A

Moisture content summary tables per month

Probe: 24010						
	150mm	300mm	450mm	600mm	800mm	1000mm
Jan-14	24,6%	26,9%	27,9%	28,2%	28,4%	28,0%
Feb-14	24,6%	26,9%	27,9%	28,2%	28,4%	28,1%
Mar-14	24,6%	26,8%	27,8%	28,2%	28,4%	28,1%
Apr-14	24,7%	26,8%	27,7%	28,1%	28,3%	28,0%
May-14	24,7%	26,8%	27,6%	28,0%	28,2%	27,9%
Jun-14	24,7%	26,7%	27,5%	27,8%	28,1%	27,8%
Jul-14	24,7%	26,6%	27,4%	27,8%	28,1%	27,7%
Aug-14	24,8%	26,7%	27,5%	27,8%	28,1%	27,8%
Sep-14	24,9%	27,0%	27,6%	27,9%	28,2%	27,8%
Oct-14	24,9%	26,8%	27,6%	28,0%	28,2%	27,8%
Nov-14	24,9%	26,8%	27,7%	28,1%	28,3%	27,9%
Dec-14	24,9%	26,9%	27,8%	28,1%	28,4%	27,9%
Jan-15	24,9%	26,9%	27,9%	28,3%	28,5%	28,0%
Feb-15	24,9%	26,9%	27,9%	28,3%	28,5%	28,0%
Mar-15	24,8%	26,9%	27,9%	28,2%	28,5%	27,9%
Apr-15	24,8%	26,8%	27,8%	28,1%	28,4%	27,9%
May-15	24,7%	26,7%	27,8%	28,1%	28,3%	27,8%
Jun-15	24,6%	26,6%	27,7%	28,0%	28,2%	27,8%
Jul-15	24,6%	26,5%	27,7%	27,9%	28,2%	27,7%
Aug-15	24,9%	26,6%	27,8%	28,0%	28,2%	27,7%
Sep-15	24,9%	26,7%	27,9%	28,1%	28,3%	27,8%
Oct-15	25,0%	26,8%	28,0%	28,2%	28,4%	27,9%
Nov-15	24,9%	26,9%	28,1%	28,3%	28,5%	27,9%
Dec-15	25,0%	27,0%	28,2%	28,4%	28,6%	28,0%

APPENDIX A- Table 1- Summary of moisture content data for probe 24010

Probe: 24008						
	150mm	300mm	450mm	600mm	800mm	1000mm
Jan-14	26,2%	28,6%	28,4%	28,8%	29,0%	29,0%
Feb-14	26,4%	28,6%	28,4%	28,8%	29,0%	29,1%
Mar-14	26,5%	28,4%	28,4%	28,8%	29,0%	29,0%
Apr-14	26,5%	28,3%	28,2%	28,7%	28,9%	29,0%
May-14	26,6%	28,2%	28,1%	28,6%	28,9%	28,9%
Jun-14	26,6%	28,1%	28,0%	28,5%	28,8%	28,8%
Jul-14	26,8%	28,0%	28,0%	28,4%	28,7%	28,8%
Aug-14	26,9%	28,1%	28,0%	28,5%	28,7%	28,8%
Sep-14	26,9%	28,2%	28,1%	28,5%	28,8%	28,8%
Oct-14	26,7%	28,3%	28,2%	28,6%	28,8%	28,9%
Nov-14	26,3%	28,4%	28,3%	28,7%	28,9%	29,0%
Dec-14	26,3%	28,5%	28,4%	28,8%	29,0%	29,0%
Jan-15	26,4%	28,6%	28,5%	28,8%	29,1%	29,1%
Feb-15	26,4%	28,6%	28,4%	28,8%	29,1%	29,1%
Mar-15	26,3%	28,5%	28,4%	28,8%	29,0%	29,1%
Apr-15	26,3%	28,4%	28,3%	28,7%	29,0%	29,0%
May-15	26,0%	28,4%	28,3%	28,7%	28,9%	29,0%
Jun-15	26,0%	28,2%	28,2%	28,6%	28,9%	28,9%
Jul-15	26,1%	28,2%	28,2%	28,5%	28,8%	28,9%
Aug-15	26,1%	28,3%	28,2%	28,5%	28,8%	28,9%
Sep-15	26,4%	28,4%	28,4%	28,6%	28,9%	28,9%
Oct-15	26,4%	28,6%	28,5%	28,7%	29,0%	29,0%
Nov-15	26,3%	28,6%	28,5%	28,8%	29,1%	29,1%
Dec-15	26,4%	28,8%	28,7%	29,0%	29,2%	29,3%

APPENDIX A- Table 2- Summary of moisture content data for probe 24008

Probe: 24007						
	150mm	300mm	450mm	600mm	800mm	1000mm
Jan-14	22,7%	24,5%	24,3%	25,3%	25,3%	25,4%
Feb-14	22,7%	24,5%	24,3%	25,3%	25,3%	25,4%
Mar-14	22,7%	24,5%	24,3%	25,2%	25,3%	25,4%
Apr-14	22,6%	24,4%	24,3%	25,2%	25,3%	25,4%
May-14	22,5%	24,4%	24,4%	25,1%	25,2%	25,3%
Jun-14	22,4%	24,3%	24,5%	25,0%	25,1%	25,2%
Jul-14	22,4%	24,2%	24,6%	24,9%	25,0%	25,2%
Aug-14	22,4%	24,2%	24,6%	24,9%	25,0%	25,2%
Sep-14	22,4%	24,2%	24,6%	24,9%	25,1%	25,2%
Oct-14	22,5%	24,3%	24,5%	25,0%	25,1%	25,2%
Nov-14	22,5%	24,4%	24,5%	25,1%	25,2%	25,3%
Dec-14	22,6%	24,5%	24,4%	25,2%	25,3%	25,4%
Jan-15	22,7%	24,5%	24,4%	25,3%	25,4%	25,5%
Feb-15	22,7%	24,5%	24,4%	25,3%	25,4%	25,5%
Mar-15	22,6%	24,5%	24,4%	25,2%	25,4%	25,5%
Apr-15	22,5%	24,4%	24,3%	25,2%	25,3%	25,4%
May-15	22,5%	24,4%	24,3%	25,1%	25,2%	25,4%
Jun-15	22,4%	24,3%	24,2%	25,0%	25,2%	25,3%
Jul-15	22,4%	24,3%	24,1%	24,9%	25,1%	25,3%
Aug-15	22,4%	24,3%	24,2%	25,0%	25,1%	25,3%
Sep-15	22,5%	24,4%	24,3%	25,1%	25,2%	25,3%
Oct-15	22,7%	24,5%	24,4%	25,2%	25,3%	25,4%
Nov-15	22,7%	24,6%	24,5%	25,3%	25,4%	25,5%
Dec-15	22,8%	24,7%	24,6%	25,3%	25,4%	25,5%

APPENDIX A- Table 3- Summary of moisture content data for probe 24007

Probe: 24005						
	150mm	300mm	450mm	600mm	800mm	1000mm
Jan-14	32,1%	34,0%	32,0%	34,3%	34,1%	34,0%
Feb-14	32,3%	34,1%	32,1%	34,4%	34,2%	34,2%
Mar-14	32,1%	33,9%	32,0%	34,3%	34,2%	34,2%
Apr-14	31,8%	33,6%	31,9%	34,1%	34,1%	34,0%
May-14	31,5%	33,2%	31,7%	33,8%	33,8%	33,7%
Jun-14	31,1%	32,8%	31,4%	33,5%	33,5%	33,3%
Jul-14	31,0%	32,5%	31,2%	33,3%	33,3%	32,9%
Aug-14	31,1%	32,6%	31,3%	33,3%	33,4%	32,8%
Sep-14	31,4%	33,0%	31,7%	33,6%	33,6%	32,9%
Oct-14	31,6%	33,3%	32,0%	33,9%	33,8%	33,1%
Nov-14	31,8%	33,5%	32,2%	34,1%	34,1%	33,3%
Dec-14	32,0%	33,8%	32,6%	34,4%	34,3%	33,5%
Jan-15	32,3%	34,1%	32,8%	34,7%	34,6%	33,7%
Feb-15	32,2%	34,0%	32,8%	34,6%	34,7%	33,8%
Mar-15	32,1%	33,9%	32,7%	34,5%	34,5%	33,7%
Apr-15	31,8%	33,6%	32,5%	34,3%	34,3%	33,5%
May-15	31,7%	33,5%	32,3%	34,2%	34,2%	33,4%
Jun-15	31,4%	33,1%	32,1%	33,9%	34,0%	33,1%
Jul-15	31,4%	33,0%	31,9%	33,8%	33,8%	32,9%
Aug-15	31,6%	33,2%	32,0%	33,8%	33,8%	32,9%
Sep-15	31,9%	33,5%	32,3%	34,1%	34,0%	33,1%
Oct-15	32,4%	34,0%	32,9%	34,6%	34,5%	33,4%
Nov-15	32,5%	34,1%	32,9%	34,7%	34,5%	33,7%
Dec-15	32,8%	34,4%	33,2%	34,9%	34,8%	33,9%

APPENDIX A- Table 4- Summary of moisture content data for probe 24005

Probe: 23998						
	150mm	300mm	450mm	600mm	800mm	1000mm
Jan-14	9,8%	6,8%	26,2%	18,4%	24,3%	26,6%
Feb-14	9,9%	6,8%	26,4%	18,6%	24,6%	26,8%
Mar-14	9,9%	6,6%	26,4%	18,8%	24,8%	26,9%
Apr-14	14,3%	6,3%	27,6%	24,9%	27,2%	25,3%
May-14	15,4%	5,5%	27,5%	25,5%	27,4%	24,9%
Jun-14	15,7%	4,6%	27,2%	25,4%	27,2%	24,5%
Jul-14	12,4%	4,0%	26,5%	22,4%	27,4%	25,3%
Aug-14	10,0%	4,1%	26,3%	22,8%	27,7%	26,4%
Sep-14	10,0%	4,8%	26,5%	26,3%	27,4%	26,4%
Oct-14	10,2%	5,4%	26,7%	26,5%	27,3%	26,5%
Nov-14	10,2%	5,7%	26,9%	23,8%	27,3%	26,7%
Dec-14	10,4%	6,1%	27,0%	24,8%	27,3%	26,8%
Jan-15	10,5%	6,8%	27,1%	21,2%	27,5%	27,1%
Feb-15	10,5%	7,0%	27,1%	21,2%	26,6%	27,2%
Mar-15	10,5%	6,8%	27,1%	21,2%	26,4%	27,3%
Apr-15	10,4%	6,2%	26,9%	21,1%	26,3%	27,2%
May-15	10,3%	5,8%	26,8%	21,0%	26,2%	27,1%
Jun-15	10,2%	5,3%	26,7%	20,9%	26,1%	27,0%
Jul-15	10,1%	4,5%	26,4%	20,7%	25,9%	26,8%
Aug-15	10,4%	4,5%	26,5%	21,0%	25,7%	26,7%
Sep-15	10,6%	5,1%	26,8%	21,2%	25,9%	26,9%
Oct-15	10,9%	6,0%	27,1%	21,4%	26,1%	27,1%
Nov-15	10,9%	6,3%	27,3%	21,6%	26,3%	27,4%
Dec-15	11,1%	7,0%	27,5%	21,8%	26,5%	27,6%

APPENDIX A- Table 5- Summary of moisture content data for probe 23998

Probe: 24004						
	150mm	300mm	450mm	600mm	800mm	1000mm
Jan-14	14,4%	20,7%	27,9%	25,5%	27,3%	25,1%
Feb-14	14,7%	20,8%	28,0%	25,7%	27,5%	25,3%
Mar-14	14,9%	20,8%	28,0%	25,8%	27,6%	25,3%
Apr-14	15,1%	20,7%	28,0%	25,8%	27,7%	25,3%
May-14	15,6%	20,7%	27,7%	25,8%	27,6%	25,1%
Jun-14	15,9%	20,5%	27,4%	25,6%	27,4%	24,7%
Jul-14	15,5%	20,3%	27,1%	25,4%	27,2%	24,3%
Aug-14	15,9%	20,5%	27,1%	25,5%	27,2%	24,2%
Sep-14	16,5%	21,1%	27,4%	25,7%	27,4%	24,4%
Oct-14	16,2%	21,1%	27,6%	26,0%	27,6%	24,5%
Nov-14	16,1%	21,0%	27,6%	26,1%	27,7%	24,7%
Dec-14	16,0%	21,0%	27,7%	26,2%	27,7%	24,7%
Jan-15	16,1%	21,3%	27,9%	26,4%	27,9%	25,0%
Feb-15	16,1%	21,3%	28,0%	26,5%	28,0%	25,2%
Mar-15	16,0%	21,3%	27,9%	26,5%	28,0%	25,3%
Apr-15	15,8%	21,1%	27,7%	26,3%	27,8%	25,1%
May-15	15,6%	21,0%	27,6%	26,2%	27,7%	25,0%
Jun-15	15,3%	20,7%	27,3%	25,9%	27,5%	24,7%
Jul-15	15,1%	20,6%	27,2%	25,8%	27,3%	24,5%
Aug-15	15,3%	20,9%	27,4%	26,0%	27,5%	24,7%
Sep-15	15,7%	21,3%	27,9%	26,5%	27,9%	25,0%
Oct-15	15,8%	21,4%	28,0%	26,7%	28,0%	25,2%
Nov-15	15,3%	21,2%	28,2%	26,8%	28,2%	25,4%
Dec-15	14,2%	20,5%	28,2%	27,0%	28,4%	25,6%

APPENDIX A- Table 6- Summary of moisture content data for probe 24004

Probe: 24003						
	150mm	300mm	450mm	600mm	800mm	1000mm
Jan-14	25,0%	25,6%	29,2%	29,5%	29,8%	29,0%
Feb-14	25,0%	25,6%	29,2%	29,6%	29,8%	29,0%
Mar-14	25,0%	25,5%	29,1%	29,6%	29,8%	29,0%
Apr-14	25,0%	25,6%	29,1%	29,5%	29,8%	29,0%
May-14	24,9%	25,8%	29,0%	29,5%	29,8%	29,0%
Jun-14	24,9%	25,8%	28,9%	29,4%	29,7%	28,8%
Jul-14	24,9%	25,7%	28,8%	29,3%	29,7%	28,7%
Aug-14	24,9%	25,8%	28,8%	29,3%	29,7%	28,7%
Sep-14	24,5%	25,3%	27,9%	28,7%	29,3%	29,2%
Oct-14	24,1%	24,8%	26,9%	28,0%	29,0%	29,7%
Nov-14	24,2%	24,8%	26,7%	28,4%	28,8%	29,7%
Dec-14	24,1%	24,5%	26,0%	27,8%	28,7%	29,6%
Jan-15	24,2%	24,6%	25,8%	27,4%	28,7%	29,6%
Feb-15	24,2%	24,6%	25,8%	27,4%	28,7%	29,6%
Mar-15	24,2%	24,6%	26,1%	27,7%	28,7%	29,7%
Apr-15	24,1%	24,5%	25,7%	27,1%	28,6%	29,4%
May-15	24,1%	24,5%	25,6%	27,1%	28,6%	29,4%
Jun-15	24,1%	24,5%	25,5%	27,0%	28,5%	29,3%
Jul-15	24,1%	24,5%	25,5%	27,0%	28,4%	29,2%
Aug-15	24,1%	24,5%	25,4%	26,9%	28,4%	29,2%
Sep-15	24,1%	24,5%	25,6%	27,2%	28,5%	29,3%
Oct-15	24,2%	24,6%	25,7%	27,3%	28,6%	29,4%
Nov-15	24,2%	24,6%	25,8%	27,4%	28,7%	29,4%
Dec-15	24,3%	24,7%	25,7%	27,3%	28,7%	29,5%

APPENDIX A- Table 7- Summary of moisture content data for probe 24003

Probe: 24009						
	150mm	300mm	450mm	600mm	800mm	1000mm
Jan-14	21,3%	24,3%	25,5%	26,2%	26,7%	26,8%
Feb-14	21,4%	24,4%	25,5%	26,2%	26,7%	26,8%
Mar-14	21,4%	24,4%	25,5%	26,2%	26,7%	26,8%
Apr-14	21,4%	24,4%	25,5%	26,2%	26,7%	26,8%
May-14	21,3%	24,4%	25,4%	26,1%	26,7%	26,8%
Jun-14	21,3%	24,5%	25,3%	26,1%	26,6%	26,7%
Jul-14	21,3%	24,4%	25,3%	26,0%	26,5%	26,6%
Aug-14	21,3%	24,8%	25,3%	26,0%	26,5%	26,6%
Sep-14	21,6%	24,8%	25,5%	26,1%	26,6%	26,5%
Oct-14	22,4%	24,0%	26,1%	26,1%	26,6%	26,1%
Nov-14	22,2%	23,9%	25,9%	26,1%	26,7%	26,4%
Dec-14	21,6%	24,7%	25,6%	26,3%	26,8%	26,8%
Jan-15	21,6%	24,7%	25,6%	26,4%	26,8%	26,9%
Feb-15	21,6%	24,7%	25,6%	26,4%	26,9%	26,9%
Mar-15	21,6%	24,7%	25,6%	26,4%	26,8%	26,9%
Apr-15	21,5%	24,6%	25,6%	26,3%	26,8%	26,9%
May-15	21,5%	24,6%	25,5%	26,3%	26,8%	26,8%
Jun-15	21,5%	24,5%	25,5%	26,2%	26,7%	26,8%
Jul-15	21,4%	24,5%	25,4%	26,2%	26,6%	26,7%
Aug-15	21,6%	24,6%	25,5%	26,2%	26,7%	26,7%
Sep-15	21,7%	24,6%	25,6%	26,3%	26,8%	26,8%
Oct-15	21,8%	24,8%	25,7%	26,4%	26,8%	26,9%
Nov-15	21,8%	24,8%	25,8%	26,5%	26,9%	26,9%
Dec-15	21,9%	24,9%	25,8%	26,5%	27,0%	27,0%

APPENDIX A- Table 8- Summary of moisture content data for probe 24009

APPENDIX: B

Graphs of average temperatures over time

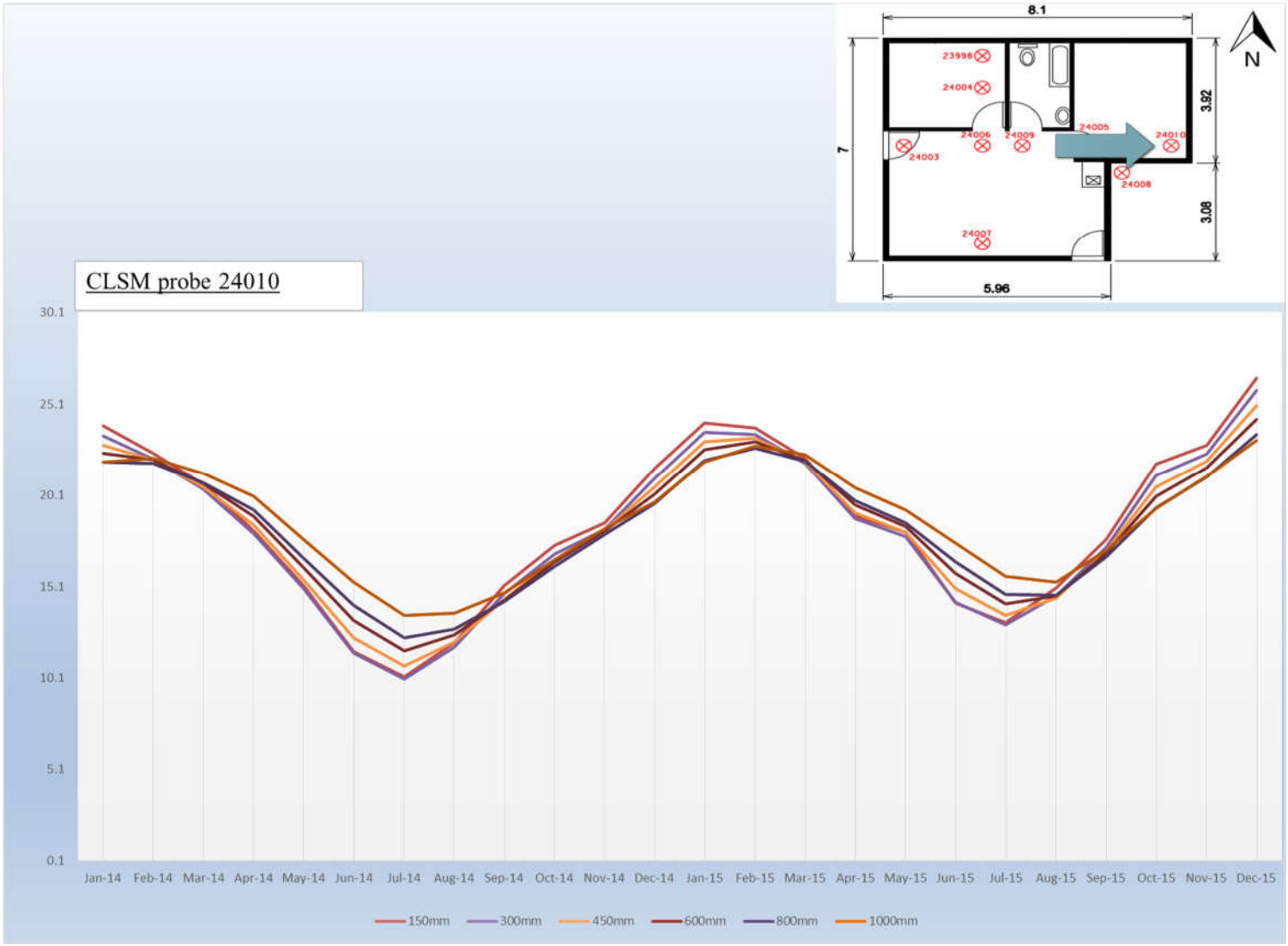

APPENDIX B- Figure 1- Graph of temperature over time for probe 24010

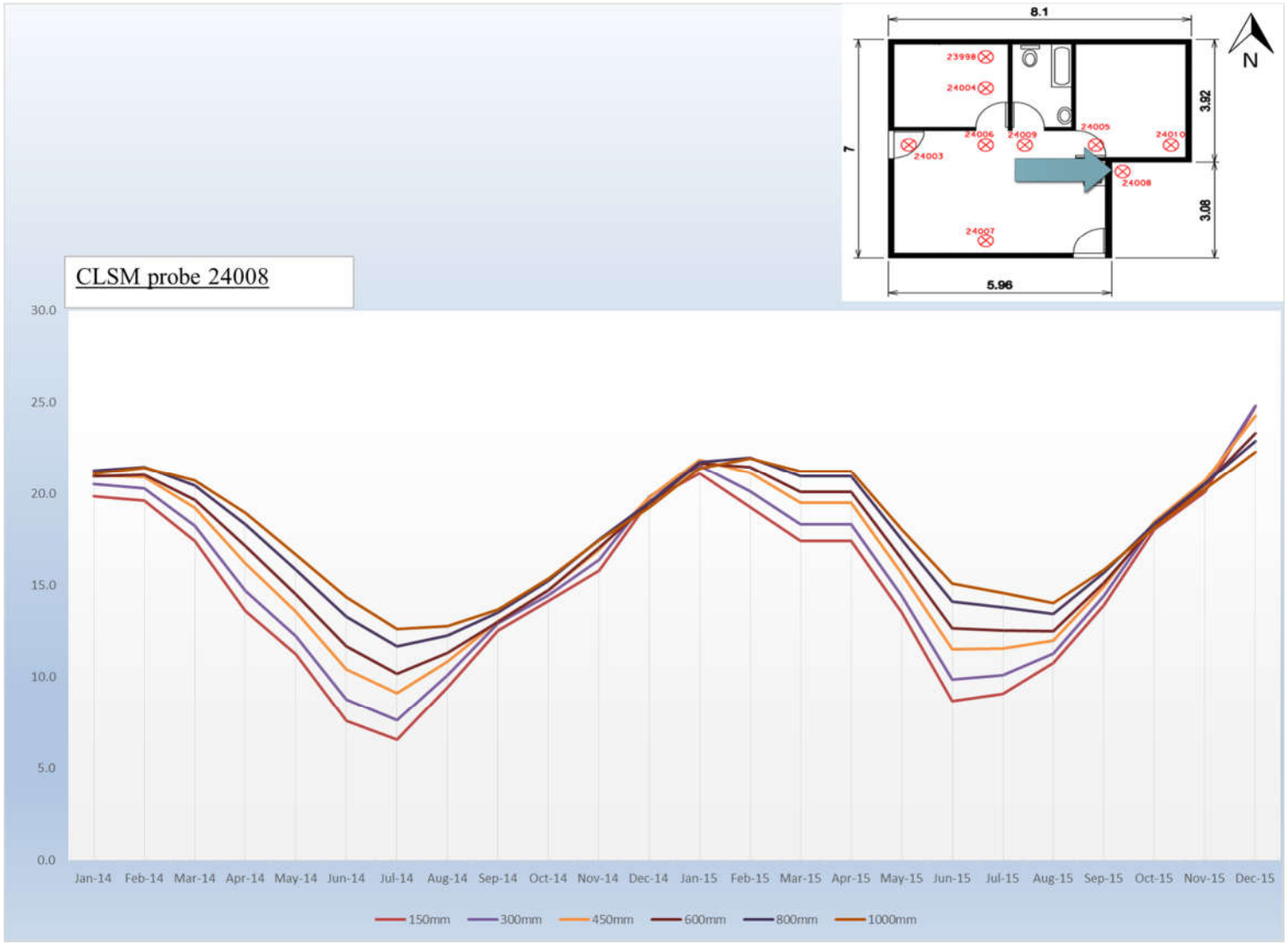

APPENDIX B- Figure 2- Graph of temperature over time for probe 24008

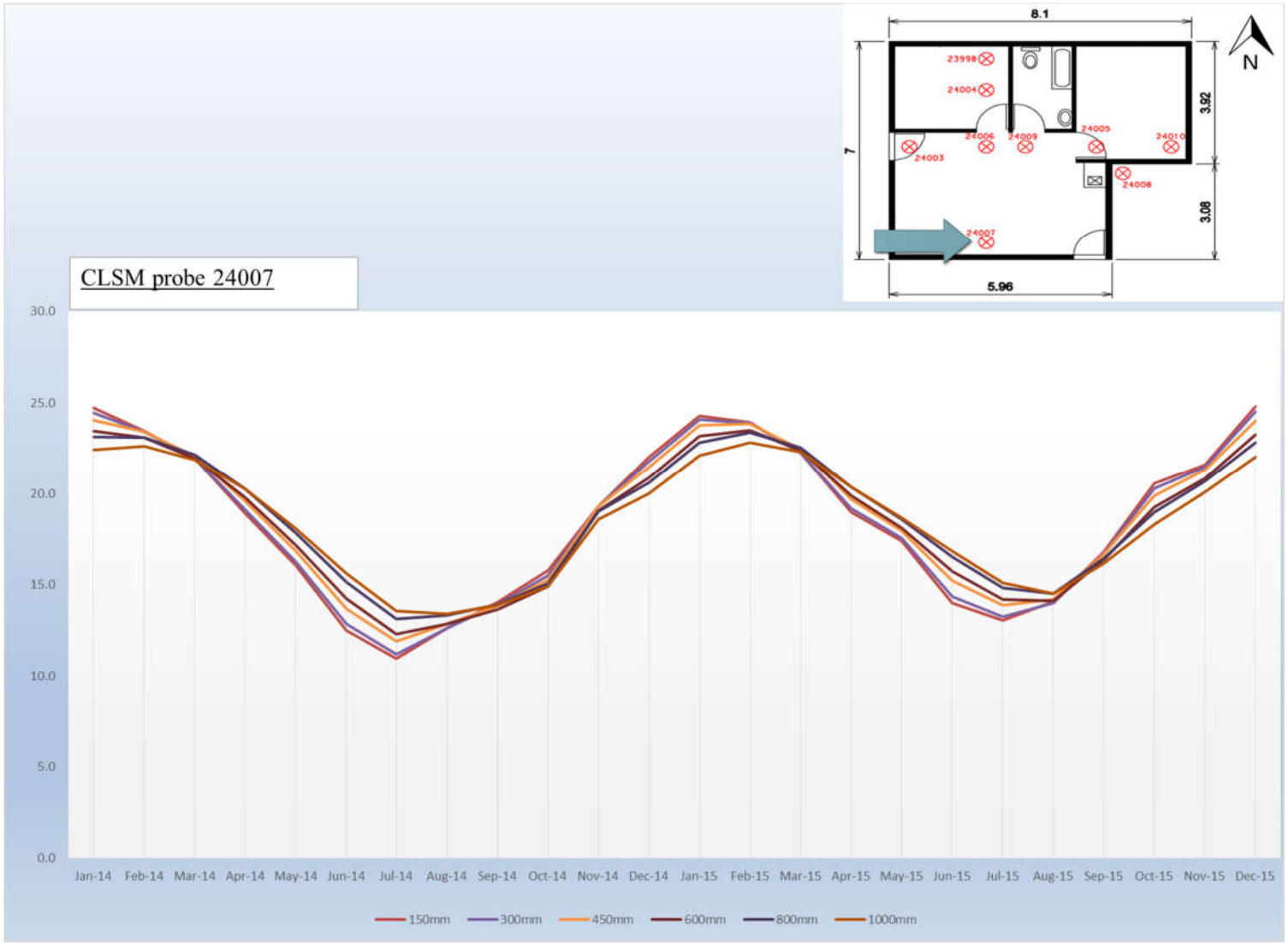

APPENDIX B- Figure 3- Graph of temperature over time for probe 24007

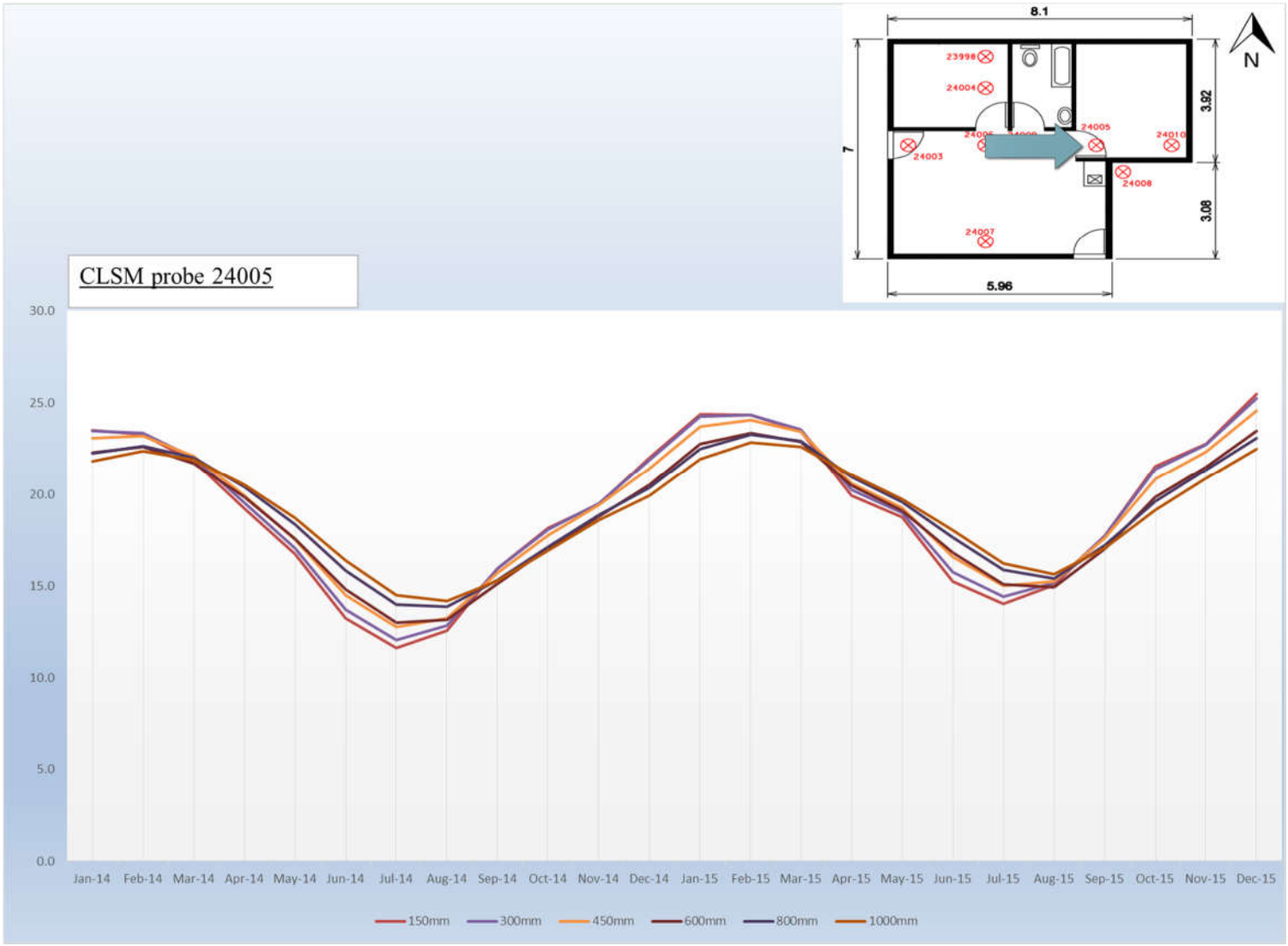

APPENDIX B- Figure 4- Graph of temperature over time for probe 24005

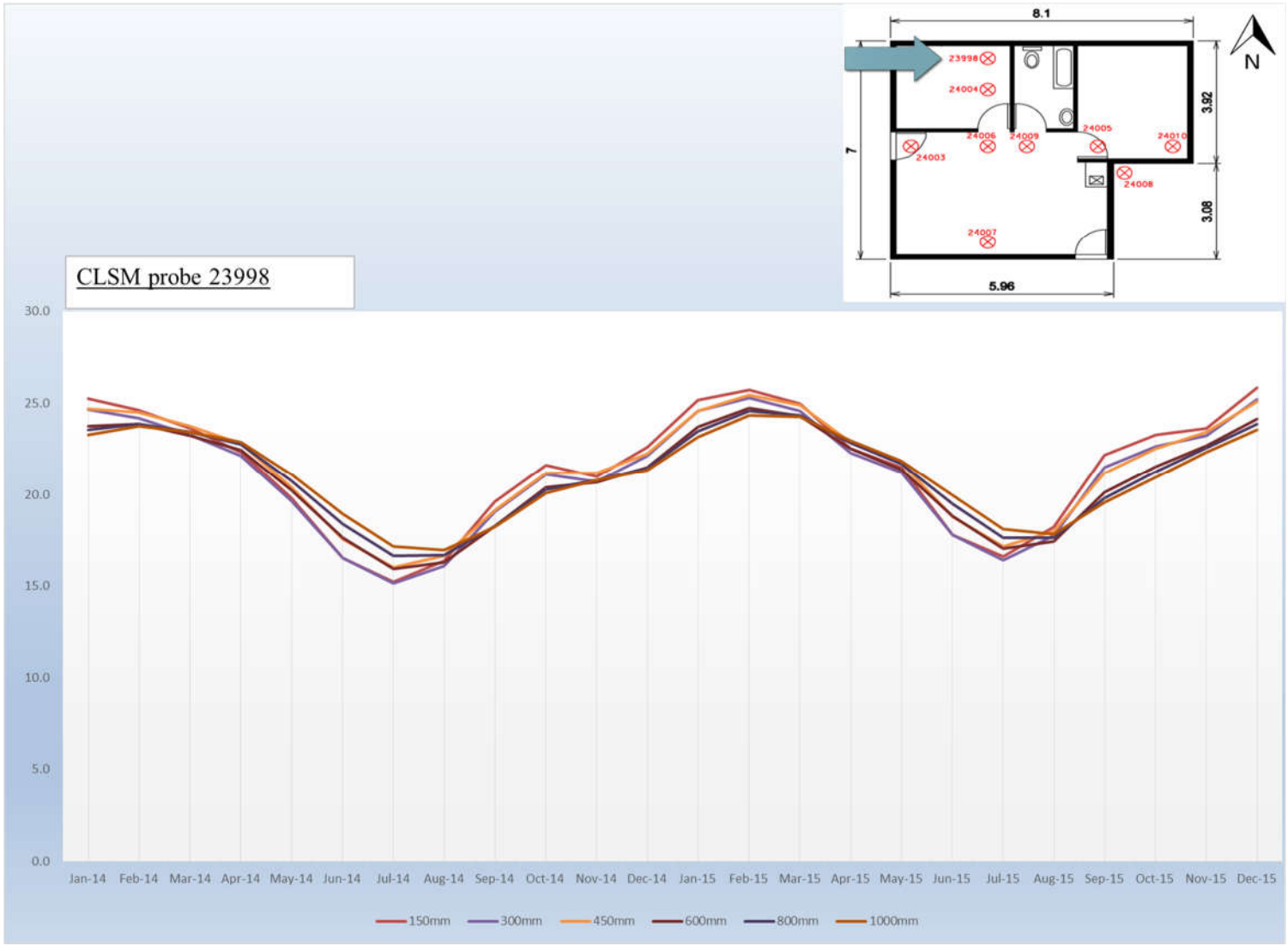

APPENDIX B- Figure 5- Graph of temperature over time for probe 23998

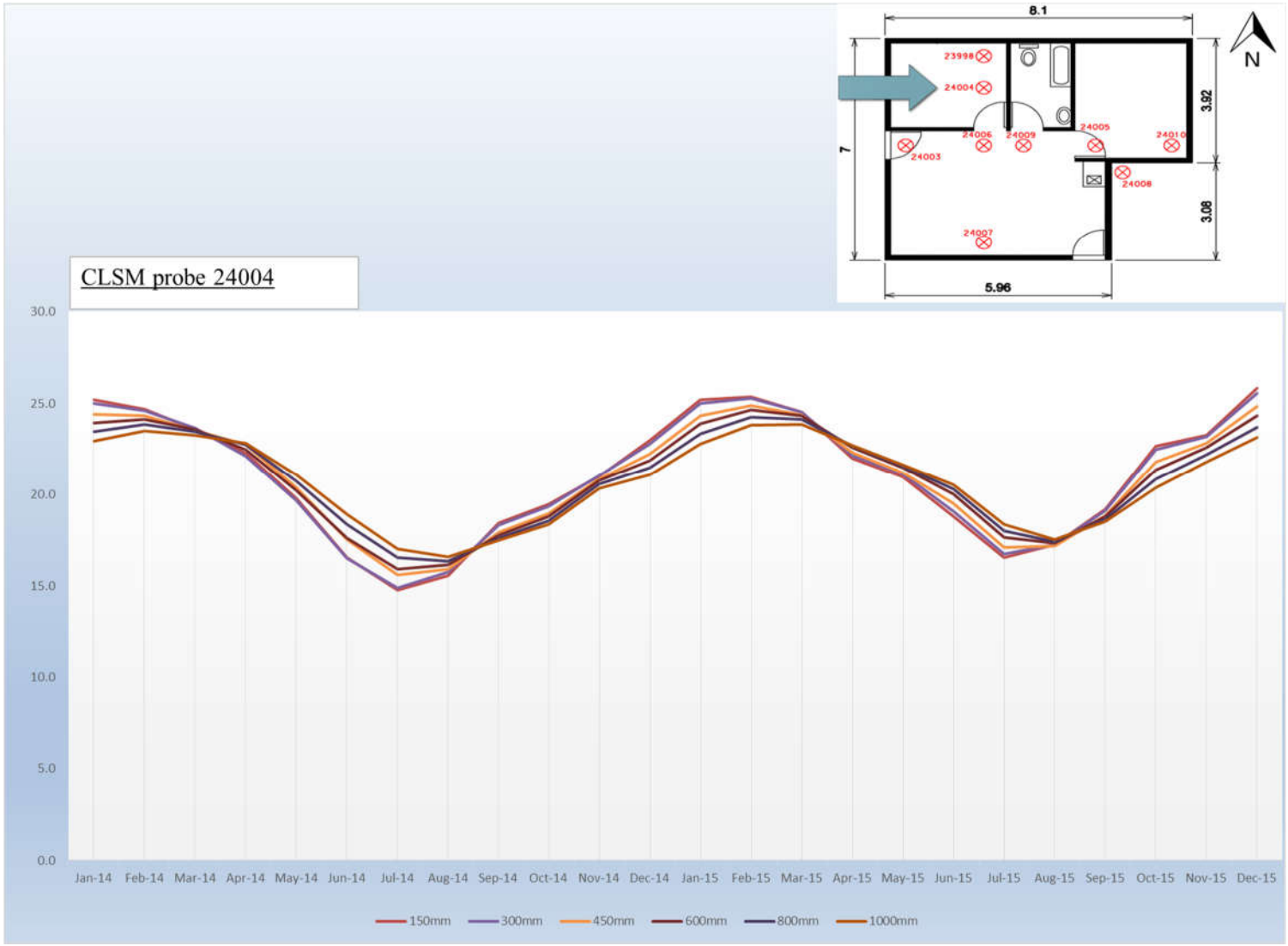

APPENDIX B- Figure 6- Graph of temperature over time for probe 24004

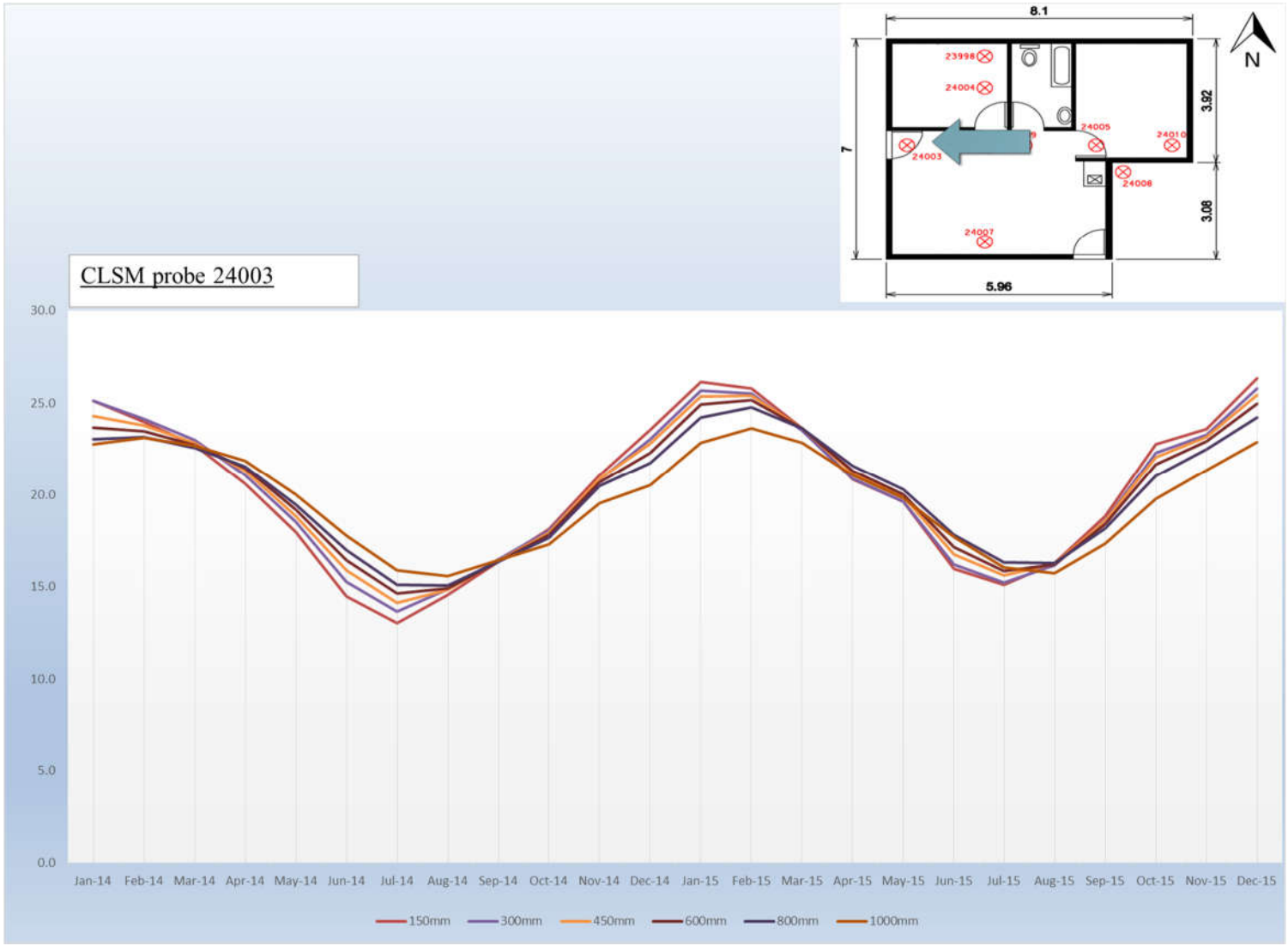

APPENDIX B- Figure 7- Graph of temperature over time for probe 24003

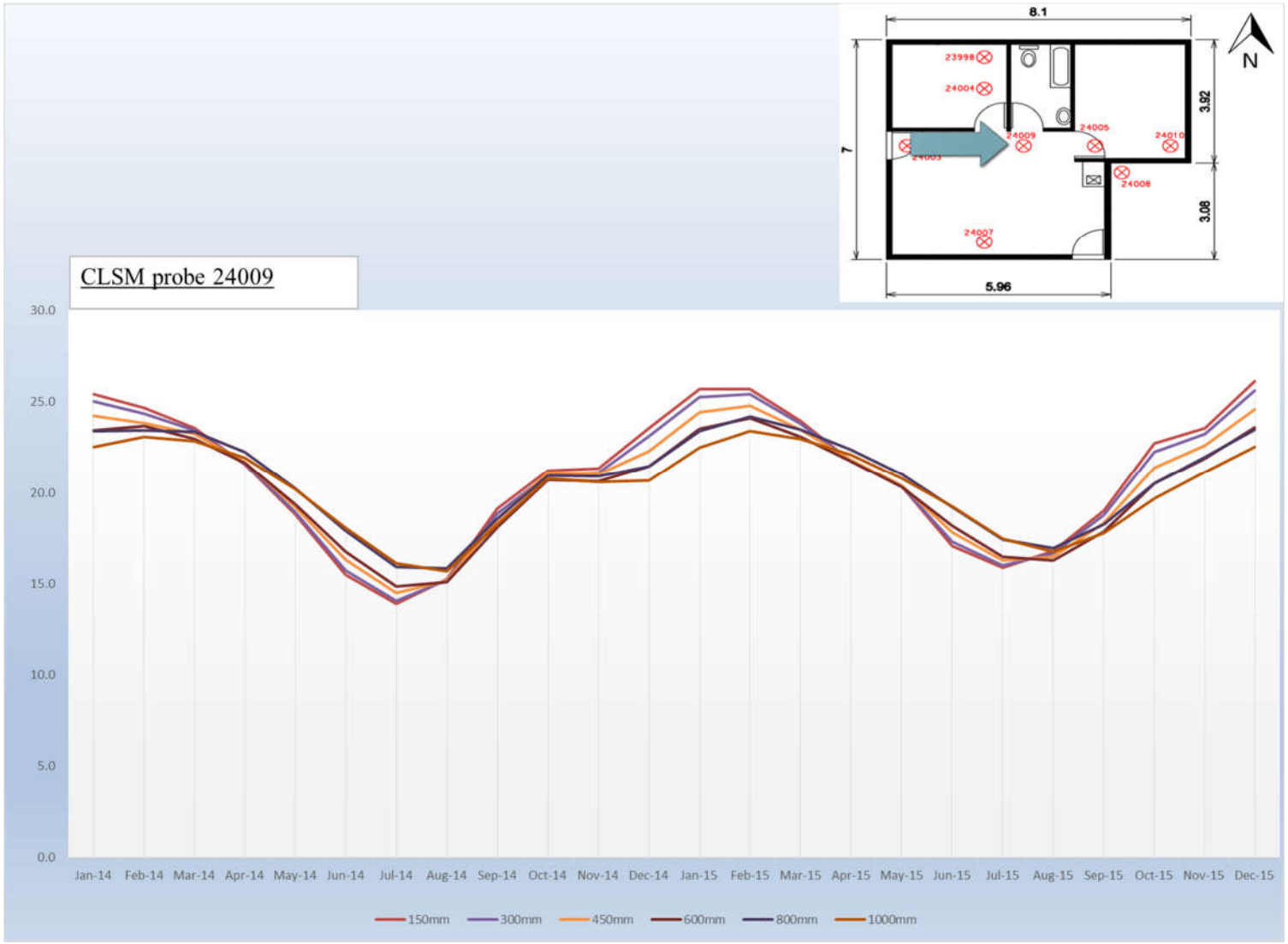

APPENDIX B- Figure 8- Graph of temperature over time for probe 24009

APPENDIX: C

Moisture content change at specific depths for all CLSM probes

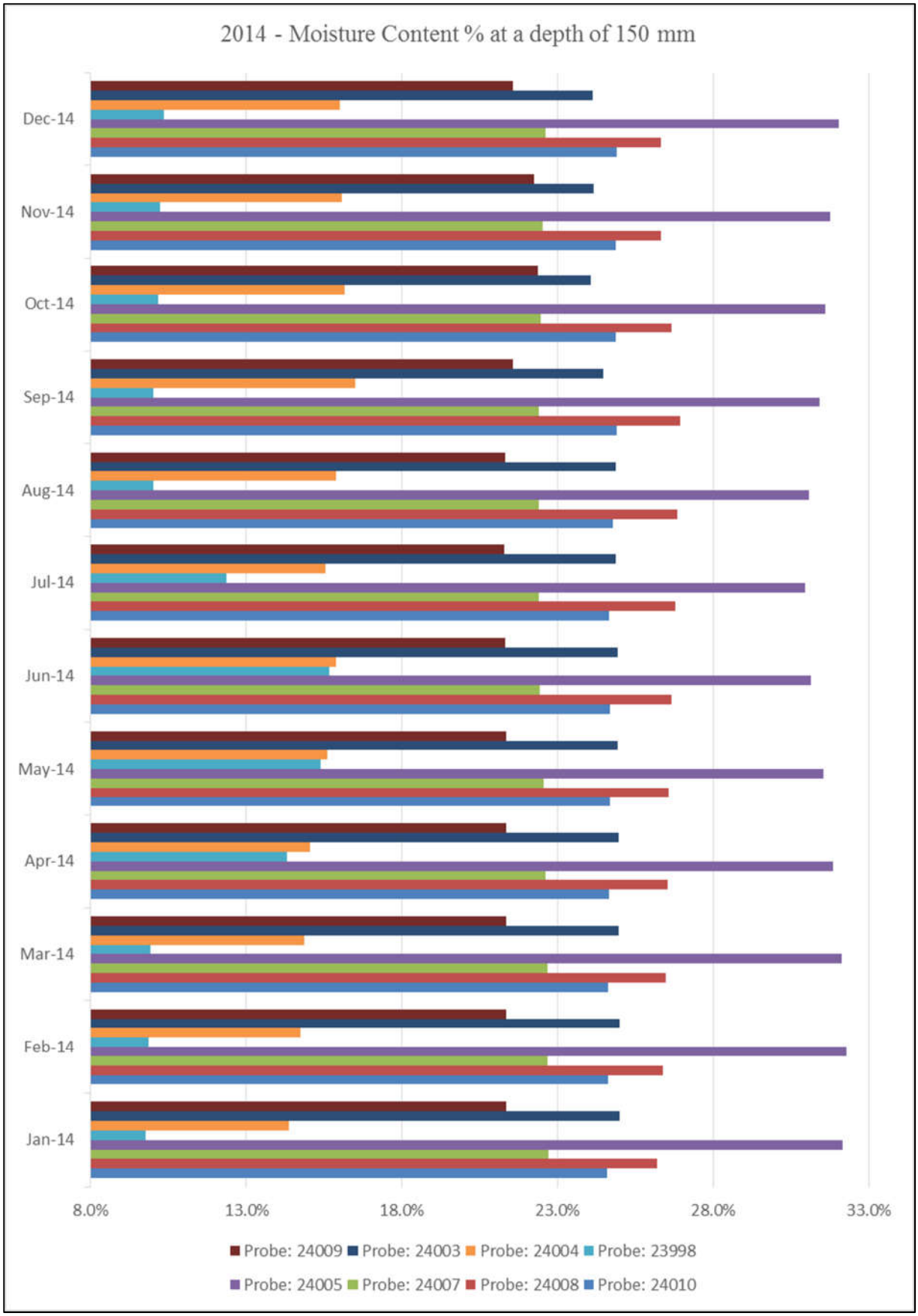

APPENDIX C - Figure: 1 – Moisture content at a depth of 150mm for 2014

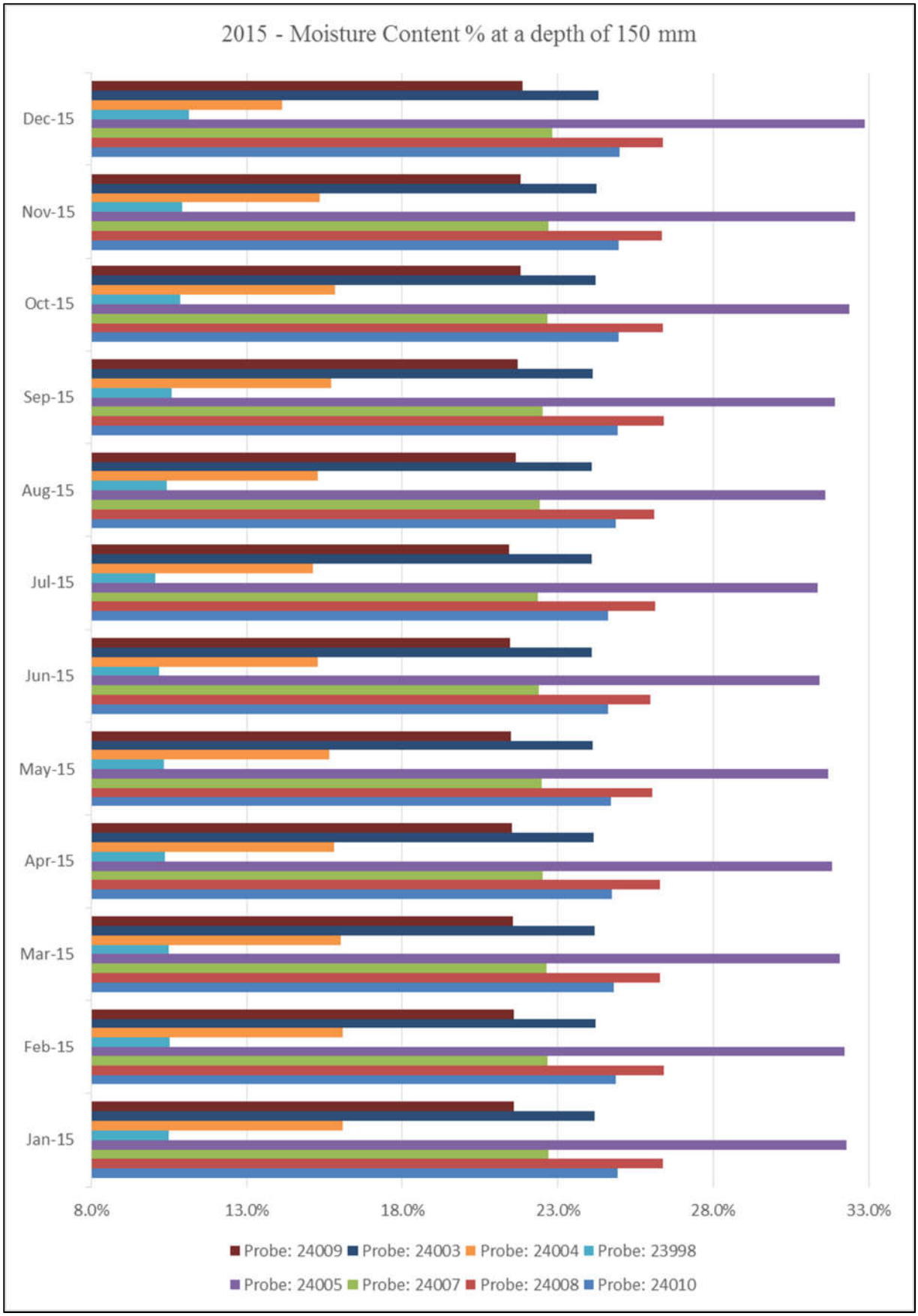

APPENDIX C - Figure: 2– Moisture content at a depth of 150mm for 2015

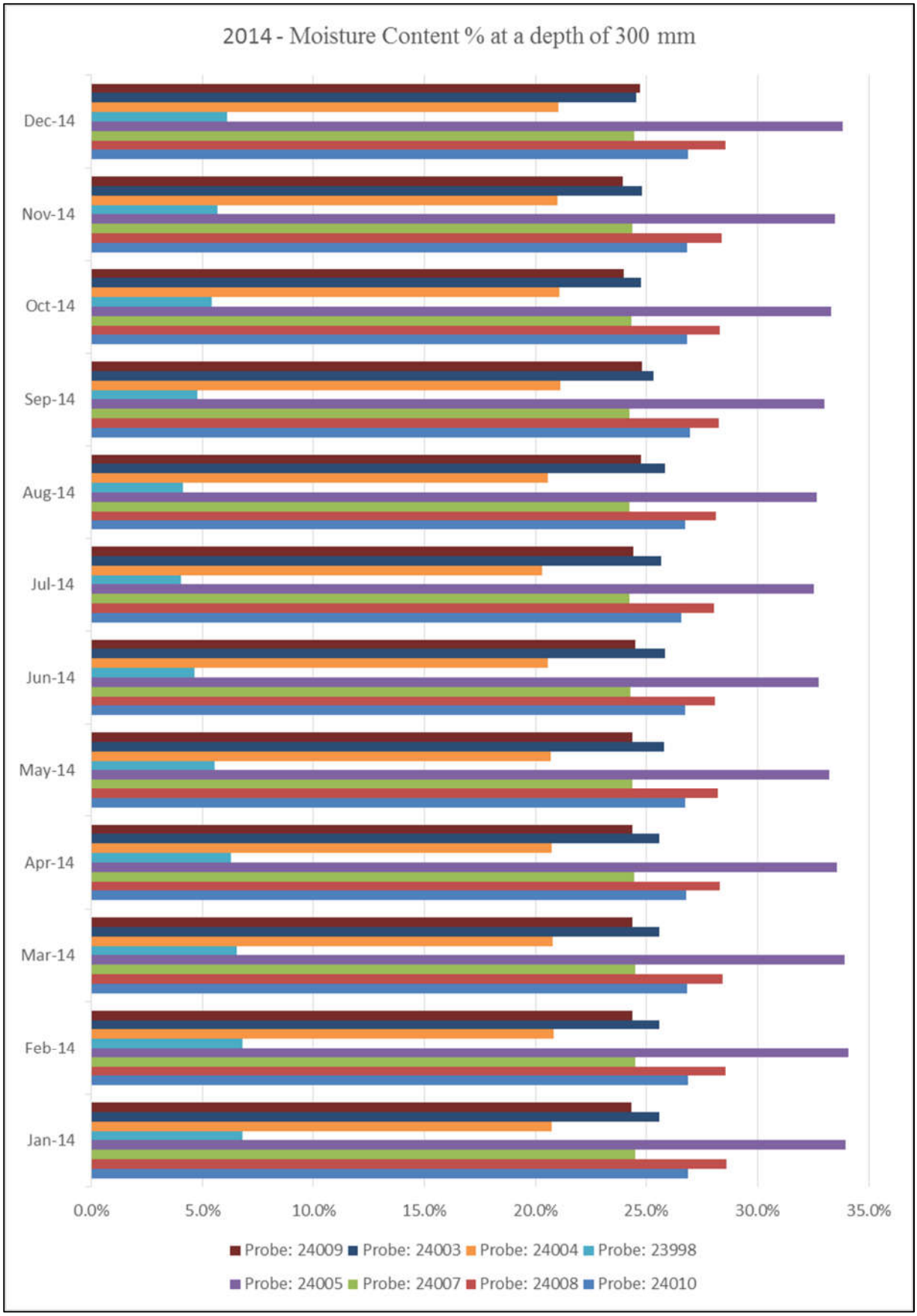

APPENDIX C - Figure: 3– Moisture content at a depth of 300mm for 2014

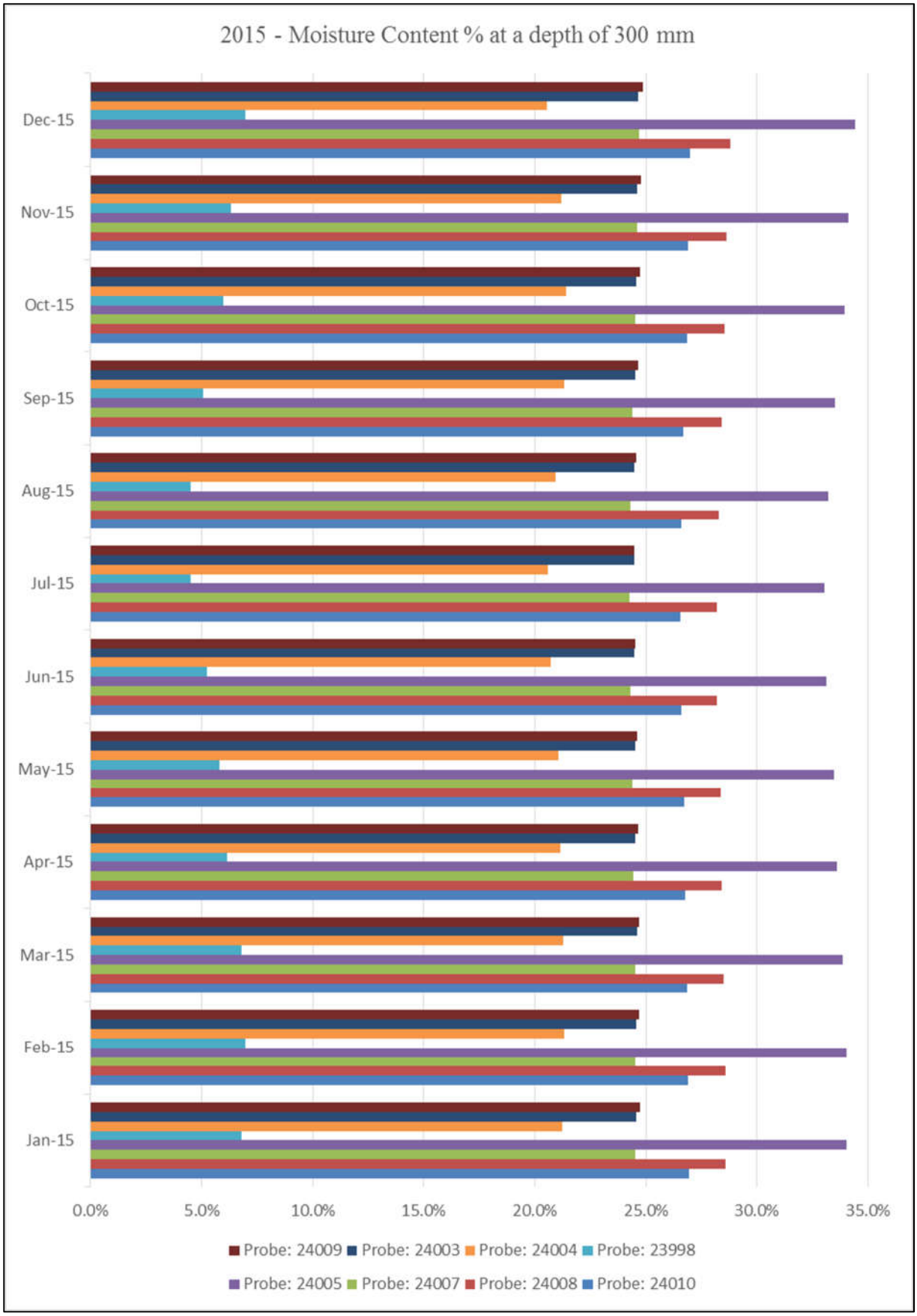

APPENDIX C - Figure: 4– Moisture content at a depth of 300mm for 2015

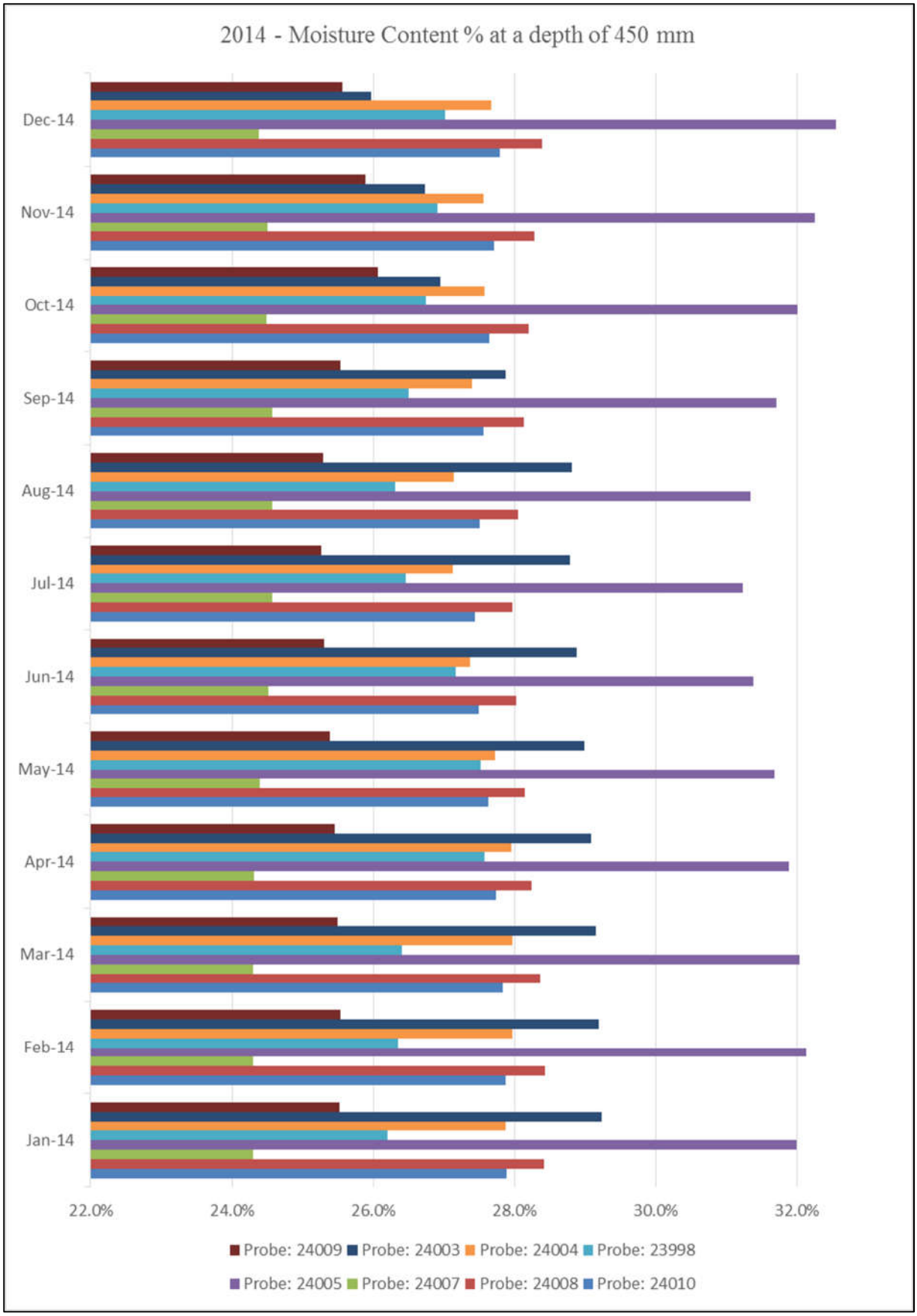

APPENDIX C - Figure: 5– Moisture content at a depth of 450mm for 2014

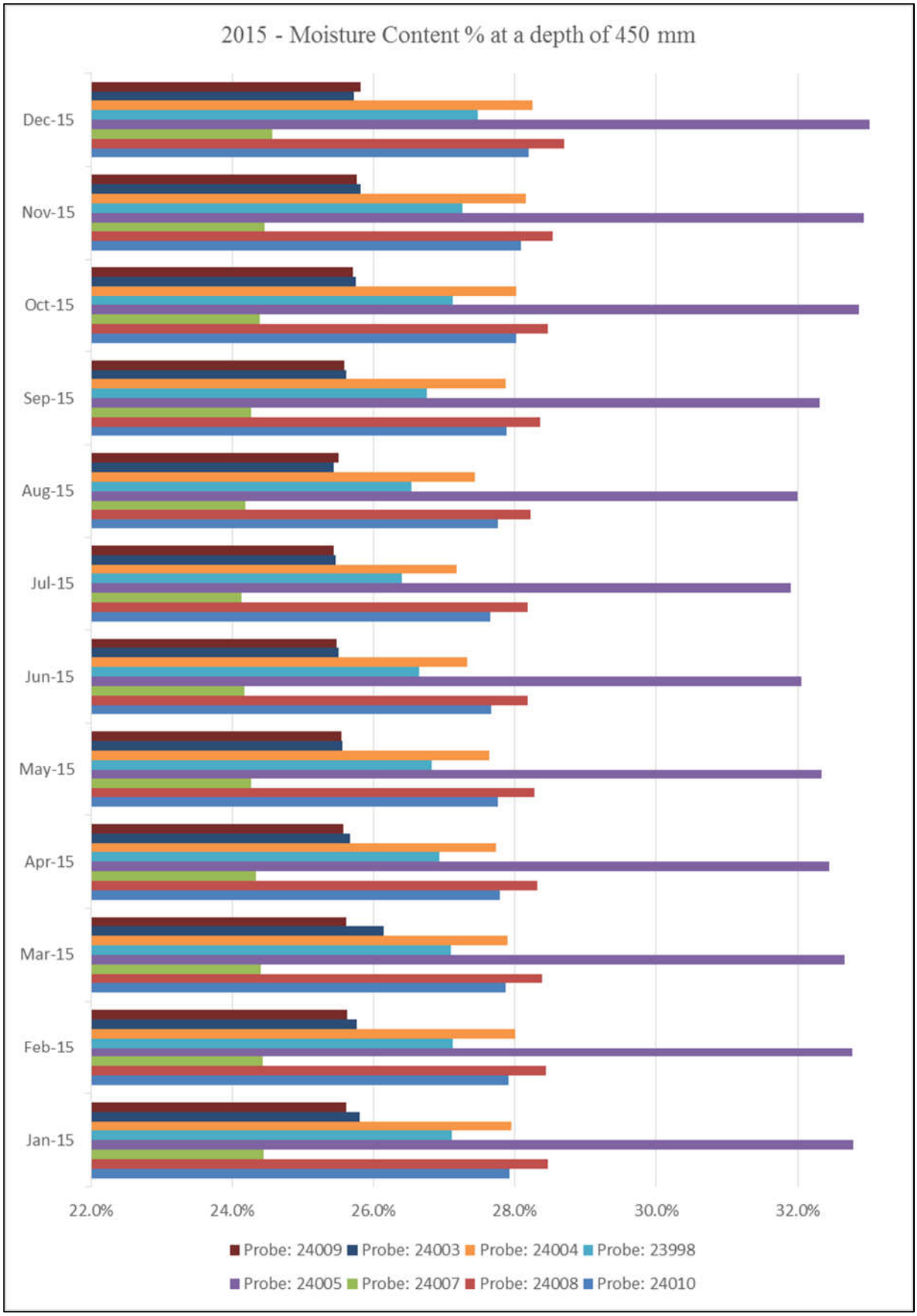

APPENDIX C - Figure: 6– Moisture content at a depth of 450mm for 2015

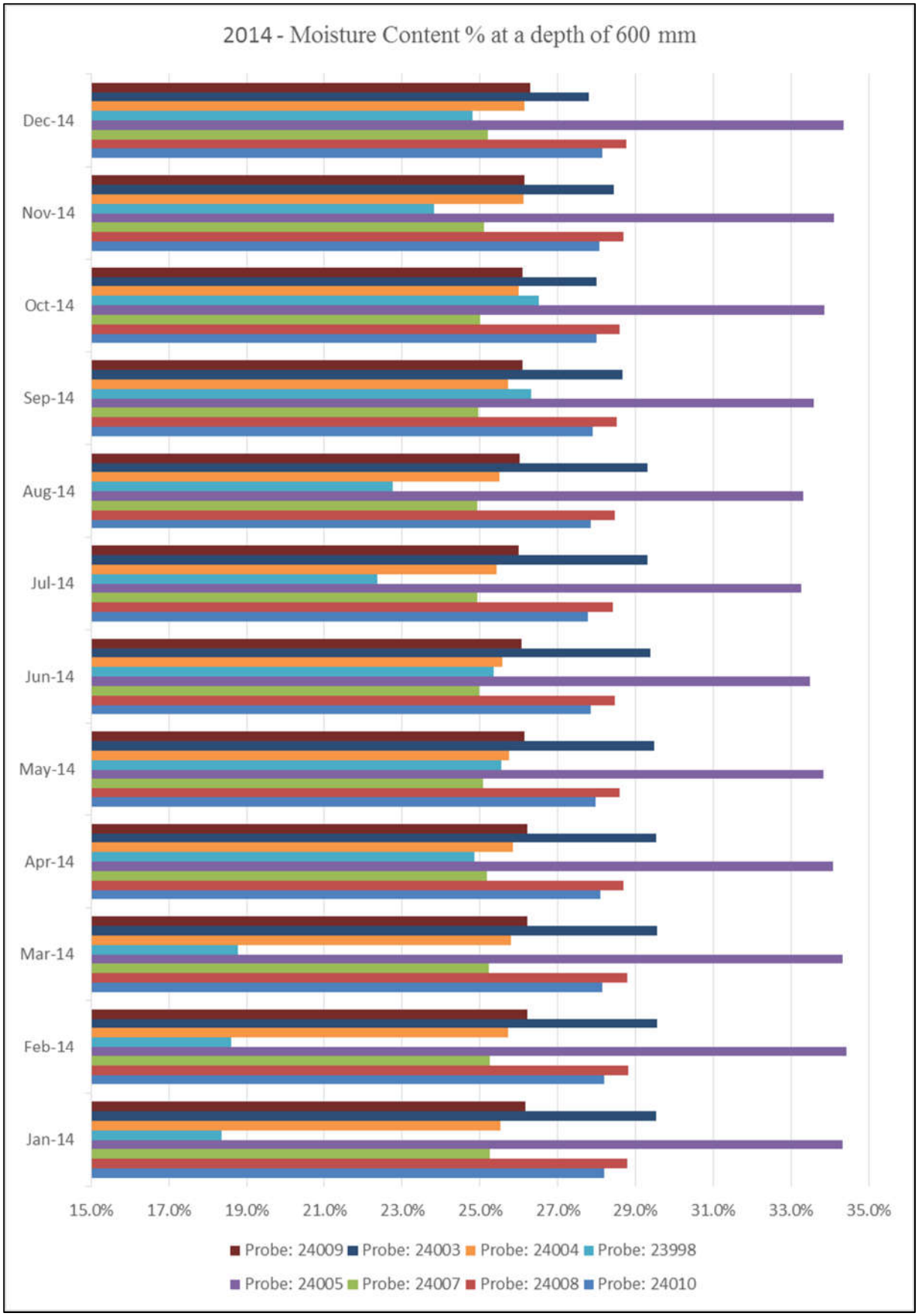

APPENDIX C - Figure: 7– Moisture content at a depth of 600mm for 2014

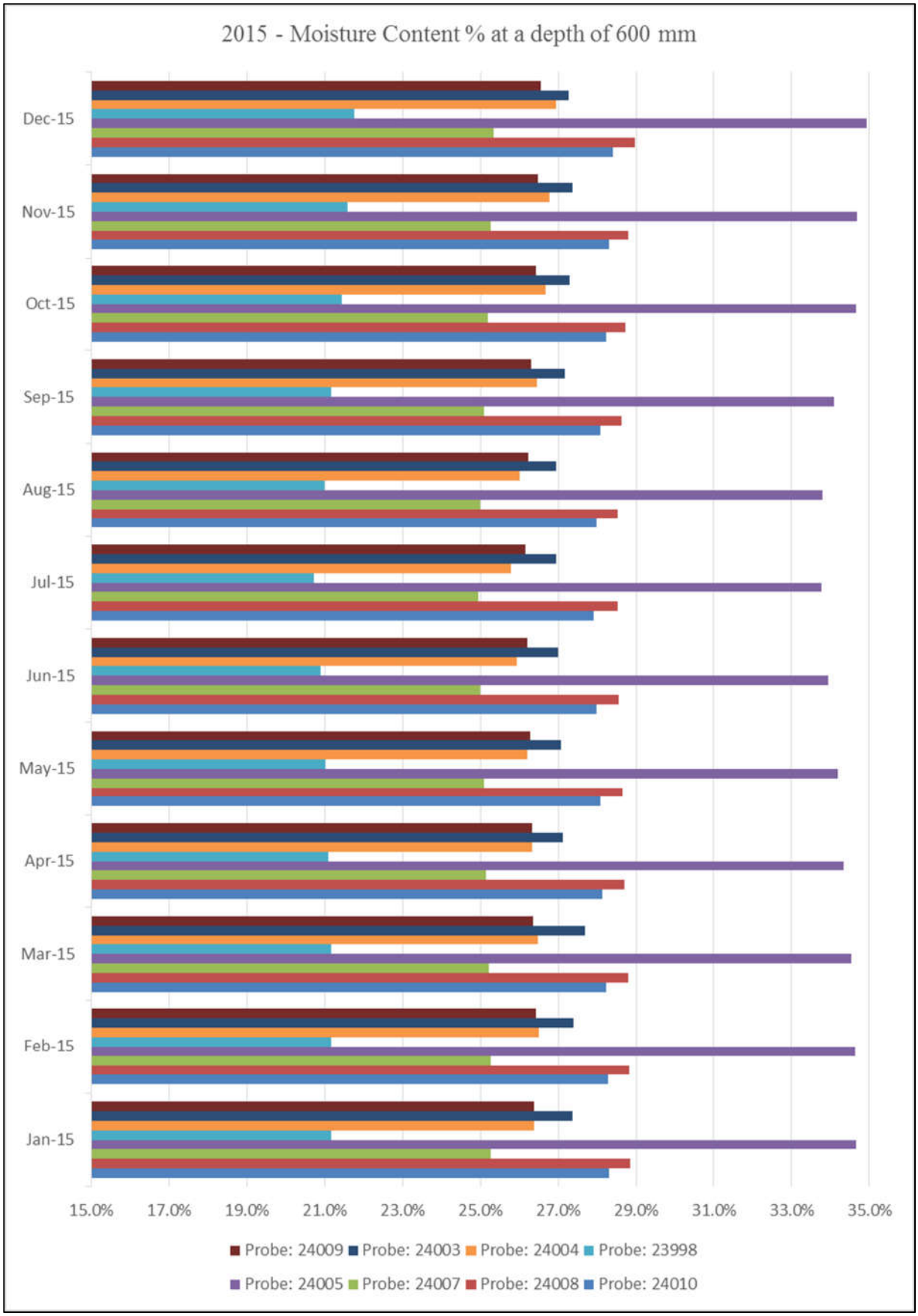

APPENDIX C - Figure: 8– Moisture content at a depth of 600mm for 2015

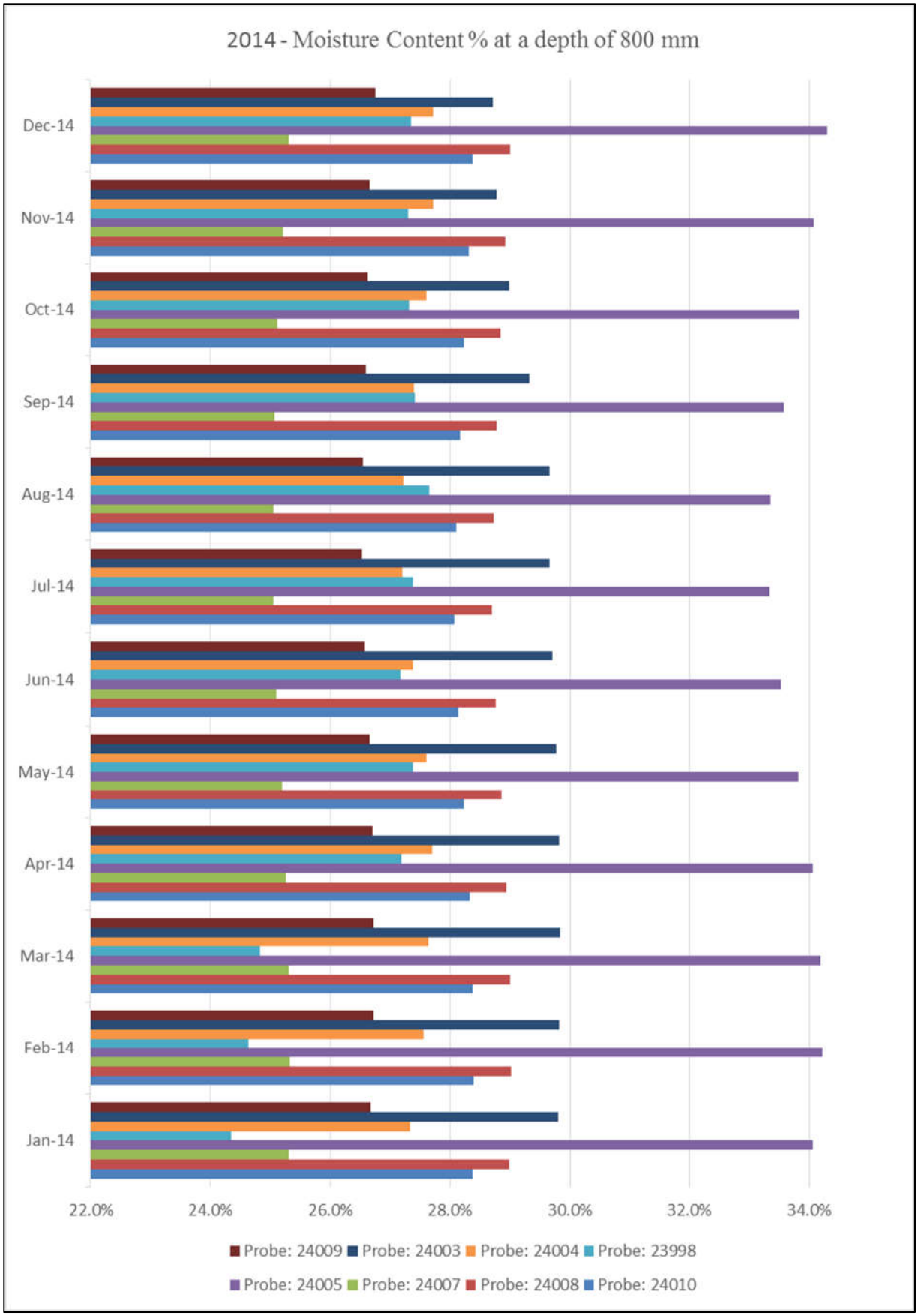

APPENDIX C - Figure: 9– Moisture content at a depth of 800mm for 2014

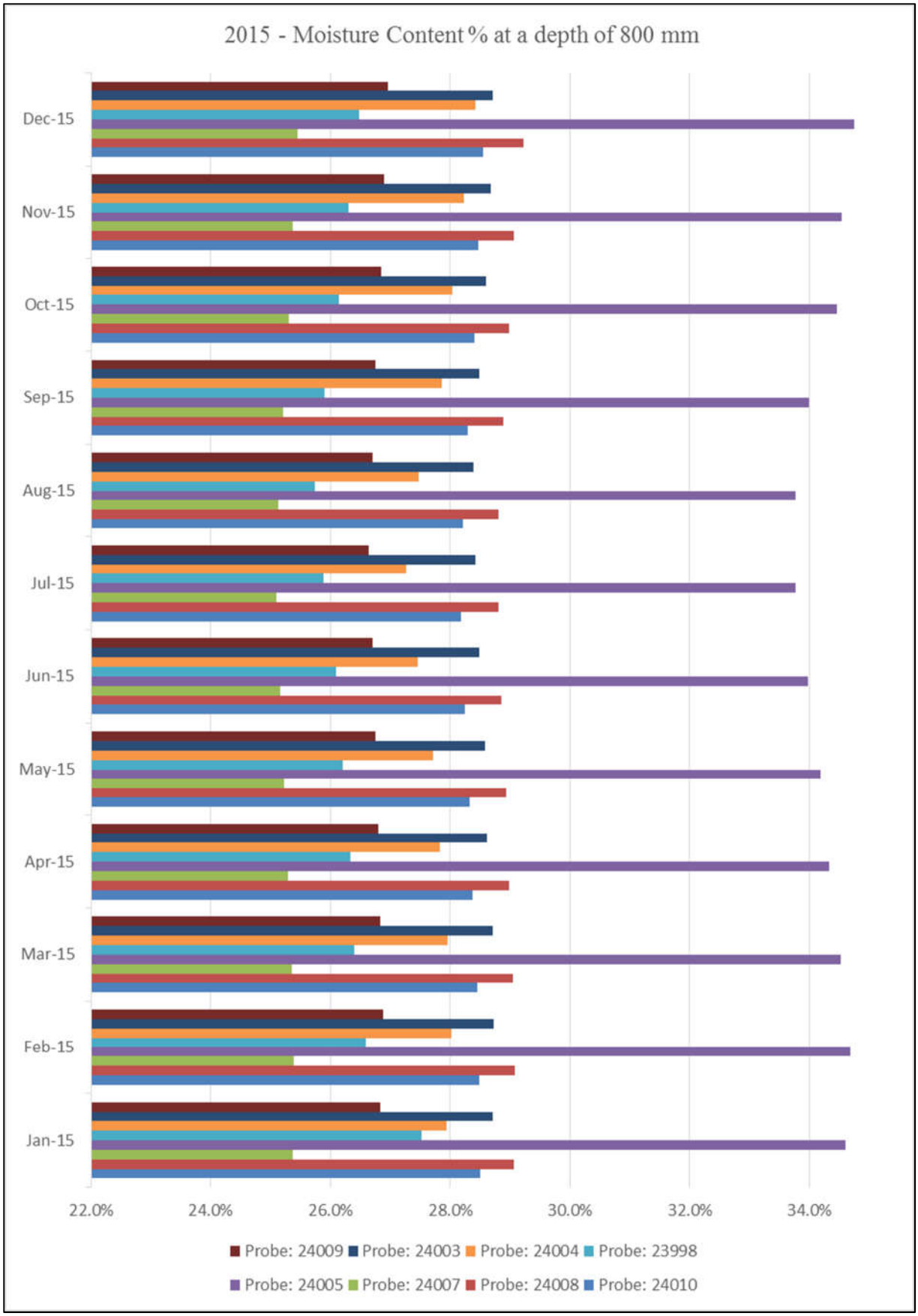

APPENDIX C - Figure: 10– Moisture content at a depth of 800mm for 2015

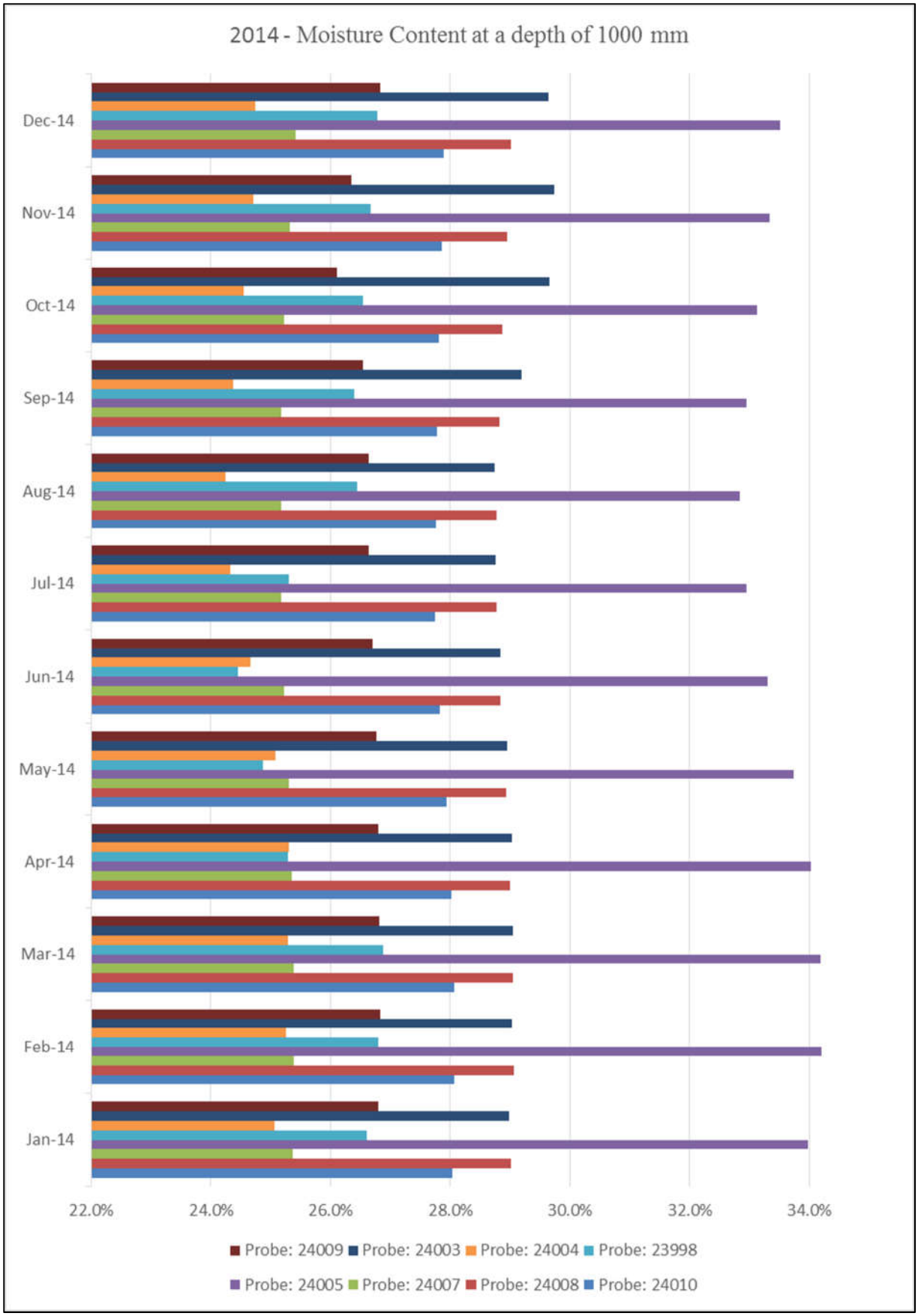

APPENDIX C - Figure: 11– Moisture content at a depth of 1000mm for 2014

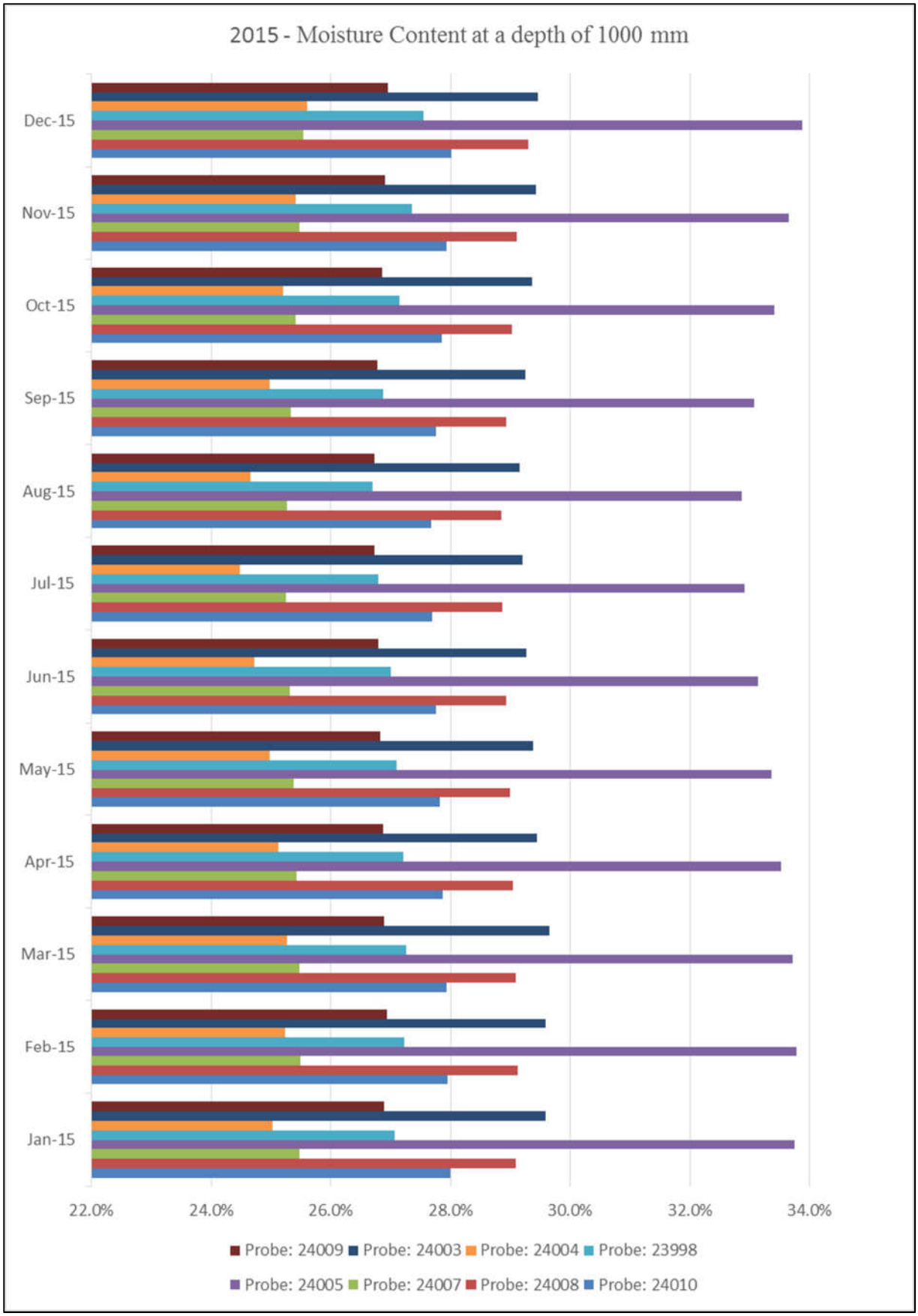

APPENDIX C - Figure: 12– Moisture content at a depth of 1000mm for 2015

APPENDIX: D

Moisture Content seasonal change models using 3D Field

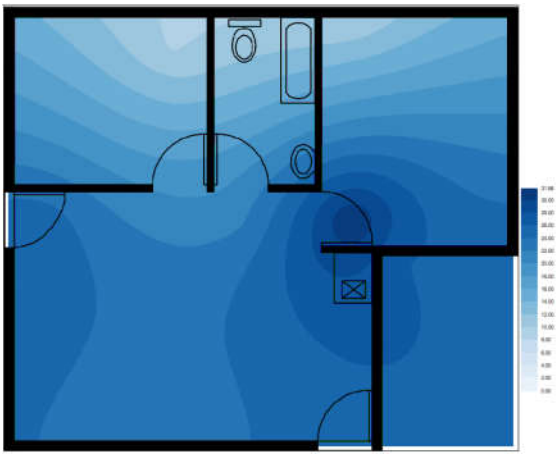

APPENDIX D - Figure: 1: 2014 January 150mm MC: 9%-32%

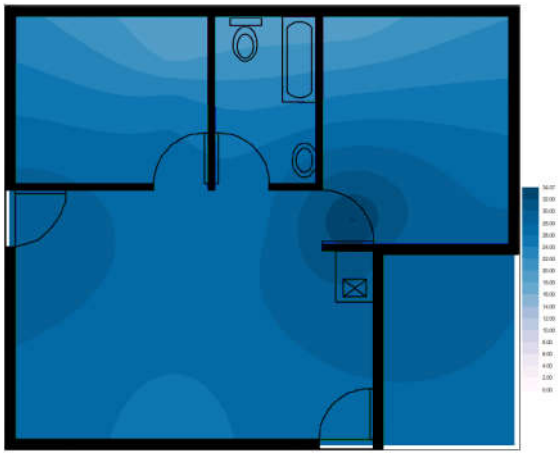

APPENDIX D - Figure: 4: 2014 January 600mm MC: 18%-35%

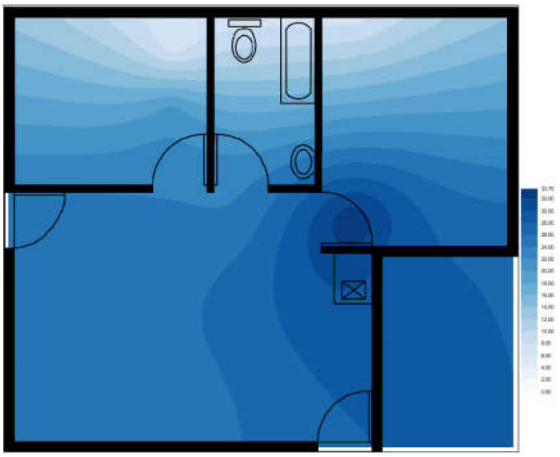

APPENDIX D - Figure: 2: 2014 January 300mm MC: 7%-34%

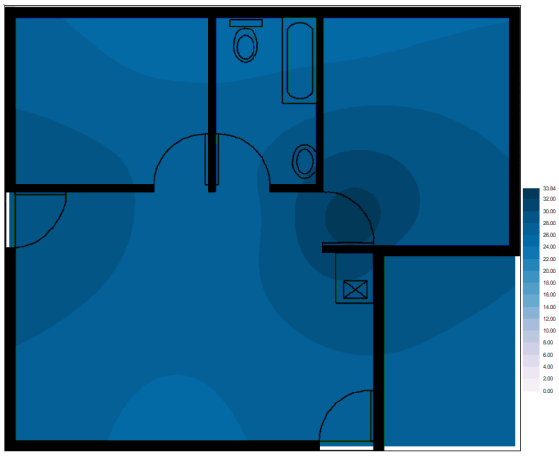

APPENDIX D - Figure: 5: 2014 January 800mm MC: 24%-34%

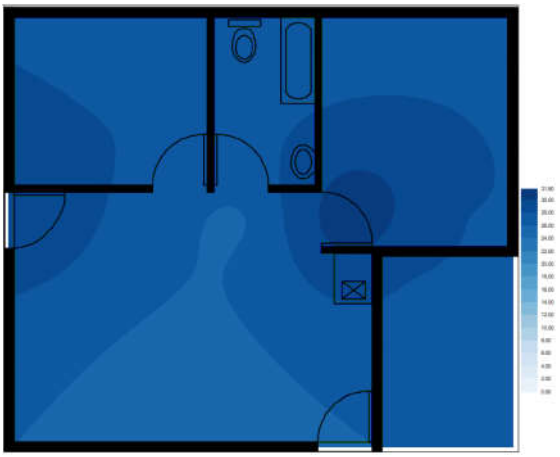

APPENDIX D - Figure: 3: 2014 January 450mm MC: 24%-32%

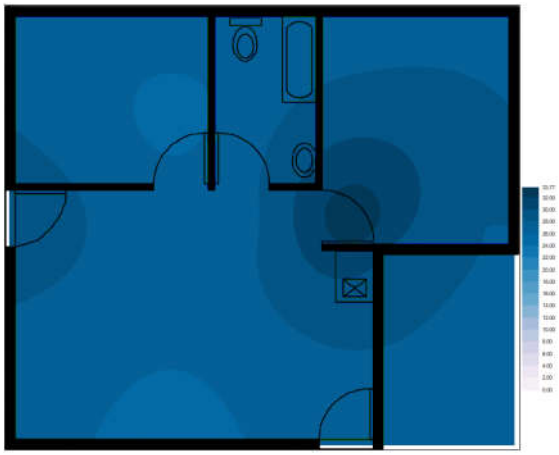

APPENDIX D - Figure: 6: 2014 January 1000mm MC: 25%-34%

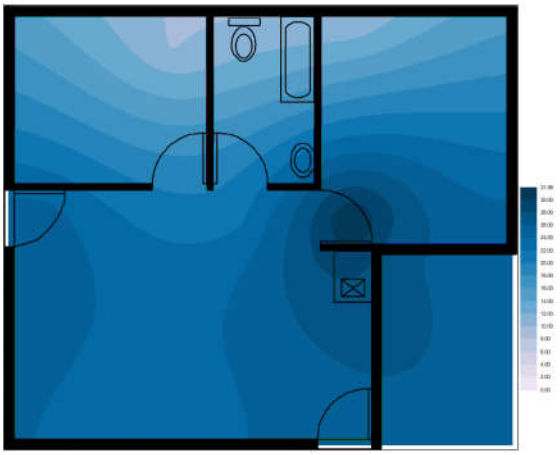

APPENDIX D - Figure: 7: 2014 February 150mm MC: 9%-32%

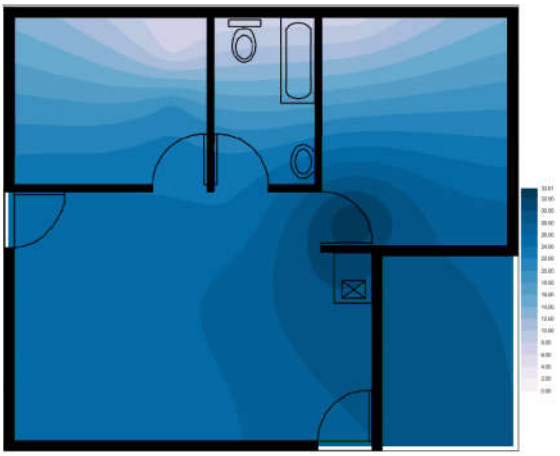

APPENDIX D - Figure: 8: 2014 February 300mm MC: 6%-34%

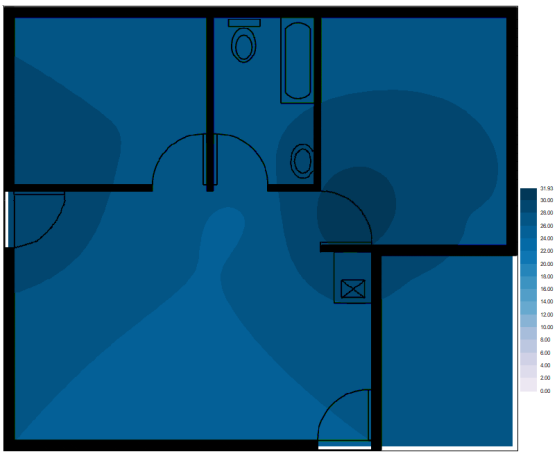

APPENDIX D - Figure: 9: 2014 February 450mm MC: 24%-32%

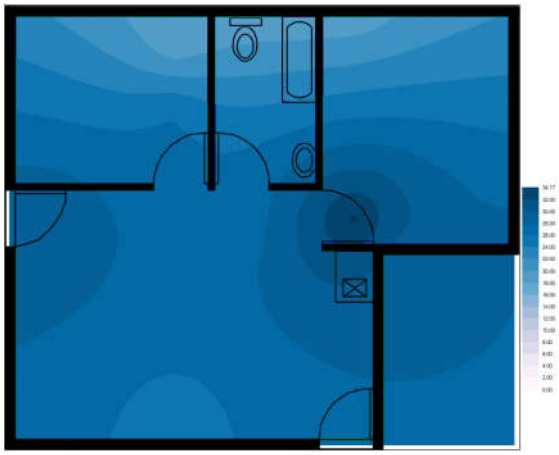

APPENDIX D - Figure: 10: 2014 February 600mm MC: 18%-35%

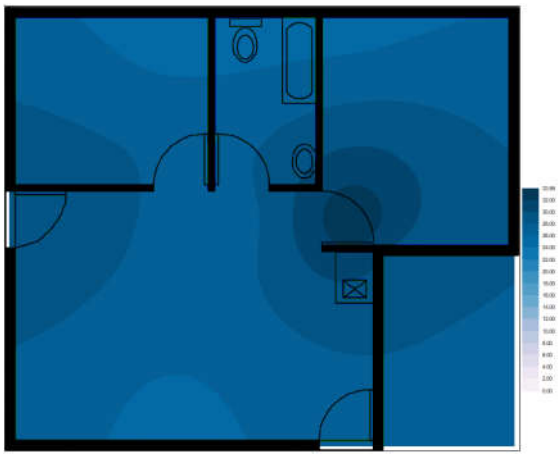

APPENDIX D - Figure: 11: 2014 February 800mm MC: 24%-34%

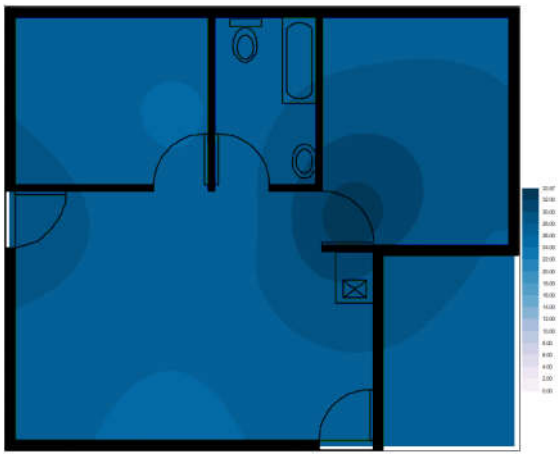

APPENDIX D - Figure: 12: 2014 February 1000mm MC: 25%-34%

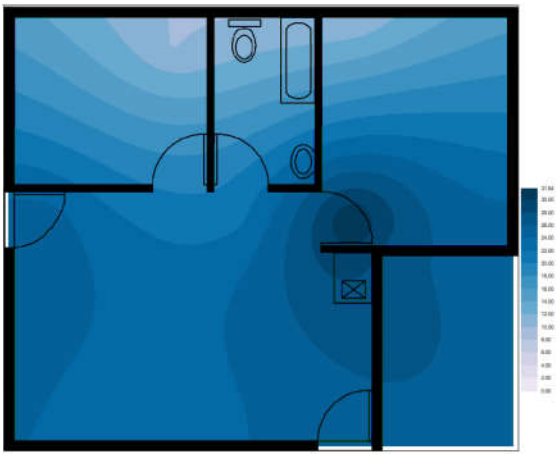

APPENDIX D - Figure: 13: 2014 March 150mm MC: 10%-32%

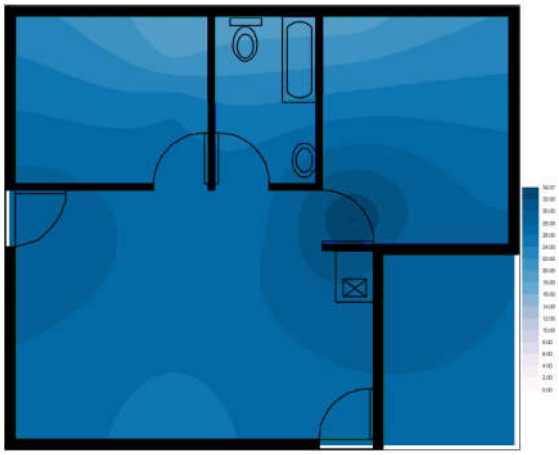

APPENDIX D - Figure: 16: 2014 March 600mm MC: 18%-34%

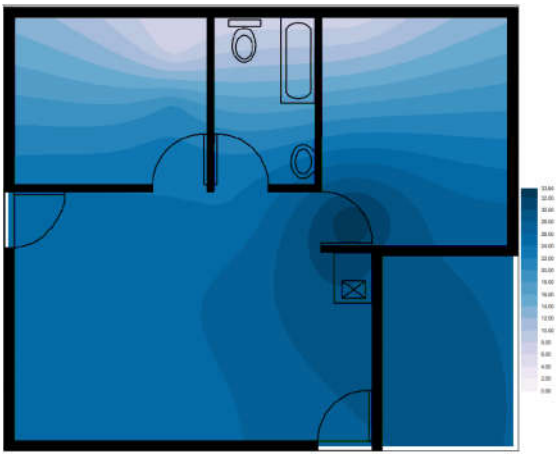

APPENDIX D - Figure: 14: 2014 March 300mm MC: 6%-34%

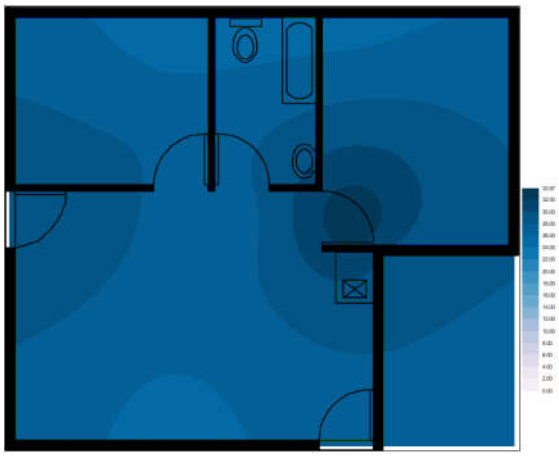

APPENDIX D - Figure: 17: 2014 March 800mm MC: 24%-34%

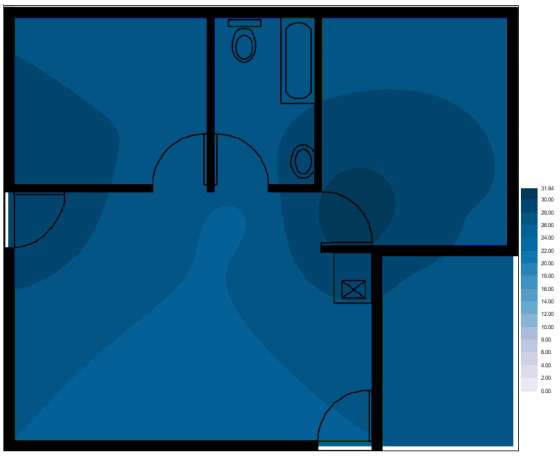

APPENDIX D - Figure: 15: 2014 March 450mm MC: 24%-32%

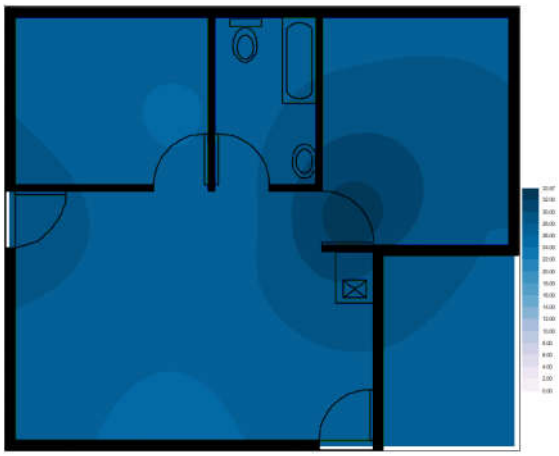

APPENDIX D - Figure: 18: 2014 March 150mm MC: 25%-34%

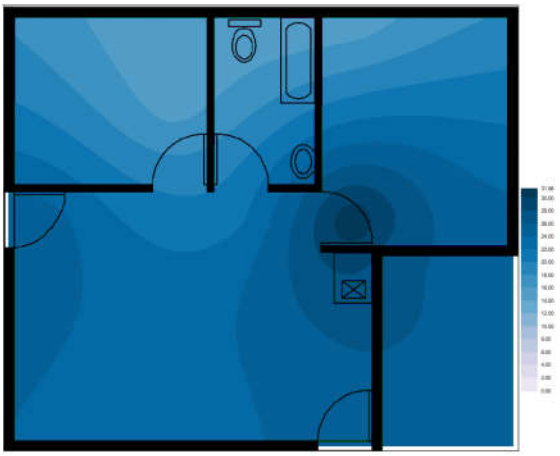

APPENDIX D - Figure: 19: 2014 April 150mm MC: 14%-32%

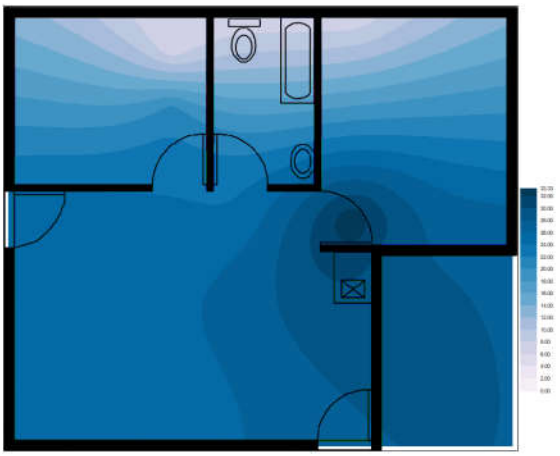

APPENDIX D - Figure: 20: 2014 April 300mm MC: 6%-34%

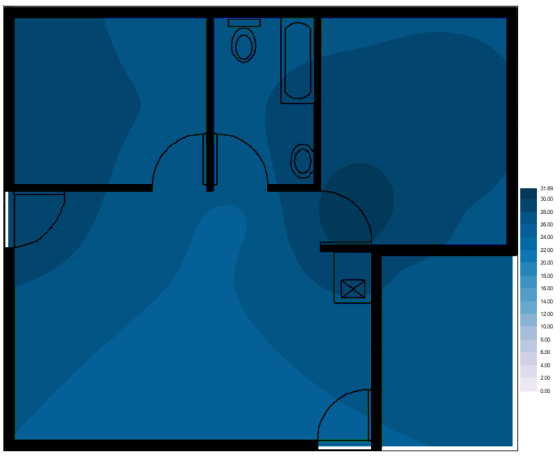

APPENDIX D - Figure: 21: 2014 April 450mm MC: 24%-32%

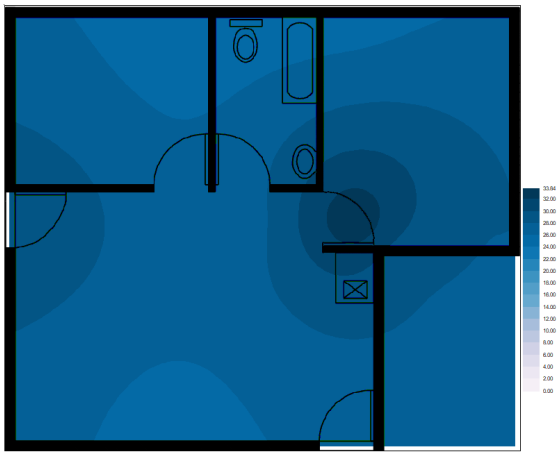

APPENDIX D - Figure: 22: 2014 April 600mm MC: 25%-34%

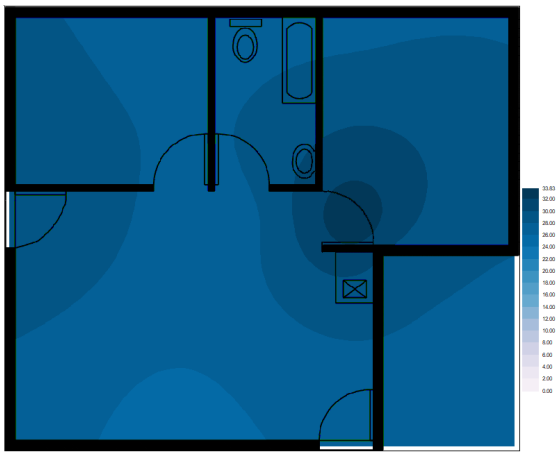

APPENDIX D - Figure: 23: 2014 April 800mm MC: 25%-34%

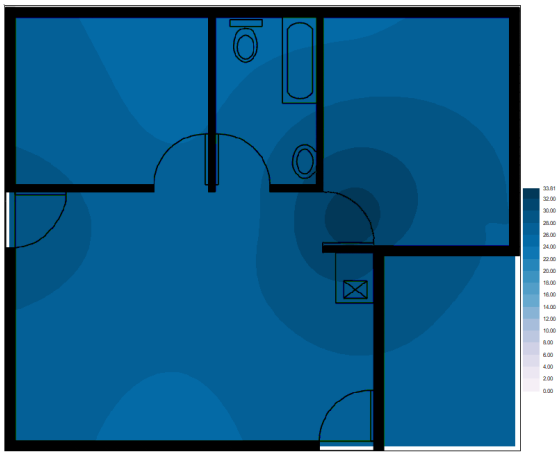

APPENDIX D - Figure: 24: 2014 April 1000mm MC: 25%-34%

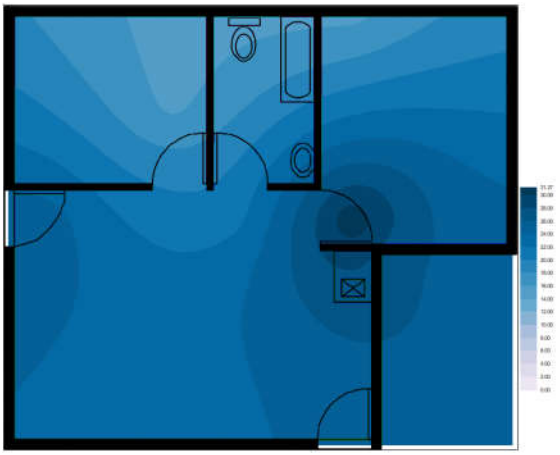

APPENDIX D - Figure: 25: 2014 May 150mm MC: 15%-31%

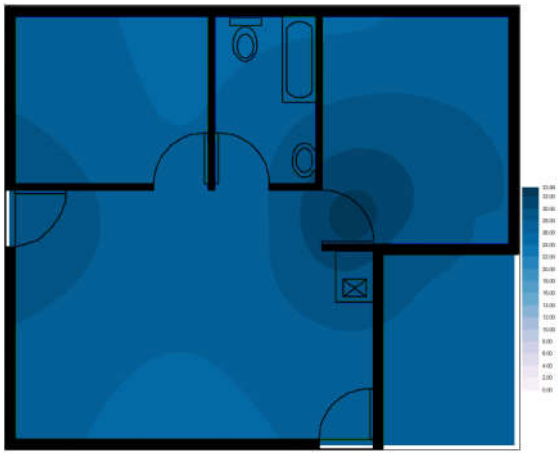

APPENDIX D - Figure: 28: 2014 May 600mm MC: 25%-34%

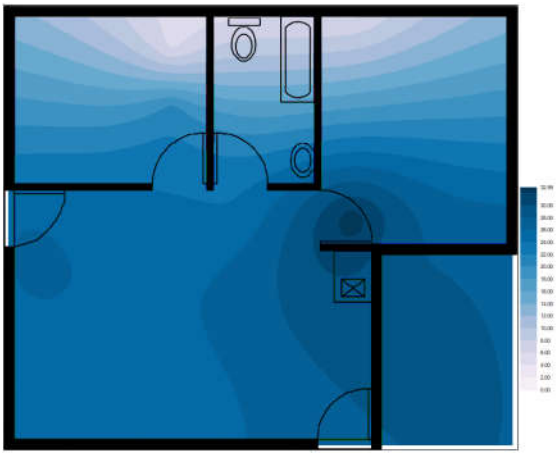

APPENDIX D - Figure: 26: 2014 May 300mm MC: 6%-33%

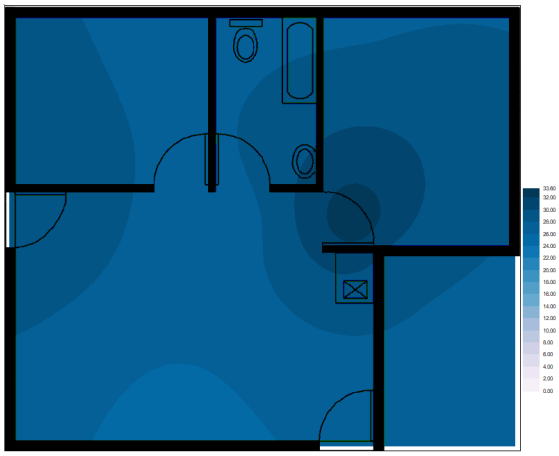

APPENDIX D - Figure: 29: 2014 May 800mm MC: 25%-34%

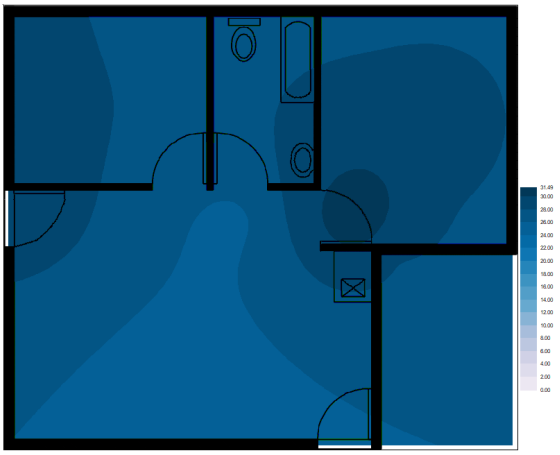

APPENDIX D - Figure: 27: 2014 May 450mm MC: 24%-32%

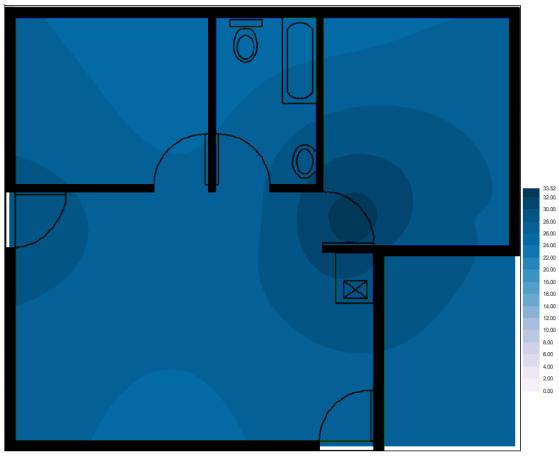

APPENDIX D - Figure: 30: 2014 May 1000mm MC: 25%-34%

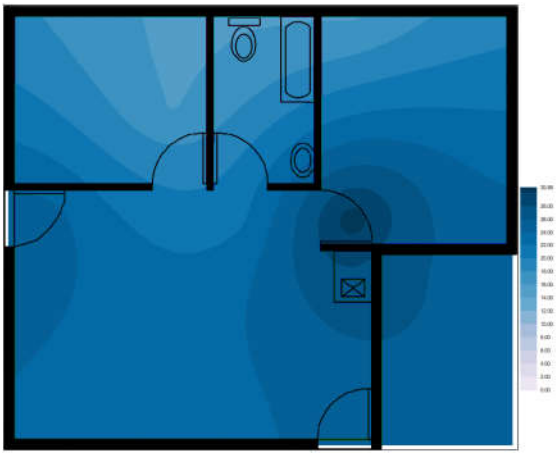

APPENDIX D - Figure: 31: 2014 June 150mm MC: 16%-31%

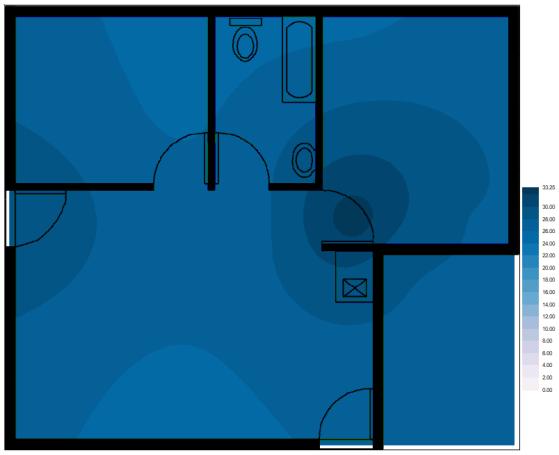

APPENDIX D - Figure: 34: 2014 June 600mm MC: 25%-33%

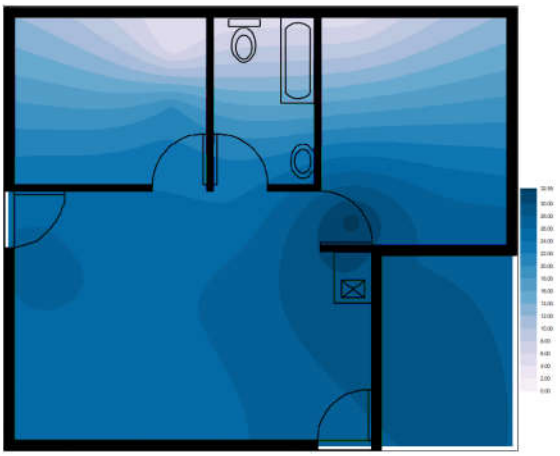

APPENDIX D - Figure: 32: 2014 June 300mm MC: 5%-33%

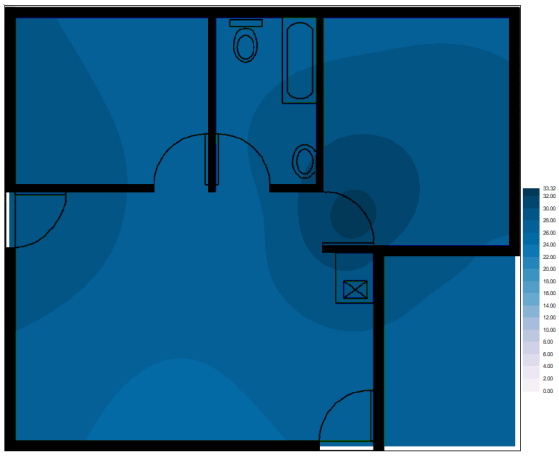

APPENDIX D - Figure: 35: 2014 June 800mm MC: 25%-33%

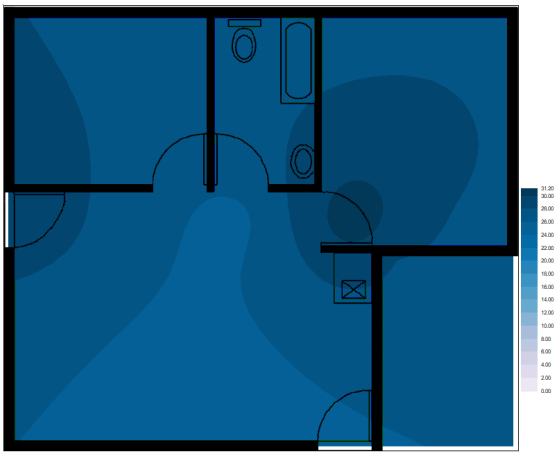

APPENDIX D - Figure: 33: 2014 June 450mm MC: 24%-31%

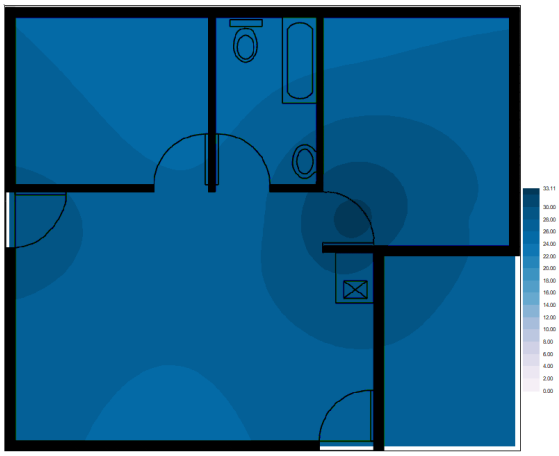

APPENDIX D - Figure: 36: 2014 June 1000mm MC: 24%-33%

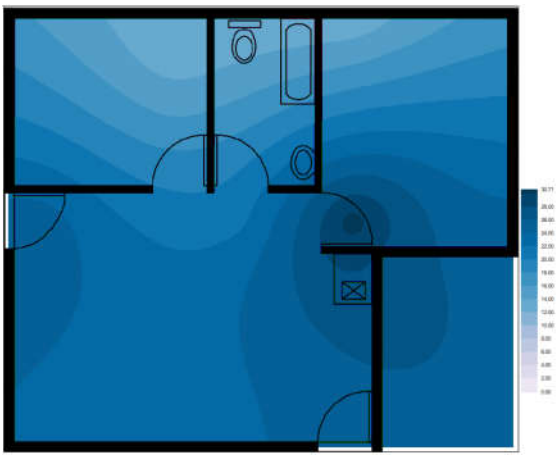

APPENDIX D - Figure: 37: 2014 July 150mm MC: 12%-31%

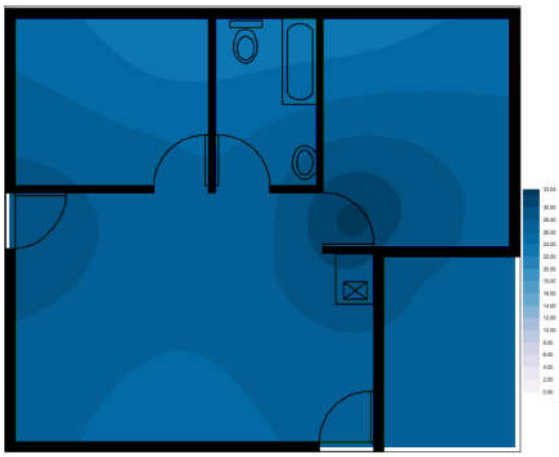

APPENDIX D - Figure: 40: 2014 July 600mm MC: 22%-33%

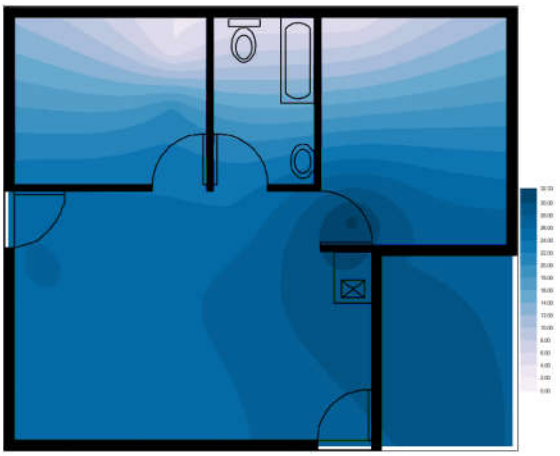

APPENDIX D - Figure: 38: 2014 July 300mm MC: 4%-32%

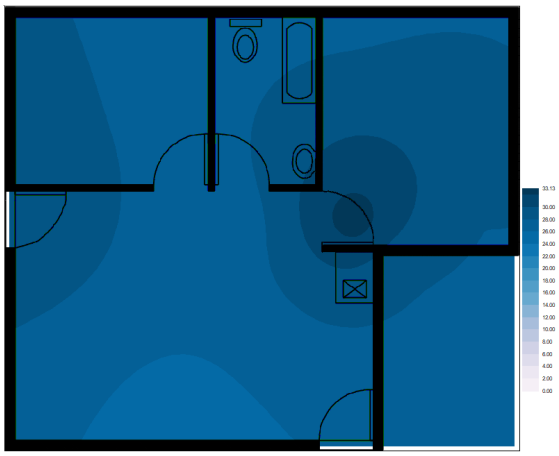

APPENDIX D - Figure: 41: 2014 July 800mm MC: 25%-33%

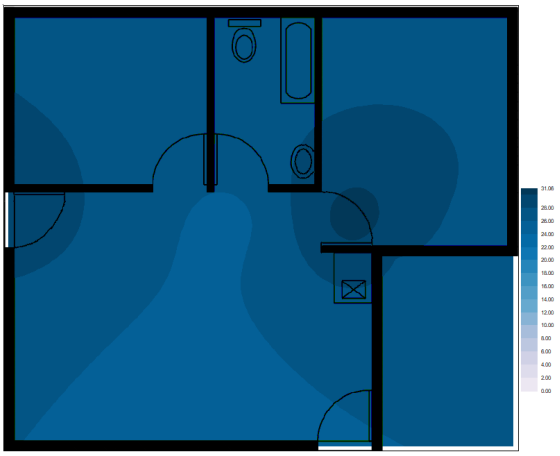

APPENDIX D - Figure: 39: 2014 July 450mm MC: 24%-31%

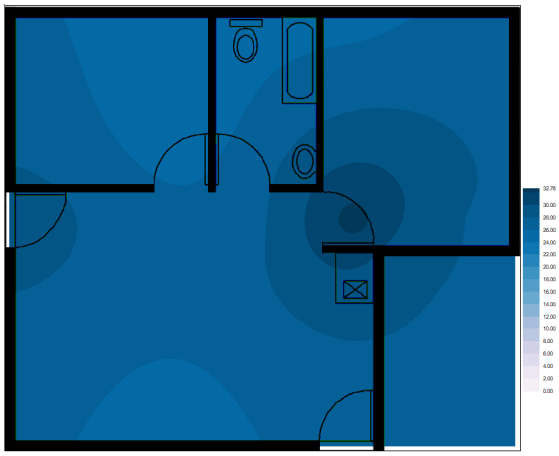

APPENDIX D - Figure: 42: 2014 July 1000mm MC: 24%-33%

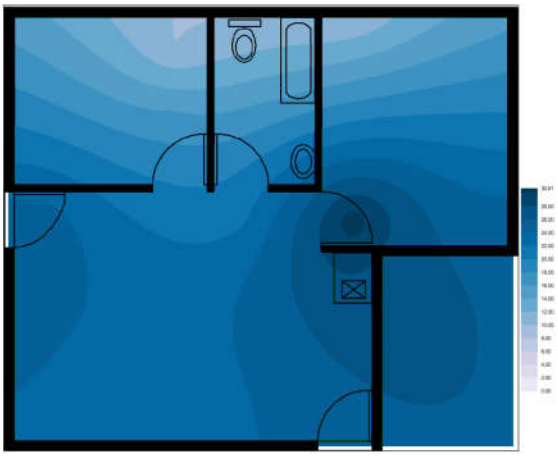

APPENDIX D - Figure: 43: 2014 August 150mm MC: 10%-31%

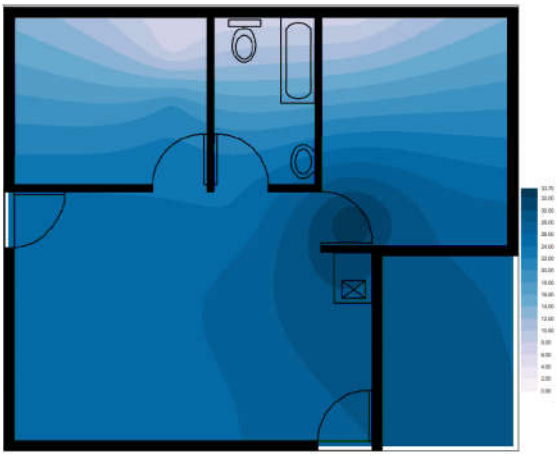

APPENDIX D - Figure: 44: 2014 August 300mm MC: 4%-33%

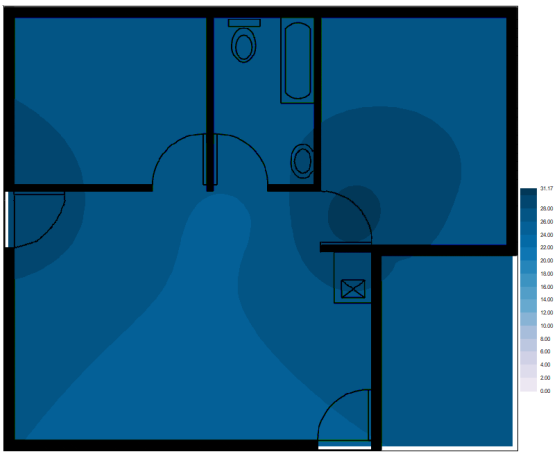

APPENDIX D - Figure: 45: 2014 August 450mm MC: 24%-31%

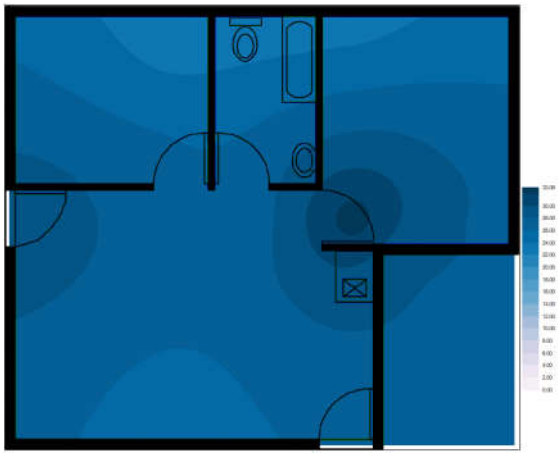

APPENDIX D - Figure: 46: 2014 August 600mm MC: 23%-33%

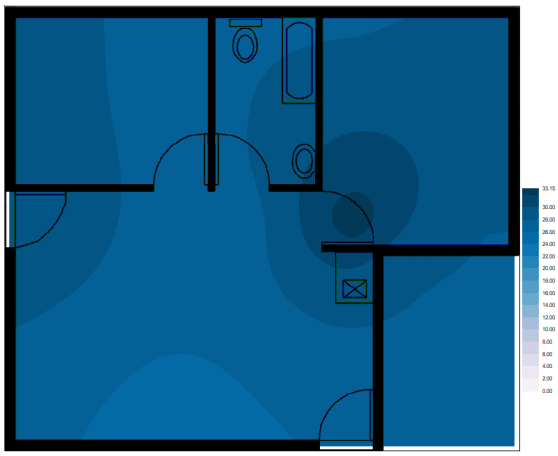

APPENDIX D - Figure: 47: 2014 August 800mm MC: 25%-33%

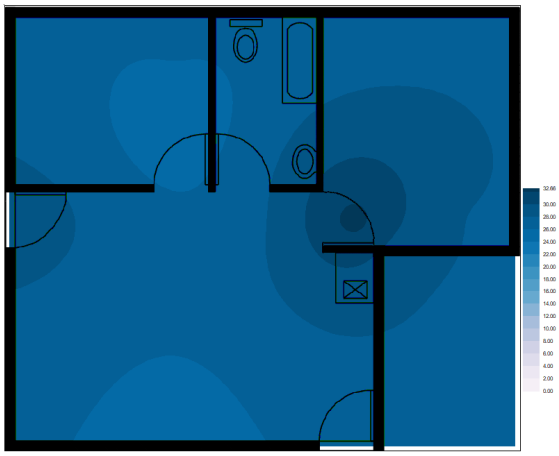

APPENDIX D - Figure: 48: 2014 August 1000mm MC: 24%-33%

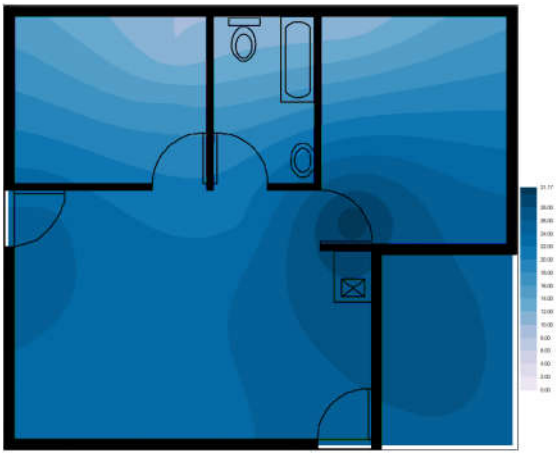

APPENDIX D - Figure: 49: 2014 September 150mm MC: 10%-31%

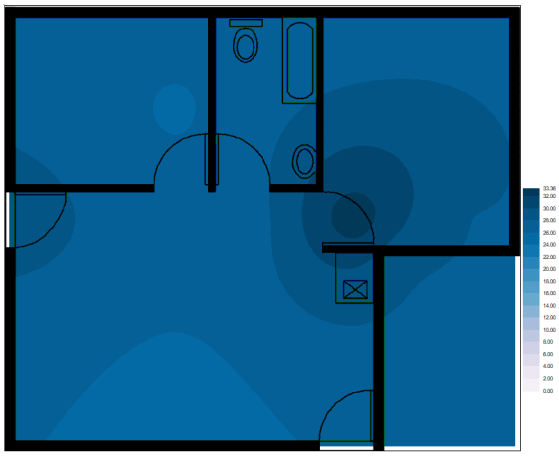

APPENDIX D - Figure: 52: 2014 September 600mm MC: 25%-34%

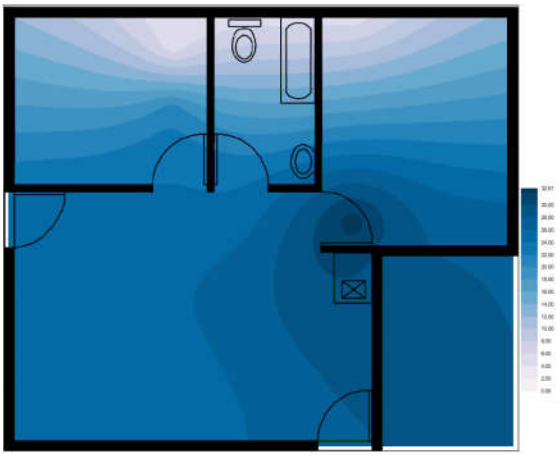

APPENDIX D - Figure: 50: 2014 September 300mm MC: 5%-33%

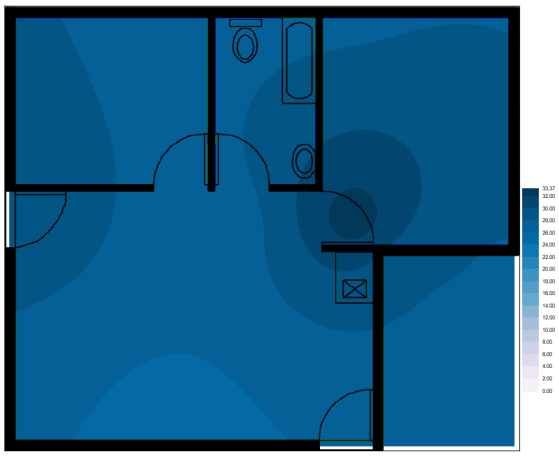

APPENDIX D - Figure: 53: 2014 September 800mm MC: 25%-34%

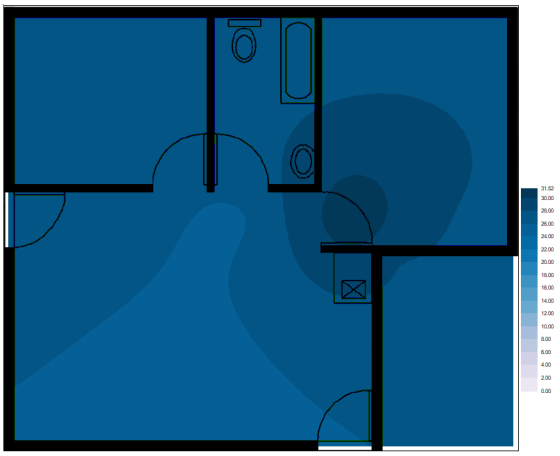

APPENDIX D - Figure: 51: 2014 September 450mm MC: 24%-32%

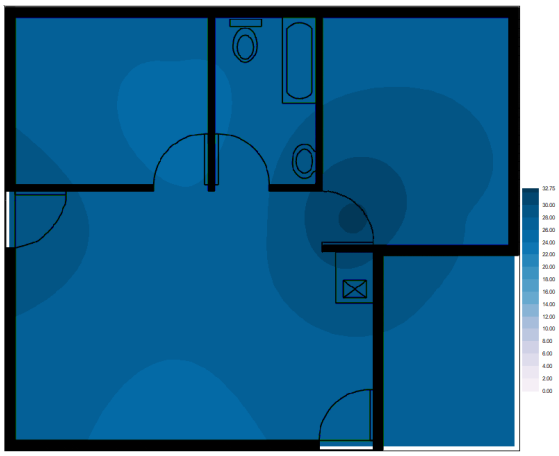

APPENDIX D - Figure: 54: 2014 September 150mm MC: 24%-33%

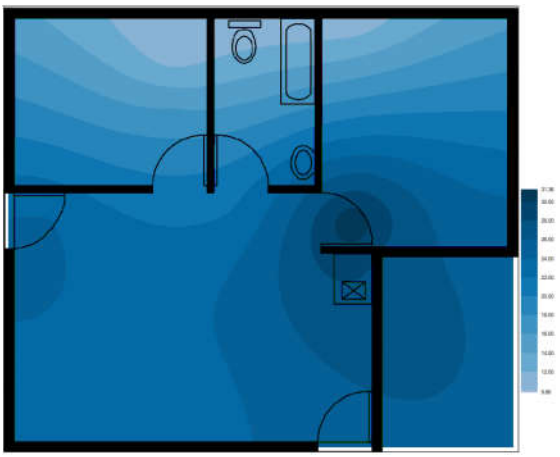

APPENDIX D - Figure: 55: 2014 October 150mm MC: 10%-32%

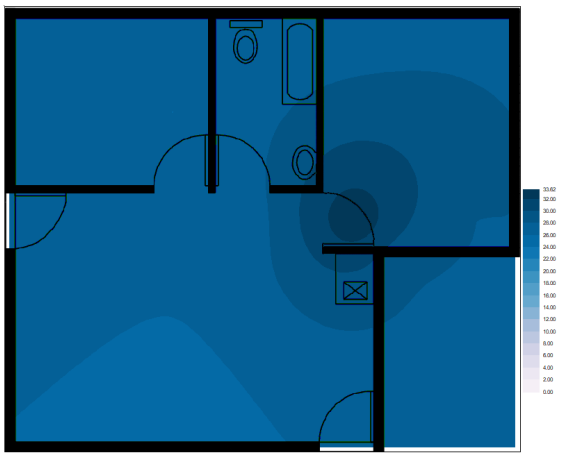

APPENDIX D - Figure: 58: 2014 October 600mm MC: 25%-34%

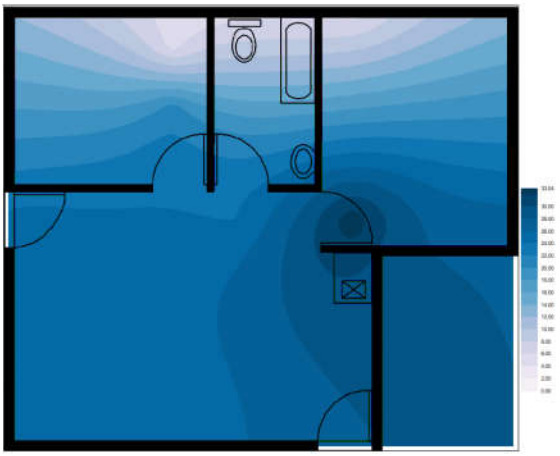

APPENDIX D - Figure: 56: 2014 October 300mm MC: 5%-33%

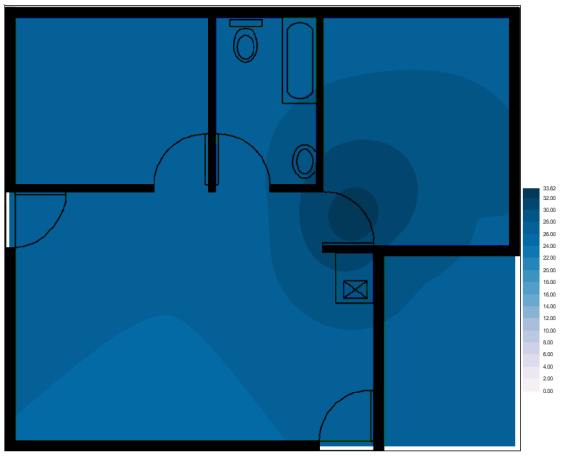

APPENDIX D - Figure: 59: 2014 October 800mm MC: 25%-34%

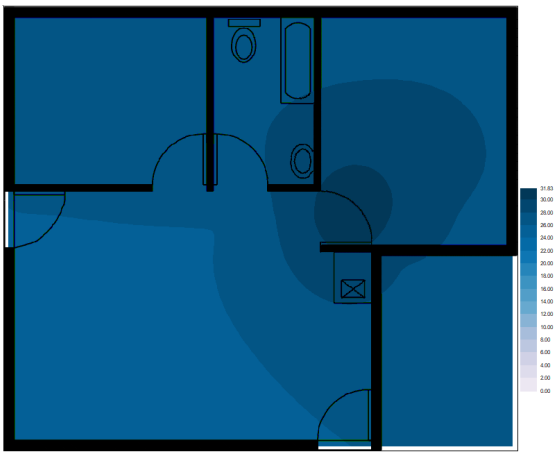

APPENDIX D - Figure: 57: 2014 October 450mm MC: 24%-32%

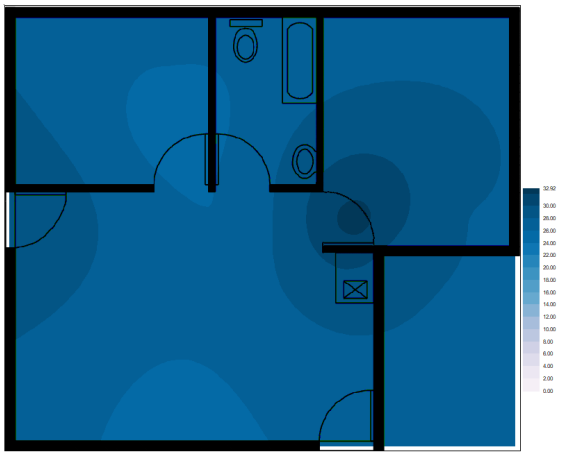

APPENDIX D - Figure: 60: 2014 October 1000mm MC: 24%-33%

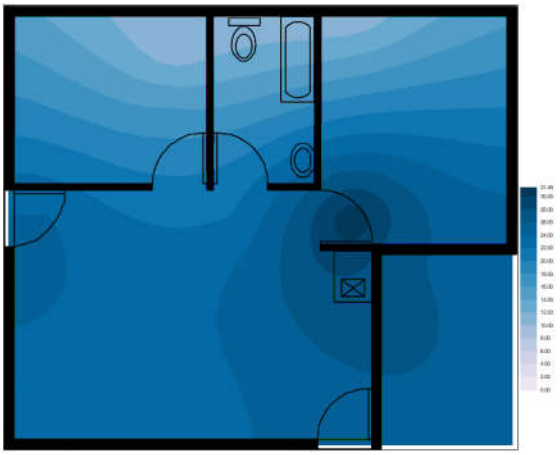

APPENDIX D - Figure: 61: 2014 November 150mm MC: 10%-32%

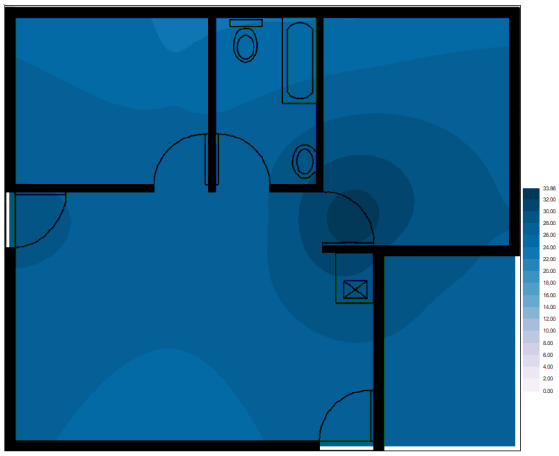

APPENDIX D - Figure: 64: 2014 November 600mm MC: 23%-34%

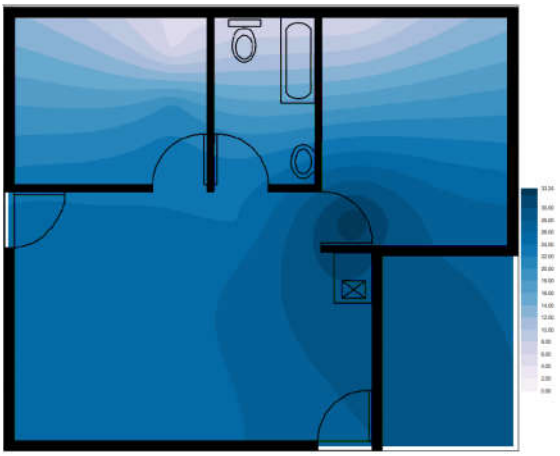

APPENDIX D - Figure: 62: 2014 November 300mm MC: 6%-34%

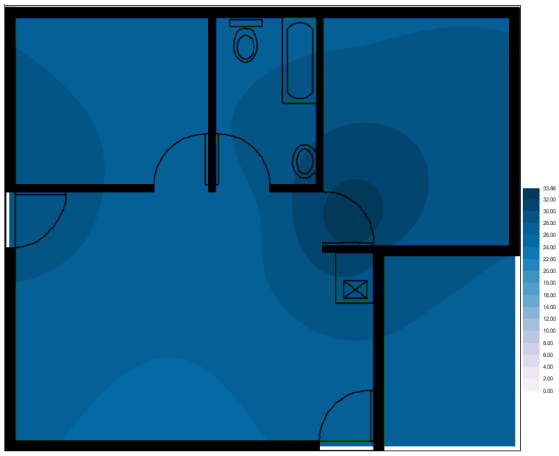

APPENDIX D - Figure: 65: 2014 November 800mm MC: 25%-34%

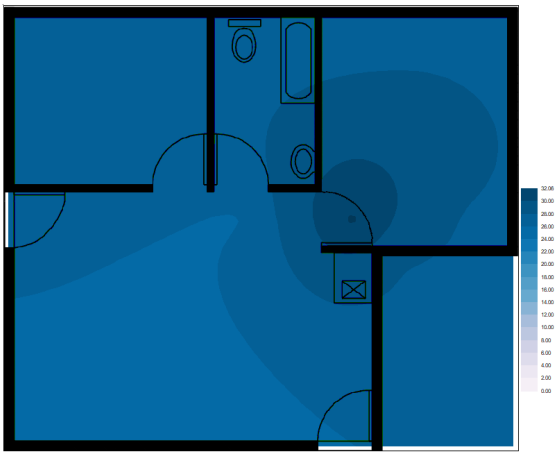

APPENDIX D - Figure: 63: 2014 November 450mm MC: 24%-32%

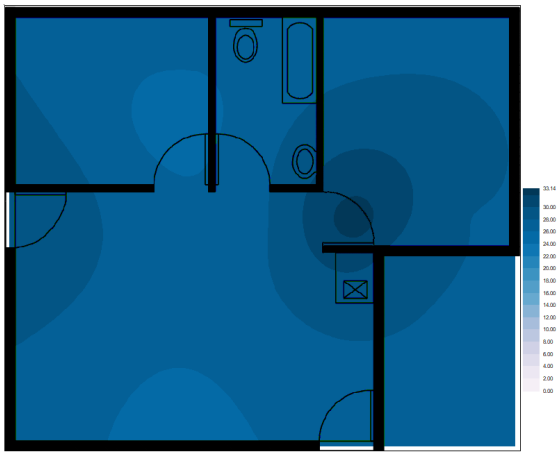

APPENDIX D - Figure: 66: 2014 November 1000mm MC: 24%-33%

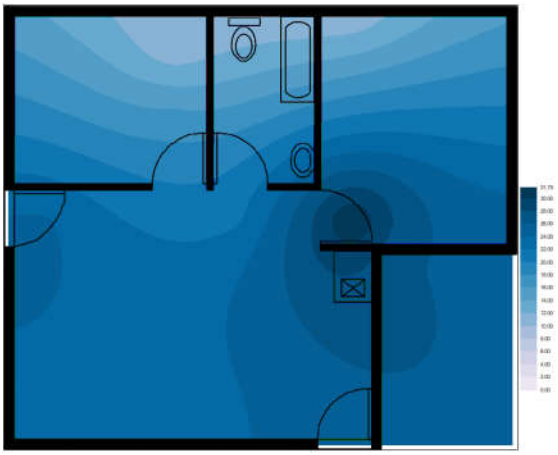

APPENDIX D - Figure: 67: 2014

December 150mm MC: 10%-32%

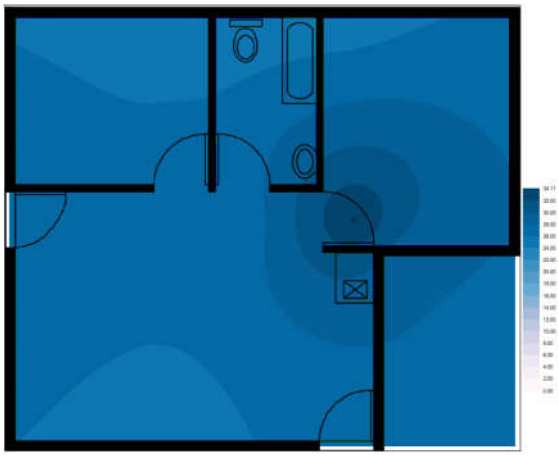

APPENDIX D - Figure: 70: 2014

December 600mm MC: 25%-34%

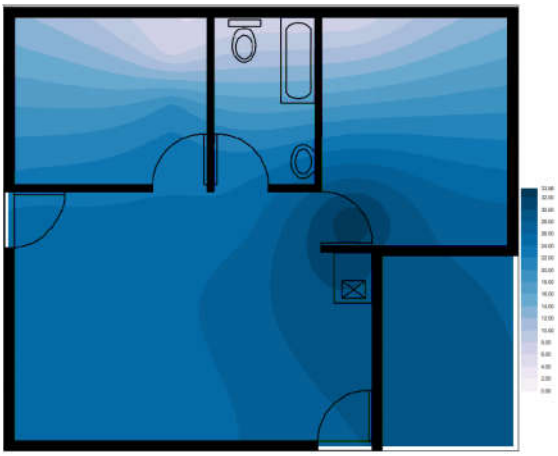

APPENDIX D - Figure: 68: 2014

December 300mm MC: 6%-34%

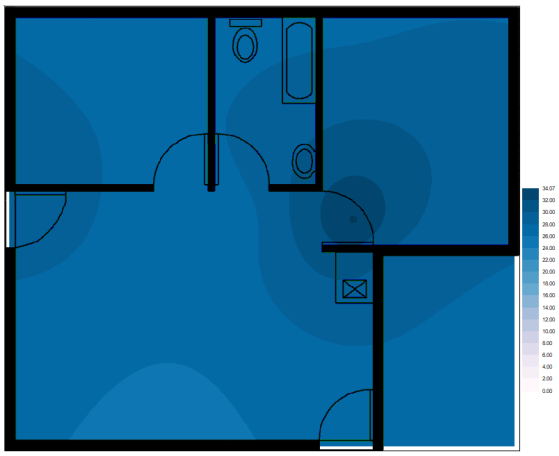

APPENDIX D - Figure: 71: 2014

December 800mm MC: 25%-34%

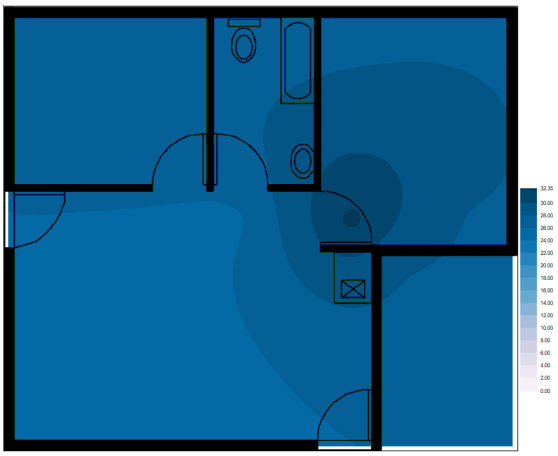

APPENDIX D - Figure: 69: 2014

December 450mm MC: 24%-33%

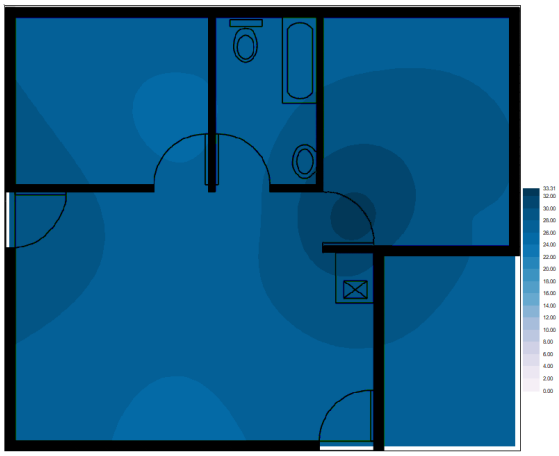

APPENDIX D - Figure: 72: 2014

December 1000mm MC: 24%-34%

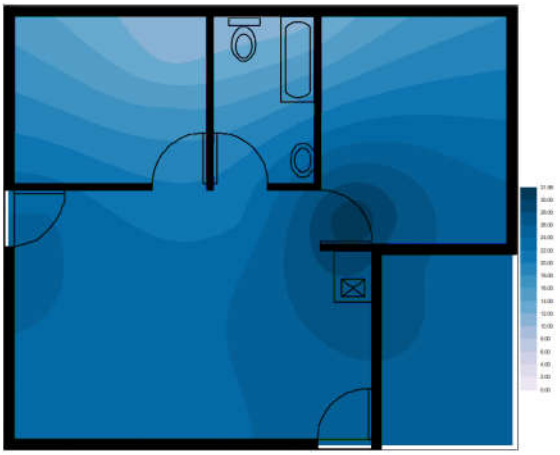

APPENDIX D - Figure: 73: 2015 January 150mm MC: 10%-32%

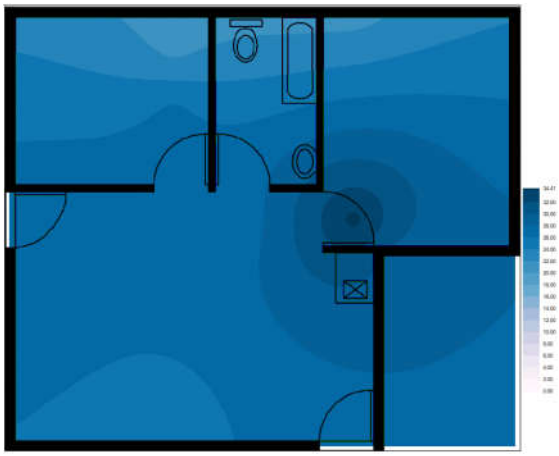

APPENDIX D - Figure: 76: 2015 January 600mm MC: 20%-35%

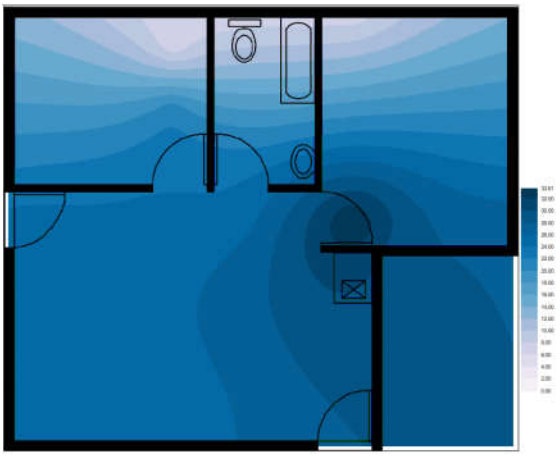

APPENDIX D - Figure: 74: 2015 January 300mm MC: 7%-34%

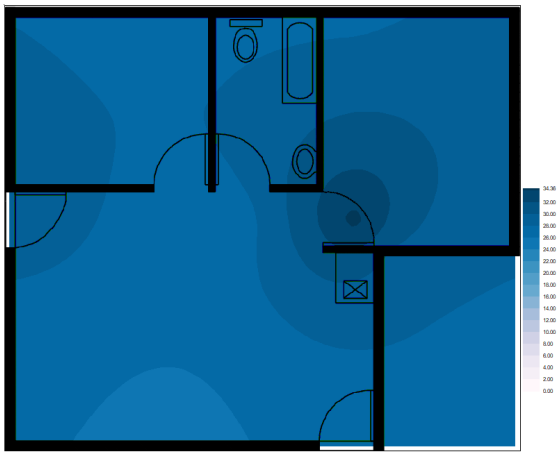

APPENDIX D - Figure: 77: 2015 January 800mm MC: 25%-35%

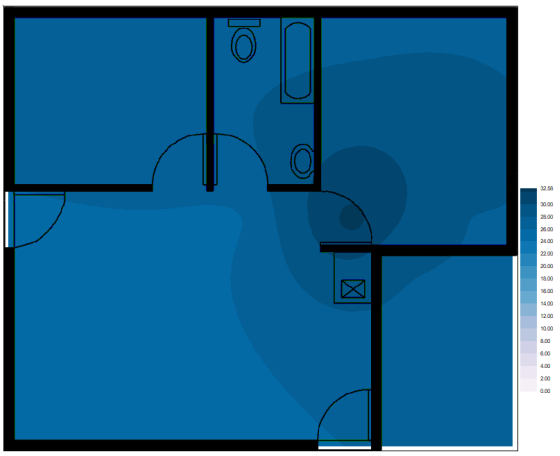

APPENDIX D - Figure: 75: 2015 January 450mm MC: 24%-33%

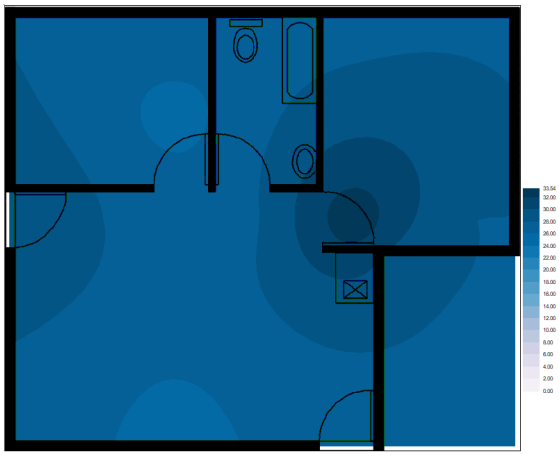

APPENDIX D - Figure: 78: 2015 January 1000mm MC: 25%-34%

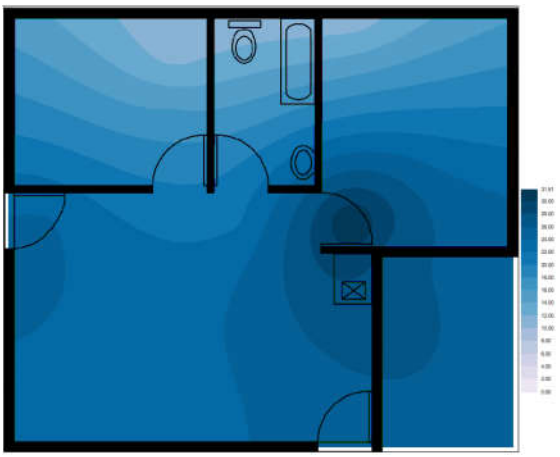

APPENDIX D - Figure: 79: 2015 February 150mm MC: 10%-32%

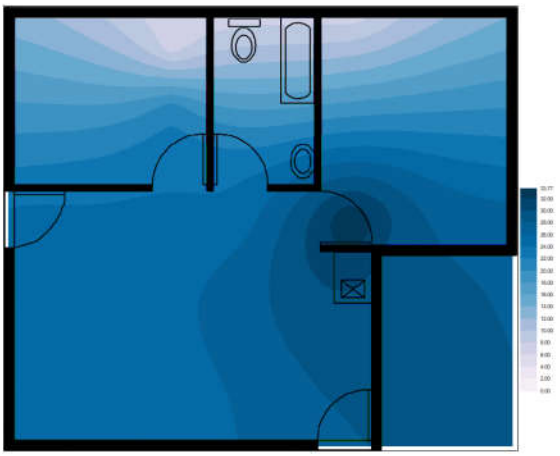

APPENDIX D - Figure: 80: 2015 February 300mm MC: 7%-34%

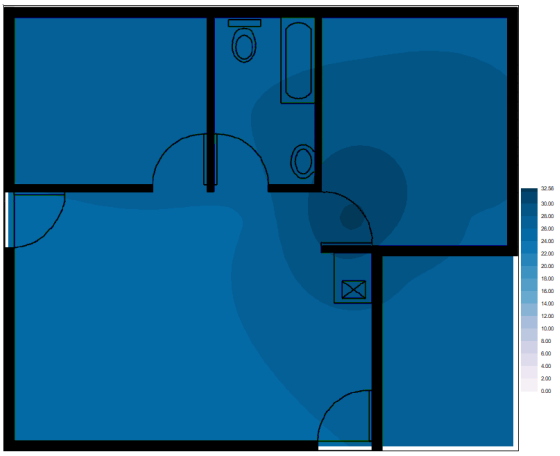

APPENDIX D - Figure: 81: 2015 February 450mm MC: 24%-33%

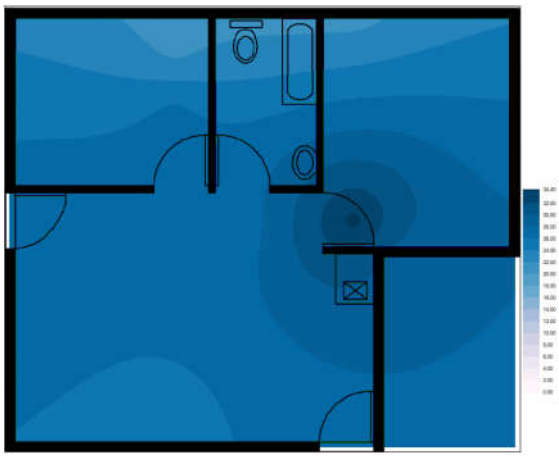

APPENDIX D - Figure: 82: 2015 February 600mm MC: 20%-35%

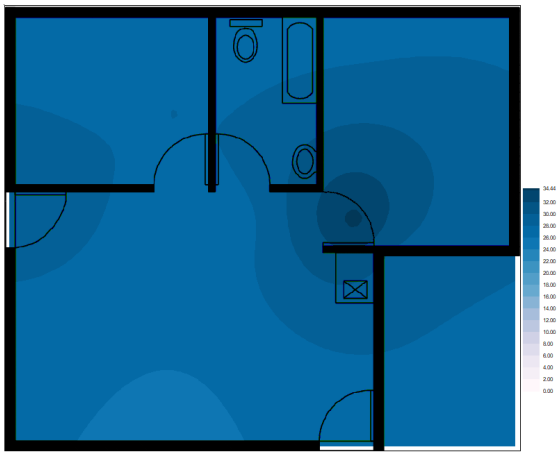

APPENDIX D - Figure: 83: 2015 February 800mm MC: 25%-35%

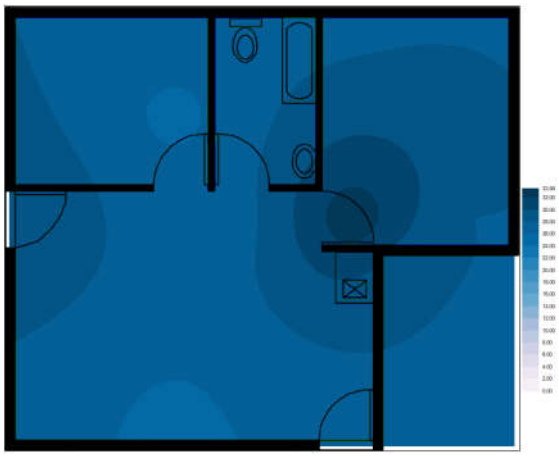

APPENDIX D - Figure: 84: 2015 February 1000mm MC: 25%-34%

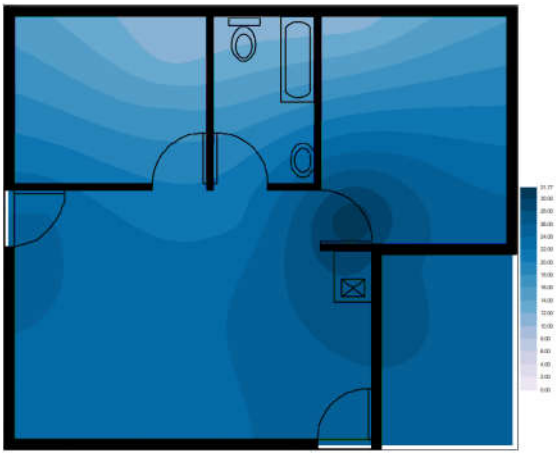

APPENDIX D - Figure: 85: 2015 March 150mm MC: 10%-32%

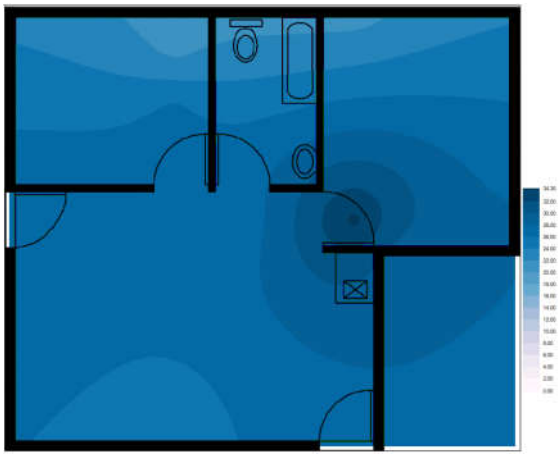

APPENDIX D - Figure: 88: 2015 March 600mm MC: 10%-35%

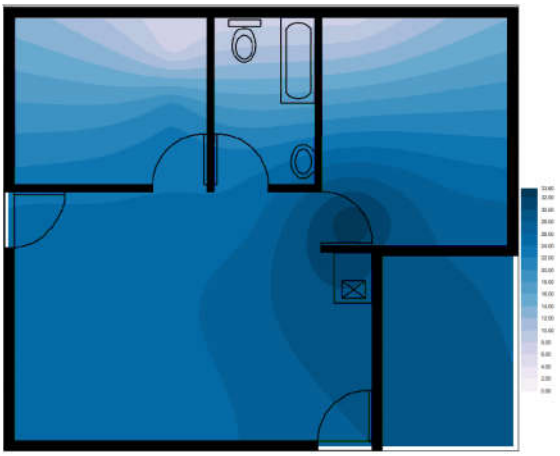

APPENDIX D - Figure: 86: 2015 March 300mm MC: 7%-34%

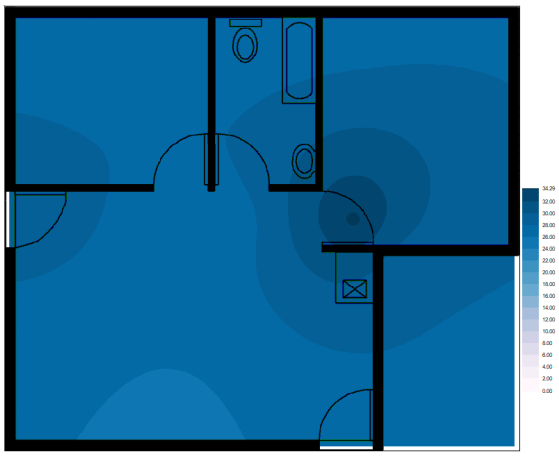

APPENDIX D - Figure: 89: 2015 March 800mm MC: 25%-35%

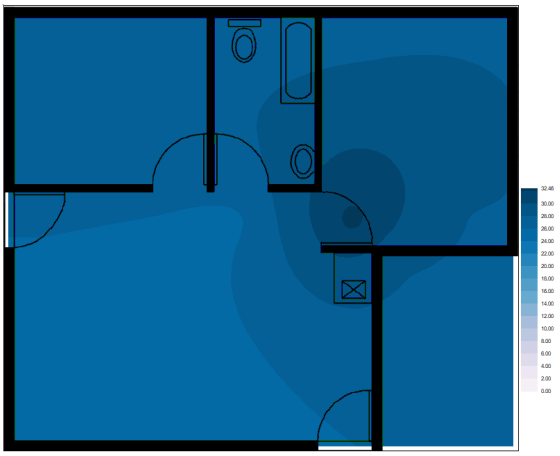

APPENDIX D - Figure: 87: 2015 March 450mm MC: 24%-33%

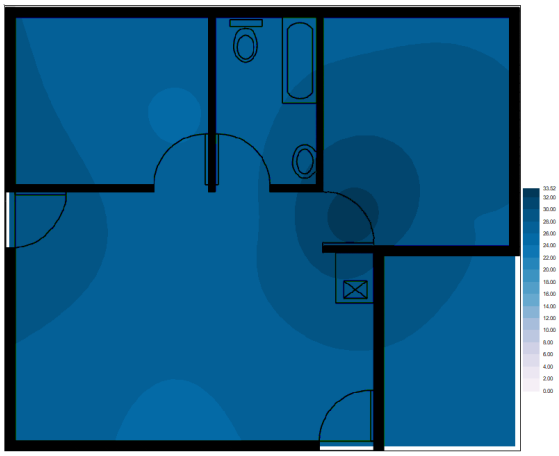

APPENDIX D - Figure: 90: 2015 March 1000mm MC: 25%-34%

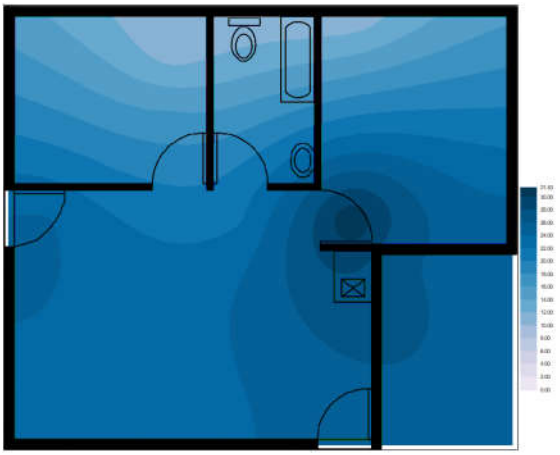

APPENDIX D - Figure: 91: 2015 April 150mm MC: 10%-32%

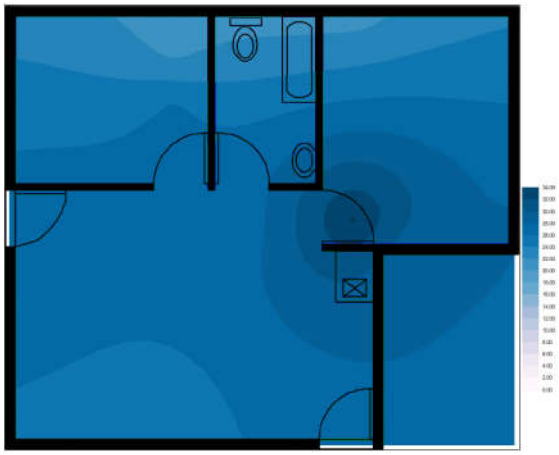

APPENDIX D - Figure: 94: 2015 April 600mm MC: 20%-34%

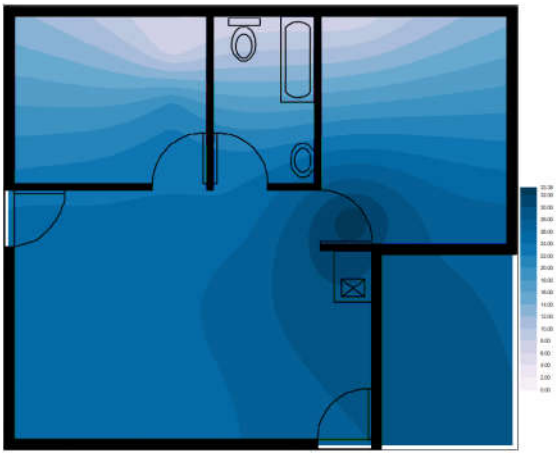

APPENDIX D - Figure: 92: 2015 April 300mm MC: 6%-34%

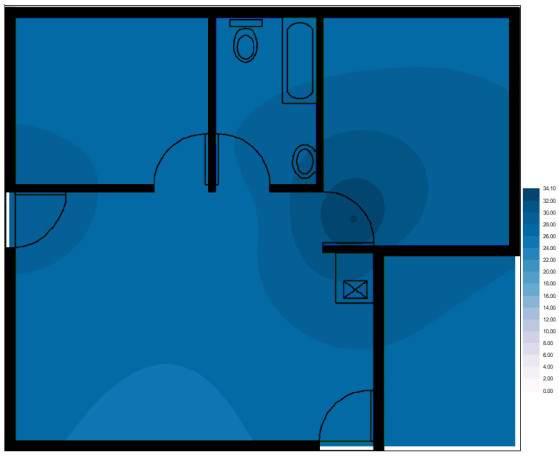

APPENDIX D - Figure: 95: 2015 April 800mm MC: 25%-34%

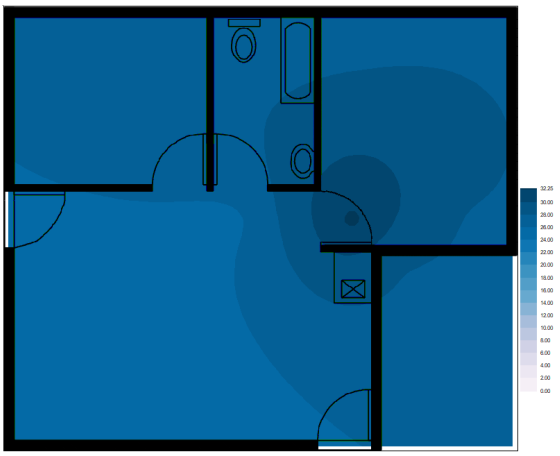

APPENDIX D - Figure: 93: 2015 April 450mm MC: 24%-32%

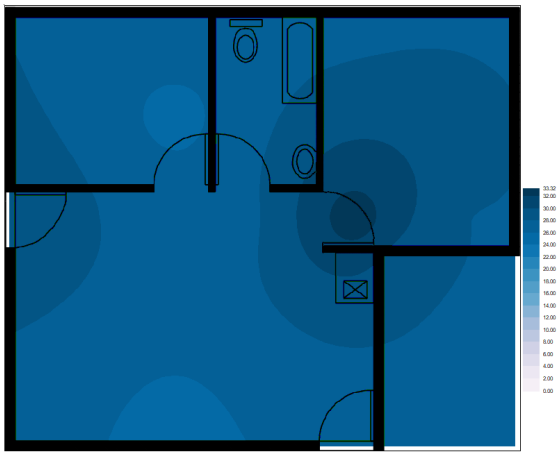

APPENDIX D - Figure: 96: 2015 April 1000mm MC: 25%-34%

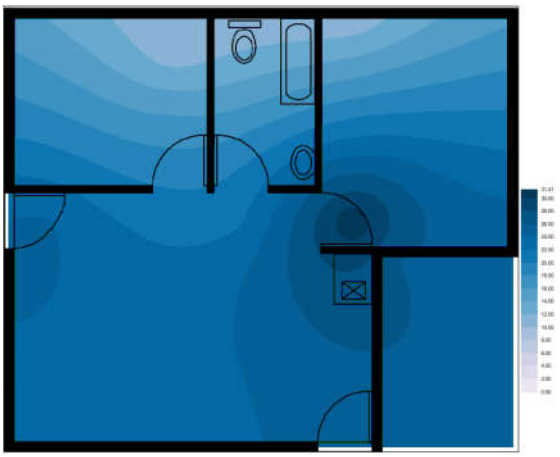

APPENDIX D - Figure: 97: 2015 May 150mm MC: 10%-32%

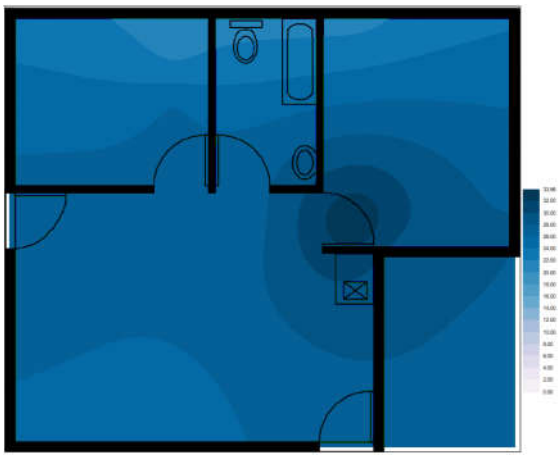

APPENDIX D - Figure: 100: 2015 May 600mm MC: 20%-34%

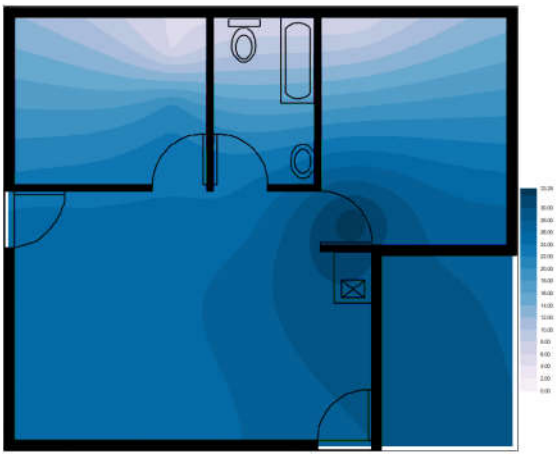

APPENDIX D - Figure: 98: 2015 May 300mm MC: 6%-33%

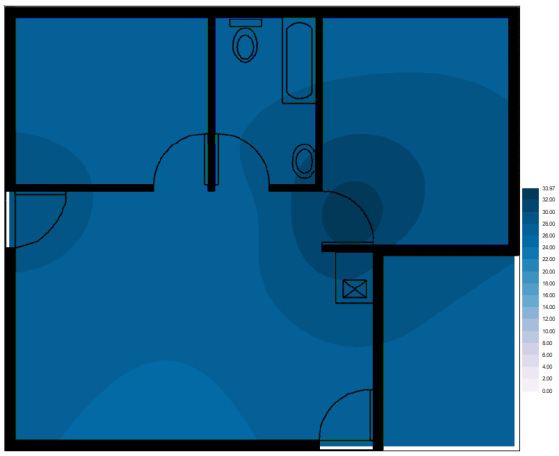

APPENDIX D - Figure: 101: 2015 May 800mm MC: 25%-34%

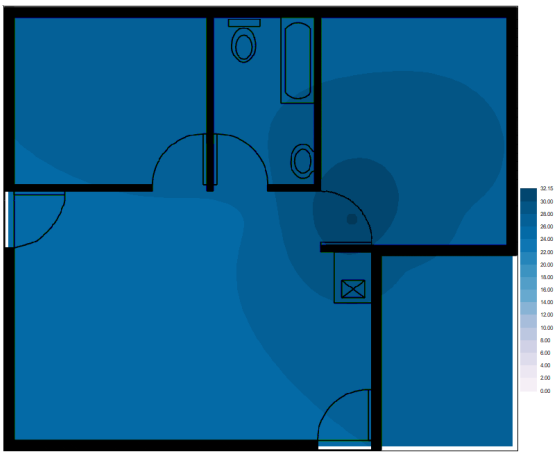

APPENDIX D - Figure: 99: 2015 May 450mm MC: 24%-32%

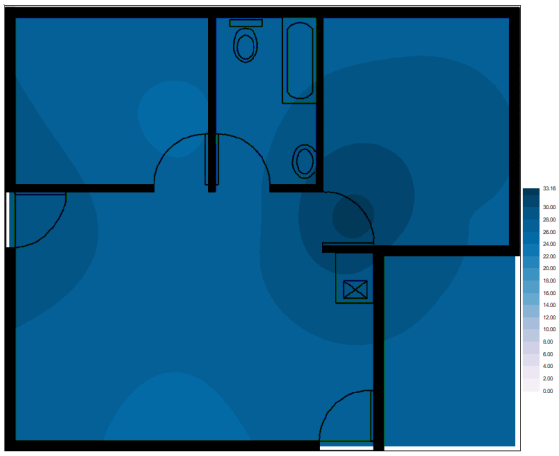

APPENDIX D - Figure: 102: 2015 May 1000mm MC: 25%-33%

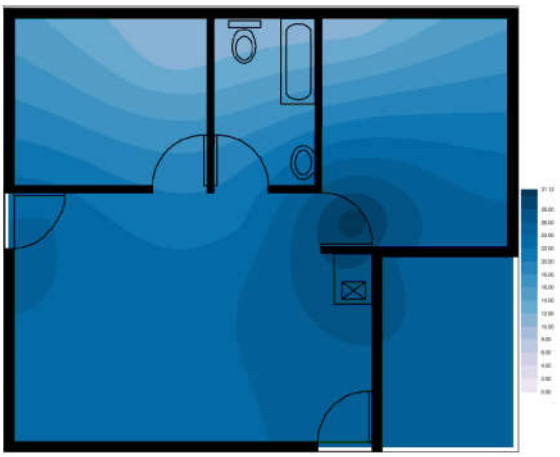

APPENDIX D - Figure: 103: 2015 June 150mm MC: 10%-31%

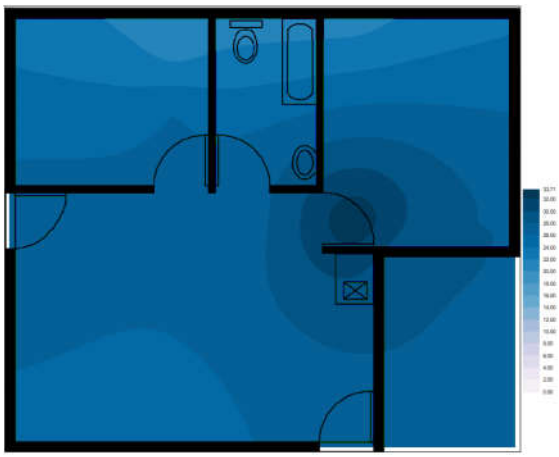

APPENDIX D - Figure: 106: 2015 June 600mm MC: 20%-34%

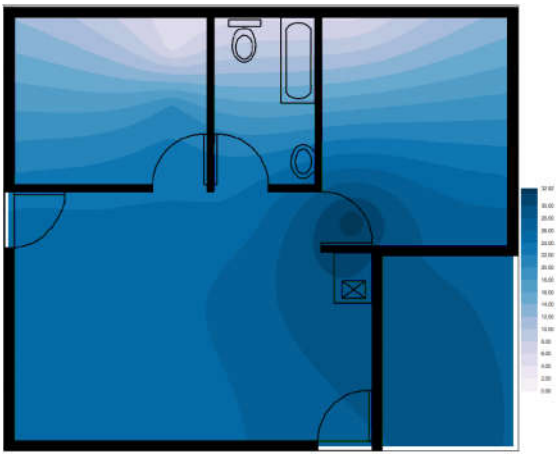

APPENDIX D - Figure: 104: 2015 June 300mm MC: 5%-33%

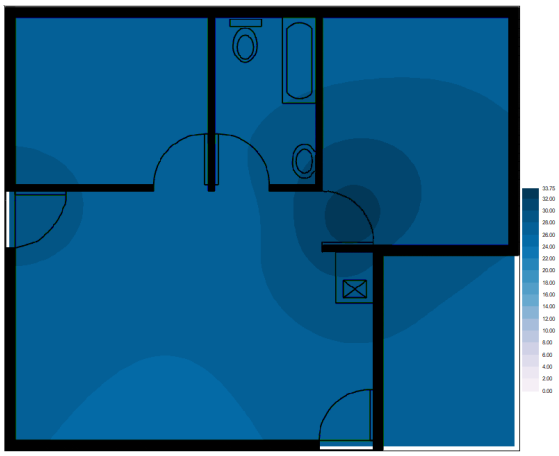

APPENDIX D - Figure: 107: 2015 June 800mm MC: 25%-34%

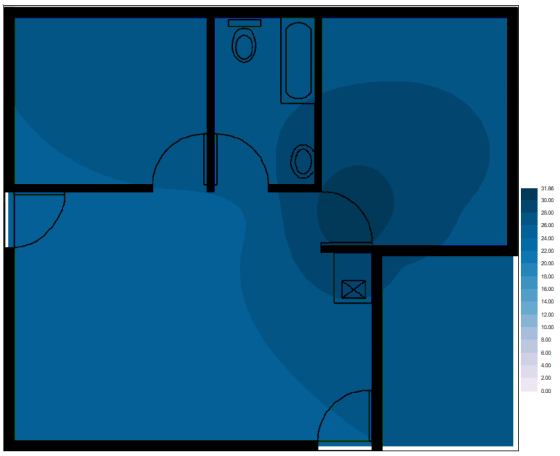

APPENDIX D - Figure: 105: 2015 June 450mm MC: 24%-32%

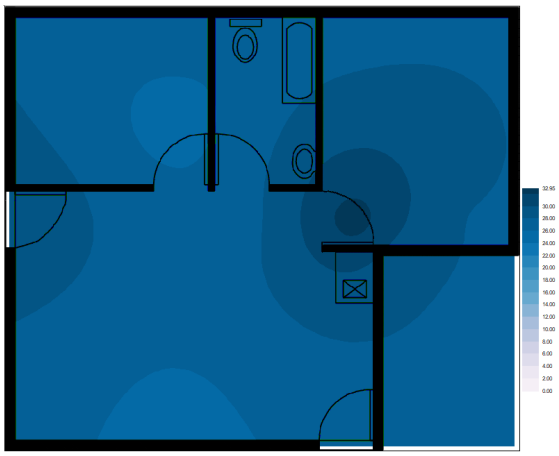

APPENDIX D - Figure: 108: 2015 June 1000mm MC: 24%-33%

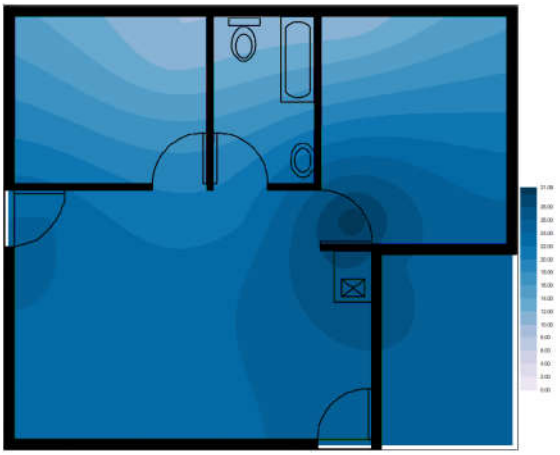

APPENDIX D - Figure: 109: 2015 July 150mm MC: 10%-31%

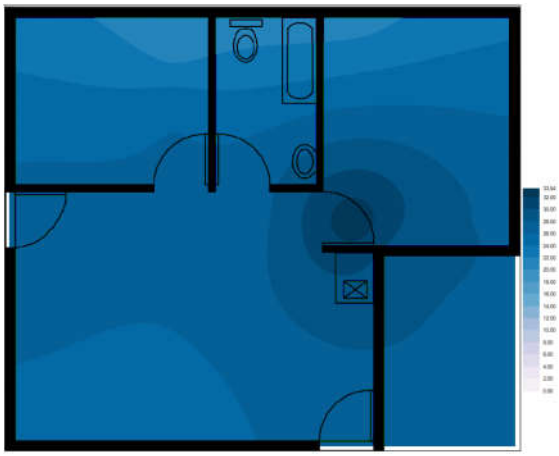

APPENDIX D - Figure: 112: 2015 July 600mm MC: 20%-34%

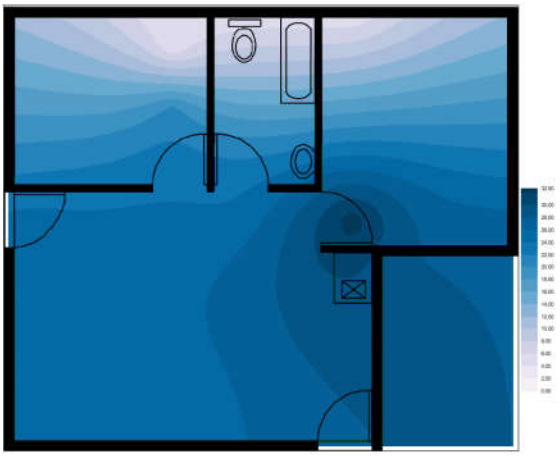

APPENDIX D - Figure: 110: 2015 July 300mm MC: 5%-33%

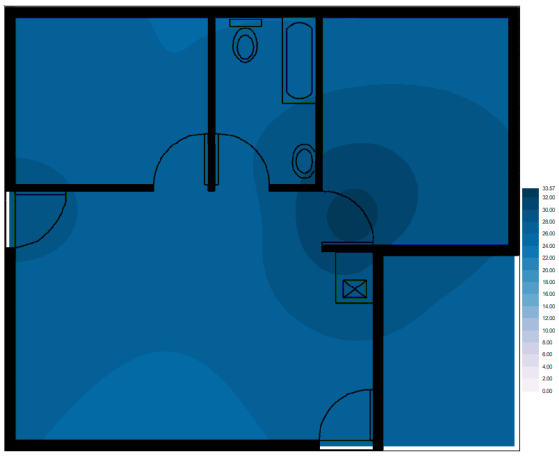

APPENDIX D - Figure: 113: 2015 July 800mm MC: 25%-34%

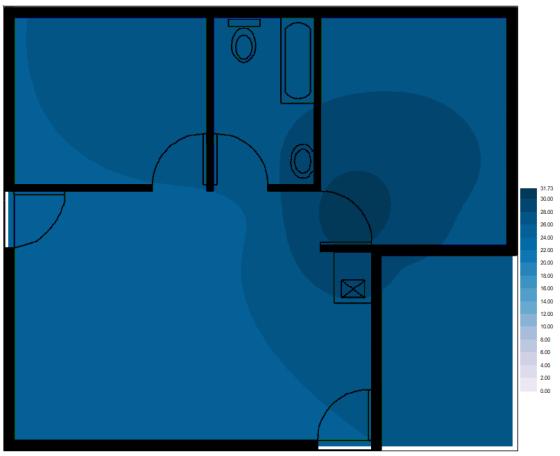

APPENDIX D - Figure: 111: 2015 July 450mm MC: 24%-32%

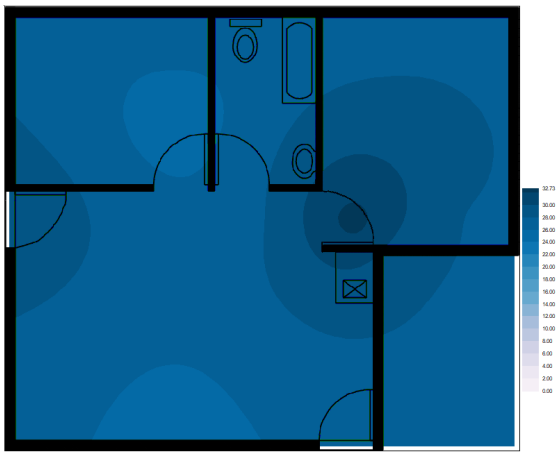

APPENDIX D - Figure: 114: 2015 July 1000mm MC: 24%-33%

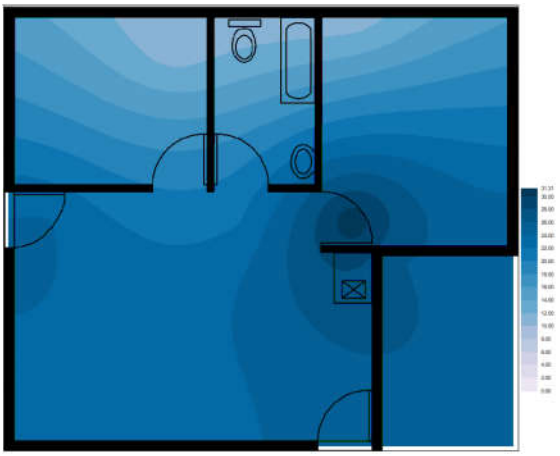

APPENDIX D - Figure: 115: 2015 August 150mm MC: 10%-32%

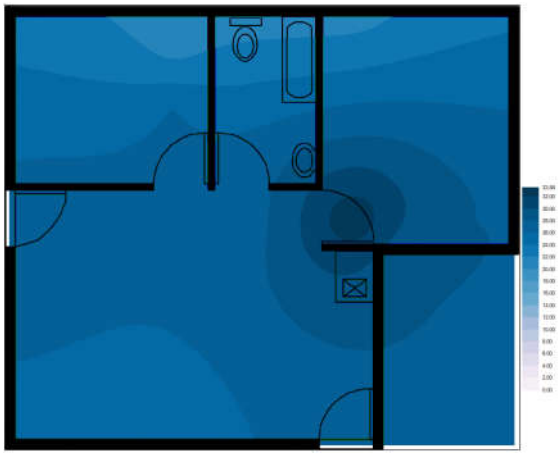

APPENDIX D - Figure: 118: 2015 August 600mm MC: 20%-34%

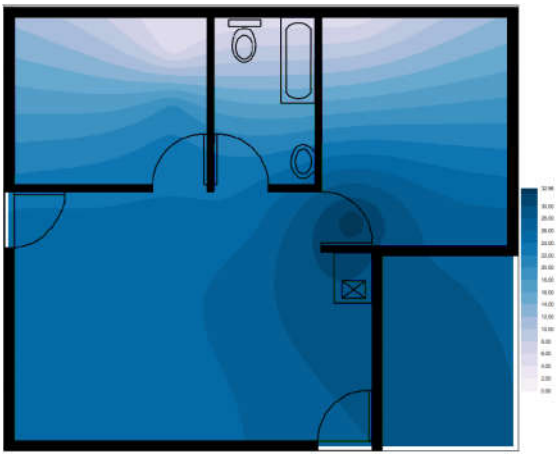

APPENDIX D - Figure: 116: 2015 August 300mm MC: 5%-33%

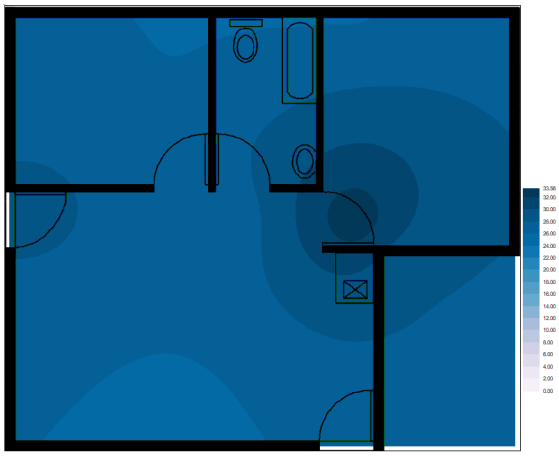

APPENDIX D - Figure: 119: 2015 August 800mm MC: 25%-34%

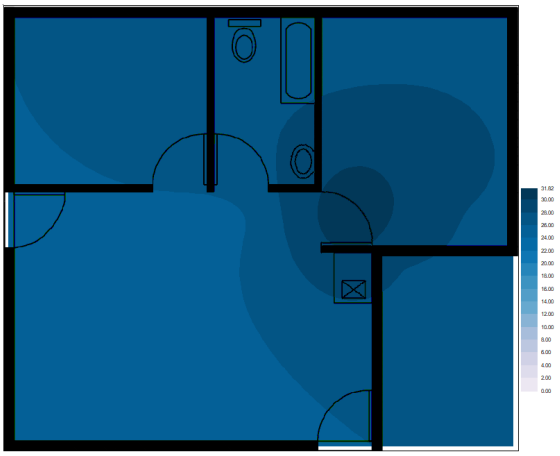

APPENDIX D - Figure: 117: 2015 August 450mm MC: 24%-32%

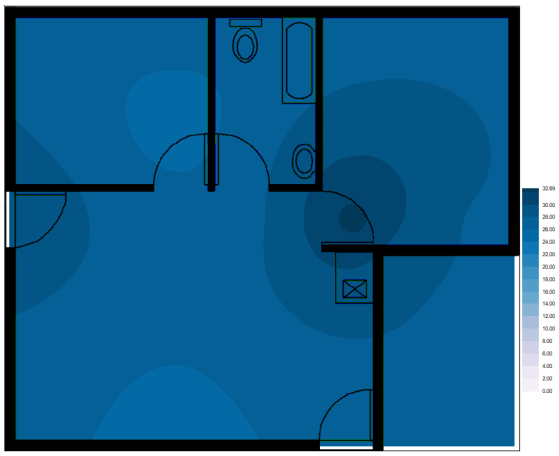

APPENDIX D - Figure: 120: 2015 August 1000mm MC: 24%-33%

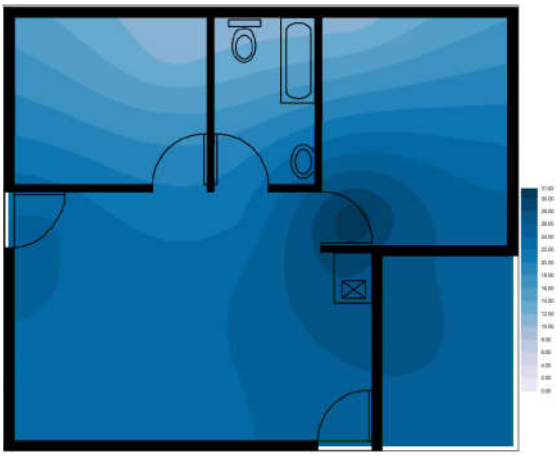

APPENDIX D - Figure: 121: 2015 September 150mm MC: 10%-32%

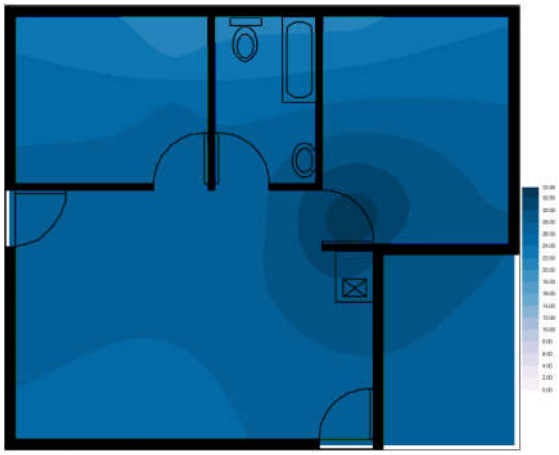

APPENDIX D - Figure: 124: 2015 September 600mm MC: 20%-34%

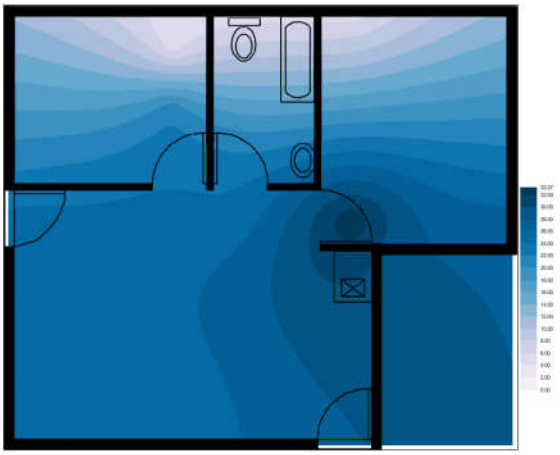

APPENDIX D - Figure: 122: 2015 September 300mm MC: 5%-34%

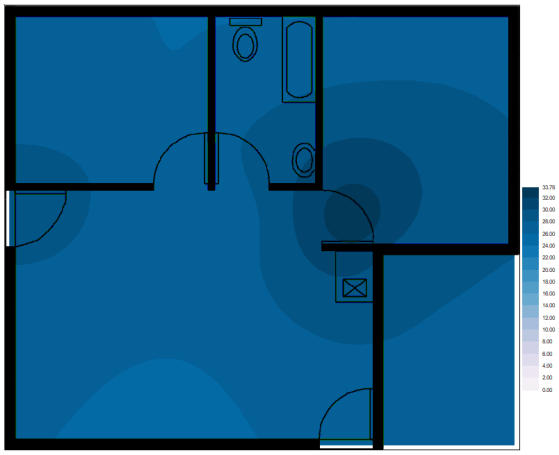

APPENDIX D - Figure: 125: 2015 September 800mm MC: 25%-34%

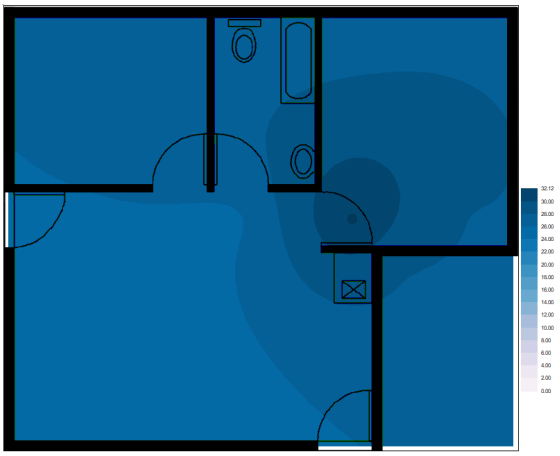

APPENDIX D - Figure: 123: 2015 September 450mm MC: 24%-32%

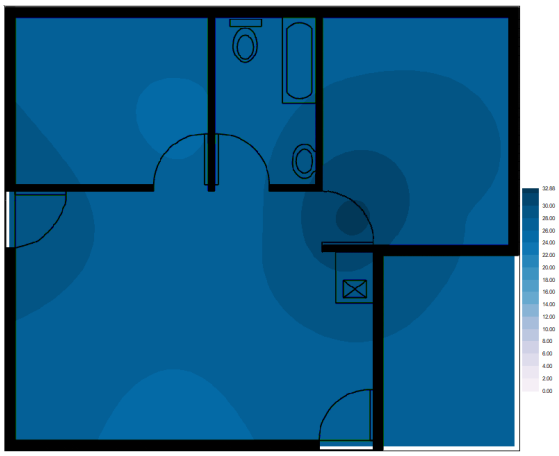

APPENDIX D - Figure: 126: 2015 September 1000mm MC: 25%-33%

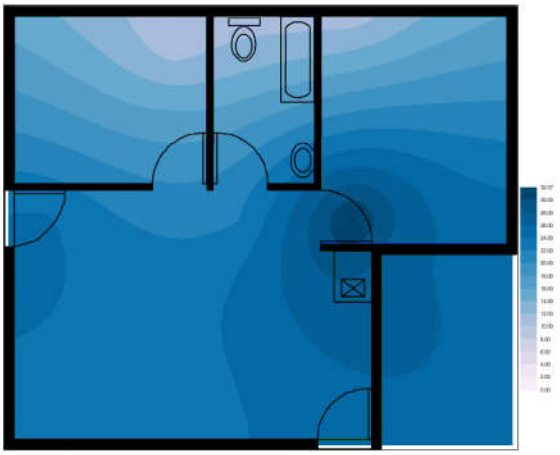

APPENDIX D - Figure: 127: 2015 October 150mm MC: 10%-32%

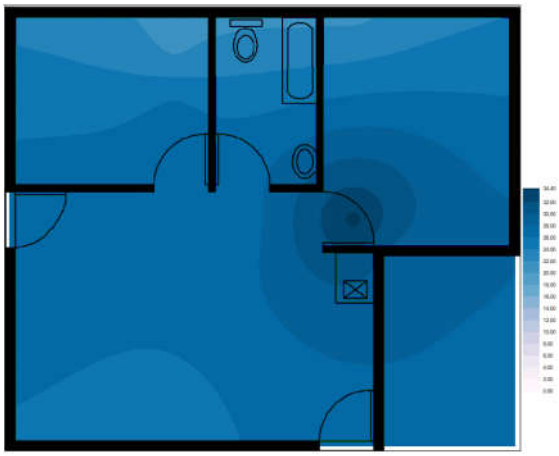

APPENDIX D - Figure: 130: 2015 October 600mm MC: 21%-35%

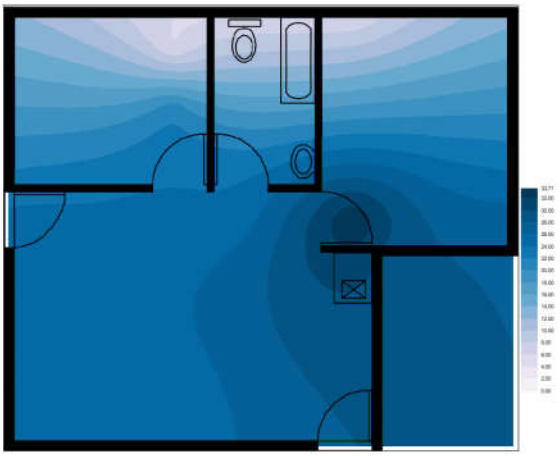

APPENDIX D - Figure: 128: 2015 October 300mm MC: 6%-34%

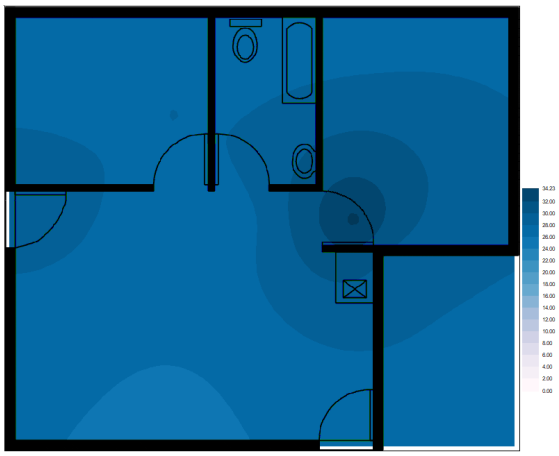

APPENDIX D - Figure: 131: 2015 October 800mm MC: 25%-34%

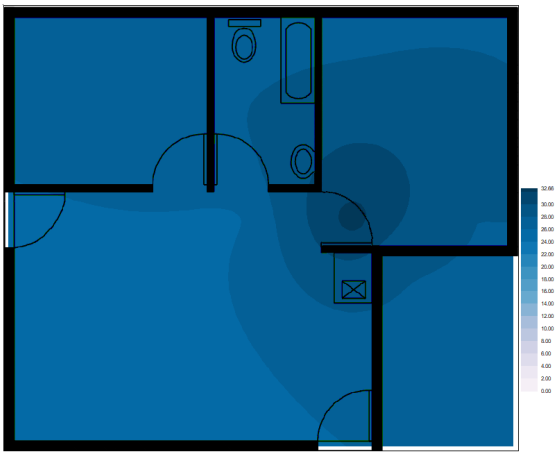

APPENDIX D - Figure: 129: 2015 October 450mm MC: 24%-33%

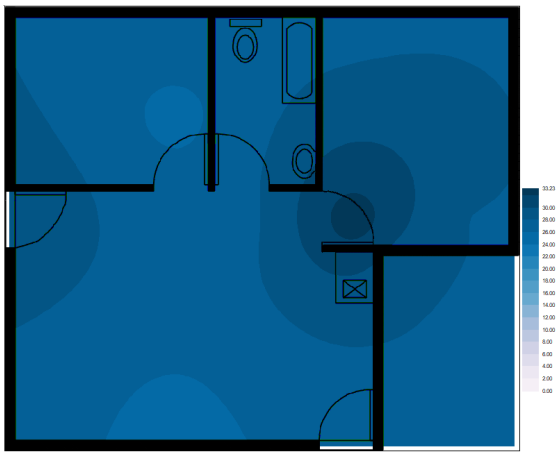

APPENDIX D - Figure: 132: 2015 October 1000mm MC: 25%-33%

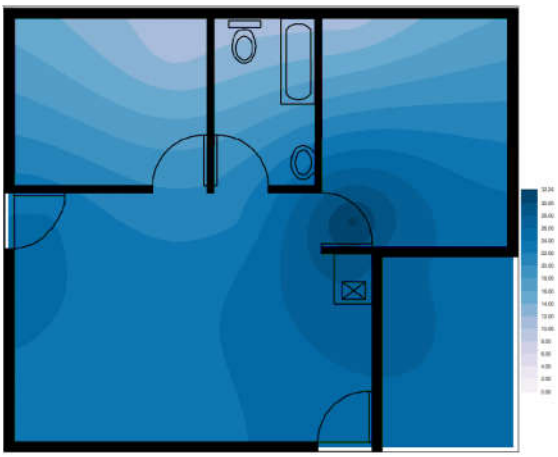

APPENDIX D - Figure: 133: 2015 November 150mm MC: 10%-33%

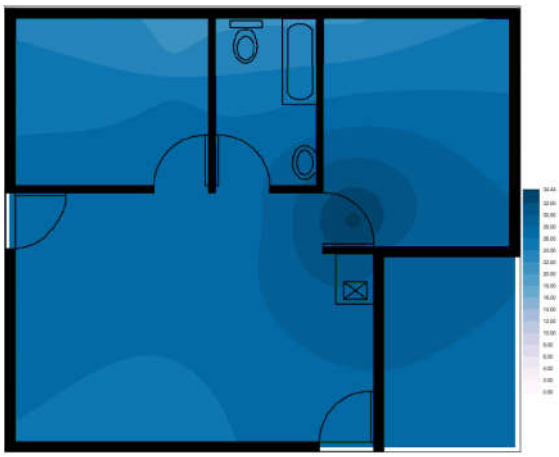

APPENDIX D - Figure: 136: 2015 November 600mm MC: 21%-35%

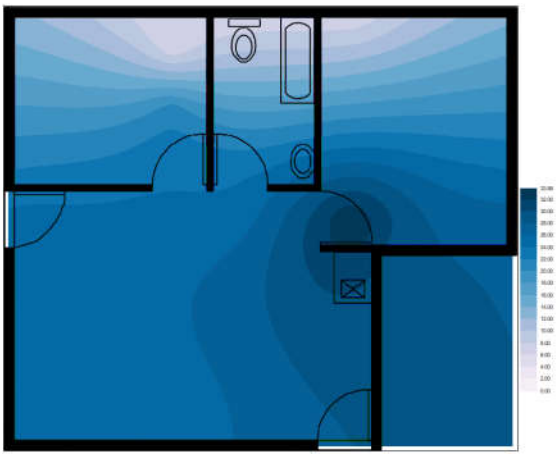

APPENDIX D - Figure: 134: 2015 November 300mm MC: 6%-34%

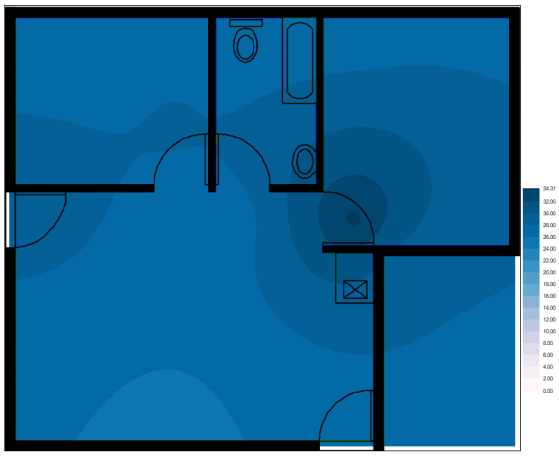

APPENDIX D - Figure: 137: 2015 November 800mm MC: 24%-35%

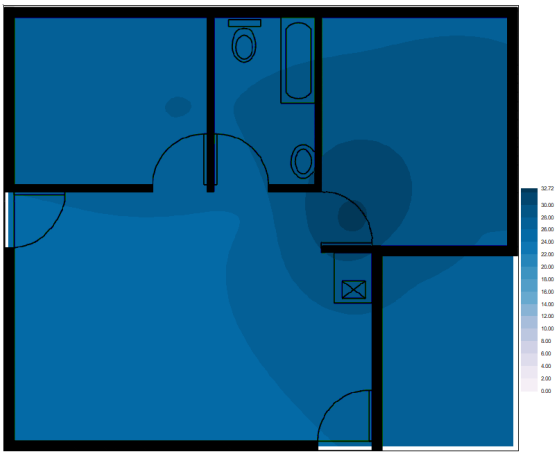

APPENDIX D - Figure: 135: 2015 November 450mm MC: 24%-33%

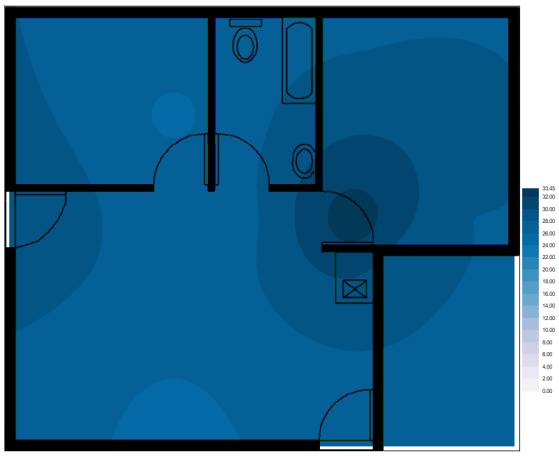

APPENDIX D - Figure: 138: 2015 November 1000mm MC: 25%-34%

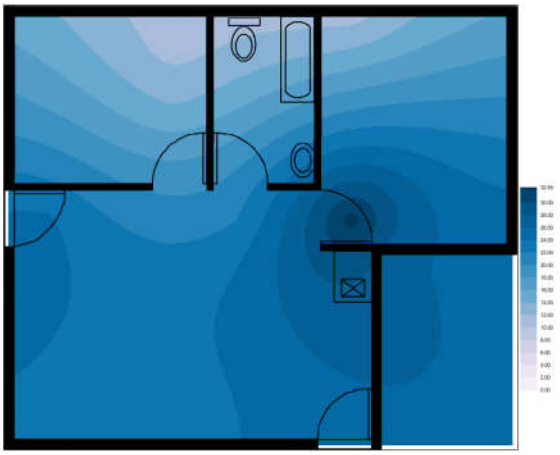

APPENDIX D - Figure: 139: 2015 December 150mm MC: 10%-33%

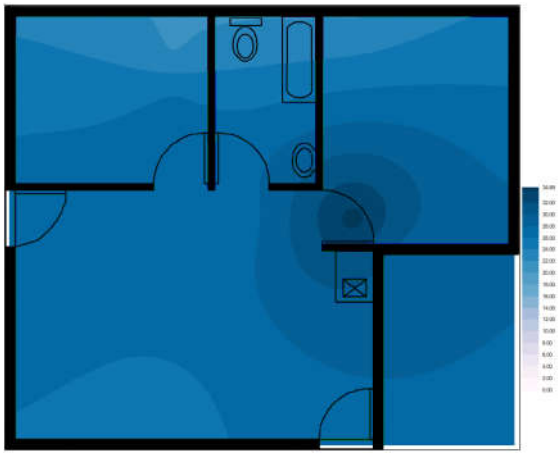

APPENDIX D - Figure: 142: 2015 December 600mm MC: 22%-35%

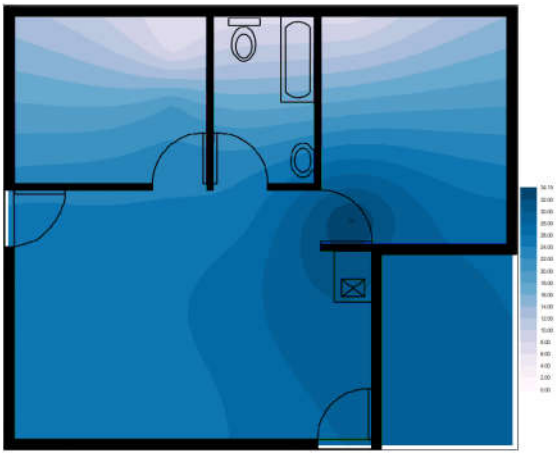

APPENDIX D - Figure: 140: 2015 December 300mm MC: 7%-34%

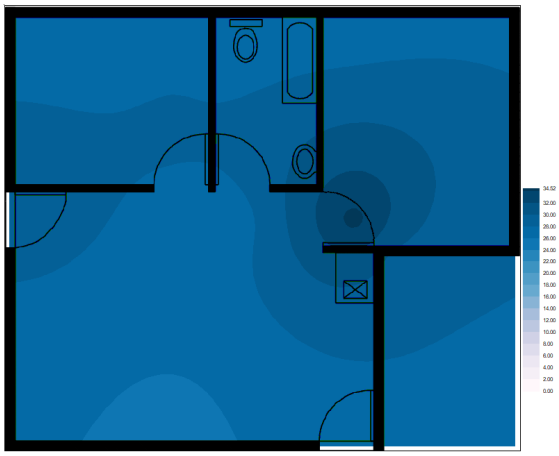

APPENDIX D - Figure: 143: 2015 December 800mm MC: 25%-35%

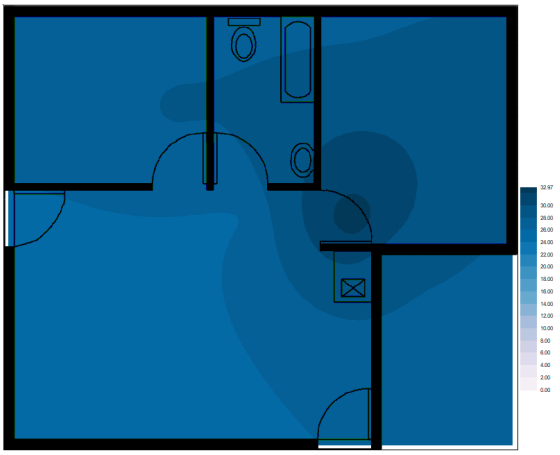

APPENDIX D - Figure: 141: 2015 December 450mm MC: 24%-33%

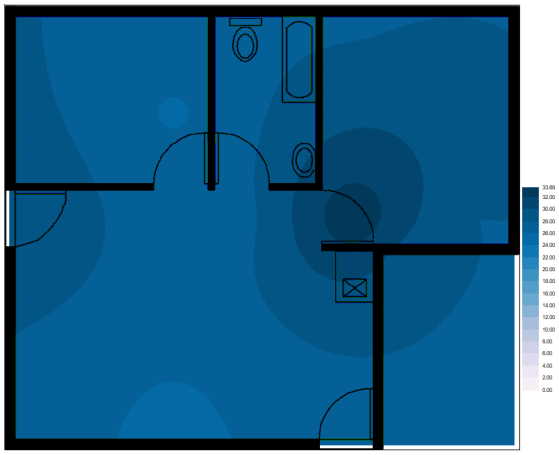

APPENDIX D - Figure: 144: 2015 December 1000mm MC: 25%-34%

APPENDIX: E

Temperature change models using 3D Field

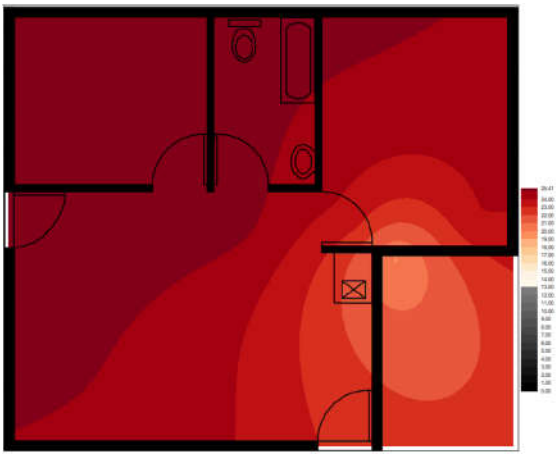

APPENDIX E - Figure: 145: 2014 January 150mm Temperature: 19.9°C – 25.4°C

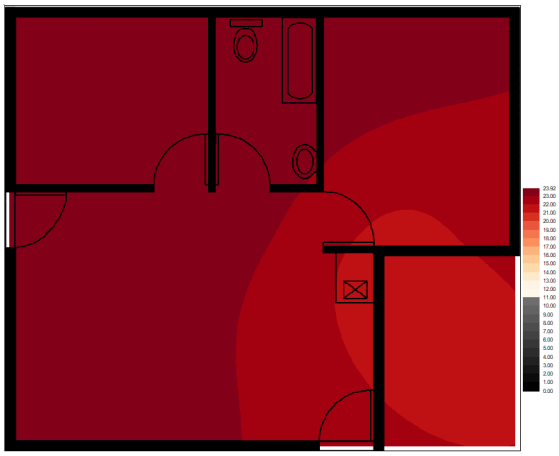

APPENDIX E - Figure: 148: 2014 January 600mm Temperature: 21°C - 0°C

APPENDIX E - Figure: 146: 2014 January 300mm Temperature: 20.5°C – 25.1°C

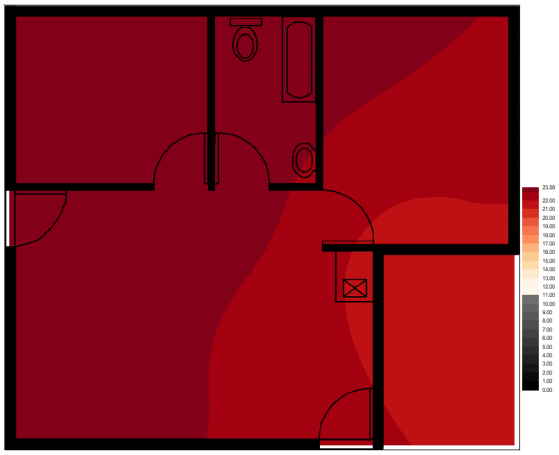

APPENDIX E - Figure: 149: 2014 January 800mm Temperature: 21.3°C – 23.6°C

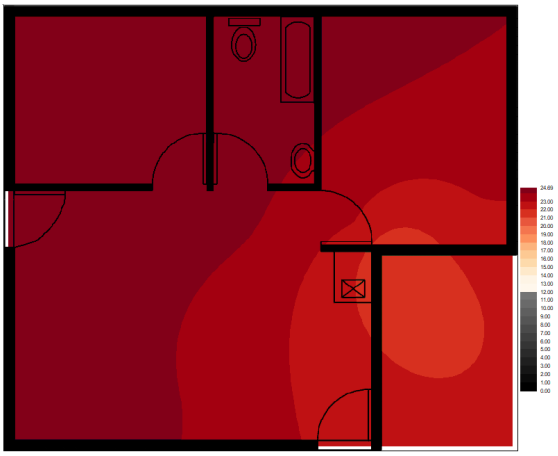

APPENDIX E - Figure: 147: 2014 January 450mm Temperature: 21.0°C – 24.7°C

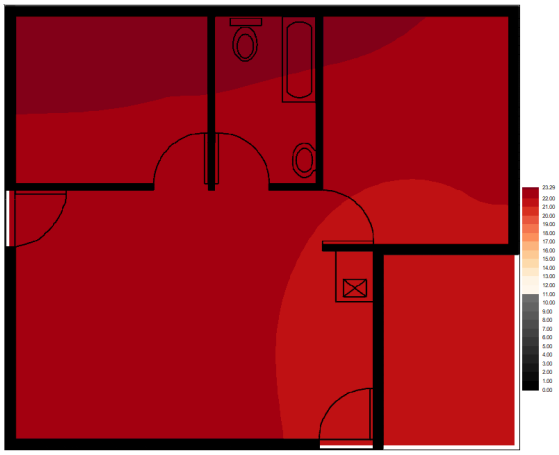

APPENDIX E - Figure: 150: 2014 January 1000mm Temperature: 23.3°C – 21.1°C

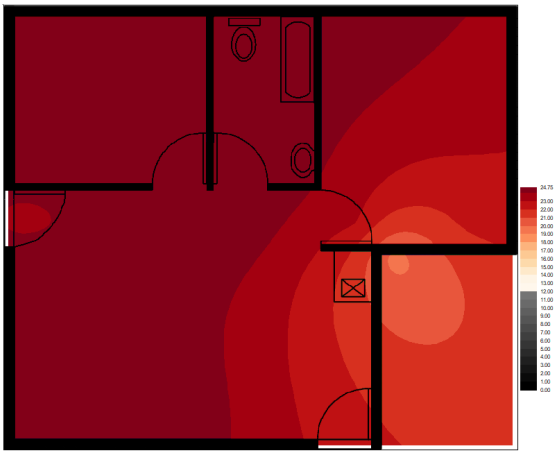

APPENDIX E - Figure: 151: 2014

February 150mm Temp: 19.6°C – 24.7°C

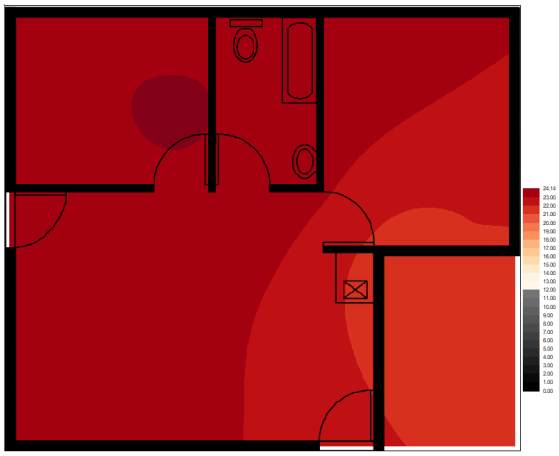

APPENDIX E - Figure: 154: 2014

February 600mm Temp: 21.0°C – 24.1°C

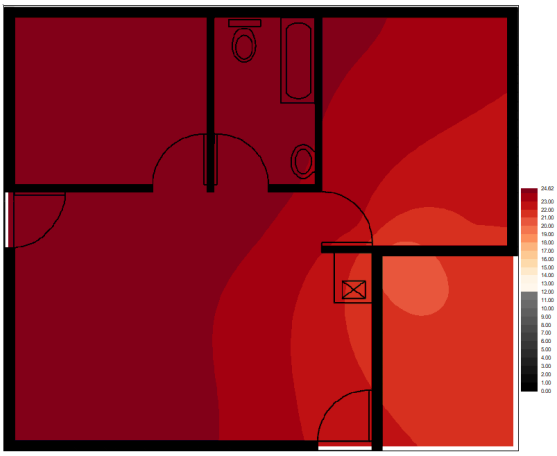

APPENDIX E - Figure: 152: 2014

February 300mm Temp: 20.3°C – 24.6°C

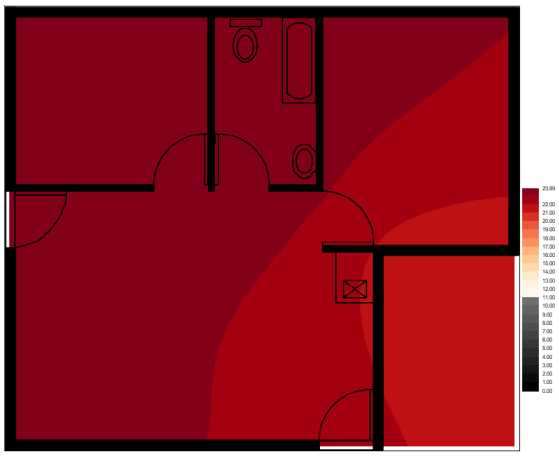

APPENDIX E - Figure: 155: 2014

February 800mm Temperature: 21.5°C – 23.9°C

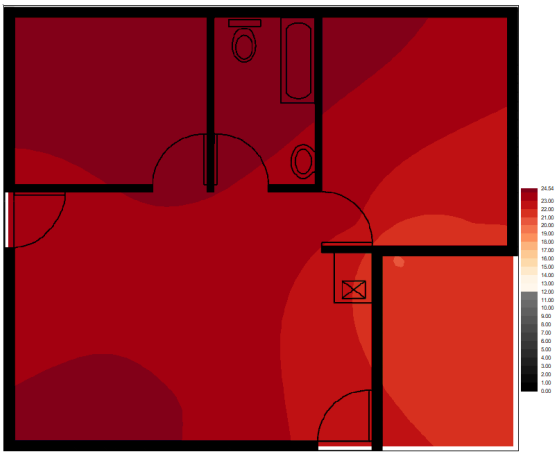

APPENDIX E - Figure: 153: 2014

February 450mm Temp: 20.9°C – 24.5°C

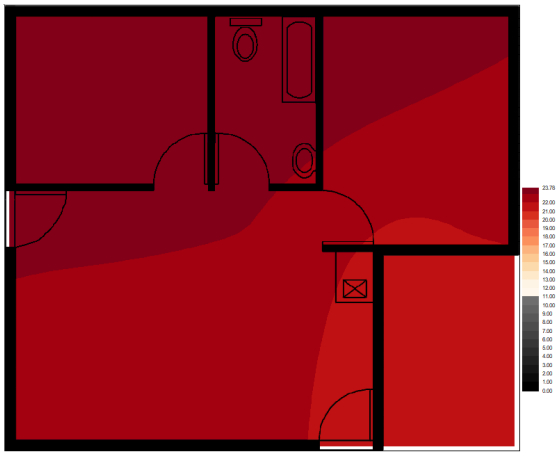

APPENDIX E - Figure: 156: 2014

February 1000mm Temp: 21.5°C – 23.8°C

APPENDIX E - Figure: 157: 2014 March 150mm Temperature: 17.4°C – 23.6°C

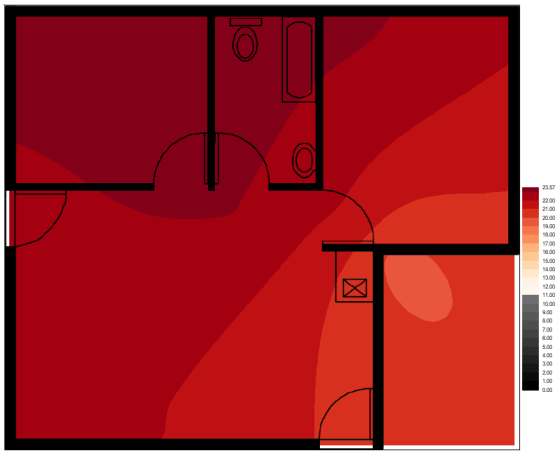

APPENDIX E - Figure: 160: 2014 March 600mm Temperature: 19.7°C – 23.6°C

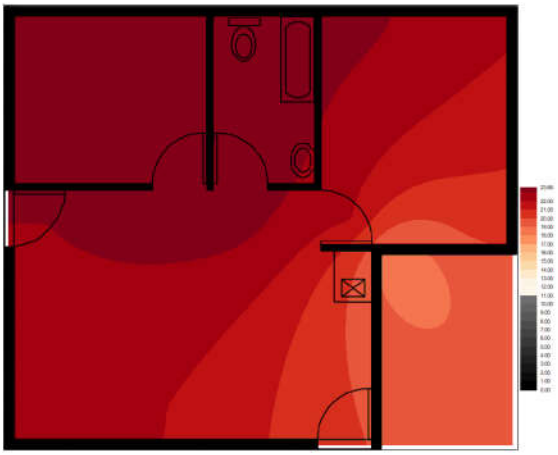

APPENDIX E - Figure: 158: 2014 March 300mm Temperature: 18.3°C – 23.5°C

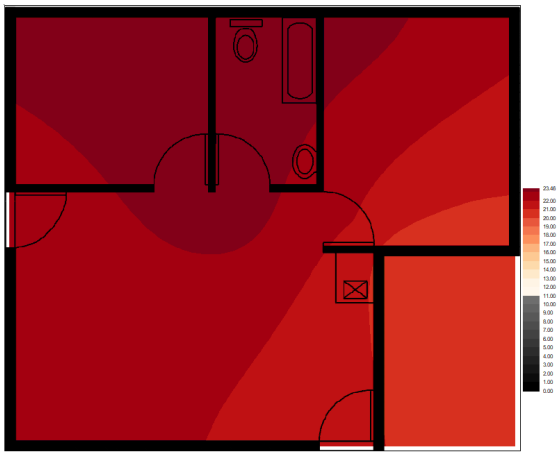

APPENDIX E - Figure: 161: 2014 March 800mm Temperature: 20.5°C – 23.4°C

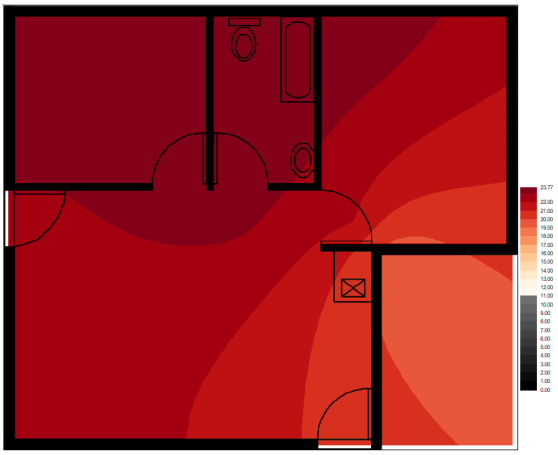

APPENDIX E - Figure: 159: 2014 March 450mm Temperature: 19.2°C – 23.6°C

APPENDIX E - Figure: 162: 2014 March 150mm Temperature: 20.7°C – 23.4°C

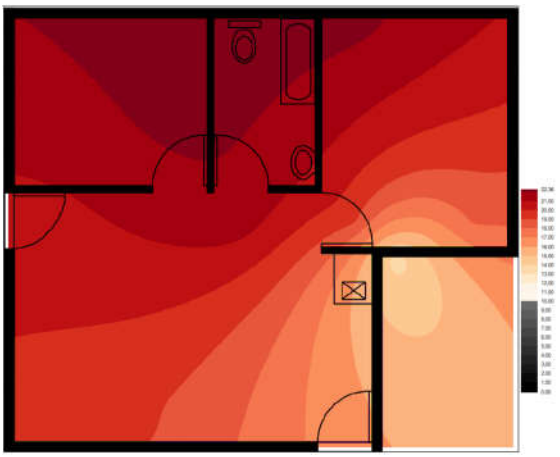

APPENDIX E - Figure: 163: 2014 April 150mm Temperature: 13.6°C – 22.3°C

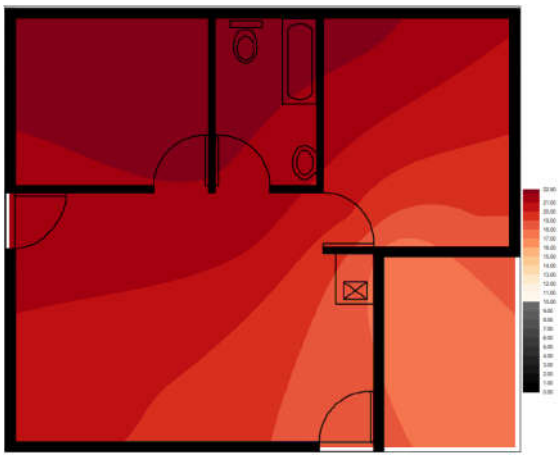

APPENDIX E - Figure: 166: 2014 April 600mm Temperature: 17.1°C – 22.5°C

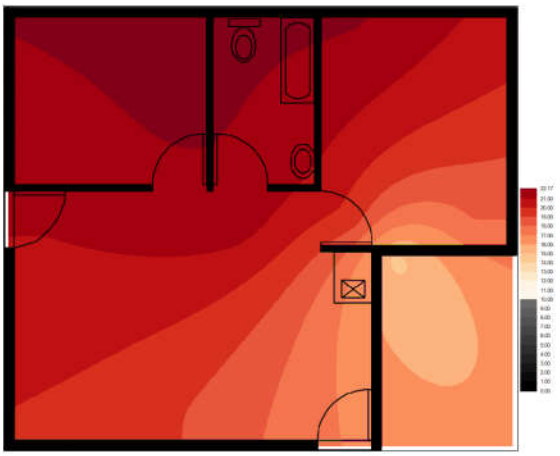

APPENDIX E - Figure: 164: 2014 April 300mm Temperature: 18.0°C – 22.1°C

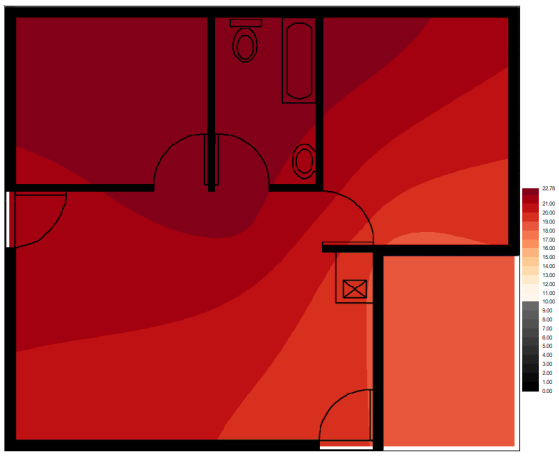

APPENDIX E - Figure: 167: 2014 April 800mm Temperature: 18.3°C – 22.8°C

APPENDIX E - Figure: 165: 2014 April 450mm Temperature: 16.2°C – 22.8°C

APPENDIX E - Figure: 168: 2014 April 1000mm Temperature: 19.0°C – 22.9°C

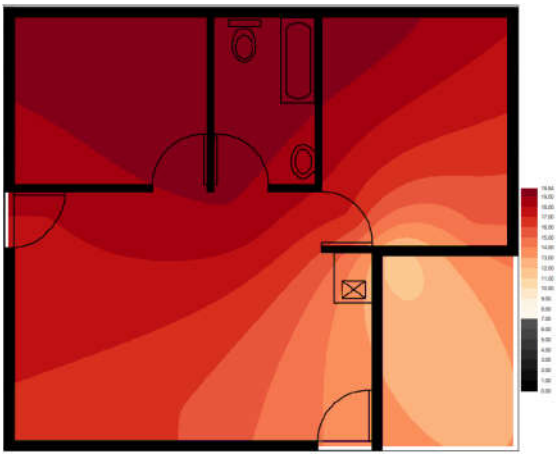

APPENDIX E - Figure: 169: 2014 May 150mm Temperature: 11.3°C – 18.8°C

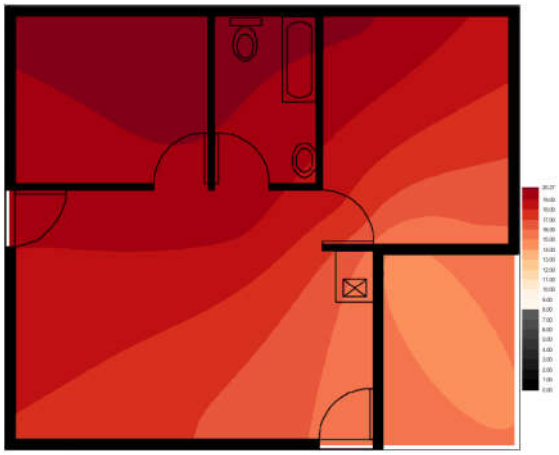

APPENDIX E - Figure: 172: 2014 May 600mm Temperature: 14.5°C – 20.2°C

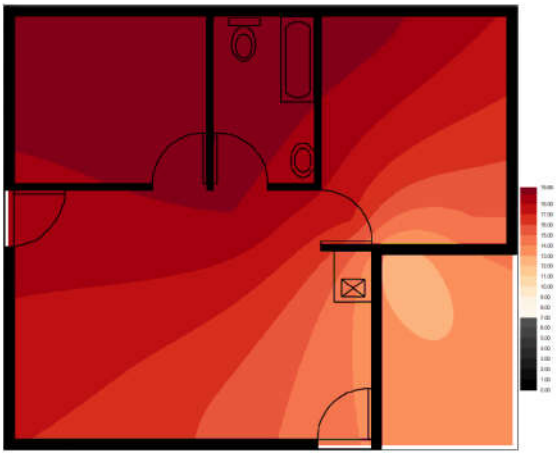

APPENDIX E - Figure: 170: 2014 May 300mm Temperature: 12.2°C – 18.9°C

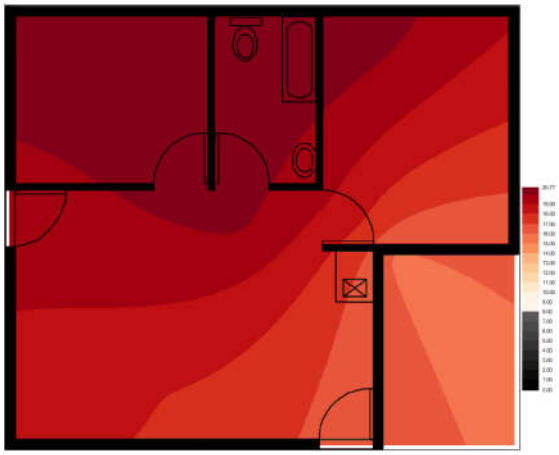

APPENDIX E - Figure: 173: 2014 May 800mm Temperature: 15.9°C – 20.2°C

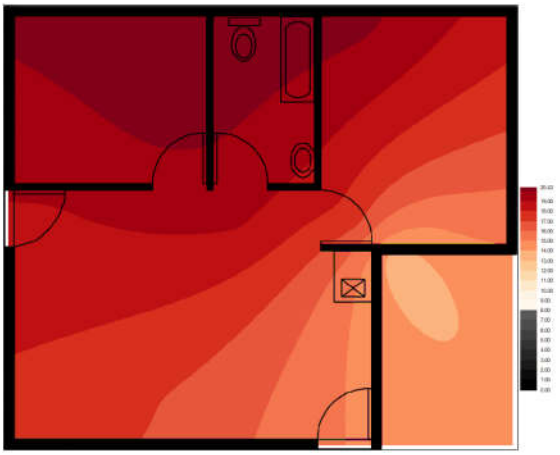

APPENDIX E - Figure: 171: 2014 May 450mm Temperature: 13.6°C – 20.4°C

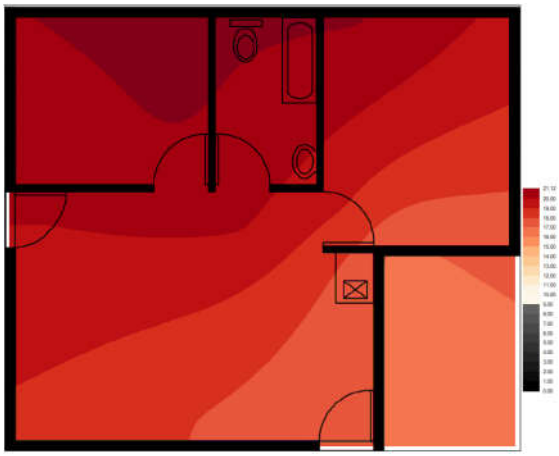

APPENDIX E - Figure: 174: 2014 May 1000mm Temperature: 16.7°C – 20.2°C

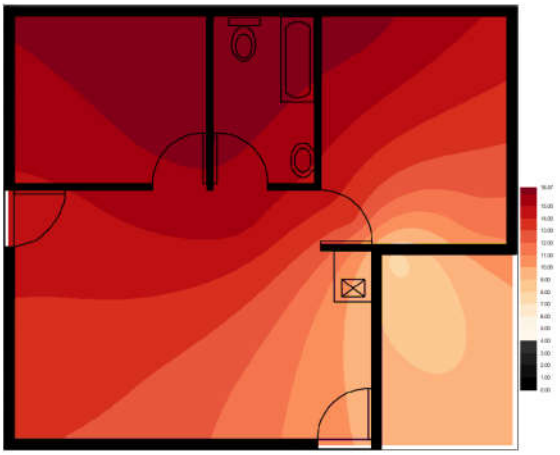

APPENDIX E - Figure: 175: 2014 June 150mm Temperature: 7.6°C – 16.5°C

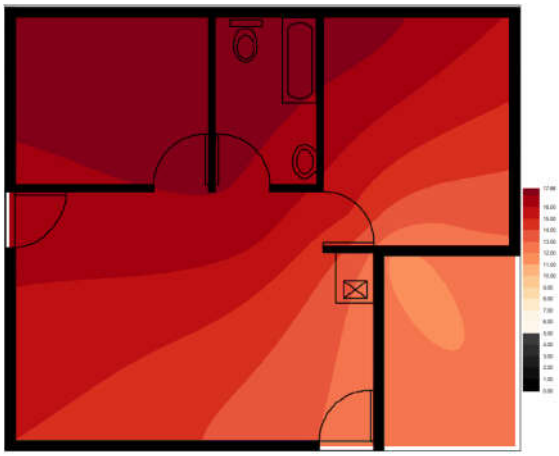

APPENDIX E - Figure: 178: 2014 June 600mm Temperature: 11.2°C – 17.6°C

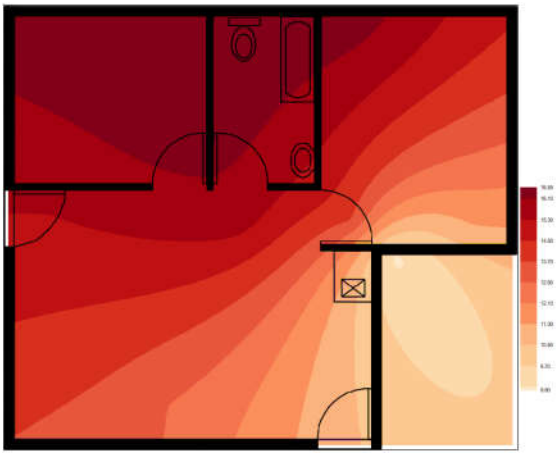

APPENDIX E - Figure: 176: 2014 June 300mm Temperature: 8.8°C – 16.5°C

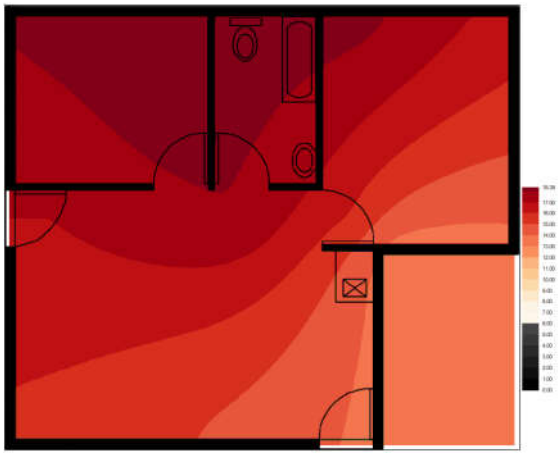

APPENDIX E - Figure: 179: 2014 June 800mm Temperature: 13.3°C – 18.4°C

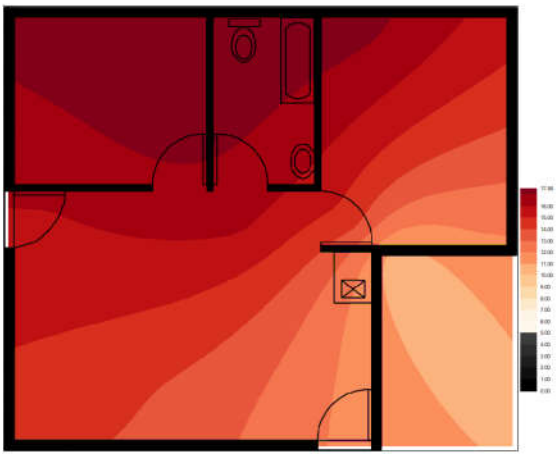

APPENDIX E - Figure: 177: 2014 June 450mm Temperature: 10.4°C – 17.6°C

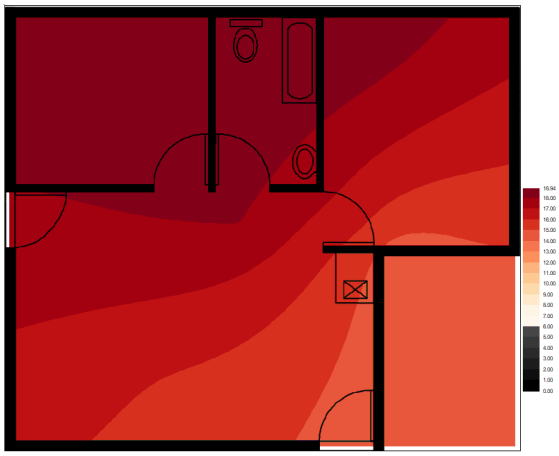

APPENDIX E - Figure: 180: 2014 June 1000mm Temperature: 14.3°C – 18.9°C

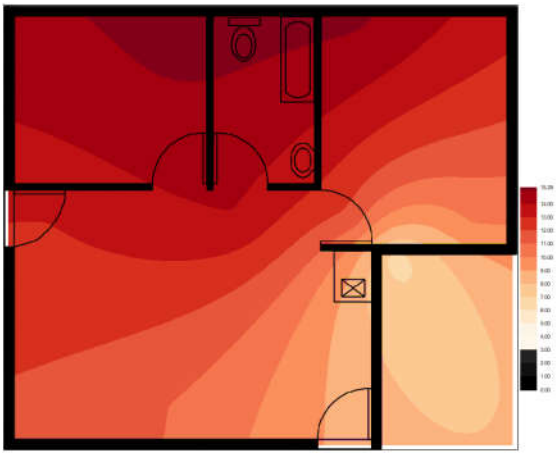

APPENDIX E - Figure: 181: 2014 July
150mm Temperature: 6.6°C – 15.2°C

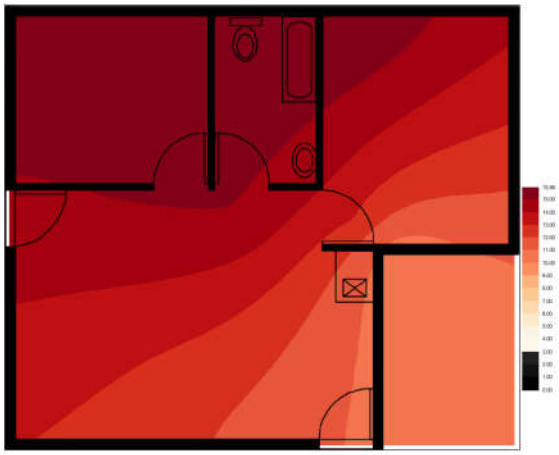

APPENDIX E - Figure: 184: 2014 July
600mm Temperature: 10.2°C – 16.0°C

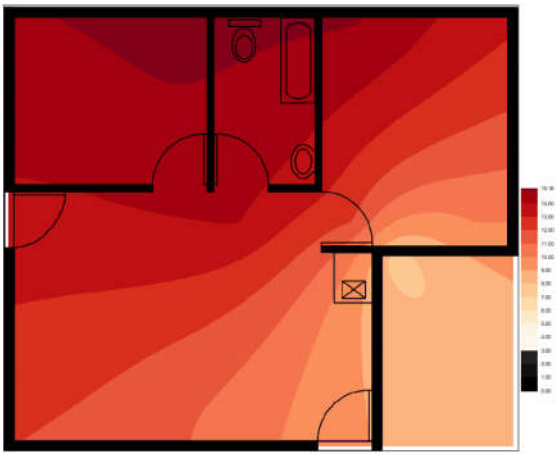

APPENDIX E - Figure: 182: 2014 July
300mm Temperature: 7.6°C – 15.1°C

APPENDIX E - Figure: 185: 2014 July
800mm Temperature: 11.7°C – 16.6°C

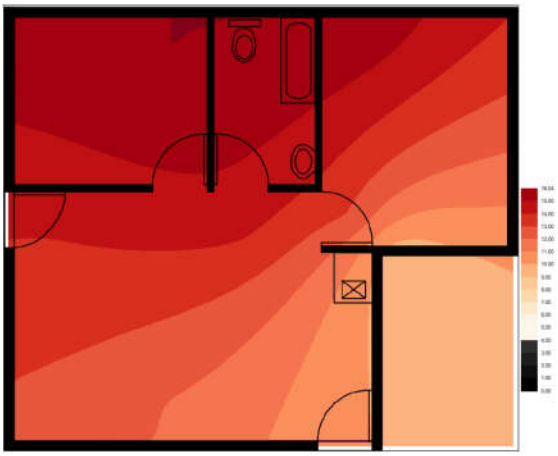

APPENDIX E - Figure: 183: 2014 July
450mm Temperature: 9.1°C – 16.0°C

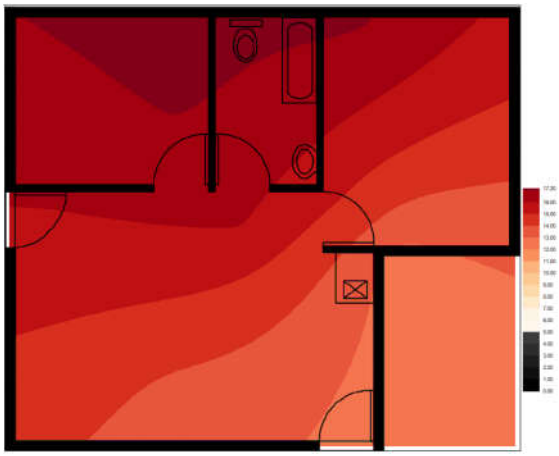

APPENDIX E - Figure: 186: 2014 July
1000mm Temperature: 12.6°C – 17.2°C

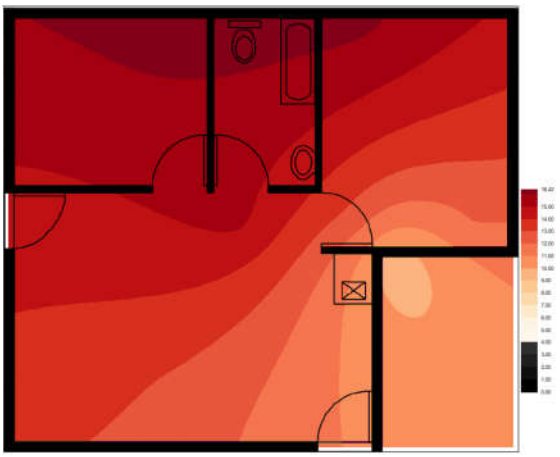

APPENDIX E - Figure: 187: 2014 August 150mm Temperature: 9.4°C – 16.4°C

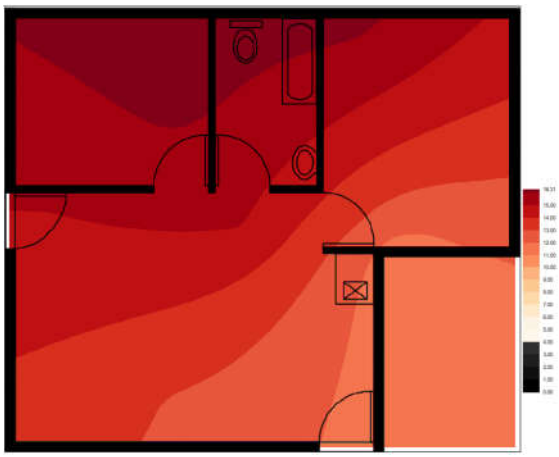

APPENDIX E - Figure: 190: 2014 August 600mm Temperature: 11.3°C – 16.3°C

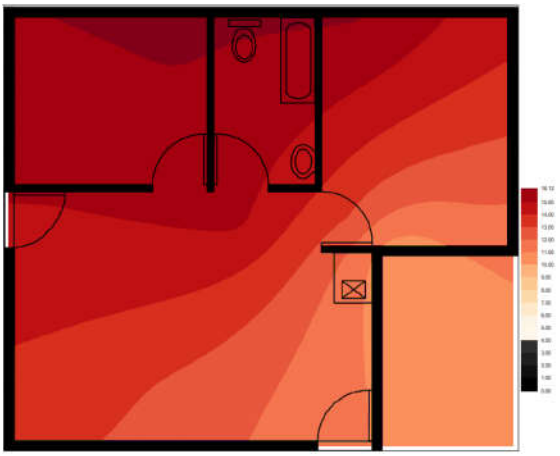

APPENDIX E - Figure: 188: 2014 August 300mm Temperature: 10.1°C – 15.8°C

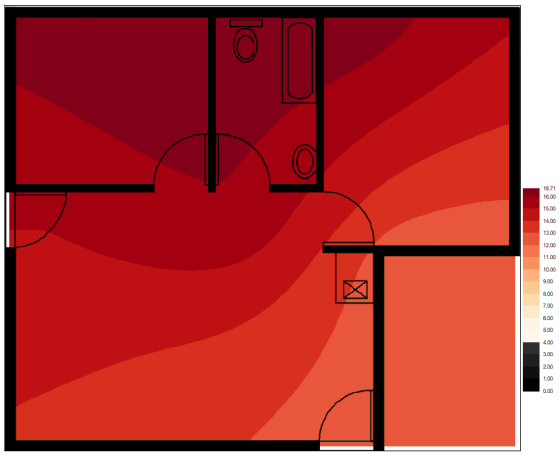

APPENDIX E - Figure: 191: 2014 August 800mm Temperature: 12.3°C – 15.9°C

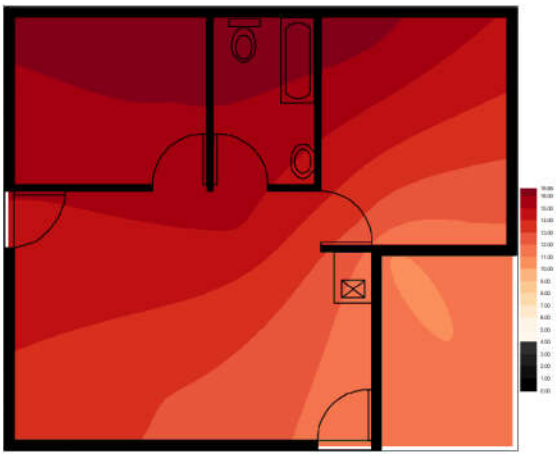

APPENDIX E - Figure: 189: 2014 August 450mm Temperature: 10.9°C – 16.6°C

APPENDIX E - Figure: 192: 2014 August 1000mm Temperature: 12.8°C – 17.0°C

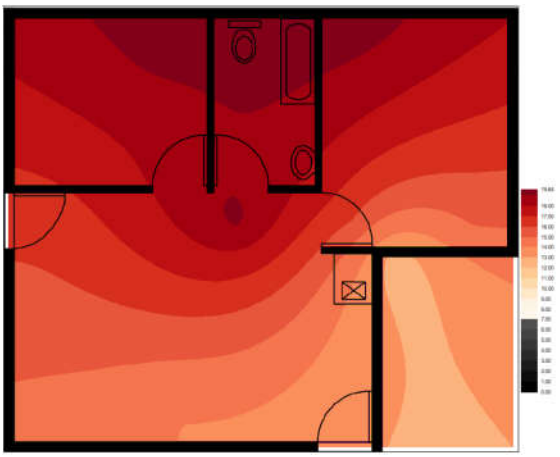

APPENDIX E - Figure: 193: 2014

September 150mm Temp: 12.5°C– 19.2°C

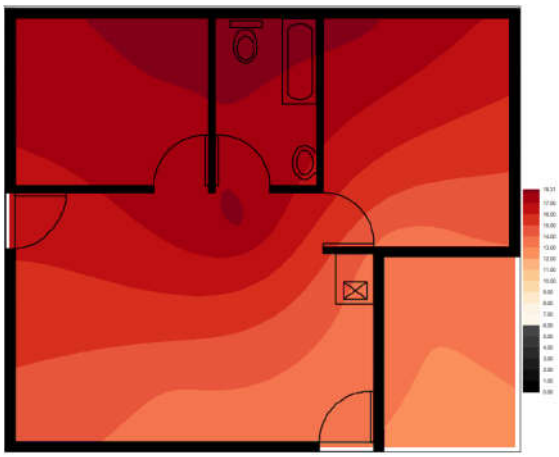

APPENDIX E - Figure: 196: 2014

September 600mm Temp: 13.0°C- 18.3°C

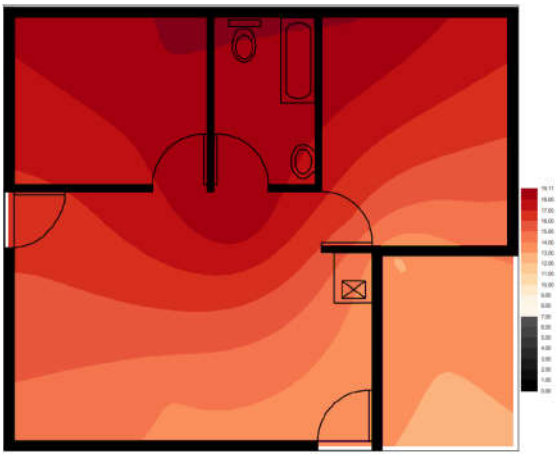

APPENDIX E - Figure: 194: 2014

September 300mm Temp: 12.9°C- 19.1°C

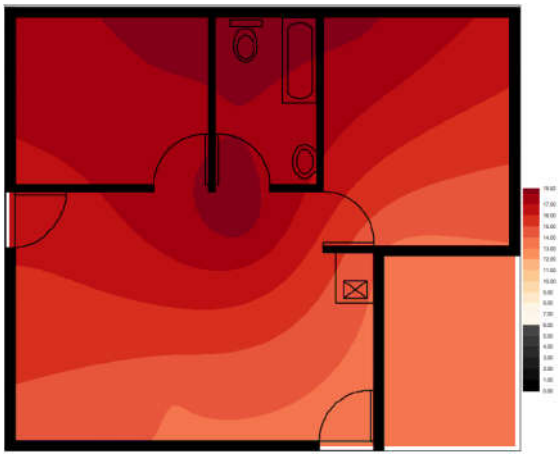

APPENDIX E - Figure: 197: 2014

September 800mm Temp: 13.5°C- 18.6°C

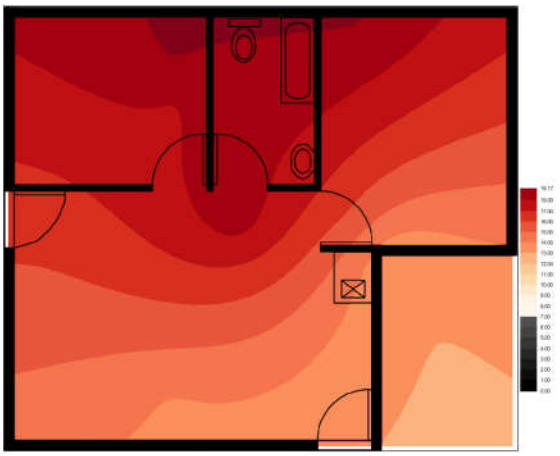

APPENDIX E - Figure: 195: 2014

September 450mm Temp: 13.1°C- 18.5°C

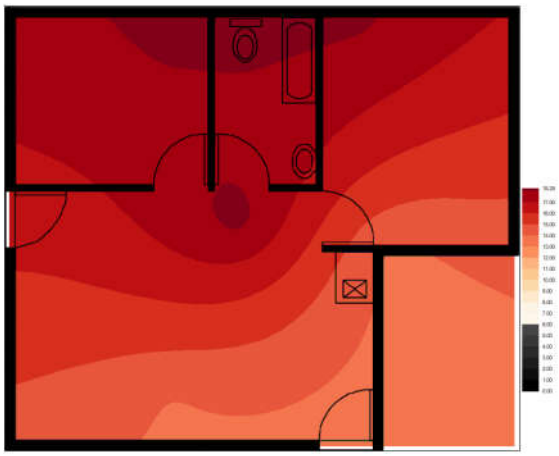

APPENDIX E - Figure: 198: 2014

September 150mm Temp: 13.7°C- 18.3°C

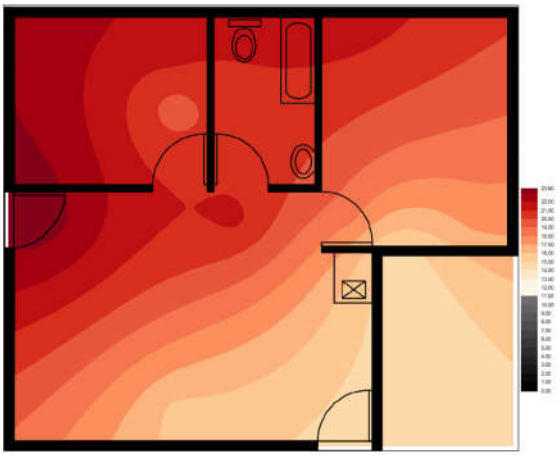

APPENDIX E - Figure: 199: 2014 October 150mm Temperature: 14.2°C – 23.6°C

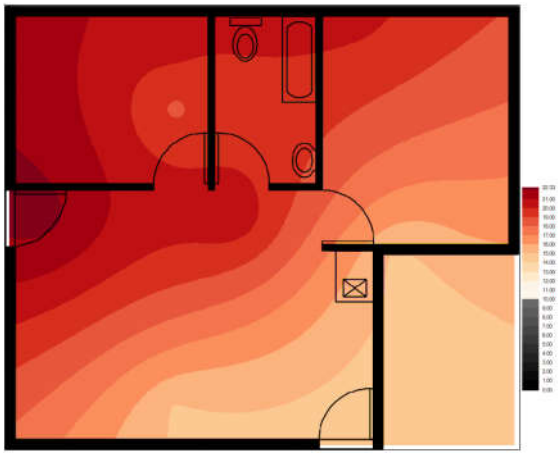

APPENDIX E - Figure: 202: 2014 October 600mm Temperature: 14.8°C – 22.3°C

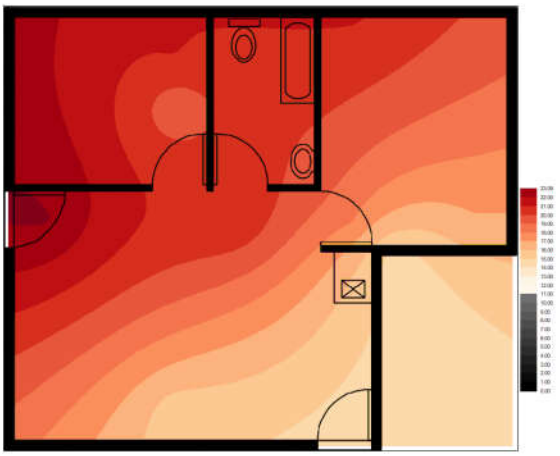

APPENDIX E - Figure: 200: 2014 October 300mm Temperature: 14.5°C – 23.1°C

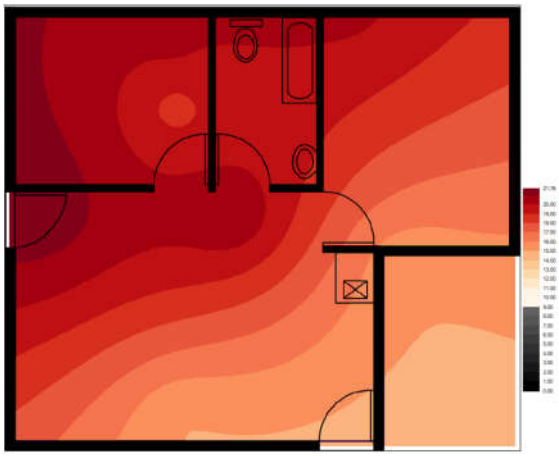

APPENDIX E - Figure: 203: 2014 October 800mm Temperature: 15.1°C – 21.7°C

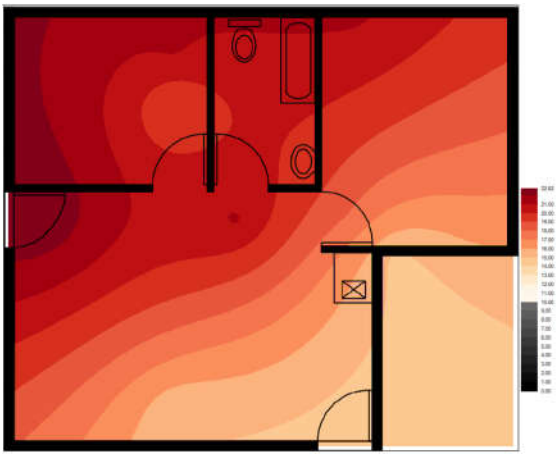

APPENDIX E - Figure: 201: 2014 October 450mm Temperature: 14.7°C – 22.8°C

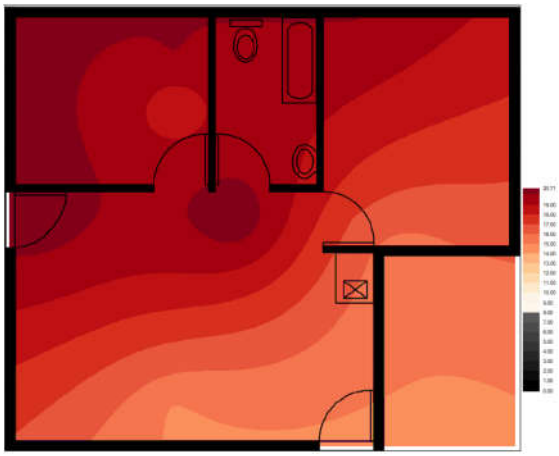

APPENDIX E - Figure: 204: 2014 October 1000mm Temperature: 14.9°C – 20.8°C

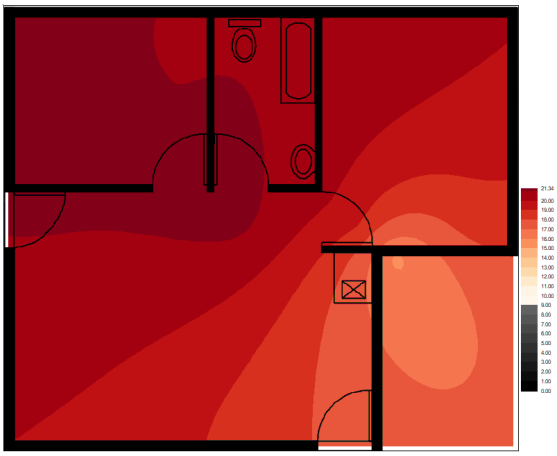

APPENDIX E - Figure: 205: 2014

November 150mm Temp: 15.8°C – 21.1°C

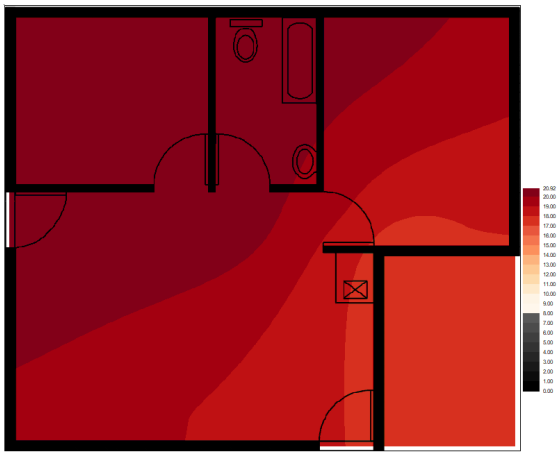

APPENDIX E - Figure: 208: 2014

November 600mm Temp: 17.1°C – 20.8°C

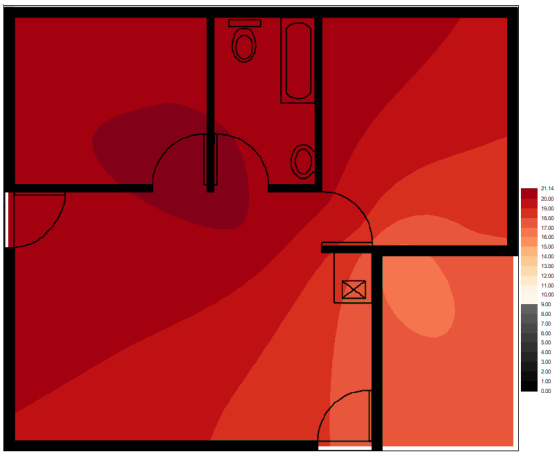

APPENDIX E - Figure: 206: 2014

November 300mm Temp: 16.4°C – 20.8°C

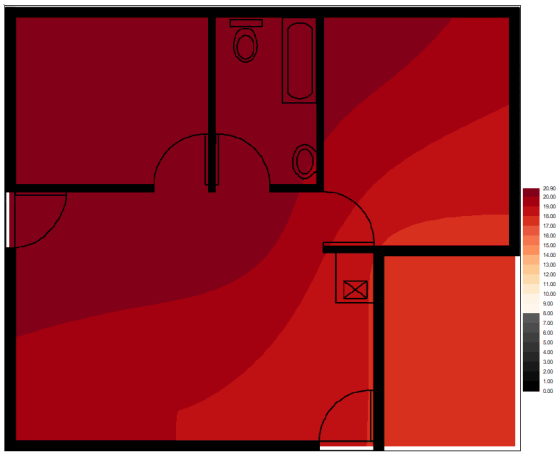

APPENDIX E - Figure: 209: 2014

November 800mm Temp: 17.5°C – 20.9°C

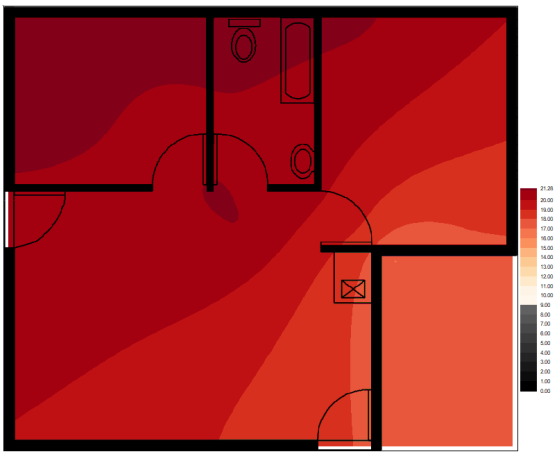

APPENDIX E - Figure: 207: 2014

November 450mm Temp: 17.0°C – 21.0°C

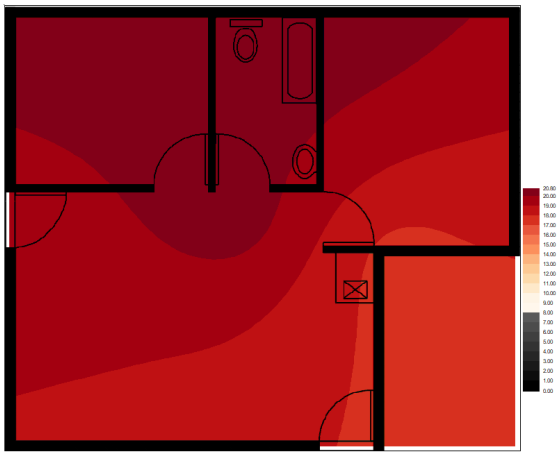

APPENDIX E - Figure: 210: 2014

November 1000mm Temp: 17.5° –20.6°C

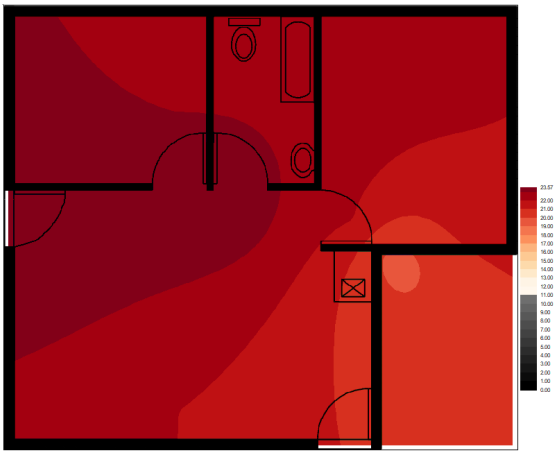

APPENDIX E - Figure: 211: 2014

December 150mm Temp: 19.6°C – 23.6°C

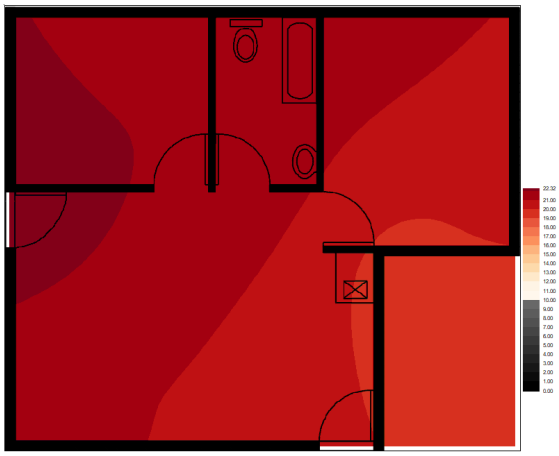

APPENDIX E - Figure: 214: 2014

December 600mm Temp: 19.5°C – 22.3°C

APPENDIX E - Figure: 212: 2014

December 300mm Temp: 19.8°C – 23.1°C

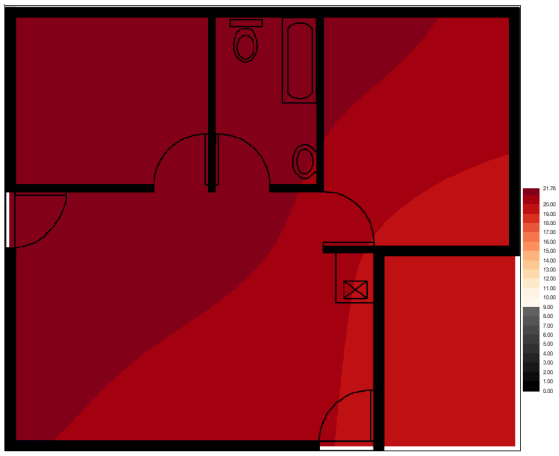

APPENDIX E - Figure: 215: 2014

December 800mm Temp: 19.5°C – 21.7°C

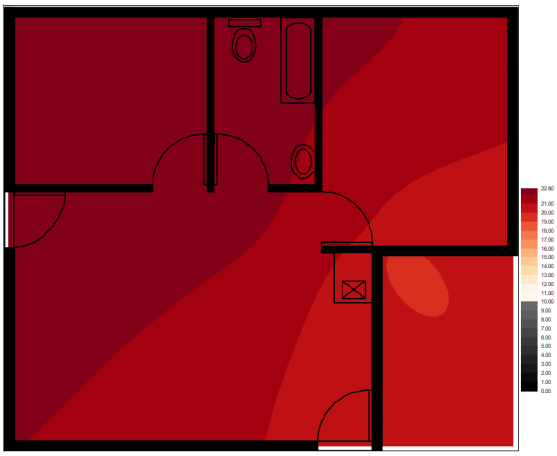

APPENDIX E - Figure: 213: 2014

December 450mm Temp: 19.8°C – 22.8°C

APPENDIX E - Figure: 216: 2014

December 1000mm Temp: 19.2°C–21.4°C

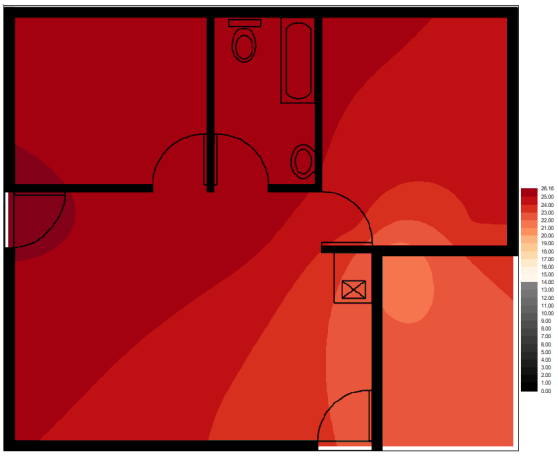

APPENDIX E - Figure: 217: 2015 January 150mm Temperature: 21.1°C – 26.2°C

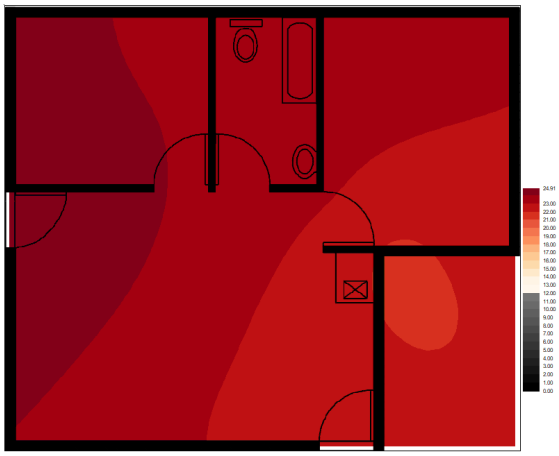

APPENDIX E - Figure: 220: 2015 January 600mm Temperature: 21.7°C – 24.9°C

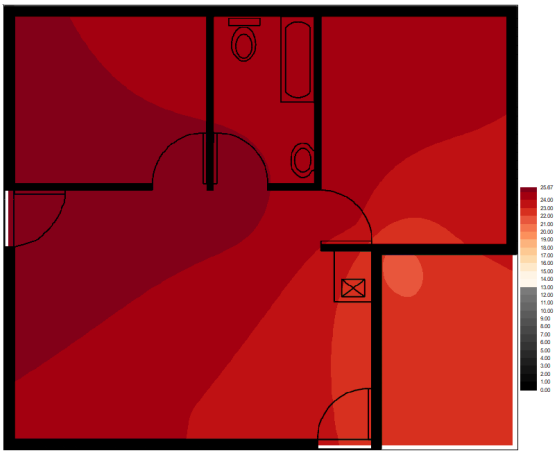

APPENDIX E - Figure: 218: 2015 January 300mm Temperature: 21.6°C – 25.7°C

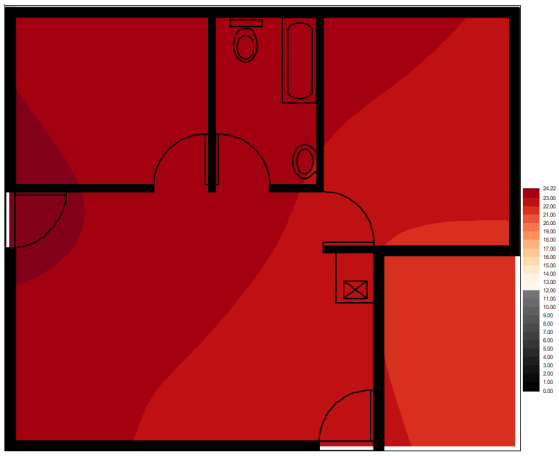

APPENDIX E - Figure: 221: 2015 January 800mm Temperature: 21.8°C – 24.2°C

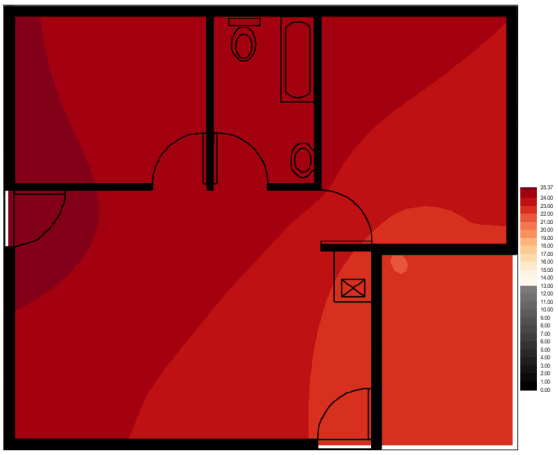

APPENDIX E - Figure: 219: 2015 January 450mm Temperature: 21.9°C – 25.4°C

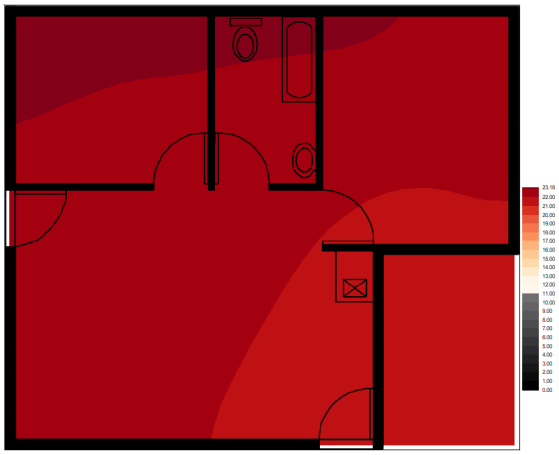

APPENDIX E - Figure: 222: 2015 January 1000mm Temperature: 21.9°C – 22.8°C

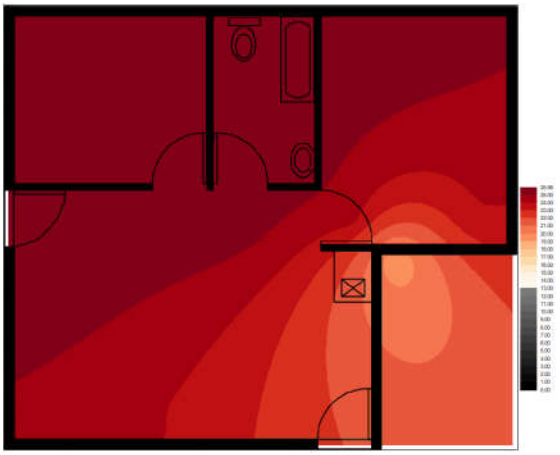

APPENDIX E - Figure: 223: 2015 Feb 150mm Temperature: 19.3°C – 25.8°C

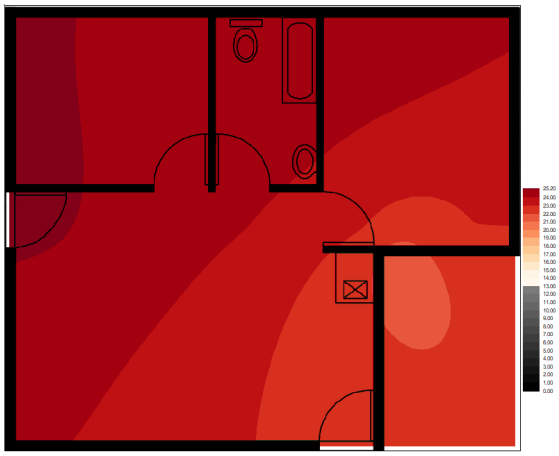

APPENDIX E - Figure: 226: 2015 Feb 600mm Temperature: 21.5°C – 25.2°C

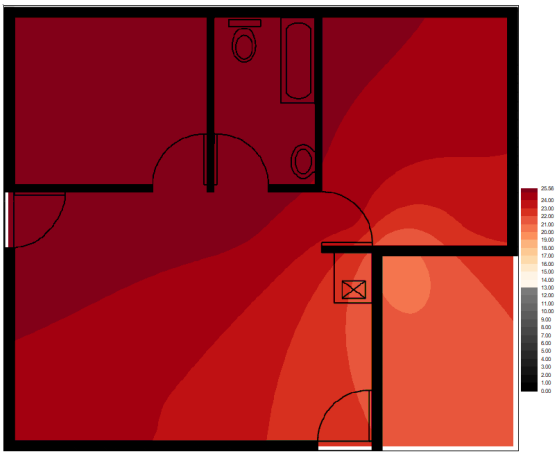

APPENDIX E - Figure: 224: 2015 Feb 300mm Temperature: 20.2°C – 25.5°C

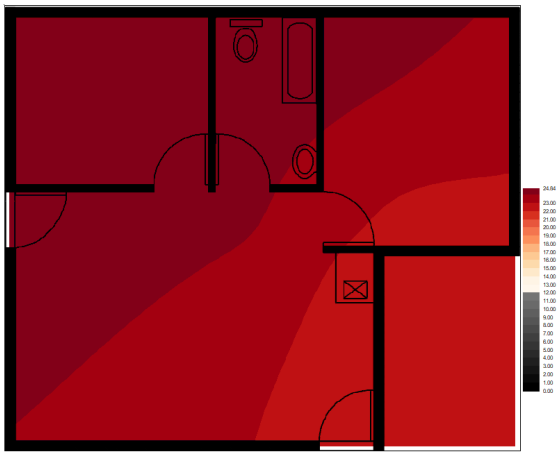

APPENDIX E - Figure: 227: 2015 Feb 800mm Temperature: 22.0°C – 24.8°C

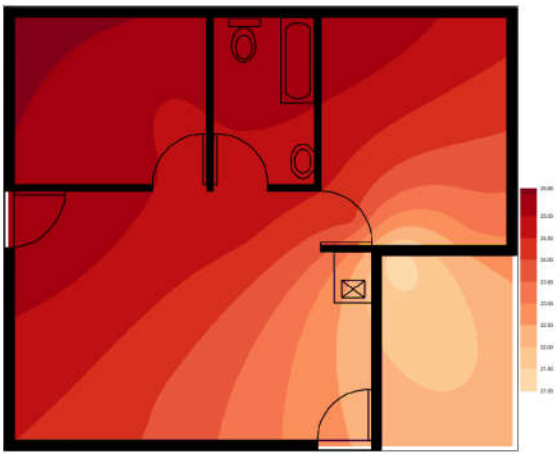

APPENDIX E - Figure: 225: 2015 Feb 450mm Temperature: 21.2°C – 25.5°C

APPENDIX E - Figure: 228: 2015 Feb 1000mm Temperature: 21.9°C – 24.3°C

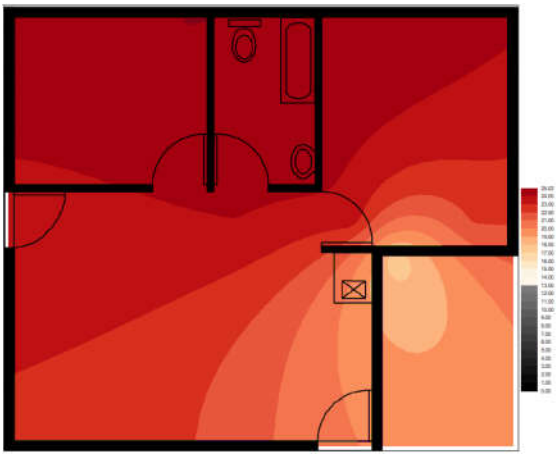

APPENDIX E - Figure: 229: 2015 March 150mm Temperature: 17.4°C – 25.0°C

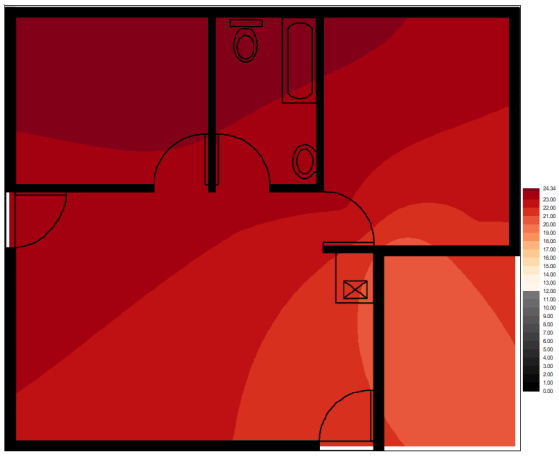

APPENDIX E - Figure: 232: 2015 March 600mm Temperature: 20.1°C – 23.6°C

APPENDIX E - Figure: 230: 2015 March 300mm Temperature: 18.3°C – 24.6°C

APPENDIX E - Figure: 233: 2015 March 800mm Temperature: 21.0°C – 24.3°C

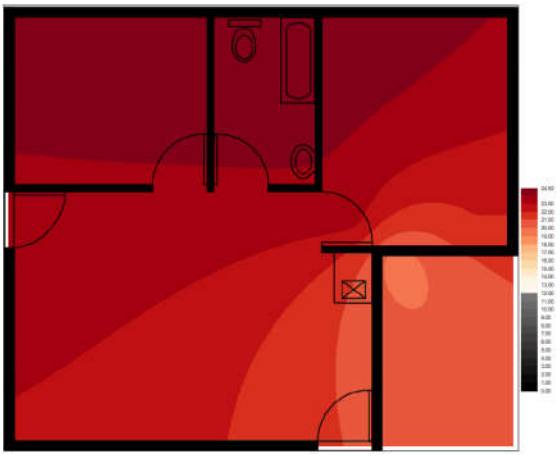

APPENDIX E - Figure: 231: 2015 March 450mm Temperature: 19.5°C – 24.9°C

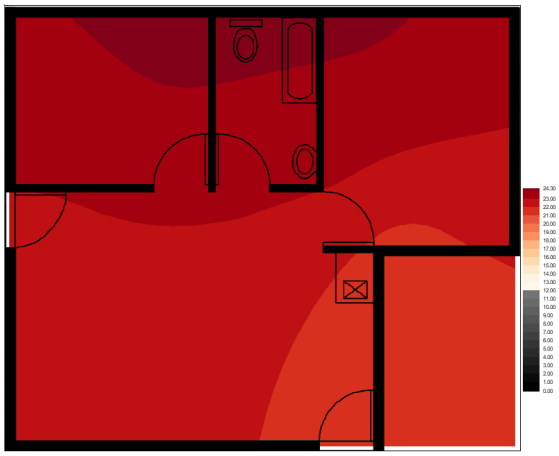

APPENDIX E - Figure: 234: 2015 March 1000mm Temperature: 21.3°C – 24.3°C

APPENDIX E - Figure: 235: 2015 April 150mm Temperature: 17.4°C – 22.0°C

APPENDIX E - Figure: 238: 2015 April 600mm Temperature: 19.5°C – 22.6°C

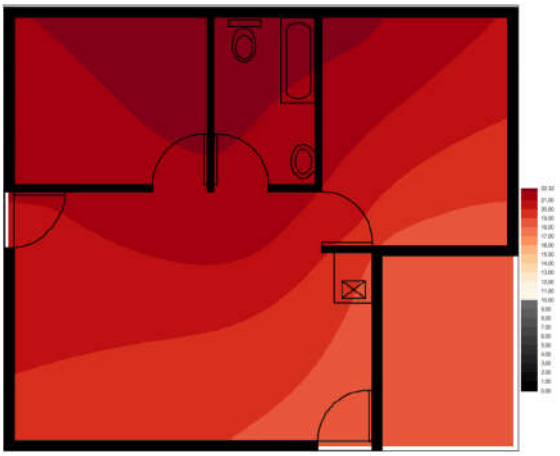

APPENDIX E - Figure: 236: 2015 April 300mm Temperature: 18.3°C – 22.3°C

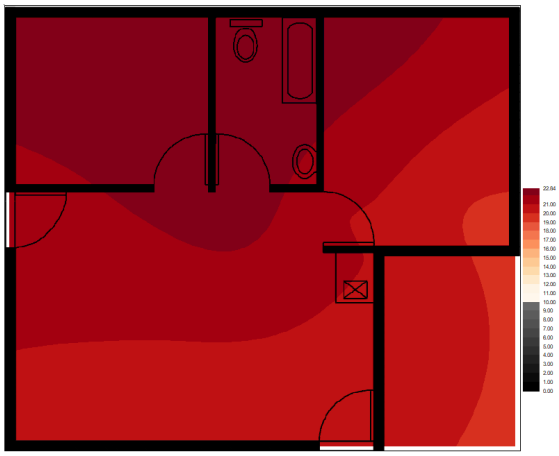

APPENDIX E - Figure: 239: 2015 April 800mm Temperature: 19.8°C – 22.8°C

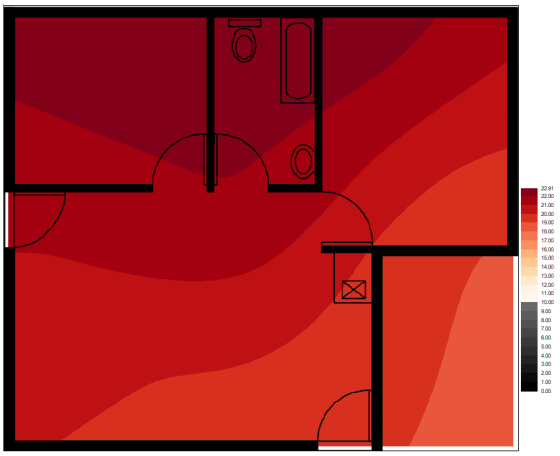

APPENDIX E - Figure: 237: 2015 April 450mm Temperature: 19.1°C – 22.9°C

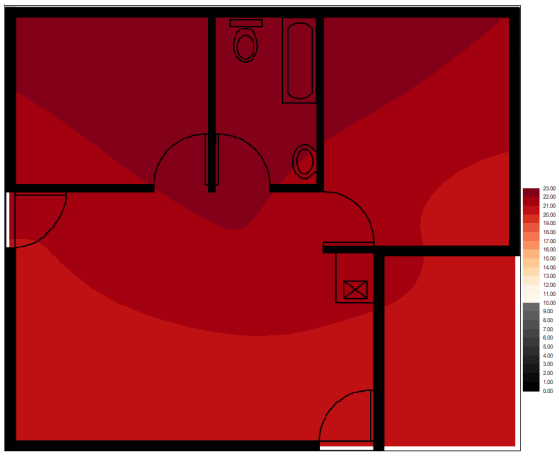

APPENDIX E - Figure: 240: 2015 April 1000mm Temperature: 20.4°C – 23.0°C

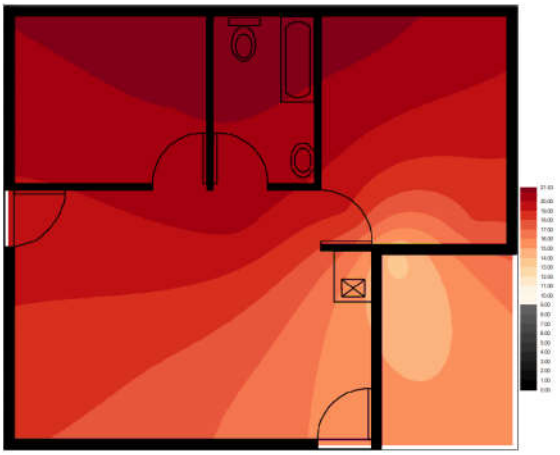

APPENDIX E - Figure: 241: 2015 May 150mm Temperature: 13.5°C – 20.4°C

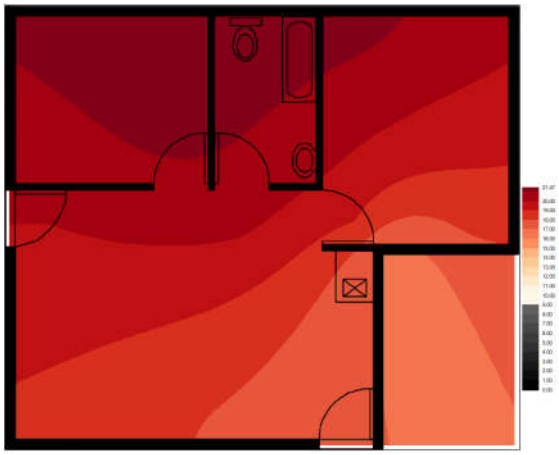

APPENDIX E - Figure: 244: 2015 May 600mm Temperature: 16.4°C – 21.5°C

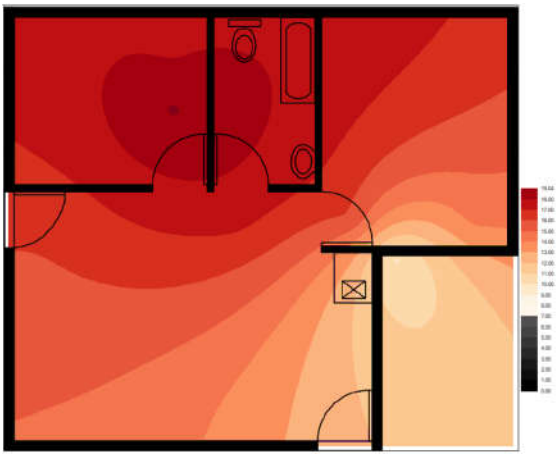

APPENDIX E - Figure: 242: 2015 May 300mm Temperature: 14.4°C – 21.2°C

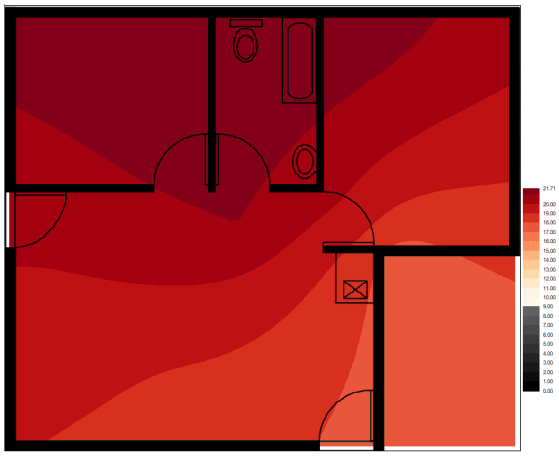

APPENDIX E - Figure: 245: 2015 May 800mm Temperature: 17.5°C – 21.7°C

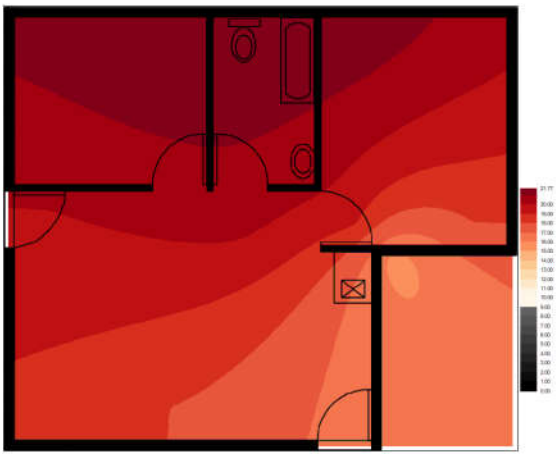

APPENDIX E - Figure: 243: 2015 May 450mm Temperature: 15.7°C – 21.7°C

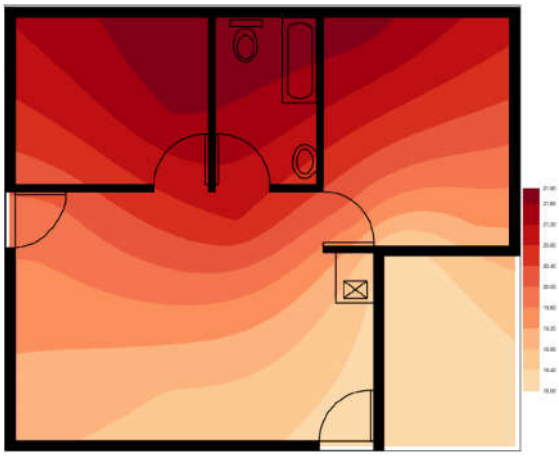

APPENDIX E - Figure: 246: 2015 May 1000mm Temperature: 18.1°C – 21.9°C

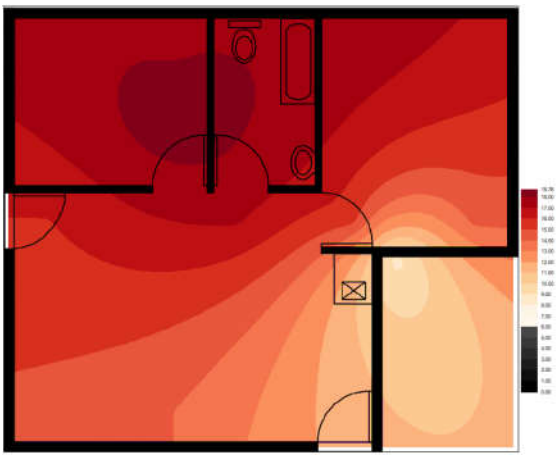

APPENDIX E - Figure: 247: 2015 June 150mm Temperature: 8.7°C – 18.8°C

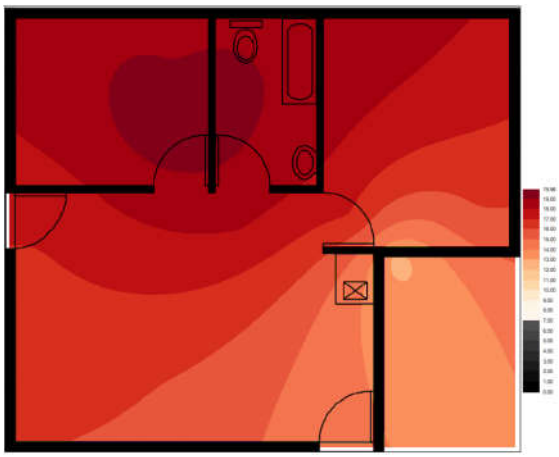

APPENDIX E - Figure: 250: 2015 June 600mm Temperature: 12.7°C – 20.0°C

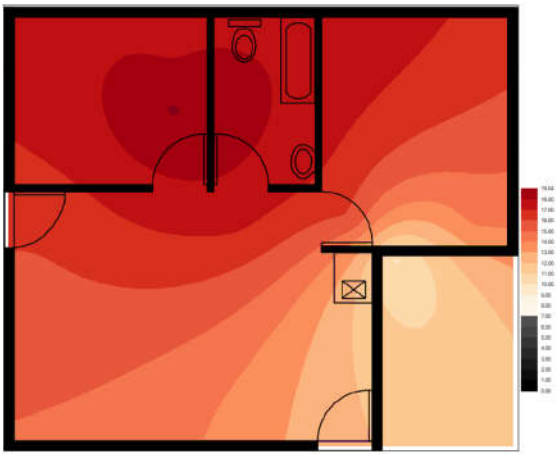

APPENDIX E - Figure: 248: 2015 June 300mm Temperature: 9.9°C – 19.1°C

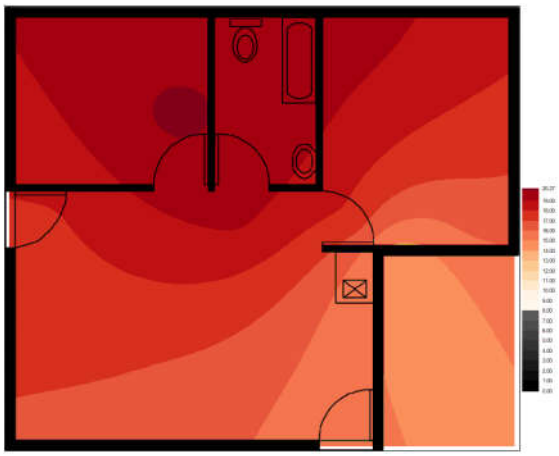

APPENDIX E - Figure: 251: 2015 June 800mm Temperature: 14.1°C – 20.3°C

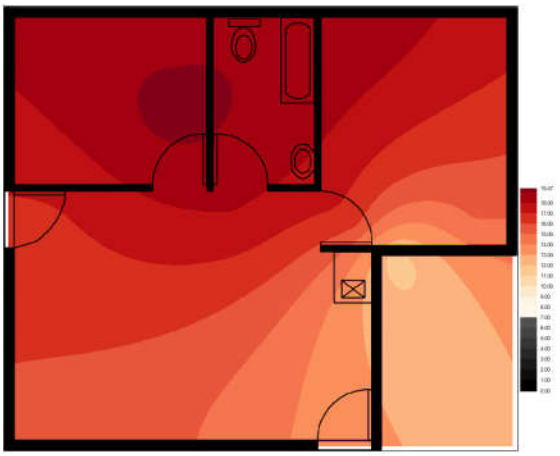

APPENDIX E - Figure: 249: 2015 June 450mm Temperature: 11.5°C – 19.5°C

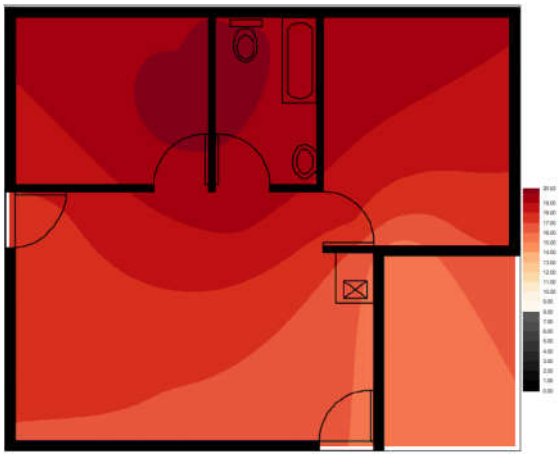

APPENDIX E - Figure: 252: 2015 June 1000mm Temperature: 15.1°C – 20.6°C

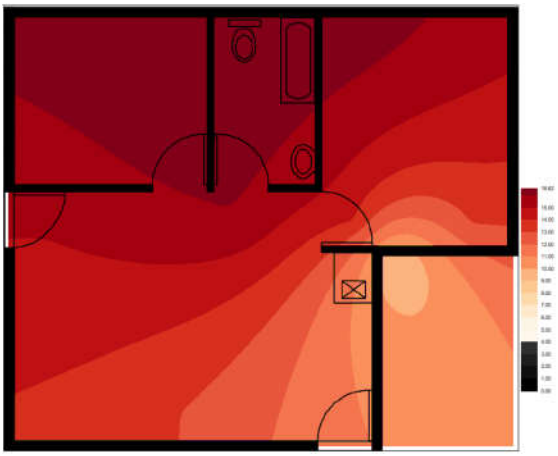

APPENDIX E - Figure: 253: 2015 July
150mm Temperature: 9.1°C – 15.9°C

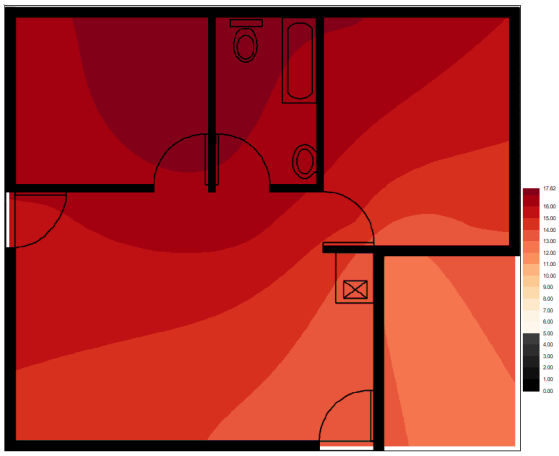

APPENDIX E - Figure: 256: 2015 July
600mm Temperature: 12.5°C – 17.6°C

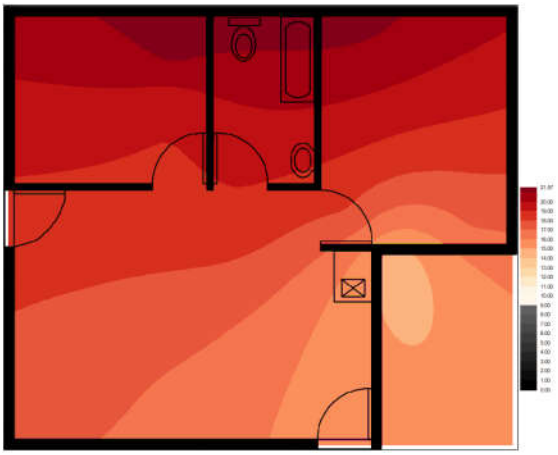

APPENDIX E - Figure: 254: 2015 July
300mm Temperature: 10.1°C – 16.0°C

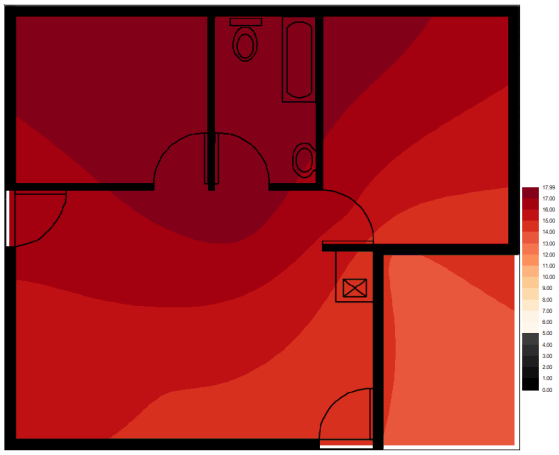

APPENDIX E - Figure: 257: 2015 July
800mm Temperature: 13.8°C – 18.0°C

APPENDIX E - Figure: 255: 2015 July
450mm Temperature: 13.9°C – 17.2°C

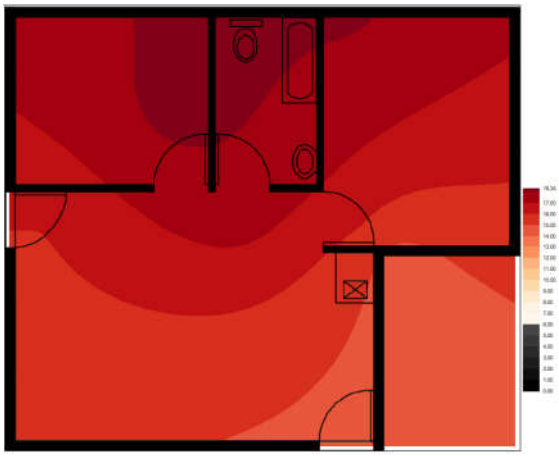

APPENDIX E - Figure: 258: 2015 July
1000mm Temperature: 14.6°C – 18.3°C

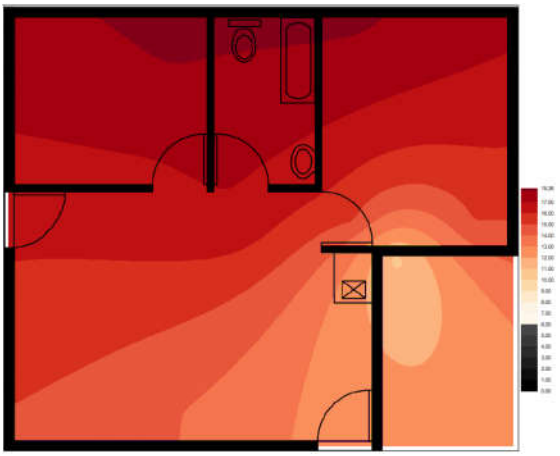

APPENDIX E - Figure: 259: 2015 August 150mm Temperature: 10.8°C – 18.2°C

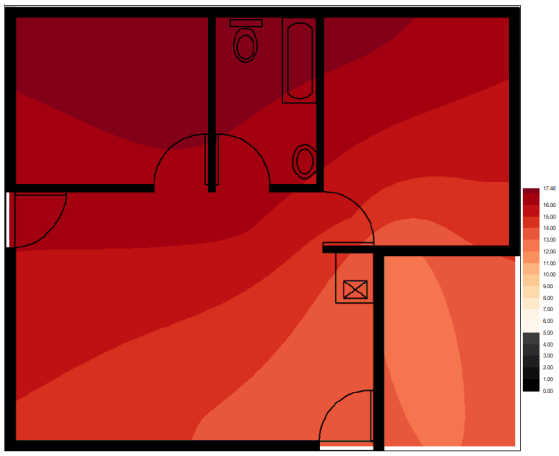

APPENDIX E - Figure: 262: 2015 August 600mm Temperature: 12.5°C – 17.4°C

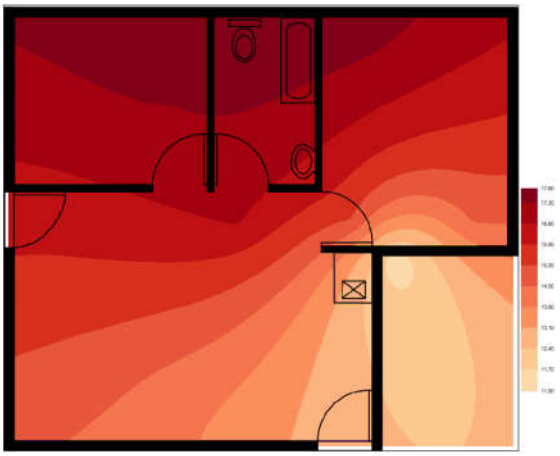

APPENDIX E - Figure: 260: 2015 August 300mm Temperature: 11.3°C – 17.8°C

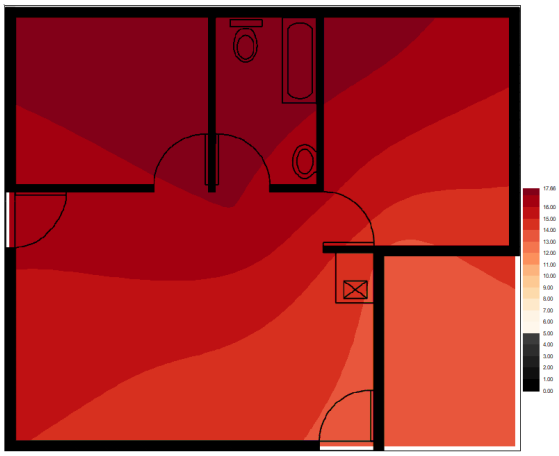

APPENDIX E - Figure: 263: 2015 August 800mm Temperature: 13.5°C – 17.6°C

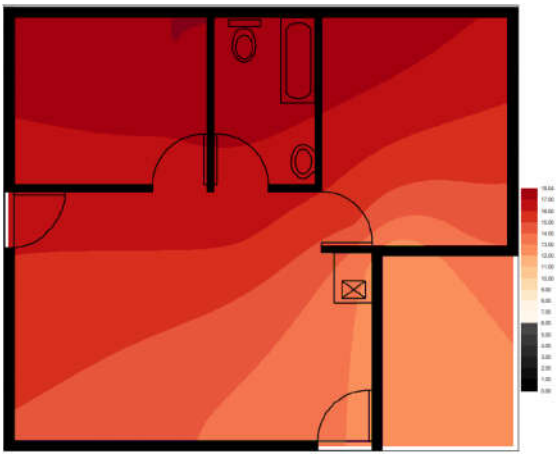

APPENDIX E - Figure: 261: 2015 August 450mm Temperature: 12.0°C – 18.0°C

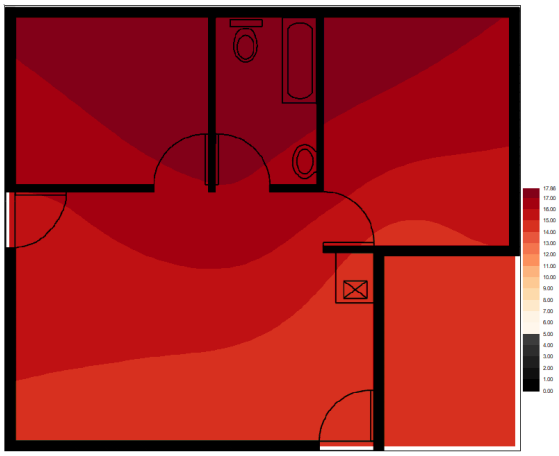

APPENDIX E - Figure: 264: 2015 August 1000mm Temperature: 14.0°C – 17.8°C

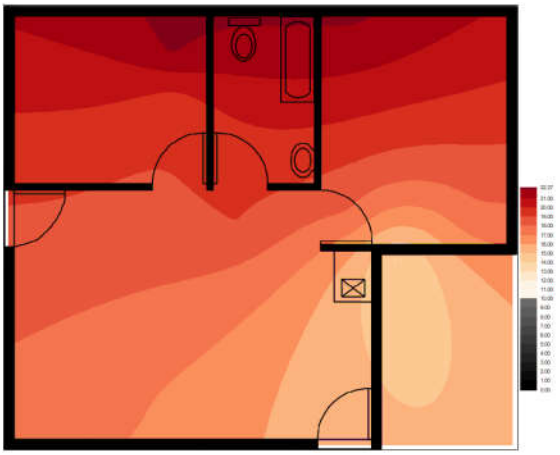

APPENDIX E - Figure: 265: 2015

September 150mm Temp: 13.9°C –22.2°C

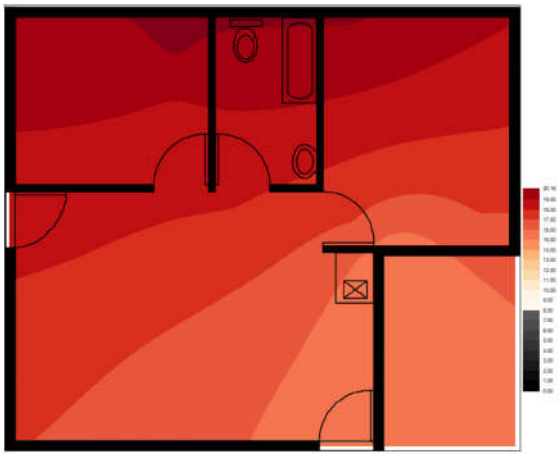

APPENDIX E - Figure: 268: 2015

September 600mm Temp: 15.1°C -20.1°C

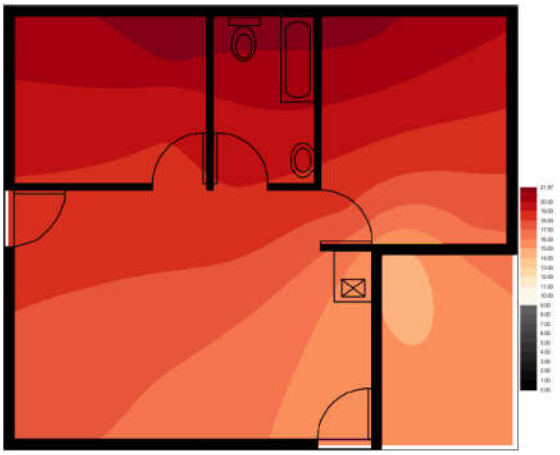

APPENDIX E - Figure: 266: 2015

September 300mm Temp: 14.4°C -21.5°C

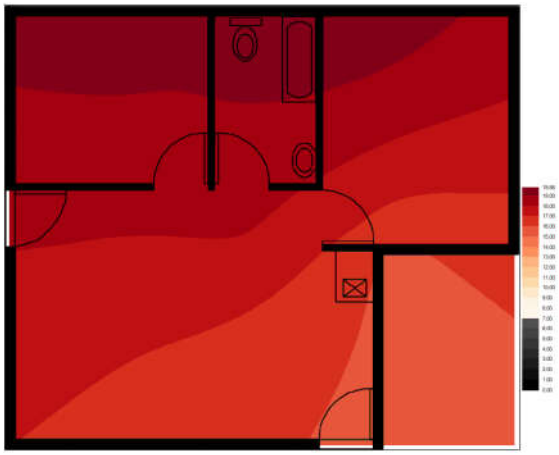

APPENDIX E - Figure: 269: 2015

September 800mm Temp: 15.7°C -19.8°C

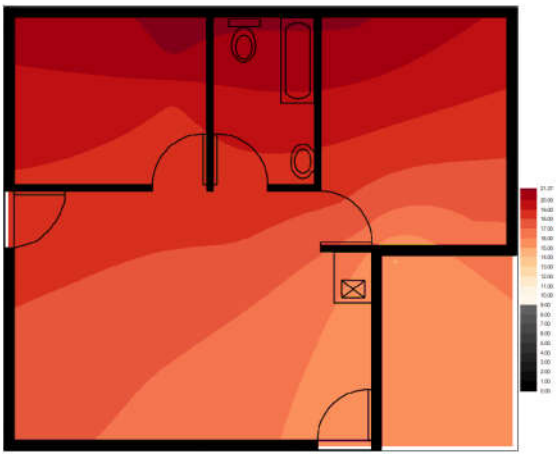

APPENDIX E - Figure: 267: 2015

September 450mm Temp: 15.0°C -21.2°C

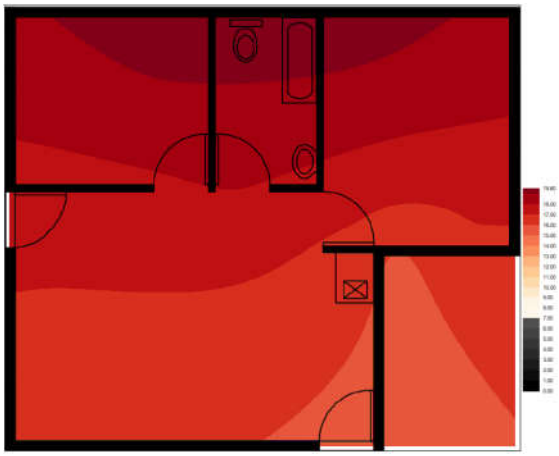

APPENDIX E - Figure: 270: 2015

September 1000mm Temp:18.2°C-19.8°C

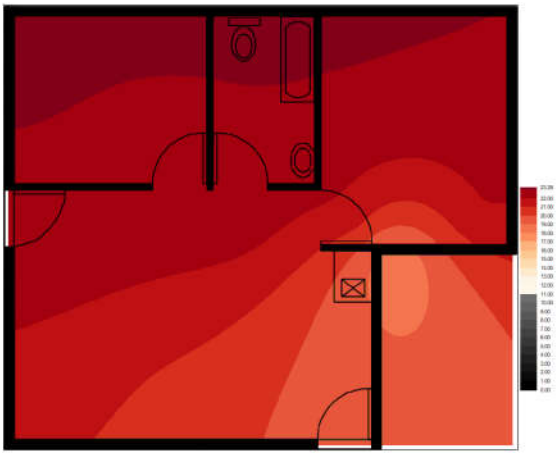

APPENDIX E - Figure: 271: 2015 October 150mm Temperature: 18.1°C – 23.3°C

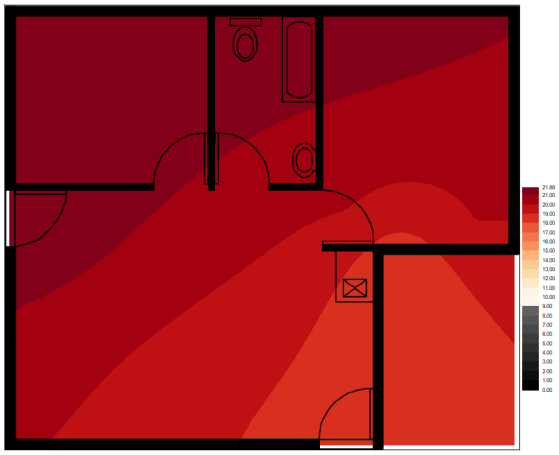

APPENDIX E - Figure: 274: 2015 October 600mm Temperature: 18.2°C – 21.7°C

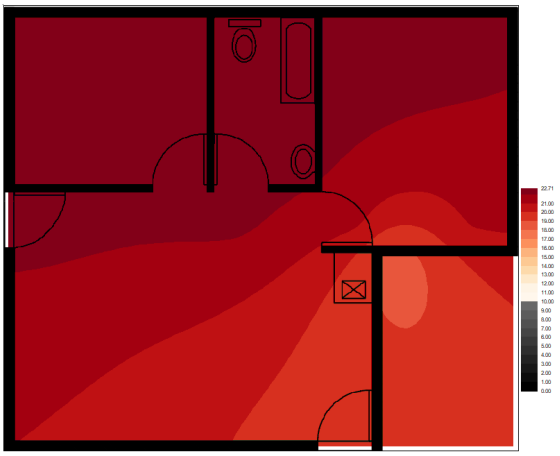

APPENDIX E - Figure: 272: 2015 October 300mm Temperature: 18.4°C – 22.6°C

APPENDIX E - Figure: 275: 2015 October 800mm Temperature: 18.4°C – 21.3°C

APPENDIX E - Figure: 273: 2015 October 450mm Temperature: 18.5°C – 22.1°C

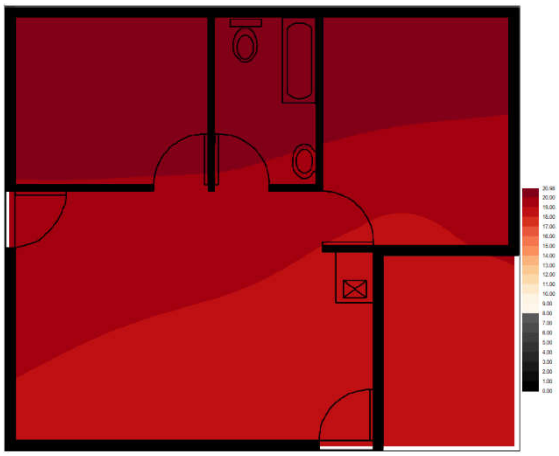

APPENDIX E - Figure: 276: 2015 October 1000mm Temperature: 18.1°C – 21.0°C

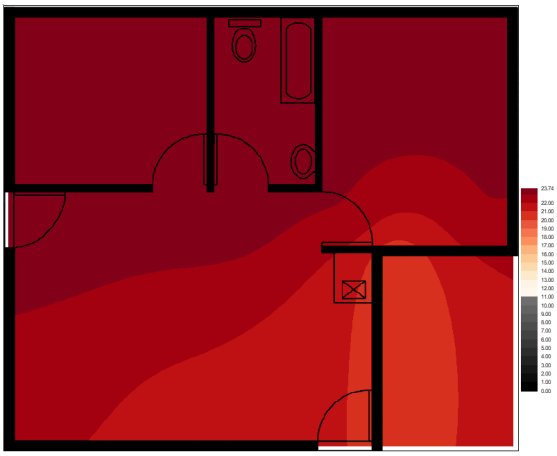

APPENDIX E - Figure: 277: 2015

November 150mm Temp: 20.1°C – 23.6°C

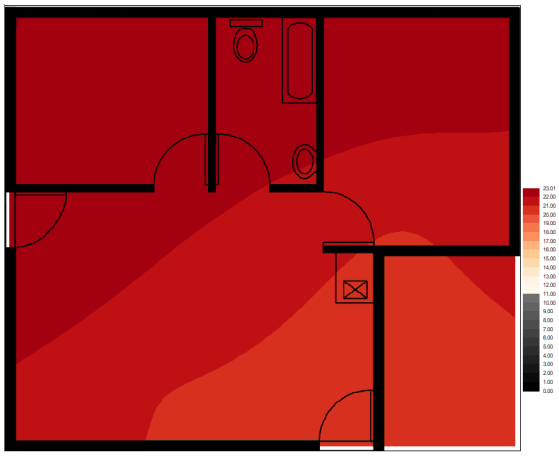

APPENDIX E - Figure: 280: 2015

November 600mm Temp: 20.5°C – 22.9°C

APPENDIX E - Figure: 278: 2015

November 300mm Temp: 20.5°C – 23.3°C

APPENDIX E - Figure: 281: 2015

November 800mm Temp: 20.6°C – 22.6°C

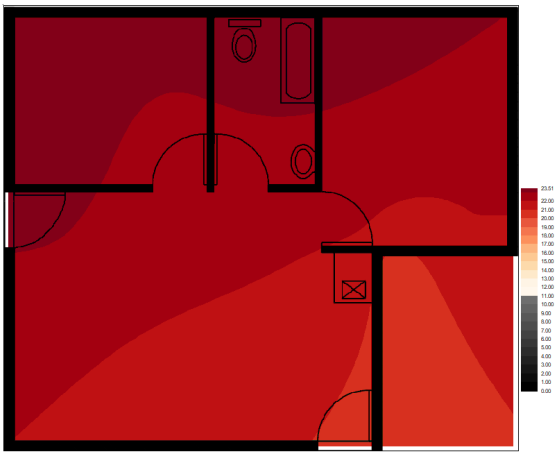

APPENDIX E - Figure: 279: 2015

November 450mm Temp: 20.7°C – 23.2°C

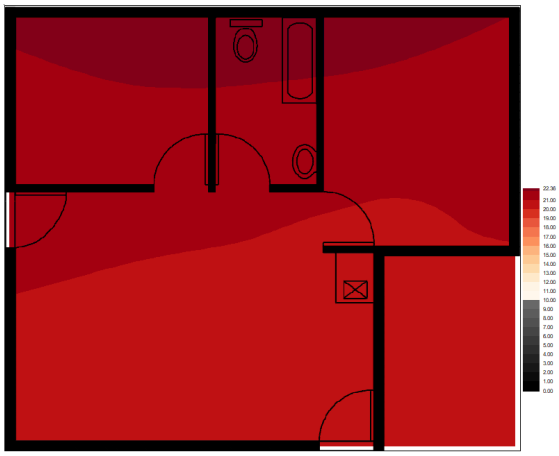

APPENDIX E - Figure: 282: 2015

November 1000mm Temp: 20.1°C–21.8°C

APPENDIX E - Figure: 283: 2015

December 150mm Temp: 24.8°C – 26.4°C

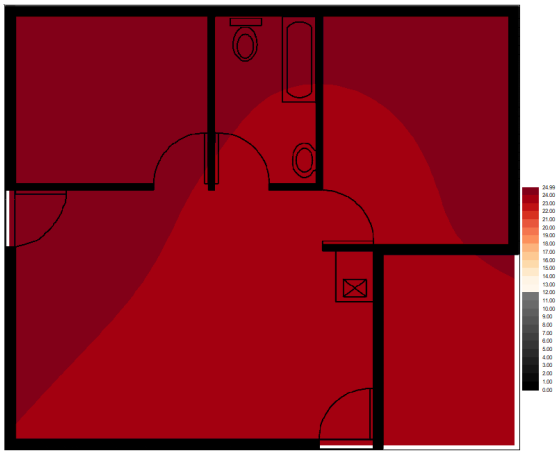

APPENDIX E - Figure: 286: 2015

December 600mm Temp: 23.3°C – 25.0°C

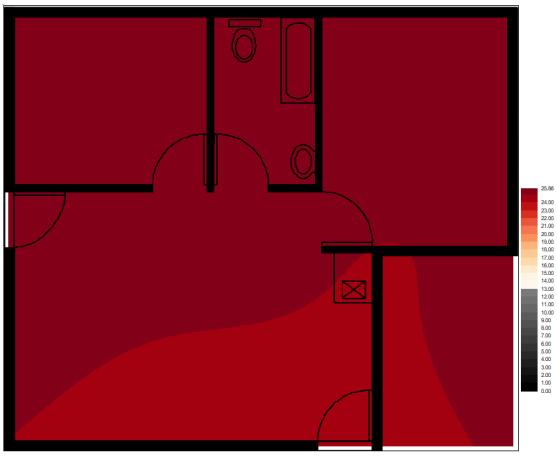

APPENDIX E - Figure: 284: 2015

December 300mm Temp: 24.5°C – 25.3°C

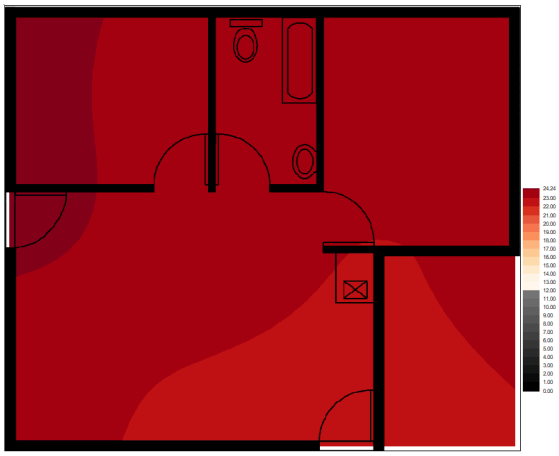

APPENDIX E - Figure: 287: 2015

December 800mm Temp: 22.9°C – 24.2°C

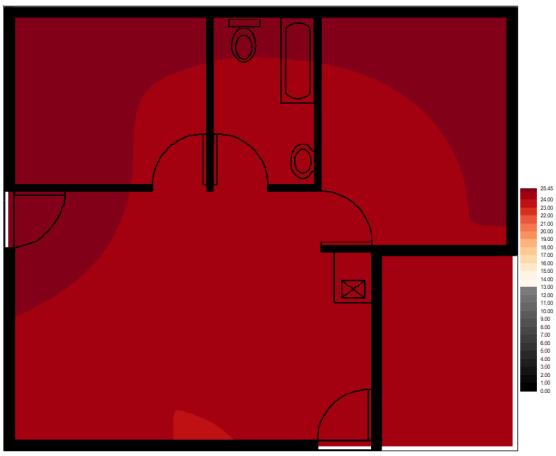

APPENDIX E - Figure: 285: 2015

December 450mm Temp: 24.0°C – 25.1°C

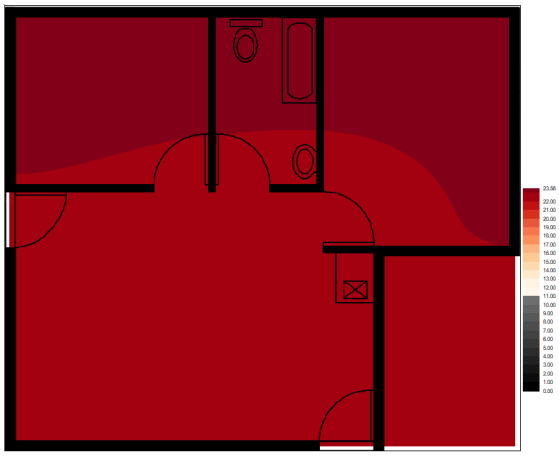

APPENDIX E - Figure: 288: 2015

December 1000mm Temp: 22.0°C–23.1°C

APPENDIX: F

Orientation of the sun in Botshabelo

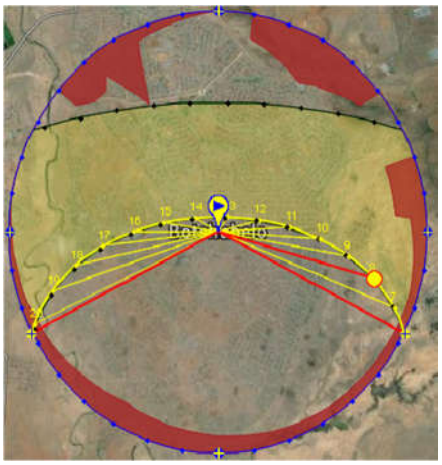

APPENDIX F- Figure 1: Orientation of the sun at January in Botshabelo

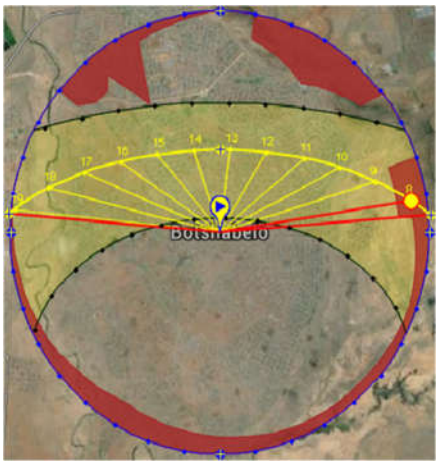

APPENDIX F- Figure 4: Orientation of the sun at April in Botshabelo

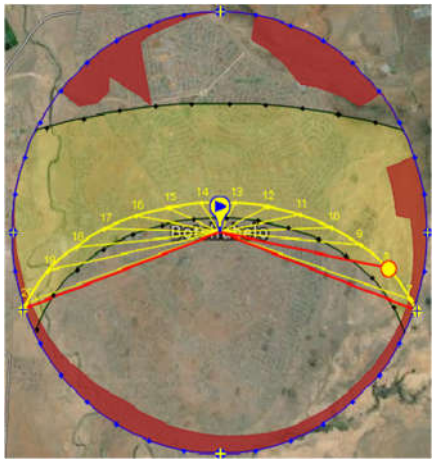

APPENDIX F- Figure 2: Orientation of the sun at February in Botshabelo

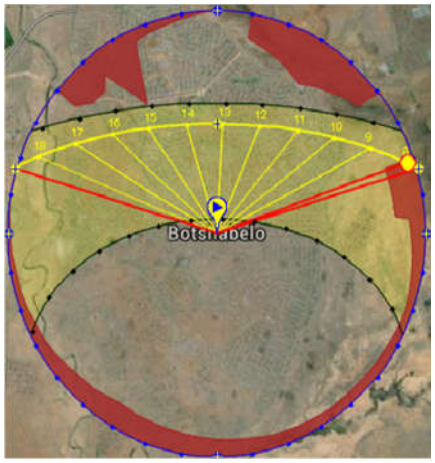

APPENDIX F- Figure 5: Orientation of the sun at May in Botshabelo

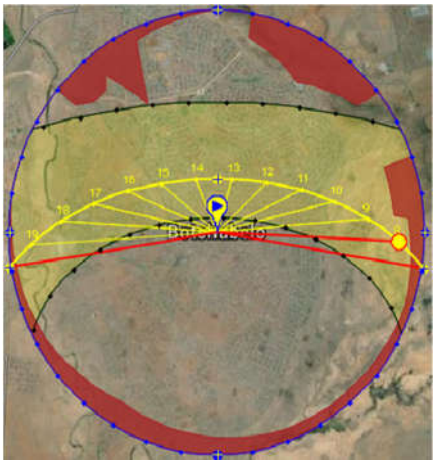

APPENDIX F- Figure 3: Orientation of the sun at March in Botshabelo

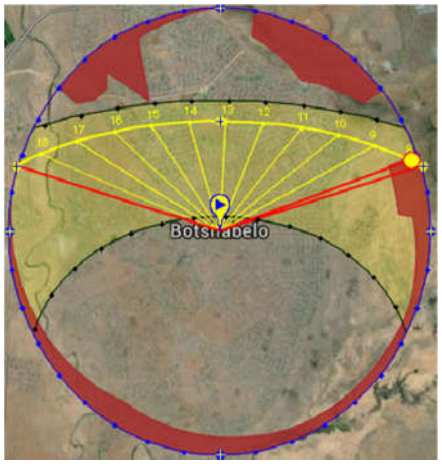

APPENDIX F- Figure 6: Orientation of the sun at June in Botshabelo

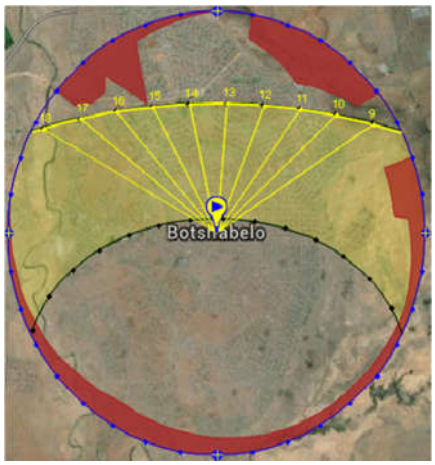

APPENDIX F- Figure 7: Orientation of the sun at July in Botshabelo

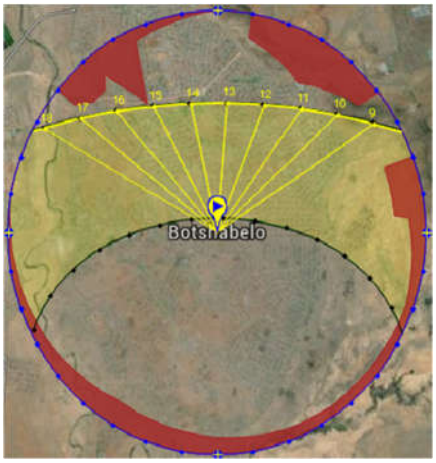

APPENDIX F- Figure 8: Orientation of the sun at August in Botshabelo

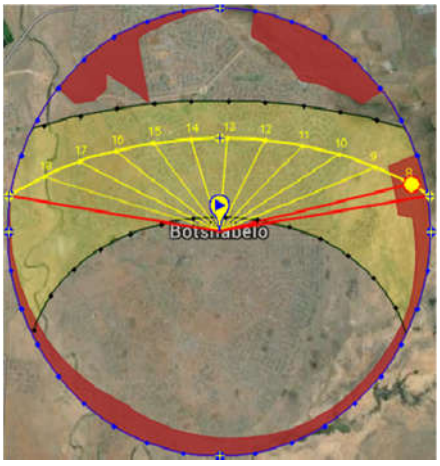

APPENDIX F- Figure 9: Orientation of the sun at September in Botshabelo

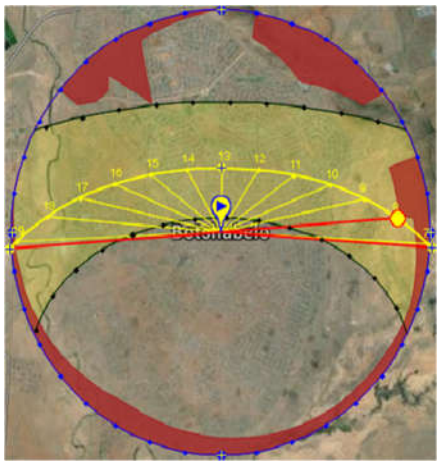

APPENDIX F- Figure 10: Orientation of the sun at October in Botshabelo

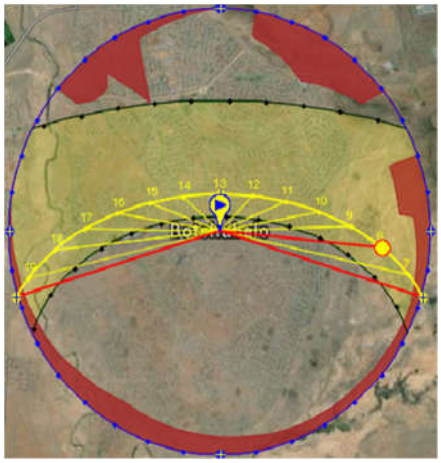

APPENDIX F- Figure 11: Orientation of the sun at November in Botshabelo

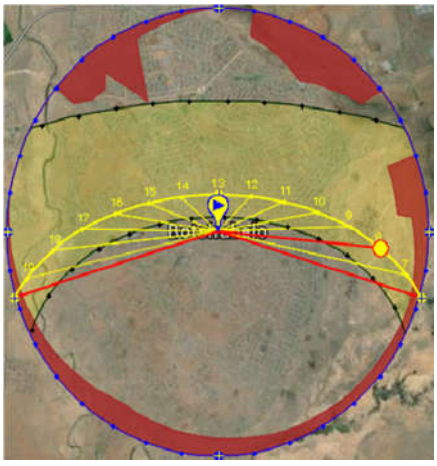

APPENDIX F- Figure 12: Orientation of the sun at December in Botshabelo